Stéphanie LIZY-DESTREZ

Operational Scenarios Optimization for Resupply of Crew and Cargo of an International Gateway Station Located near the Earth-Moon-Lagrangian Point-2

Operational scenarios optimization for resupply of crew and cargo of an International gateway Station located near the Earth-Moon-Lagrangian point-2

A thesis accepted by the Faculty of Aerospace Engineering and Geodesy of the University of Stuttgart in partial fulfillment of the requirements for the degree of Doctor of Engineering Sciences (Dr.-Ing.)

by

Stéphanie Isabelle LIZY-DESTREZ

Born in Toulon (France)

Committee chairs:
Prof. Dr. Yves Gourinat, ISAE, France
Prof. Dr. Massimiliano Vasile, University of Strathcycle, Great-Britain

Committee members:
Prof. Dr. Ernst Messerschmid, University of Stuttgart, Germany
Prof. Dr. Daniel Alazard, ISAE, France
Prof. Dr. Emmanuel Trélat, Université Pierre et Marie Curie (Paris 6), France
Prof. Dr. France Josep Masdemont, Universitat Politecnica de Catalunya, Spain

Date of defence :   15.12.2015

Institute of Space Systems
University of Stuttgart

Institut Supérieur de l'Aéronautique et de l'Espace
Université Fédérale de Toulouse Midi Pyrénées

2016

CONTENTS

List of figures

List of tables

Acknowledgments

A travers cette thèse, je tiens à remercier tous ceux qui m'ont soutenue
à commencer par ma famille Nathan, Lou-Anne et Bruno
mes directeurs de thèse Daniel et Ernst
le directeur de l'Ecole Doctorale, Yves
mes professeurs et parmi eux, Bénédicte et Christian
mes collègues et amis
la section TEC-ECN de l'ESTEC
et surtout tous les étudiants qui ont bien voulu m'accompagner par ordre
d'apparition : Christian, Giuseppe, Chloé, Jason, Crescenzio, Bastien, Jean-
Baptiste, Pierre, Carlo, Kevin, Quentin, Mohammad, Lucas, Cécile, Alban,
Nicolas
sans oublier les deux promotions du Mastère SEN 2010 et 2011

Nomenclature

Acronym	Definition
2BP	Two-Body Problem
3BP	Three-Body Problem
3D	Three dimensions
AA	Aéronautique Astronautique
ACE	Advanced Composition Explorer
ATV	Automated Transfer Vehicle
ATV-CC	ATV Control Center
AMEML2	Available Mass in EML2
BCR4BP	Bi-Circular Restricted Four-Body Problem
CARE	Crew module Atmospheric Reentry Experiment
CoG	Center of Gravity
CSA	Canadian Space Agency
CSDV	Commande des systèmes et dynamique du vol
DCAS	Département Conception et Conduite des véhicules Aéronautiques et Spatiaux
CR3BP	Circular Restricted Three-Body Problem
DPT	NASA's Decadal Planning Team
eFFBD	Enhanced Functional Flow Block Diagram
EML	Earth-Moon Libration point
ESA	European Space Agency
ESTEC	ESA Technical Center
FISO	Future In-Space Operations
EVA	Extra -Vehicular Activity
FOM	Figure of Merit
GRAIL	Gravity Recovery and Interior Laboratory
HOI	Halo Orbit Insertion
ICE	International Cometary Explorer
IMCCE	Institut de Mécanique Céleste et de Calcul des Ephémérides
IMLEO	Initial Mass in LEO
INCOSE	International Council of Systems Engineering
ISAE	Institut Supérieur de l'Aéronautique et de l'Espace
ISECG	International Space Exploration Coordination Group
ISEE-3	International Sun-Earth Explorer 3
I_{SP}	Specific impulse
ISS	International Space Station
IRS	Institut für Raumfahrtsysteme at Stuttgart University
JAXA	Japan Aerospace Exploration Agency
JWST	James Webb Space Telescope
KAM	Kolomogorov, Arnold and Moser
LBT	Lunar FlyBy Trajectory

Acronym	Definition
LEO	Low Earth Orbit
LH_2	Liquid diHydrogen
LP	Libration Point
LOX	Liquid Oxygen
MDRS	Mars Desert Research Station
MOI	Stable Manifold Orbit Insertion
MOL	Manned Orbiting Laboratory
MORL	Manned Orbiting Research Laboratory
MPCV	Multi-Purpose Crew Vehicle
NASA	National Aeronautics and Space Agency
NEO	Near Earth Object
NEXT	NASA Exploration Team
ODE	Ordinary Differential Equation
PhD	Philosophiæ Doctor
PM	Poincaré Map
ROSCOSMOS	Russian Federal Space Agency
SE	Systems Engineering
SEL	Sun-Earth Lagrangian point
SEN	Systems Engineering ISAE Advanced Master
SK	Station Keeping
SLS	Space Launch System
SMART	Small Missions for Advanced Research in Technology
SMC	Space Medical Center
SOHO	Solar and Heliospheric Observatory
SPDM	Special Purpose Dexterous Manipulator
SPM	State Propagation Matrix
SSF	Space Station Freedom
STM	State Transition Matrix
STS	Space Transportation System
TEC-ECN	Guidance, Navigation, and Control Systems section of ESTEC
THEMIS	Time History of Events and Macroscale Interactions during Substorms
THOR	Trans-lunar Human explORation
TOF	Time Of Flight
USA	United States of America
WMAP	Wilkinson Microwave Anisotropy Probe
WSB	Weak Stability Boundary
WSBE	Weak Stability Boundary exotic family
WSBT	Weak Stability Boundary traditional family

Abstract

In the context of future human space exploration missions in the solar system (with an horizon of 2025) and according to the roadmap proposed by ISECG (International Space Exploration Coordination Group) [1], a new step could be to maintain as an outpost, at one of the libration points of the Earth-Moon system, a space station. This would ease access to far destinations as Moon, Mars and asteroids and would allow testing some innovative technologies, before employing them for far distant human missions. One of the main challenges will be to maintain permanently, and ensure on board crew health thanks to an autonomous space medical center docked to the proposed space station, as a Space haven. Then the main problem to solve is to manage the station servitude, during deployment (modules integration) and operational phase. Challenges lie, on a global point of view, in the design of the operational scenarios and, on a local point of view, in trajectories selection, so as to minimize velocity increments (energy consumption) and transportation duration (crew safety). Which recommendations could be found out as far as trajectories optimization is concerned, that would fulfill energy consumption, transportation duration and safety criterion? What would technological hurdles be to rise for the building of such Space haven? What would be performances to aim at for critical sub-systems? Expected results of this study could point out research and development perspectives for human spaceflight missions and above all, in transportation field for long lasting missions.
Thus, the thesis project, presented here, aims starting from global system life-cycle decomposition, to identify by phase operational scenario and optimize resupply vehicle mission.

The main steps of this project consist of:
- Bibliographical survey, that covers all involved disciplines like mission analysis (Astrodynamics, Orbital mechanics, Orbitography, N-Body Problem, Rendezvous…), Applied Mathematics, Optimization, Systems Engineering….
- Entire system life-cycle analysis, so as to establish the entire set of scenarios for deployment and operations (nominal cases, degraded cases, contingencies…) and for all trajectories legs (Low Earth Orbit, Transfer, Rendezvous, re-entry…)
- Trade-off analysis for Space Station architecture
- Modeling of the mission legs trajectories
- Trajectories optimization

Three main scenarios have been selected from the results of the preliminary design of the Space Station, named THOR: the Space Station deployment, the resupply cargo missions and the crew transportation. The deep analysis of those three main steps pointed out the criticality of the rendezvous strategies in the vicinity of Lagrangian points. A special effort has been set on those approach maneuvers. The optimization of those rendezvous trajectories led to consolidate performances (in term of energy and duration) of the global transfer from the Earth to the Lagrangian point

neighborhood and return. Finally, recommendations have been deduced that support the Lagrangian points importance for next steps of Human Spaceflight exploration of the Solar system.

Résumé

Ce projet se place dans le contexte des futures missions habitées d'exploration du système solaire (avec un horizon de 2025), en respect de la feuille de route proposée par l'ISECG (International Space Exploration Coordination Group) [1]. Une nouvelle avancée serait de maintenir, à un des points de Lagrange du système Terre-Lune, en avant-poste, une station spatiale qui faciliterait l'accès vers les destinations telles que la Lune, Mars et les astéroïdes et permettrait de tester certaines technologies, notamment avant de les employer pour des missions plus lointaines. Un des principaux défis sera de maintenir en permanence et de garantir à bord la santé de l'équipage, à l'aide d'un centre médical (SMC) autonome arrimé à cette station. Se pose alors la problématique de la servitude d'une telle station, pendant la phase de déploiement (assemblage des différents modules constitutifs du centre médical) et la phase opérationnelle. Les enjeux résident, d'un point de vue global, dans la construction des scénarios opérationnels et, d'un point de vue local, la sélection de trajectoires, cherchant notamment à minimiser les incréments de vitesse (la dépense énergétique) et les temps de transport (sauvegarde des équipages). Quelles recommandations pourrait-on apporter en terme d'optimisation de trajectoire, satisfaisant des critères de dépense énergétique, durée de transport et sécurité ? Quels sont les verrous technologiques à lever pour permettre la réalisation d'une telle station spatiale? Quelles seraient les performances à viser pour les sous-systèmes critiques impliqués? Les résultats d'une telle étude permettraient d'ouvrir des perspectives de recherche et développement dans le domaine des vols habités, notamment dans le domaine du transport mais également dans l'optique d'une occupation de longue durée.

Le projet cherche donc à partir de la décomposition du cycle de vie du système complet, à identifier des scénarios opérationnels par phase et optimiser la mission du véhicule de ravitaillement.

Les principales étapes de ce projet consistent en :
- Etat de l'art qui couvre l'ensemble des disciplines abordées, allant de l'analyse mission (Astrodynamique, Mécanique spatiale, orbitographie, Problème à N-corps, Rendez-vous ...), aux Mathématiques appliquées et l'Ingénierie Système
- Analyse approfondie du cycle de vie du système complet afin d'élaborer l'ensemble des scénarios du déploiement jusqu'aux opérations (Cas nominaux, Cas dégradés, Cas de contingences, ...) et pour toutes les branches des trajectoires (Orbite basse, transfert, rendez-vous, rentrée ...)
- Architecture fonctionnelle et organique de la Station Spatiale
- Modélisation des branches de trajectoires
- Optimisation des trajectoires

Sur la base des résultats de la conception préliminaire de la Station Spatiale, nommée THOR, trois scénarios ont été sélectionnés : la construction de la station, les missions de ravitaillement par cargo et le transport des équipages. De l'étude approfondie de ces trois étapes principales, les stratégies de rendez-vous au voisinage des points de

Lagrange sont apparues essentielles et critiques. Un effort tout particulier a été mis sur l'indentification de ces manœuvres d'approche. Des analyses d'optimisation des trajectoires de rendez-vous ont été effectuées, qui ont permis de consolider des performances au niveau des trajectoires globales (depuis la Terre jusqu'au point de Lagrange et retour), réalistes en terme de d'énergie et de durée. Enfin, des recommandations ont pu être déduites, soutenant l'intérêt des points de Lagrange pour les prochaines étapes majeures de l'exploration du système solaire par des équipages.

Kurzfassung

Im Zusammenhang mit den künftigen bemannten Raumfahrt-Missionen zur Exploration des Sonnensystems (mit einem Horizont vom Jahr 2025) und entsprechend dem von der ISECG (International Space Exploration Coordination Group) [1] vorgeschlagenen Zeitplan, könnte ein neuer Schritt darin bestehen, eine Raumstation in einem der Librationspunkte des Erde-Mond-Systems als Vorposten zu einzurichten. Dies würde den Zugang zu weiten Zielen wie Mond, Mars und Asteroiden erleichtern und es ermöglichen, einige innovative Technologien zu testen, bevor sie für weit entfernte bemannte Missionen eingesetzt werden. Eine der wichtigsten Herausforderungen ist es, die Crew auf lange Dauer in der Station zu halten und ihre Gesundheit an Bord sicherzustellen, dank eines autonomen medizinischen Zentrums (SMC für Space Medical Center), das an die Raumstation angedockt ist und wie ein Hafen funktioniert. Dann wird das Hauptproblem zu lösen sein, wie die Betreibung des Zentrums während der Phase der Integration (Zusammenbau der verschiedenen Elemente) und der Betriebsphase zu bewältigen ist. Die Herausforderungen liegen, aus einer globalen Sicht, in der Aufstellung der Betriebsszenarien und, aus einer lokalen Sicht, in der Auswahl der Flugbahnen, um so Geschwindigkeitsinkremente (Energieverbrauch) und Transportdauer (Sicherheit der Crew) zu minimieren. Welche Empfehlungen könnte man machen für die Optimierung der Flugroute, um die Kriterien von Energieverbrauch, Transportdauer und Sicherheit möglichst zu erfüllen? Welche technologischen Hürden würden bei dem Bau einer solchen Raumstation zu überwinden sein? Welche Meisterwerke müssten für die notwendigen schwierigen Subsysteme vollbracht werden ? Die Ergebnisse solch einer Studie könnten Wegweiser sein für Forschung und Weiterentwicklung im Bereich der bemannten Raumfahrt-Missionen, insbesondere im Rahmen des Transportwesens für Langzeitflüge.

Somit hat die hier vorgestellte Dissertation das Ziel, anhand der Zerlegung des Lebenszyklus des globalen Systems, die verschiedenen Phasen der Betriebsszenarien zu identifizieren und somit die Missionen des Versorgungstransporters zu optimieren.

Die Hauptphasen des Projektes bestehen aus:

- Bibliographische Übersicht, die alle betroffenen Disziplinen abdeckt wie Missionsanalyse (Astrodynamik, Orbitalmechanik, Orbitography, N-Körper-Problem, Rendezvous...), angewandte Mathematik, Optimierung, Systems Engineering ....
- Analyse des Lebenszyklus des kompletten Systems, um so die gesamte Reihe von Szenarien für die Installation und den Betrieb (nominale Fälle, degradierte Fälle, Eventualfälle...) zu etablieren und dies für alle Zweige der Trajektorien (Low Earth Orbit, Transfer, Rendezvous, Wiedereintritt...)
- Architekturanalyse der Raumstation, funktions- und elementbezogen
- Modellierung der Trajektorienzweige
- Optimierung der Flugroute

Drei Hauptszenarien sind aus den Ergebnissen des vorläufigen Entwurfs der Raumstation, THOR genannt, ausgewählt: die Installation der Raumstation, die Missionen für die Versorgung durch Weltraumtransporter und der Transport der Besatzung. Die genaue Analyse dieser drei Hauptphasen macht die kritische Situation der Rendezvous-strategien in der Nähe der Librationspunkte deutlich. Eine besondere Aufmerksamkeit wurde deshalb dieser Annäherungsmanöver gewidmet. Die Optimierung dieser Rendezvous-trajektorien führte zur Verbesserung von Leistungen (in Bezug auf Energie und Dauer) auf dem Gesamtweg von der Erde bis zum Lagrange-Punkt und Rückflug. Schließlich konnten Empfehlungen gegeben werden, die die Bedeutung der Lagrange-Punkte bestätigen für die nächsten Schritte bei der Erforschung des Sonnensystems durch bemannte Raumflüge.

Schlüsselworte:
Rendezvous, Transfer, Trajektorien, N-Körper-Problem, Lagrange-Punkt, Halo Orbit, Optimierung

1   Introduction

"Space: the final frontier. These are the voyages of the starship Enterprise. Its five-year mission: to explore strange new worlds, to seek out new life and new civilizations, to boldly go where no man has gone before."

Star Trek

1.1   Motivations

Space exploration takes an active part in the Humanity evolution, as an answer to the human desire for discovery and conquest. In the coming decades, setting up human missions for new space exploration of the solar system will be an ambitious challenge for the entire humanity. Human and robotic exploration of the Moon, Near Earth Objects (NEOs), and Mars will strengthen and enrich humanity's future, bringing nations together for a common cause, revealing new knowledge, inspiring people, and stimulating technical and commercial innovation. These are the substantial benefits delivered to society.

Placing humans in space for a long duration mission beyond Earth's neighborhood implies the design of a highly complex system to travel, live and work safely in the hostile deep space environment. Thanks to lessons learned acquired since Apollo missions, first robotics missions towards Mars or asteroids, and exploitation of the International Space Station (ISS), a next step might be to set up a permanent outpost in the Earth-Moon system. This gateway could also serve for test bed for missions to Near Earth Objects (NEOs), lunar surface and Mars.

Main space agencies (like NASA, ESA, JAXA, Roscosmos…) participating in ISECG (International Space Exploration Coordination Group) have defined a long-range human exploration strategy, beginning with the utilization of ISS and expands human presence throughout the Solar System and leading to human missions to explore the surface of Mars. The *Global Exploration Strategy* [1] also identified the common goals, among all the nations, for space exploration:
- Search for life,
- Extend human presence,
- Develop exploration technologies and capabilities,
- Perform science to support human exploration,
- Stimulate economic expansion,
- Perform Space, Earth and applied sciences,
- Engage the public in exploration,
- Enhance the Earth's safety.

Human exploration preparatory activities are necessary to achieve the ultimate goal: the Mars human mission. In both scenarios presented in ISECG roadmap, the Lagrangian points of the Earth-Moon system appear to be a very promising waypoint on route to Mars. Actually, due to the particular dynamic of the solar system, the Earth-Moon Lagrangian points are directly connected to the targeted final destination (like Moon, Asteroids and Mars). As a consequence, the main goal of this project is to analyze the feasibility of a Space Station in the vicinity of the Earth-Moon Lagrangian points. It will mainly deal with methodologies to design the station and mission analysis to deploy and maintain the station. In all envisaged scenarios, the Rendezvous strategy appears to be a critical hurdle.

Although the dynamics of the Lagrangian Points is now a classical topic for Astrodynamics, rendezvous in their vicinity has not yet been deeply studied, in particular in the human space exploration context.

1.2 Objectives

The project presented results from the design of such an exploration gateway as an endeavor to better understand what technical challenges would have to be faced and better formalize and model so as to identify potential solution for an optimal architecture.

In this context, main challenges aim at:
- Taking into account go and return. Crew has to come back on Earth.
- Reducing not only the mission costs but also the flight duration.
- Ensuring rendezvous
- Interlacing Design and Mission analysis goals.

As a consequence, in this report, a wide range of topics will be exhibited, among them Systems Engineering, Systems Dynamics, N-Body Problem and Optimization.

1.3 Thesis context

This thesis project results from a fruitful collaboration between ISAE (Institut Supérieur de l'Aéronautique et de l'Espace) and IRS (Stuttgart University Space System Institute). Thank to this project, we welcomed one Master student from Stuttgart University during his Master Thesis internship. Also I was personally hosted by IRS and had the opportunity to meet Professors and PhD students from the University. During the last period, I was welcomed by TEC-ECN (Guidance, Navigation and Control Section) at ESTEC (ESA, European Space Agency, Technical Center) in Noordwijk (the Nederlands) during six months.

This thesis conducted to nine conference publications that are listed here below:
1. **Lizy-Destrez S., Blank C.,** *Mission analysis for a space medical center of an exploration gateway at lunar libration point*, IAC-11.A5.4.8 - IAC 2011 - 3-7 October 2011 Cape Town - South Africa
2. **Stéphanie Lizy-Destrez, Giuseppe Ferraioli, Chloé Audas, Jason Piat**,

How to save delta-V and time for a round trip to EML2 Lagrangian point? IAC-12.A5.4.12, x13323 - IAC 2012 - 1-5 October 2012 Naples – Italy

3. **Crescenzio Amendola, Stéphanie Lizy-Destrez**, *Panorama of ideas on structure and materials for the design of a multi-modular Space Station at EML2*, IAC-2013, D3.1, 6x17742 – 23-27 Septembre 2013 Beijing - China

4. **Giuseppe Ferraioli, Dr. Mickael Causse, Mrs. Stéphanie Lizy-Destrez, Prof. Yves Gourinat,** *Habitability of manned vehicles: the impact of human factors on future long duration human space exploration missions en route to Mars***,** IAC-13, A1.1.1, 23-27 Septembre 2013 Beijing - China

5. **Pierre Kokou, Bastien Le Bihan, Jean-Baptiste Receveur, Stéphanie Lizy-Destrez,** *Computing an optimized trajectory between Earth and an EML2 Halo orbit***,** SciTech 2014, 13-17 National Harbor, Maryland, USA

6. **Stéphanie Lizy-Destrez, Bastien Le Bihan, Mohammad Iranmanesh,** *Transfer and rendezvous strategies for the deployment and the servicing of an inhabited space station at Earth-Moon L2***,** IAC-14, C1.8.10, 29 September – 03 October 2014, Toronto, Canada

7. **Stéphanie Lizy-Destrez, Chloé Audas,** *Scenarios optimization for a servicing inhabited space station at Earth-Moon Lagrangian point (EML2)*, IAC-14, C1.8.10, 29 September – 03 October 2014, Toronto, Canada

8. **Crescenzio Amendola, Stéphanie Lizy-Destrez, Regine Leconte,** *The THOR space station at EML2: Analysis and preliminary design of an innovative adaptable docking system,* IAC-14, C2.1.21593, 29 September – 03 October 2014, Toronto, Canada

9. **Stéphanie Lizy-Destrez.,** *Rendezvous optimization with an inhabited space station at EML2*, 25th International Symposium on Space Flight Dynamics ISSFD - October 19 – 23, 2015, Munich, Germany

1.4 Report organization

The manuscript falls into five main parts:

- The first part (chapter 1) introduces the motivations and the context of this project,
- The second part (chapter 2) describes the historical overview of Human spaceflight and solar system exploration dynamics,
- The third part (chapter 0) provides the methodology applied to design the Space Station,
- The fourth part (chapter 4) gives the mathematical theoretical background for the trajectories optimization (space dynamics system, Three-body problem, genetic algorithms),
- The fifth and last part (chapter 5) performs the mission analysis for deployment and the resupply of the THOR space station in orbit around EML2.
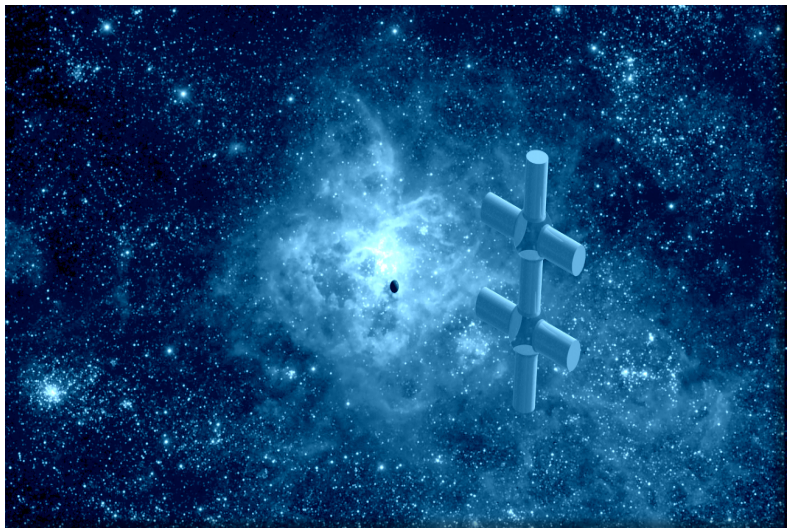
Figure 1: Artistic view of the Space Station

2 Space exploration context

2.1 Three-body problem history

Since some years, there is a growing interest of the space scientific community for trajectories towards, around and from Lagrangian points (also called Libration points); this topic is directly related to the n-body problem (see 4.2). The three-body problem, as a particular case, is one of the most studied models not only in celestial mechanics, but also in mathematics. After a prehistoric period with C. Ptolemée and N. Copernicus, its history started with the first steps of celestial orbital mechanics, with J. Kepler's laws [2] and G. Galileo's [3] theories, thanks to combination of experiments and mathematics. Moreover, I. Newton [4] set the fundamental basis of the three-body problem so as to predict the Moon motion, while unifying Kepler's and Galileo's works.
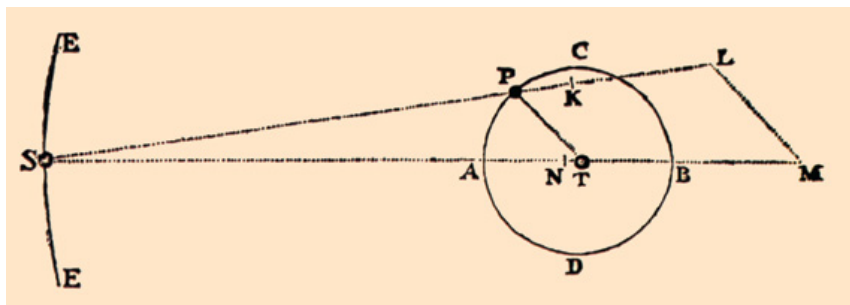
Figure 2: Earth, Moon and Sun motion by I. Newton [4]

Figure 2 presents the motion of Earth (T), Moon (P) and Sun (S), subjected to their gravitational forces, as depicted by I. Newton in Principia [4].

Many famous astronomers and mathematicians, like L. Euler, A. Clairaut, J. D'Alembert, J-L. Lagrange [5], P. Laplace, S. Poisson, C. Jacobi, U. Le Verrier, F. Tisserand … succeeded him, so as to prove formally the solar system stability. Particularly, Laplace thought to demonstrate it thanks to the perturbation theory. Unfortunately, first order development (Keplerian ellipse) is no more correct when at least three-body are involved and was not enough to conclude definitively.

The N-body problem has to be taken into account so as to find those non-Keplerian complex trajectories. H. Poincaré, in the late 1800s, developed the modern dynamical systems theory [6] and [7]. Even his work is essential to the modern period of celestial mechanics and astrodynamics; there has been a large gap, about seventy years, without any real advanced research on the topic. Just one year after H. Poincaré's death, H. Birkhoff brought to an end Poincaré's work with the proof of the Poincaré-Birkhoff fixed-point theorem.

During the XX° century, the n-body problem was taken to a new step thanks to the works of A. Kolomogorov, V. Arnold and J. Moser with the KAM theorem and recently thanks to the "Chaos theory".

Figure 3 provides a chronology of the main astronomers and mathematicians studying actively and participating in the n-body problem description. Nevertheless, as a schema, it is not exhaustive. Its main goal is to present the temporal sequence of their influence.
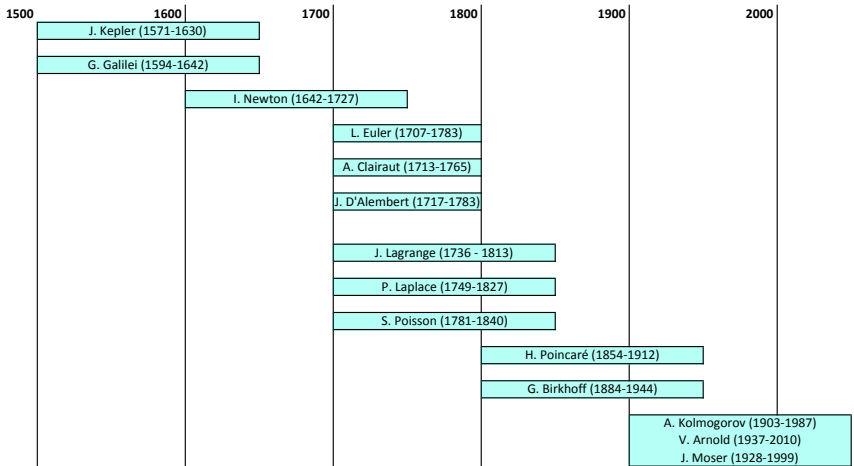
Figure 3: Chronology of N-body problem mathematicians and astronomers

Even if brilliant scientists tried hardest to solve the n-body problem, all along the history, only some exotic configurations lead to exact solutions. As a consequence, only two approaches are possible:
- The perturbation theory with approximation by using decomposition in series
- The numerical methods taking into account all gravitational interactions.

Moreover, the n-body problem also exists in the frame of the general relativity, which is even more complicated than in the Newtonian frame.

The history presented in this paragraph mostly deals with celestial mechanics, that is to say, the natural motion of the celestial bodies. Next paragraph is then focusing on exploration missions that take benefit of this natural dynamics.

2.2 History of space missions towards the Lagrangian point
For first solar system exploration missions (like Voyager), patched conic model was satisfactory to compute the trajectory. But, space missions became more demanding (as far as fuel consumption is considered), so other strategies had to be applied.

Moreover, some science space missions take advantage of particular properties of the Lagrangian points. Among them, the SOHO satellite orbits around the Solar Lagrangian point SEL1 for Sun observation, and the James Webb Space Telescope is scheduled for 2018, replacing the Hubble telescope, orbiting around the Solar Lagrangian point SEL2 for astrophysics observation. Many theoretical studies have demonstrated the benefits of the application of the three (and further) bodies problem to space exploration missions like communication satellites [8], navigation satellites, scientific satellites or human spaceflight ([9], [10]). This paragraph provides first a brief overview of existing studies of the space exploration background in the Sun-Earth system or in the Earth-Moon system, then some examples of probes mission towards the Lagrangian points.

First synthesis (see Table 1) presents an overview of space missions implementing low energy transfer in the Sun-Earth system or in the Earth-Moon system. The second ones (Table 2) focus on future missions towards Lagrangian Points. Those tables have been established thanks to Parker's work (see [11]).

System	Mission	Space Agency	Launch year	Location
Sun-Earth	ISEE-3	ESA - NASA	1978	Halo orbit about SEL1
	Wind	NASA	1994	Halo orbit about SEL1
	SOHO	ESA - NASA	1995	Quasi-Halo orbit about SEL1
	ACE	NASA	1997	Lissajous orbit about SEL1
	WMAP	NASA	2001	Small amplitude Lissajous orbit about SEL2
	Genesis	NASA	2001	Halo orbit about SEL1, then SEL2 and return to Earth
	Herschel	ESA	2009	Lissajous orbit about SEL2
	Planck	ESA- NASA	2009	Lissajous orbit about SEL2
	GAIA	ESA	2013	Lissajous orbit about SEL2
Earth-Moon	HITEN (MUSES-A)	JAXA	1990	Low energy transfer to the Moon
	SMART-1	ESA	2003	Low energy transfer to the Moon
	THEMIS	NASA	2007	Insertion about EML2, then one satellite transferred to EML1, then both inserted around the Moon
	GRAIL	NASA	2011	Moon insertion with low-energy transfer

Table 1: Historical overview of space missions implementing low energy transfer

System	Mission	Space Agency	Launch year	Location
Sun-Earth	Lisa Pathfinder	ESA	Expected 2015	Halo orbit about SEL1
	JWST	NASA-ESA-CSA	Expected 2018	SEL2

Table 2: Example of expected space missions implementing low energy transfer

Those tables show that most of the missions are travelling in the Sun-Earth system. There seems to be a lack of interest for the Lagrangian points of the Earth-Moon system. Moreover, most of the missions in the Earth-Moon systems aimed at a Moon insertion.

The Appendix 2 presents a chronological synthesis of those types of missions, in parallel to Human spaceflight chronology. The main objective of this synthesis is to demonstrate the lack of studies and projects about human spaceflight missions towards Lagrangian points and support by consequence the main contribution of the thesis.

2.3 Space exploration missions history

The paragraph does not intend to present the global chronology of human spaceflights: it neither focuses on the early first stages, nor lists all the flights. It presents a synthesis of the large and detailed history of space stations provided in [12].
It gives the major historical achievements so as to highlight the evolution. Human space exploration history mainly falls into three main steps:
- Early concepts of space stations (from 1865 to 1957)
- National programs (from 1957 to 1998)
- International cooperation (from 1998 to nowadays)

This paragraph will also deal with a synthetic of overview of next perspectives in the context of Human spaceflight and solar system exploration.

2.3.1 Early concepts of space stations

Space as a final frontier has always fascinated Humanity. Despite some unknown confidential attempts, some forward-thinking authors like E. Hale (1822-1909), J. Verne (1828-1905) or K. Lasswitz (1848-1910) proposed first concepts of inhabited space vehicles. In two of his books [13] and [14], Jules Verne, the most famous of those three storytellers, imagined many life support systems that could have inspired space programs, not only like concentrated food or oxygen resupply, but also for example observation windows.
Afterwards, arrived the pioneers' area with the Russian K. Tsiolkovsky (1857-1935), the American R. Goddard (1882-1945), the German H. Oberth (1894-1989), the Slovenian H. Noordung (1892-1929), the British H.E. Ross and Smith and the German then American W. Von Braun (1912-1977). That moment was also the time of

development of launch system and transportation vehicles since space stations operations cannot take place without them.

K. Tsiolkovsky [15] not only proposed the famous rocket equation (see (5-12)) and the usage of rocket for human beings, but also in 1933 described a concept of a space habitat (see Figure 4, He identified not only the necessity for the space station to rotate around its longitudinal axis as to maintain on board some simulated gravity, but also promote the idea to embed trees and others plants for life support.
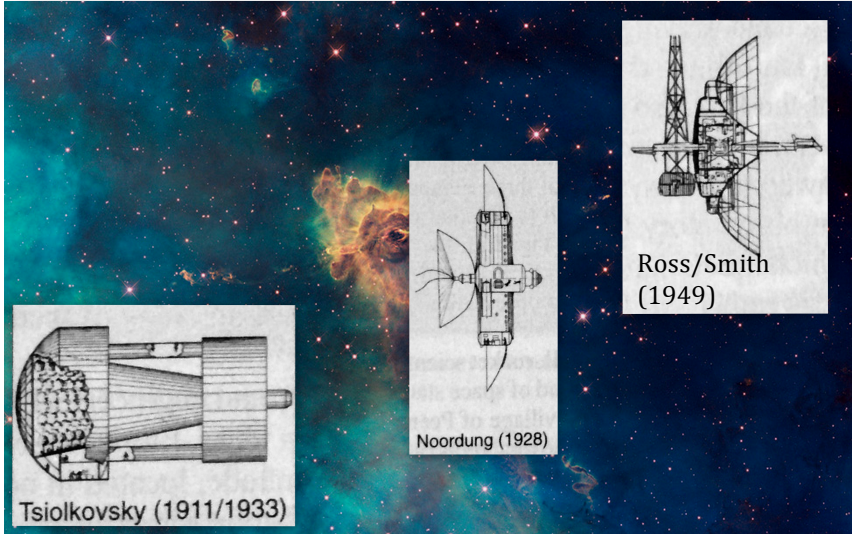
Figure 4: Some examples of early concepts of Space stations

H. Oberth (see [16]) was interested to maintain a space station in Low Earth Orbit for many purposes, Astronomy, Earth observation, military support, meteorological application, and refuelling for interplanetary flights. Then, H. Noordung (see [17]) suggested a geostationary space station (see Figure 4), with Earth observation application and support to human activities.

Interest for space stations decreased for some times because of World War II. Anyways, H.E. Ross [18] and Smith worked on the design on another space station (see Figure 4), with an interdisciplinary crew. They also concluded that it would be impossible to launch such a huge and complex system with only one rocket and suggested to assemble it in orbit.

But the most well known was prepared by W. Von Braun (see [19]) with a wheel-shape structure, orbiting on a polar orbit. He considered it as a milestone on the roadmap towards Mars exploration.
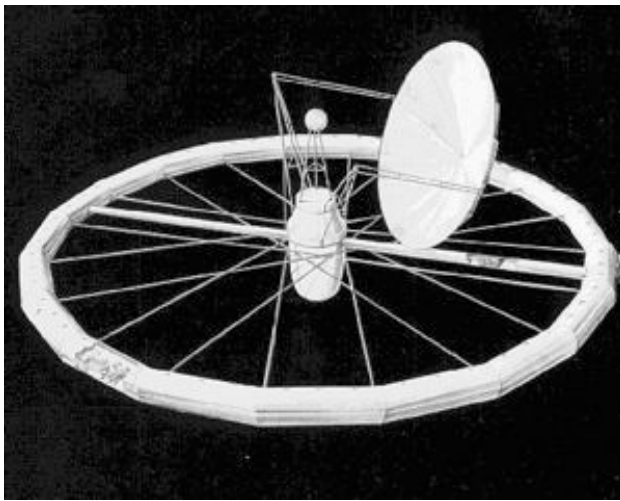
Figure 5: The concept of the wheel-shape space design as sketched

W. Von Braun in 1946

2.3.2 National programs

The success of Sputnik in 1957 gave a new boost to the inhabited space conquest. In the context of the cold war, the two main blocks (Russians and Americans) funded and developed enthusiastically fundamental building blocks for Human Spaceflight systems.

Table 3 provides an historical overview from the very beginning in 1958 to nowadays. The efforts of the two main nations can be seen in parallel, but also the emergence of Europe and China. A more detailed chronology of the main steps are human spaceflight history is provided in Appendix 2.

On the American side, NASA (founded in 1958), started to manage in parallel missions to the Moon and the development of an inhabited space station. Every concept assumed the availability of a large launch system, as Saturn V. The decision was undertaken in 1961 to go to the Moon in the same decade. As all the efforts were concentrated towards this fantastic final goal, the dream came true in 1969. Nevertheless, some remaining concepts of space stations were studied and came out to the Skylab project. The Skylab station was not designed as a permanent crew outpost, but it proved the ability of human being to work in space. The main lessons learned from investment of the American nation in Human Spaceflight history are: the importance of the transportation system and its modularity, but also the capability to build a space station, step by step while assembly it in orbit. Figure 6 presents some mandatory building blocks of American space stations history, with Saturn V, Skylab as first American space station and of course, the Space Shuttle. This chapter does not enlighten the Apollo missions, whereas it was an exceptional program that carried out many of useful concepts for the next steps of human exploration of the solar system, like reentry capsule, landing modules and rovers.
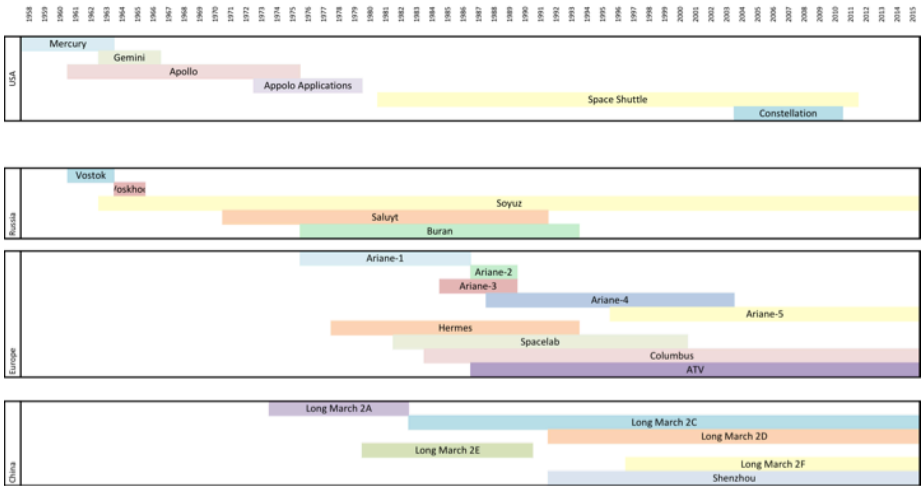
Table 3: Historical overview of Human Spaceflight program per nation

A Saturn V launch - @ NASA

Columbia space shuttle - @NASA

Skylab - @NASA
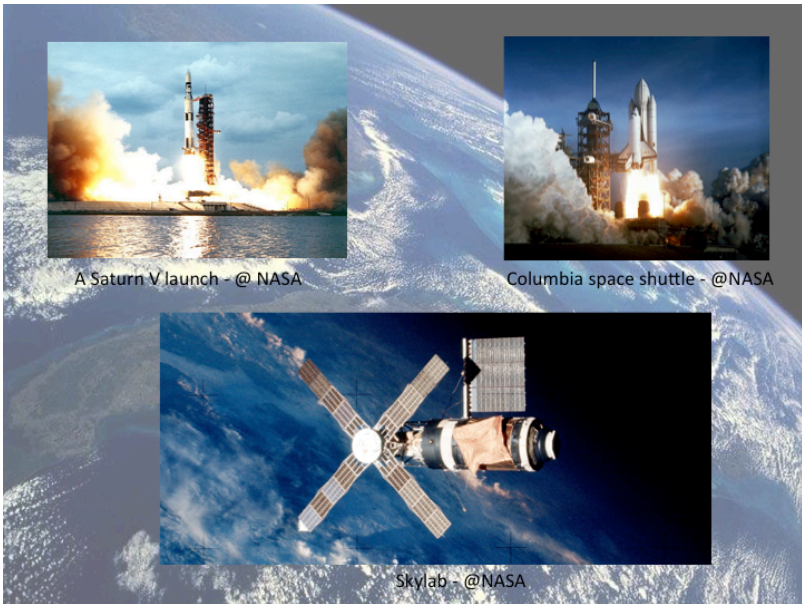
Figure 6: American building blocks for space stations

On the other side, Russians embarked, very soon, with a lot of efforts and successes on the development of human spaceflight endeavor and particular, of space stations. Main successes of Russian space conquest are:

- First artificial satellite with Sputnik 1, launched on the 4th of October 1957;
- First animal with the dog, Laika, launched on the 3rd of November 1957;
- First lunar probe with Luna 1, launched on the 4th of January 1959;
- First man with Yuri Gagarin, on board Vostok 1 on the 12th of April 1961;
- First woman with Valentina Terechkova, on the 16th of June 1963.

Then, from 1971, they operated space stations in LEO with the Salyut program. During this period of 24 years, they ensured 30 years of human being's presence in space. They also succeeded to combine military and civilian objectives. They tested in orbit rendezvous techniques for space station assembly with critical activities, like docking and undocking, boost maneuvers, etc.… and reentry capsule. Figure 7 provides sketches of Salyut-2, Sayut-3 and Mir space stations.
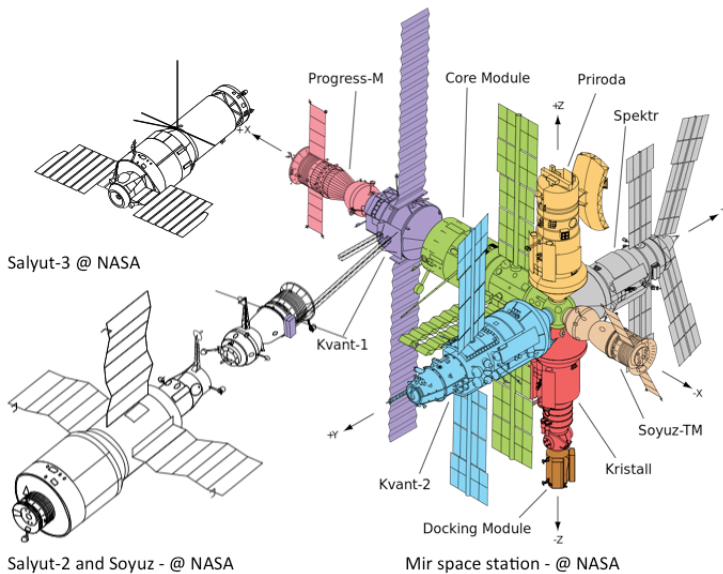
Figure 7: Example of Russian space stations

Meanwhile, Europe followed slowly, first with the launch vehicle development (Ariane family) and first satellites. In the early 1970's, Europe decided to take part to the Human spaceflight adventure by designing and operating Spacelab. It was a space laboratory, launched by the Space Shuttle, to conduct experiments in space. In the mid-1970's, Europe also invested in the design of a spaceplane, named Hermes. But

31

unfortunately, the Hermes program was cancelled, in 1992. Some lessons learned were then reused in ATV (Automated Transfer Vehicle) development.

During the same period, China, like the other space powers, developed first missiles to prepare launch systems production, while collaborating with the soviet republic. So was born the Long March family, with a first satellite in orbit in 1970. In this context, China also decided to take part in the human spaceflight adventure, but the program was aborted due to political upheavals. Nevertheless, they initiated their own reentry capsule and lander concepts.

2.3.3 International cooperation

It can be noticed after the two major steps: first man in space and first man on the Moon, the USA concentrated their efforts on the development of the crew vehicle, while the Russians developed stations. Nevertheless, in 1984, R. Reagan, president of the United States of America, invited his international partners to join and develop a space station together. Canada, Japan and Europe answered positively. The station, named in 1988 SSF (for Space Station Freedom) had to face financial constraints (because of the great number of shuttle resupply flights and crew Extra-Vehicular Activities for station assembly) and technical difficulties (particularly, after the Challenger accident in 1986). At that time, as it was the end of the Soviet Union, Russia could not afford by its own the financial efforts to support space station operations. Thus in 1993, as cold war was over, B. Clinton, president of the USA, proposed to Russia to cooperate to design a new space station, based on SSF and MIR-2 concept. This was the beginning of the ISS (International Space Station) adventure. Figure 8
presents the configuration of the ISS as it was in May 2011.

ISS Configuration
As of May 2011 (ULF6 - STS-134)
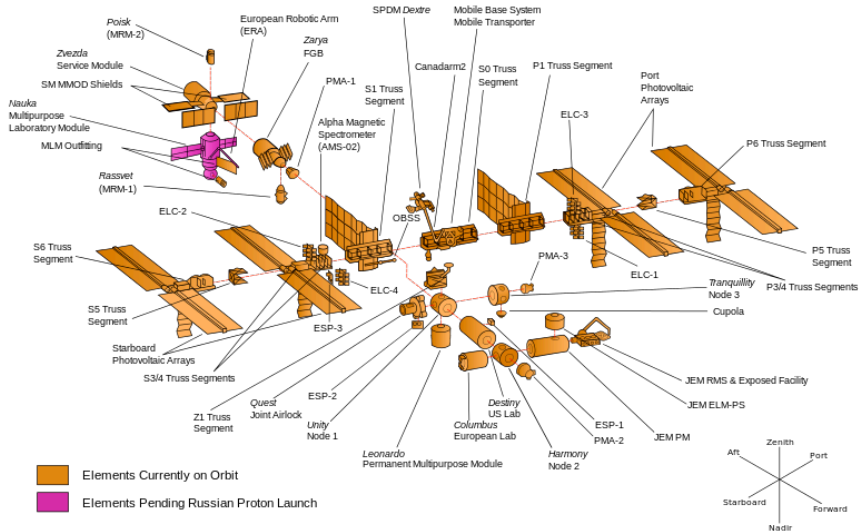
Figure 8: ISS configuration in May 2011 - Credits: NASA

The ISS collaboration falls into four main parts:
- Phase 1: Contributions to the further expansion and utilization of MIR (1994-1998)
- Phase 2: Assembly of ISS (1998-2000)
- Phase 3: Operations of ISS (2000-2015)
- Phase 4: Further expansion of ISS (from 2015 – 2020 or 2025)

During the first phase of international cooperation, the space shuttle was transporting mixed crew from US and Russia. The space shuttle was extended thanks to the American Spacehab (reduced concept compared to the European Spacelab) to carry freight and payloads to MIR. Then the collaboration entered in the second phase to assemble together the ISS, sharing missions and operations.

2.3.4   Actual situation
The international cooperation concretely started in 2008, with the third phase with the Japanese Experiment Module (Kibo), the Canadian robotic arm (SPDM – Special Purpose Dexterous) and the docking of Columbus, the European science laboratory. Japan and Europe also contribute to ISS maintenance with their resupply cargos: the European Automated Transfer Vehicle (ATV) and the Japanese H-II Transfer Vehicle (HTV). The Space shuttle mission ended in 2011. Even if new American unmanned cargos are tested (Cygnus and Dragon), the crewmember depend nowadays exclusively on Soyuz to reach the ISS. Figure 9 presents a comparative overview of the several freight cargos for the ISS.

Figure 9: Actual resupply cargos of the ISS

While the utilization of the ISS has already been extended several times, the end of mission of the space station is not strongly confirmed, and seems to be still under discussion. ISS reentry might occur between 2020 and 2025.

Meanwhile, China started Human spaceflight activities with a new program that planned the development of a space station. The first taikonaut flew in 2003, then the first Chinese EVA took place in 2008 and the first Chinese space station was launched in 2011. China became then the third space power with the ability to launch human being into space. Next step for the ambitious Chinese space program should be to land a taikonaut on the Moon.

2.3.5   Existing studies on human mission towards Lagrangian Points

Looking at the set of studies performed in the field of Lunar Libration Points one stumbles upon the fathers and main advocates of utilization concepts for these points repeatedly. R. Farquhar published the first papers on the utilization of co-linear EMLs in the late sixties and early seventies, including the application for communication relay satellites [8] and inhabited space stations in a Halo orbit around EML2 [9]. In the following decades, he contributed to many more aspects of Libration Point (LP) utilization in general - e.g. his 2004 paper is summarizing findings on the utility of LPs for human solar system exploration [10].

K. Howell summarized a wide range of knowledge concerning the mathematical representation of Libration Point orbits [20] and methods to determine transfers from, to and among them [21]. Recently, F. Renk analyzed direct, indirect and Weak Stability Boundary (WSB) trajectories in the Sun-Earth-Moon system in his

dissertation [22] and paper [23]. Mingtao and Jianhua [24] published similar findings for direct flyby trajectories.

One of the most useful publications giving an overview of the physical and mathematical background, past missions, numerical concepts, trajectory applications and future trends are ESA's Ariadna final reports [25, 26]. The first one also features an accessible description of new trends in the assessment of mission design based on Dynamical Systems Theory as well as a very well structured bibliography. The same is true for the book of Lo, Ross, Marsden and Koon [27].

In the field of exploration strategies and space policy W. Mendell promoted the concept of "Greater Earth" [28] and the use of the WSB as a gateway for future space exploration. He pointed out the technical, strategic and political advantages of an EML infrastructure compared to LEO [29] in the early nineties before the construction of the ISS began. According to him, an EML station also has the potential to "unite Moon and Mars believers".

The concept utilizing EMLs as a gateway to the Interplanetary Superhighway is strongly advocated by Martin Lo [30,31]. NASA's Decadal Planning Team (DPT) and later the NASA Exploration Team (NEXT) did a study on a "Lunar L1 Gateway Station" at the Johnson Spaceflight Center [32]. It went into quite some details on subsystems, but did not address location issues in detail. The concept however was re-discussed during the deliberations of the Augustine committee [33] in 2009 and is even seen as an "affordable near term stepping stone" for human space exploration within the next decade by some enthusiasts [34].

After the new orientation of NASA's exploration strategy, the option of human missions to EML2 is not only discussed in professional forums like [35] but also in industry whitepapers for future missions of the Orion Crew Exploration Vehicle [36]. The Orion concept is described in the next paragraph (see 2.3.6). Moreover, a grouped initiative of main space agencies discussed and refreshed constantly a Solar System exploration roadmap for Human Spaceflight. This committee is named ISECG (for International Space Exploration Coordination Group). The description of main objectives of this roadmap is given in the following paragraph.

2.3.6 Next steps

As discussed previously, since the Apollo program, mankind has not ventured further into space than the close vicinity of Earth, trying to increase the mastering of Low-Earth Orbits and succeeding to several space stations such as Salyut, Skylab, Mir and the International Space Station (ISS). Today, even private spaceships can access LEO and the ISS.

Space exploration and the presence of humans in space is now at a turning point of its history. Nowadays, space agencies build partnerships and lead common studies, such as the International Space Exploration Coordination Group (ISECG), to determine what the future of space exploration will be. They all agree to say that the main objective of upcoming decades will be to send humans to Mars. But considering the current resources, level of technology and political will, we are not capable of doing it yet. A step-by-step development program of spatial activities is needed.

Referring to [1], several scenarios, such as those reported in the Global Exploration Roadmap of ISECG, are proposed and summed up on Figure 10. Some suggest to go back to the Moon first, others to visit asteroids. But in either case, the deployment of a deep-space habitat in the vicinity of an Earth-Moon Lagrangian (EML) point, whose nature will be explained hereunder, has been pointed out as a key-point milestone to further development of future space technologies.
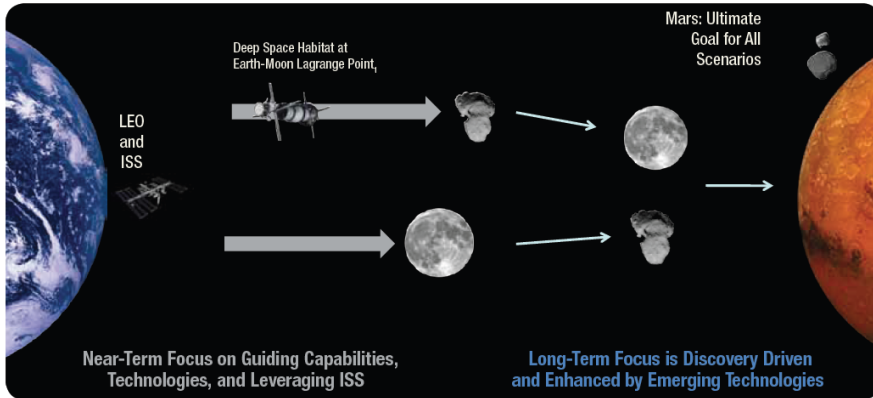
Figure 10: The Global Exploration Roadmap - Credits : ISECG

In this context, NASA with the collaboration of ESA, is designing the Orion Multi-Purpose Crew Vehicle (MPCV). This spacecraft mission will be to carry four crewmembers beyond LEO and towards the Moon, in particular for deep space transportation preparation, lunar robotic surface exploration interaction, asteroid missions, etc. Next figure presents an artistic view of Orion spacecraft in configuration with the ATV service module.

Figure 11: Orion artistic view - Credits: NASA

Moreover there are several, but few, initiatives to promote the development of a inhabited space station in the vicinity of the Earth-Moon Lagrangian points, like the FISO working group results (see Figure 12), the Russian NEM-1 concept (as an

36

extension of the ISS modules or for exploration missions) or some industrial proposals (like Lockheed Martin).
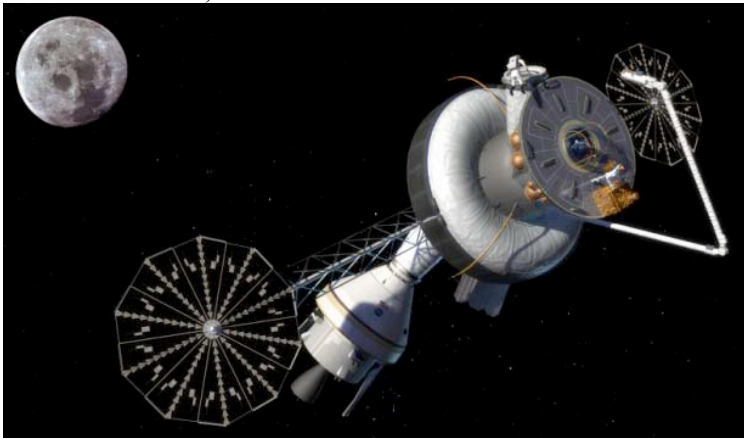
Figure 12: Concept of an EML gateway station proposed by the FISO working group

Even the general public has now the opportunity to design its own space station and locate in the Lagrangian point neighborhood thanks to videogames, like it was done with Kerbal Space Program (see Figure 13).
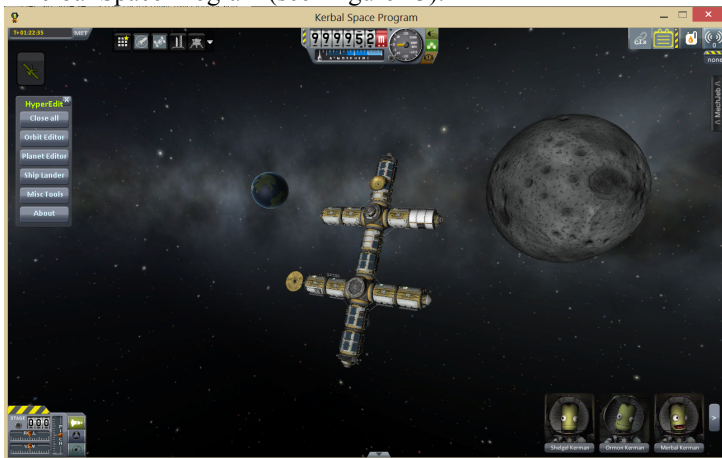
Figure 13: Concept of THOR space station in EML2 with Kerbal Space Program

3 Space station Design

According to [1], a space station located on a Halo orbit around EML2 has many advantages. First, it can serve as a gateway to other promising destinations (Moon, asteroids, Mars...) in the solar system, being linked to them by low-cost trajectories. Moreover, the set up on an appropriate EML2 Halo orbit, the deep-space habitat can maintain continuous line-of-sight communications between Earth and the far side of the Moon. The far side, which would be easily available for the first time in human space flights history, has been suggested as an advantageous location for a radio observatory, as it would be protected from radio interference with Earth. The absence of spatial debris and of the terrestrial inhomogeneous gravitational field makes a cheaper station-keeping strategy possible.

Classical approaches to spacecraft trajectory design have been quite successful in the past years with Hohmann transfers for the Apollo program but these missions were very costly in terms of propellant. The fuel requirements of these transfers would make the deployment of a massive space station in deep space unfeasible. However, a new class of low-energy trajectories have been discovered and extensively investigated in recent years. These trajectories take advantage of the natural complex dynamics arising from the presence of a third body (or more bodies) to reduce transfer costs.

On the one hand, the main contribution of this project is to identify, among these methods, optimized transfers for station deployment or cargo missions and human spaceflights, linking a Low Earth Orbit departure to the Halo orbit of the station. The selection of strategies will be based on two main criteria: the total fuel consumption required to perform the transfer and the time of flight. This trajectory optimization process is the main goal of chapter 5. Then, it also deals with the influence on some key design parameters (like the Halo orbit parameters, the position of the insertion point in the manifold....) on the total fuel consumption and on the time of flight. The actual ones focuses on the design of the proposed Space Station, named (Trans-lunar Human explORation) and most particularly on the methodology, before proposing a physical architecture as a baseline for mission analysis. An artistic view of the THOR Space Station was provided on Figure 13. A detailed presentation of its architecture is given in paragraph 3.5.

Actually, one significant challenge in implementing such a gateway is to maintain the astronauts' health by providing medical support reaching from advanced radiation monitoring to quarantine and surgery in this remote environment.

The Moon could be the first place where humans learn to live on another celestial body. This intermediate step to long-range missions is strongly recommended, firstly for financial aspects reasons and then to prove technical issues. Just three days from Earth, the Moon's natural resources and low gravity make it an ideal location to prepare people and machines for venture further into space. As a remnant of four billion years of Solar System history and as a place to observe the Earth and the Universe, it has great scientific potential. Exploration of the Moon will also reveal whether the resources available in space will allow humans to live off the land.

Given the future human space destinations en route to Mars, i.e. deep space-habitats at Earth-Moon Lagrange points, lunar bases and asteroids, the main psychosocial and psychological issues are concerning the adverse effects of prolonged co-living and co-working in small groups, under conditions of confinement and isolation. In planning any human long duration mission beyond Low Earth Orbit (LEO) with unprecedented crew autonomy level, basic human needs cannot be underestimated. Hence the integration of habitability issues in the very early stages of the mission design is essential to its outcome. This will result in a good prediction of the crew adaptation to deep space extreme conditions as well as the teamwork and social interactions. The main challenges for a sustainable and long lasting human presence in the deep space concern the coupling of engineering and human factors subsystems. In this frame, the current manuscript lies on the frontier of the so called Earth, machine and human components.

Given the complexity of the space station to be designed and of the mission analysis, a Systems Engineering approach is applied. A simplification of the approach described in INCOSE Handbook [37] and NASA SE handbook [38], falls into five main steps:
- Stakeholders needs analysis
- Requirement engineering
- Functional design
- Organic architecture
- Verification, optimization and validation
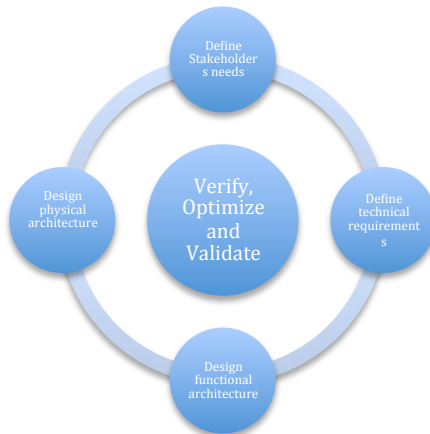
Figure 14: Simplified approach for Systems Engineering

As presented in Figure 14, these steps are not sequential: they are almost parallelized. Moreover, the approach is iterative: it has to be applied several times (between three or five times) to converge towards an organic architecture that complies with the needs expression.

3.1 Space station Stakeholders needs analysis

3.1.1 Space Station Stakeholders

At this step, the first challenge is to identify a representative set of stakeholders and elicit their requirements. A high-level synthesis of their list is represented in Figure 15. They are grouped in three categories: systems in the operational environment (orange boxes), enabling systems (green boxes) and society systems (blue boxes). This list is provided as an illustration, it is not exhaustive.
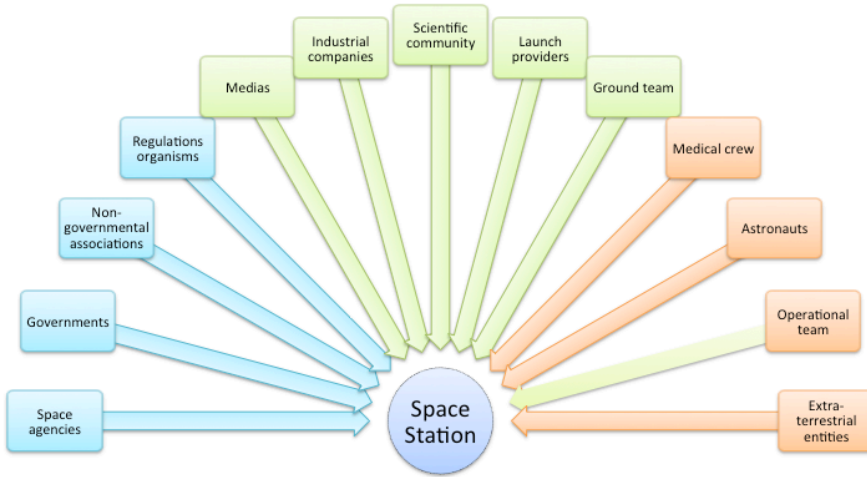
Figure 15: Space Station Stakeholders

In the **operational environment** of the Space Station, one can find the operational crew (that is to say people living « permanently » in the Space Station), the astronauts (team engaged in exploration, coming and going to the lunar surface, Mars or other distant destinations, space tourists….), the medical crew (team can be composed by doctors, nurses, experts in radiology, dental care, surgeons, chemists, biologists….) or why not, any extraterrestrial entity (in this case, crew has to know what to do facing new types of life).

Some enabling or **interoperating systems**, imposing constraints to the Space Station design by their interactions, have been identified, like ground teams (including project management, control center operators, maintenance teams, training teams, team in charge of exploration missions…), industrial companies (responsible for production, integration, companies delivering services like global positioning, telecommunications network, … or competitors), launch providers (for transportation from Earth to Low-Earth Orbit) and the scientific community composed by all scientists interested in data

processing (like biologists, psychologists, doctors, chemists, physicians, …). The media can also be considered as an interoperating system, since they may require some interfaces (voice, pictures…) with the space gateway.

The last group of stakeholders corresponds to the **social systems** like governments (nations already involved in human spaceflights or new comers), non-governmental associations (like environmentalists, banks, financial sponsors, terrorists, hackers…), space agencies, implied in largest exploration programs and regulation organisms (ensuring the respect of laws, human rights, norms, standards…).

3.1.2   Space Station Stakeholders' needs collection

Space Station Stakeholders needs have been collected thanks to several means:
- Bibliographical survey (see 2.3)
- Experts interviews (with doctors expert in Space medicine, astronauts…)
- Analogue participants questionnaires

It results that any design should take into account:
- A continuous communication between the crew and the ground segment teams,
- The impact of space radiations on the crew, and on on-board systems,
- A mandatory crew rescue in case of contingencies
- Countermeasures in case of lack of resupply

A specific survey has been conducted to investigate the behavioral effects of the prolonged co-living and co-working in analogue natural environments and ground-based test beds and determine criteria for habitability. The focus has been set on the psychological issues. Three main categories ([39] and [40]) of stressors yielded by future space stations and classified, are: latent stressors linked to emotional and interpersonal issues (for example routine, extended confinement, emotional isolation, cultural differences, gender differences…), latent stressors linked to extreme conditions issues (like communication time lag, low tolerance for errors, sleep loss…) and overt stressors (extra-vehicular activities, equipment malfunction, … crew illness, crew death). Once stressors were categorized, a non-experimental investigation has been performed based on a descriptive study, using a single measurement so as to obtain from participants to extreme experience their evaluation on the previously mentioned stressors.

The study population was composed of seventeen (17) participants that experienced co-living and co-working in the following scenarios:
- Antarctic settings (6 subjects from Kerguelen and Concordia stations),
- Caves extended exploration (2 subjects)
- Remote sea-based oil drilling platforms (1 subject)
- Remote military outpost (1 subject)
- Drone pilots (6 subjects from ATV-CC Jules Verne mission)
- Mars 520 (1 subject)

ISAE-Supaero students took part in the MDRS (Mars Desert Research Station) so as to test in an habitation analog the conditions to live and work on the planet. At the end of this experiment, students involved in the MDRS project will fill the questionnaire so as to update the results.

Every single participant has been asked, through a questionnaire, whether he/she experienced or not the stressors and to attribute to it a severity, noted G, from zero (no gravity) to five (maximum of gravity). For every stressor, a probability of occurrence, noted P, has been rated so as to evaluate the risk, noted R, to lead to mission failure. The applied formula is:

$$R = P \times G \qquad (3\text{-}1)$$

Where:
- P is the probability associated to the stressor: $P \in [0,1]$
- G is its gravity: $G \in [0,5]$
- R is the risk: $R \in [0,5]$

For each of the 6 scenarios, the criticality, noted C, is then obtained, by combining the risk (see (3-1)) and the number of stressors matched, noted N, normalized on a scale from zero to five:

$$C = N \times R \qquad (3\text{-}2)$$

Where:
- C is the criticality
- N is the number of stressors
- R is the risk

Thus, C belongs to the $[0,5] \times [0,5]$ domain.

In order to quantify the general statement that no place on Earth can reproduce the exact extreme space conditions, each scenario has been compared to the most critical one: *a Mars mission with crew landing*. The scenarios have been ranked thanks to a distance to the reference scenario. That is the reason why, the survey participants have been asked to rate their autonomy level during their experience. The shorter the distance is, the better the analogy is. The final marks are given in the following table:

Scenarios	Level of Analogy
Remote Sea-based Oil drilling platforms	3.608
Remote military outposts	3.739
Antarctic settings	4.448
Caves Extended Exploration	4.608
Drones pilots	5.179
Mars 520	5.46

Table 4: Level of analogy

The survey assessed the individual well-being and team performance effects of latent and overt stressors for habitability of space station. It demonstrated that poor and ugly design trigger negative reactions, even to small adverse events. On the contrary, welcoming environment creates peaceful state of being. Habitat should then include **recreation facilities** to counteract the effects of monotony and **fictitious places** so that the crew feels to run the daily activities as on Earth. A clear definition helps to perceive the space bigger than it is. The survey revealed that the presence of a **private area**, even very small, for each crewmember, where to stow personal items, record personal experience and have a rest is the most critical issue.

Finally, regarding the station habitability, the main criteria for design are:
- To center the habitat on the crew needs
- To ensure a eye contact on the external space
- To improve space perception
- To foster mental projections (for example: sense of verticality, horizontality)

The station architecture has been designed according to this survey results and is presented in paragraph 3.5.

3.1.2.1 Purpose
The main purpose of such a gateway should be to promote Human Solar Systems exploration in a large international collaboration.

3.1.2.2 Mission
As the Space Station will provide shelter for international crew devoted to space exploration, people shall find on board all necessities for a long stay in such a hostile environment, and particularly, anything to ensure health and medical care. It could also propose a very interesting support to science (for example: telescopes).

3.1.2.3 Objectives
Resulting from preliminary analysis, and taking into account lessons learned from previous human spaceflights, it is assumed that the top-level objectives of this Space Station are:
- To shelter permanently 6 persons,
- To welcome a maximum of thirty persons in case of contingencies of other

exploration missions,
- To be functional during at least fifteen years,
- To ensure 24h per day communications with Earth ground stations
- To be start being operational in 2025
- To comply with a crew rotation every six months
- To accept cargo delivery every three months

3.2 Rationales for THOR location

The Space Station, as a test bed for human exploration of the solar systems, may be located in the vicinity of the Earth so as to ease its deployment and maintenance and ensure continuous communications.
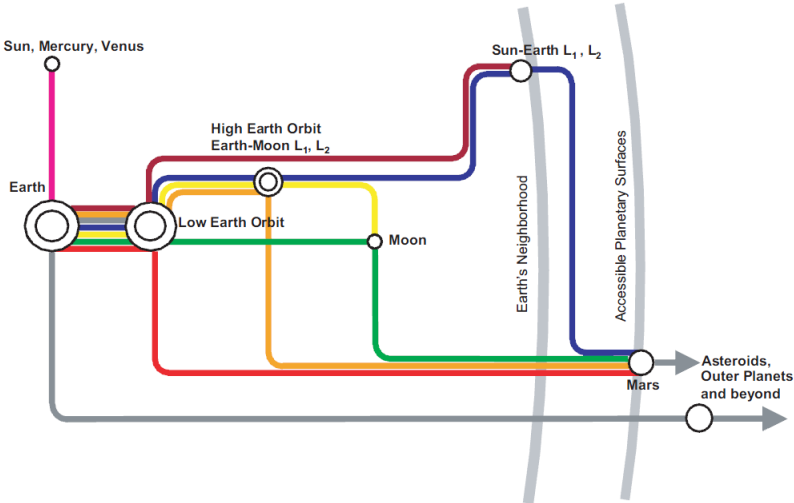
Figure 16: EML, as a gateway to the Solar system by Gary L. Martin (NASA Space Architect [41])

Due to the natural dynamics of the solar system (see 4.2), the two collinear Lagrangian points of the Earth-Moon system, EML1 and EML2, are considered. The concepts of Lagrangian point and Halo orbit are briefly reminded in paragraph 4.3. As presented on Figure 16, the space station would thus allow efficient access not only to the lunar surface, but also to many interesting destinations in the solar system like, for example, the Sun-Mars L2 or the Sun-Jupiter L1 to observe the Asteroid Belt, the Sun-Venus equilaterals L4 and L5 to provide a communications relay for Mars exploration, the Sun-Saturn L2 to look at the Kuiper Belt, the Sun-Neptune L2 to observe the Oort cloud, the Sun-Mars L1 as a waypoint to Mars and the Asteroid Belt, the Sun-Earth L1 to look at the Sun or the Sun-Earth L2 to observe the universe origins. Human missions could only visit few of these destinations, but an inhabited outpost at the gateway to these destinations may be crucial for construction and servicing missions, including robotic missions. Both points are at about the same

distance from the Moon but EML2 is almost one third further away from Earth than EML1. This induces considerable differences in access cost and transfer time. Most other properties are very similar for both locations. Those properties entail positive and negative consequences in comparison to conventional planetary orbits (like LEO) that are presented in next table.

EML properties	Consequences
No residual atmosphere	No external structures degradation due to atomic oxygen.
	No drag, so less station keeping
No inhomogeneous gravitational field	Less orbit perturbations
No magnetic field	No protection against free space radiations
No launch window	Excellent property for space exploration
No man made debris (until now)	No risk of impact
Rare Sun occultation	Almost constant thermal environment
Fixed position in the Earth Moon rotating reference frame	Same side of the Moon always visible (Near side for EML1, far side for EML2)

Table 5: Synthesis of the EML properties

The following trade-off analysis compares four possible couples, composed by location and type of orbit. Those four possibilities for the space station are Lissajous orbit around EML1, Halo orbit around EML1, Lissajous orbit around EML2 and Halo orbit around EML2. Comparison is performed through criteria rating, using a qualitative scale with the step one (bad), two (medium) and three (good). Summing up the rating for all criteria leads to a maximum value equal to twenty-four. The following table presents a synthesis of this analysis. It does not take into considerations like delta-V or duration performances since they would be fully discussed in chapter 5. Actually, the main goal of this comparison is to decide the location of the Space Station, thanks to qualitative figures of merit.

	EML1 Lissajous	EML1 Halo	EML2 Lissajous	EML2 Halo
Crew access from Earth	3	2	2	2
Deployment and resupply efficiency	2	2	3	3
Access to lunar location	3	3	3	3
Communications	2	3	2	3
Station keeping	3	3	2	3
Exploration capabilities	2	2	3	3
Long term strategy	2	2	3	3
Risk	3	3	2	2
	20	20	20	22

Table 3: Selection criteria and evaluation for location and orbit type

In this decision matrix, three couples reach twenty, while a Halo orbit around EML2 is evaluated at twenty-two points. As environmental conditions (radiation, thermal) are quite the same at EML1 or EML2, the key factors are transportation, communications and exploration strategy. The EML2 Halo orbit is the most promising location for the THOR gateway and its medical center.
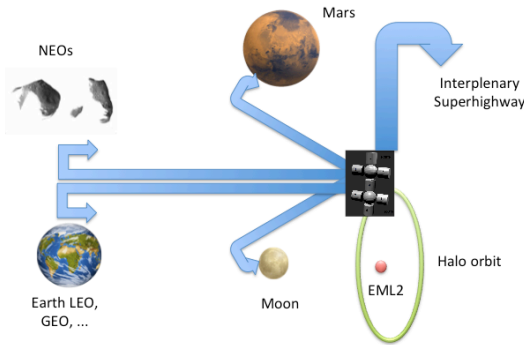
Figure 17: THOR space station location

The main recommendation is to locate:

The Space Station on Halo orbit around EML2
And the station became THOR, for Trans-Lunar Human explORation.

3.3   THOR life-profile

Going further in the Systems Engineering approach, the next step is to determine the lifecycle of the THOR space station. According to INCOSE standards [37], seven main classical stages have to be defined for the Space Station: Design, Manufacturing, Deployment, Operations and Maintenance, Training, Support and Disposal. At the very beginning of this project, it has been decided to comply with international Systems Engineering standards. Nevertheless, those stages correspond to ESA nomenclature, as described in Table 6.

INCOSE stage	ESA phase
Design	Phase 0 – Mission Analysis/Needs Identification Phase A – Feasibility Phase B – Preliminary Definition Phase C – Detailed Definition
Manufacturing	Phase D – Production/Ground Qualification Testing
Deployment	Phase E – Utilization
Operations and Maintenance	Phase E – Utilization
Training	During all phases
Support	During all phases
Disposal	Phase F – Disposal Phase

Table 6: Correspondence between ESA and INCOSE stages nomenclature

This top-level lifecycle has to be supplemented by the lifecycle of the resupply cargo and the crew vehicle. Their deployment stage starts with the Station operations and maintenance stage. Figure 18 presents scenarios.

The main objective of this thesis is to optimize those scenarios according to duration and cost criteria.

THOR life cycle
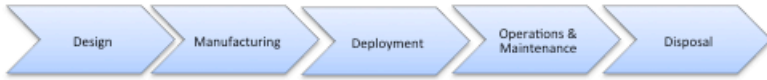
Resupply cargo life cycle
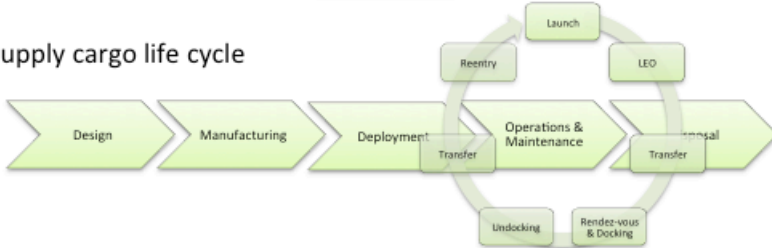
Crew vehicle life cycle
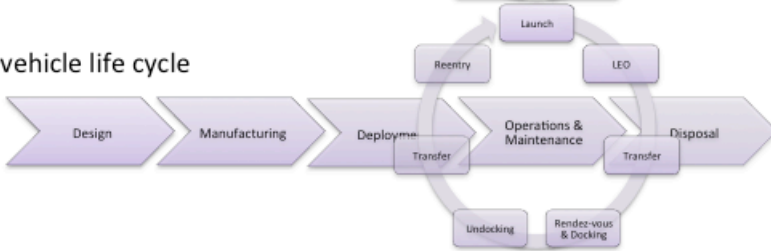
Figure 18: Space Station, resupply cargo and crew vehicle life-profile

THOR and its vehicles life-profile decomposition brought the conclusion that three important phases had to be carefully designed: the station deployment, the crew transportation (there and back) and the cargo transfer. Anyway, all trajectories carry on similar legs, presented on the Figure 19. Even if the expected performances (in term of duration and fuel consumption) vary from one phase to the other, the main legs of the cargo and the crew trajectories remain the same: Launch, station keeping in LEO (1), transfer (2), rendezvous (3), station keeping on the Halo orbit (4), return (5) and re-entry (6) as it is described on the following figure. They will be detailed in chapter 5.
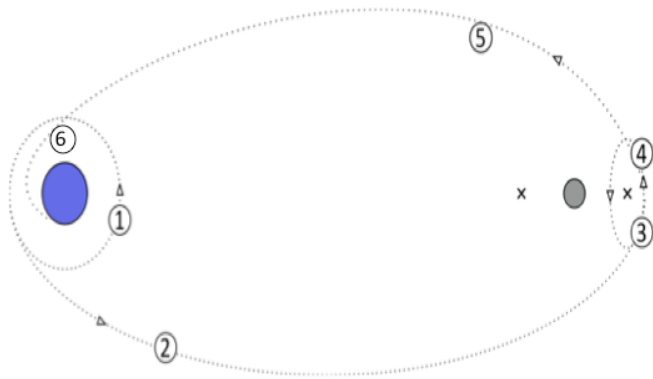
Figure 19: Trajectories main legs

The station deployment phase consists in transporting all the station components from Earth surface to the EML2. In this case, the return is not considered, but the main challenge is to find the optimal assembly scenario: is it better to integrate the module in LEO, at EML2 or somewhere else. The preliminary baseline considers that the resupply vehicle frequently delivers cargo to the Station (every 3 months). And there is one crew rotation every six months. The operational lifetime is set to fifteen years, which was coherent to the ISS duration, when the project started. Now, as ISS lifetime has been extended to thirty years, this strong assumption might be regarded as underestimated.

3.4   THOR functional architecture

Refining the purpose of THOR mission, the Space Station main functions will be:
- To ensure safe life on-board
- To guarantee permanent communications with Earth
- To always protect the crewmembers health
- To support science (astronomy, exobiology....)
- To welcome exploration crews from Moon surface, Mars or Asteroids
- To permit docking and undocking of any kind of international visiting vehicles (cargo, crew vehicles…)

As a critical sub-system of THOR Space Station, the Space Medical Center (SMC) main functions are:
- To maintain health for THOR permanent crew,
- To provide health and care to visiting astronauts,
- To plan for majors illnesses or injuries,
- To stabilize patients when emergency reentry is mandatory,
- To provide quarantine capabilities to avoid THOR contamination
- To ensure countermeasures
- To minimize microgravity and if necessary, to deal with astronaut death.
- To perform medical research,
- ....

3.5   THOR organic architecture

Taking into account all those Stakeholders' needs, the inhabited space station has been then designed. The architecture is mainly composed of seven cylindrical modules based on ATV (Automated Transfer Vehicle) proportions (a mass of twenty tons, a diameter of five meters and a length of ten meters each), completed by two spherical nodes. Each cylindrical module supports a specific function (as room, offices, kitchen, medical center, cult area...) while the spherical nodes are added to ease displacements inside the station, offer windows on space, like the Cupola on board the ISS, and support docking port. In order to avoid traffic congestion, spherical modules have been placed at the intersection of the three modules of the northern part and the three of the southern parts. These spherical modules can be compared to a crossroad and would function much the same as hubs. Windows would be added to their top parts to allow celestial viewing.

The following picture depicts the THOR station functions allocation.
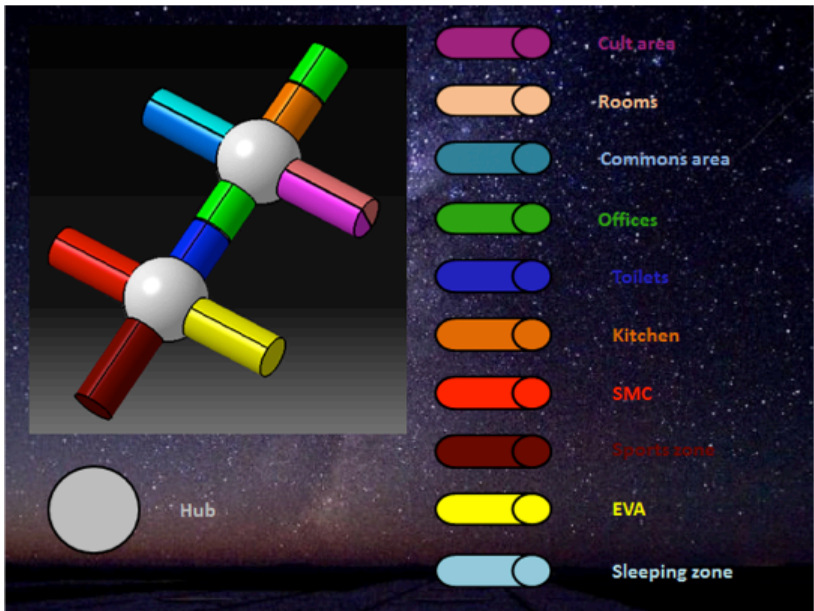
Figure 20: THOR station configuration

This functional repartition was established in order to reproduce the terrestrial way of life [42]. Thus work and leisure as well as private and public activities have been placed in different locations with respect to the functional analysis given in Figure 20. The three first modules in the northern part of the station are mostly dedicated to private and leisure activities whereas the three last modules in the southern part are dedicated to public and work activities. This creates a psychological sensation of travelling from home to work. As crew health is the most critical needs to fulfill, all life support functionalities are duplicated into several modules so as to ensure redundancy. In particular, the Space Station must be a resilient system, with one main goal related to crew survival. As a consequence, each module must be autonomous, can be rapidly separated from the space station in case of emergency and reconfigured.

As shown on Figure 20, activities are divided into four categories: private, public, group and individual activities. To these are assigned a certain set of coordinates. Typical functions were brought together and shared out among one of the seven modules of the THOR space station:

- First and third modules contain the crew quarters (sleeping compartments, hygiene facilities). Those are private and individual areas. Even a cult zone has been allocated.
- The second module is dedicated to social area (food management compartment, dining area, waste management facilities, leisure area)

- The fourth module permits transfers from the northern habitation zone to the southern working zone. It can contain storage and maintenance compartments.
- The fifth module is entirely employed for EVA (for dressing, EVA clothing maintenance, operations support, pre/post operations support and proximity operations support compartments).
- The sixth module offers sciences experiments laboratories, crew's offices and Earth communications facilities.
- The seventh module is the Space Medical Centre (SMC), encompassing an emergency shelter, exercise facility, body waste management facility, body cleansing facility, dressing and undressing compartment and quarantine compartment.

Axial orientation is a very important design issue. In order to provide crewmembers with a feeling of verticality, the seven modules were assembled so that four of them were placed in a horizontal reference plane and three of them in a vertical one. The station is space orientated so as to recreate the Earth orientation. Thus the three top modules can be qualified as the northern part of the station and the three bottom modules as the southern part. The placement of windows - allowing the observation Earth and consequently its orientation - could help crewmembers to form this mental image. Figure 20 depicts the THOR space station orientation and the way its seven modules have been assembled. The four remaining modules have been oriented at right angles to the North-South axis and a two-layered arrangement was considered to be desirable due to the similarity with the architecture of modern houses here on Earth.

Thanks to these two different configurations, interior compartments with different layout and irregular shaped rooms can be designed. This helps to provide crewmembers with a feeling of spaciousness and to combat boredom. Figure 21 proposes layout of the first and second floors for horizontal and vertical modules.
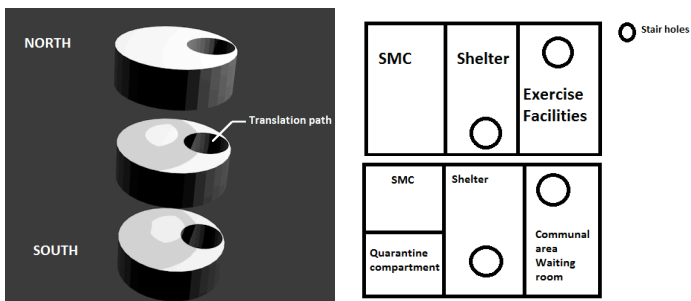
Figure 21: THOR modules internal configuration

In order to ensure space station modularity, each module has to be independent. It can travel by its own from LEO to EML2, can be individually dock and undock, particularly for safety reasons in case of emergency (fire, contaminations….). As a

52

consequence, each module has two main functions: to provide velocity increment (delta-v) during transfer and rendezvous phases (see 5) and to provide habitability when attached to the THOR space station. Each module must thus contain a propulsion subsystem (with engine, tanks...), but shall be rearranged when docked, so as to be transformed into an inhabited module. Taking into account mission analysis main results (required delta-v or transfer), four configurations of chemical propulsion have been designed and compared so as to minimize the module propulsion subsystem overall mass and the available volume after docking. Of course, considered materials are space qualified, able to resist to launch loads (compare to Ariane 5 environment). The best compromise has been found for a double set configuration with toroid tanks. The toroid shape is fixed with a maximum width compliant with diameter the minimal thickness of the module internal wall. Volume is left available for insulating material (thermal considerations).

Figure 22 presents an artistic view of the module with its propulsion sub-system and an internal design view of the propulsion subsystem with the nozzle in stowed position (a) and in deployed position (b).
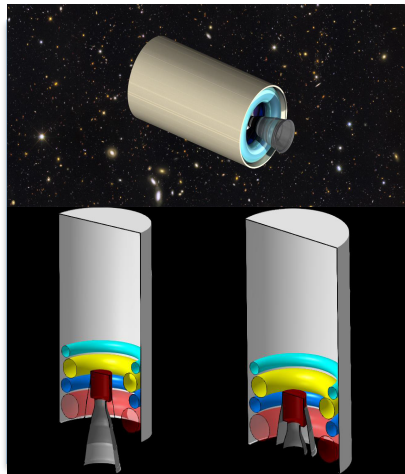
Figure 22: Module propulsion system

Another critical element to be designed is the docking sub-system, since each module may be sent separately or be attached or detached from the THOR station in case of nominal operations (cargo arrival, crew rotation, EVA) or in case of contingencies (fire, contamination, depressurization…). The main requirements to be taken into account for this docking system:
- To have a 'universal' type of joint to permit collaboration with all type of vehicles (cargo, crew vessel)
- To ensure mechanical, electrical and communication connections with the THOR space station

- To allow passageway for goods and crew in both ways (from the cargo to the station and return)

Constraints relative to the structural perspective have been deeply analyzed taking into account the different working environments during THOR space station lifetime (Launch, LEO, transfer and EML2).

Figure 23 and Figure 24 present two designs of universal docking systems that were studied

1. Closed docking system.

2. Open docking system.

3. Adaptable docking system pins.

4. Conceptual image of a rendezvous
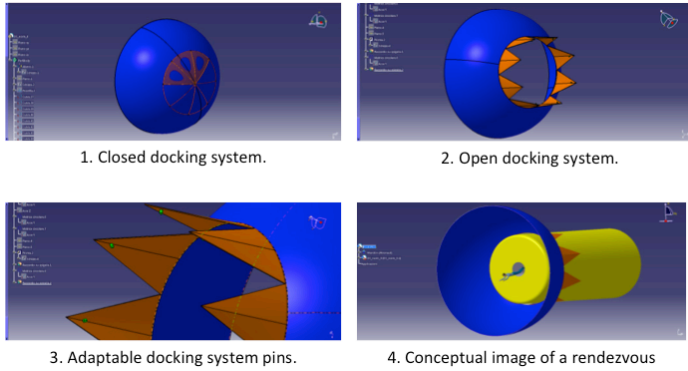
Figure 23: Adaptable pins docking system

1. Closed docking system: the black gate can be designed as a solar array.

2. Open docking system.

3. Deployed docking system

4. Conceptual image of a rendezvous
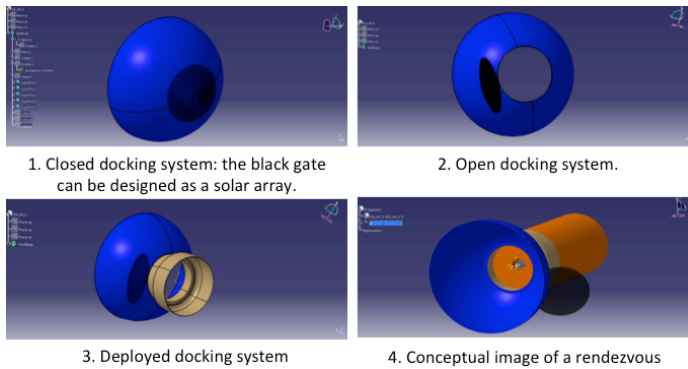
Figure 24: Inflatable docking system

54

3.6   Recommendations for mission analysis

Stakeholders' needs analysis concludes that the Space Station shall be located on a Halo orbit, around EML2. Further analysis shall now be conducted to determine the characteristics of the Halo orbit, the best trajectories for the cargo and the crew vehicle to join the Space Station and the optimal assembly scenario. The results of this analysis are presented in chapter 5.

4 Theoretical background

This chapter gives an overview of the mathematical description of the N-body problem and methodologies to compute trajectories in the dynamical systems, but also of some optimization methodologies. It falls into four parts:

- The first part provides an overview of the state-of-the art on the three-body problem, so as to explain what the Lagrangian points are,
- The second part describes the dynamics in their vicinity,
- The third part focuses on the way to travel to or from the Lagrangian points
- The last part provides mathematical tools to optimize those journeys.

4.1 Introduction

As it was explained in the context description (refer §2), the goal of this study is to design trajectories of the THOR Space Station, the cargo and the crew vehicle from a prescribed initial Low Earth orbit to the vicinity of the Earth-Moon Lagrangian point.

Concepts that are presented in this chapter are generic, but they will be instantiated with the Earth-Moon system example, the main purpose of the project. The Space station mission analysis is mostly performed in the Three-Body Problem, but the utimate change would be a description of the trajectories in the perturbed N-body ephemeris model.

4.2 N-body problem

Paragraph 2.1 provided an historical background of the N-body problem. Here the theoretical background is presented, providing the equations, describing the motion of a particle (the space station, the resupply cargo or the crew vehicle) traveling in this environment.

4.2.1 Definition

The N-body problem consists in the prediction of the motion of a particle P_0, under the gravitational influence of N-1 massive bodies $(\mathcal{P}_1 \dots \mathcal{P}_N)$ with respective masses $(m_1 \dots m_{N-1})$ and their respective positions $(P_1 \dots P_{N-1})$. In general, the massive bodies are the celestial bodies (like Earth, Moon, Sun…) and the particle is the spacecraft, like in this study, the Station, the cargo or the crew vehicle. The massive bodies are called the primaries.

As the N bodies are isolated (no other effect), the problem can be described by the following equations, developed in $\mathfrak{R}_O$, the Galilean reference frame:

$$m_k \frac{d^2 \overrightarrow{OP_k}}{dt^2} = \sum_{\substack{i=0 \\ i \neq k}}^{N-1} -G \frac{m_i m_k}{\left| \overrightarrow{P_i P_k} \right|^3} \overrightarrow{P_i P_k} \quad k = 0 \dots N-1 \qquad (4\text{-}1)$$

Where

O is the origin of the reference frame

G is the gravitational constant

Thus, the problem is modeled by a set of 3N second order scalar differential equations, by generalizing the second Newton law.

The mathematical model used to represent the Earth-Moon or Sun-Earth dynamical environments is the Circular Restricted Three-Body Problem (CR3BP). This model leads to introduce the notions of libration points (see 4.3), libration orbits (see 4.4) and invariant manifolds (see **Erreur ! Source du renvoi introuvable.**). The CR3BP is commonly used to produce quick and efficiently quantitative results for transfers between Earth and libration orbits.

The Three-Body Problem has been deeply detailed in many publications. This manuscript mainly refers to [27].

4.2.2 CR3BP model

The two-body problem has entirely been solved. On the contrary, the three-body problem does not admit any analytical solution. When the particle is assumed to be massless, the problem is said to be "Restricted." This means that the motion of the particle will not affect the trajectories of the primaries. The model becomes the Circular Restricted Three-Body Problem (CR3BP) when the primaries are supposed to be on circular orbits about their common center of mass.

In order to simplify the expressions (4-1), the masses, distances and time are normalized respectively with the sum of the primaries' masses, the distance between them and their angular velocity around their barycenter. The unit of time is taken such that the period of the orbits of the primaries is 2π. The equations are written in the synodic frame, centered on the center of mass and with the x-axis directed from the Earth to the Moon and the y-axis in the plane of the primaries' motion (see 4.2.4), the z-axis completes the right hand system.

Then, the universal constant of gravitation, G, becomes equal to 1: $G = 1$.

4.2.3 Notations

The two massive bodies (M_1 and M_2) masses are m_1 and m_2, with $m_2 < m_1$. The negligible mass of the particle is m_3.

As the main parameters have been normalized, the only remaining one in the system is the mass parameter, μ, defined as:

$$\mu = \frac{m_2}{m_1 + m_2} \qquad\qquad (\text{ 4-2})$$

Where $\mu \in \left[0, \frac{1}{2}\right]$

By consequence, the two primaries are located on the x-axis at the point $(-\mu, 0, 0)$, for M_1 and $(1 - \mu, 0, 0)$ for M_2 in the rotating frame (see 4.2.4). The position of the particle is also given by (x, y, z), in the same rotating frame.

Then, let: $\mu_1 = 1 - \mu$ and $\mu_2 = \mu$ (4-3)

4.2.4   Reference frames

Several reference frames are used:

- **Inertial reference frame**

The inertial reference frame $(O, \vec{X}, \vec{Y}, \vec{Z})$ is a Galilean reference frame where the origin, O, is at the center of gravity (CoG) of the primaries and the plane (X,Y) is the orbital plane of the primaries. The Z-axis completes the right hand system by standing normally on the x-y plane.

- **Rotating frame**

The rotating frame $(O, \vec{x}, \vec{y}, \vec{z})$ has the same origin than the inertial frame, described before. The x-axis lies along the primaries axis. It is pointing from the primary M_1 center towards M_2 center. The y-axis is perpendicular to the x-axis in the primaries orbital plane. The z-axis completes the right hand system by standing normally on the x-y plane.

- **Transformation between the inertial and the rotation frame:**

It is assumed that at the time origin (t=0), both reference frames coincide. The $(O, \vec{x}, \vec{y}, \vec{z})$ reference frame is rotating with respect to the $(O, \vec{X}, \vec{Y}, \vec{Z})$ reference frame with an angular velocity equal to the mean motion, n, of the primaries. The following figure depicts both reference frames
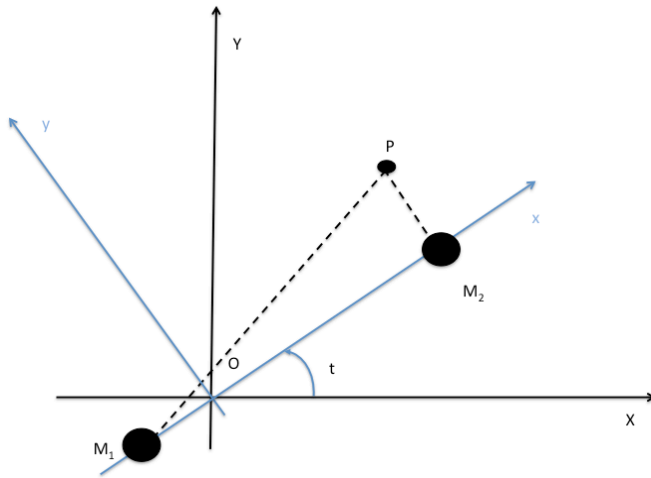
Figure 25: Inertial and rotating reference frames

When (x,y,z) and (X,Y,Z) are the positions of the particle P respectively in the rotating reference frame and in the inertial reference frame, in normalized units, the transformation equations are :

$$\begin{pmatrix} X \\ Y \\ Z \end{pmatrix} = A(t) \begin{pmatrix} x \\ y \\ z \end{pmatrix} \qquad (\text{4-4})$$

Where

$$A(t) = \begin{pmatrix} cost & -sint & 0 \\ sint & cost & 0 \\ 0 & 0 & 1 \end{pmatrix} \qquad (\text{4-5})$$

- **Halo orbit local reference frame**

Some optimization computations require a Halo orbit parameterization. A specific reference frame is defined and presented in 5.2.2.

4.2.5 Conversions

Most models presented in this document are performed in a non-dimensional system of equations. Nevertheless, the mission analysis (see 5) will give dimensional results. The units' conversions from the unprimed normalized system to the primed dimensionnalized system are:

- For distance: $d' = Ld$ where L is the distance between the center of the two primaries
- For velocity: $s' = Vs$ where V is the orbital velocity of M_1
- For time: $t' = \frac{T}{2\pi}t$ where T is the orbital period of the two primaries.

4.2.6 Equations of motion

The equations of motion describe the travel of the particle under the gravitational influence of the two primaries. There are several techniques to derive them:

- Newtonian approach
- Lagrangian approach in the inertial frame
- Lagrangian approach in the rotating frame
- Hamiltonian approach in the rotating frame

All these approaches are equivalent and will reach, fortunately, the same equations of motion starting from Newton's equation:

$$\vec{F} = \frac{d}{dt}(m\vec{v}) \qquad (\,4\text{-}6\,)$$

where : m is the mass of the particle
$\vec{v}$ is the velocity of the particle
$\vec{F}$ is the sum of the external forces on the particle

In this thesis, the **Lagrangian approach in the rotating frame** is developed like it was given in Marsden and Ratiu [43].

In the (4-1) equations, the motion of the particle in the inertial reference frame are:

$$\ddot{X} = -\frac{\partial U}{\partial X}, \ddot{Y} = -\frac{\partial U}{\partial Y}, \ddot{Z} = -\frac{\partial U}{\partial Z} \qquad (\,4\text{-}7\,)$$

Where U is the gravitational potential which the particle will experience due to m_1 and m_2, in normalized units:

$$U = -\frac{\mu_1}{r_1} - \frac{\mu_2}{r_2} - \frac{1}{2}\mu_1\mu_2 \qquad (4\text{-}8)$$

And where μ_1 and μ_2 are defined in (4-3).
r_1 and r_2 are the distances of the particle P, from the two celestial bodies, M_1 and M_2. They are given,

- In the inertial reference frame, as:

$$r_1^2 = (X + \mu_2 cost)^2 + (Y + \mu_2 sint)^2 + Z^2 \qquad (4\text{-}9)$$
$$r_2^2 = (X - \mu_1 cost)^2 + (Y + \mu_1 sint)^2 + Z^2$$

- In the rotating reference frame, as:

$$r_1^2 = (x + \mu_2)^2 + y^2 + z^2 \qquad (4\text{-}10)$$
$$r_2^2 = (x - \mu_1)^2 + y^2 + z^2$$

According to Marsden and Ratiu [43], the Euler-Lagrange equations are:

$$\frac{d}{dt}\frac{\partial L}{\partial \dot{q}^i} - \frac{\partial L}{\partial q^i} = 0 \qquad (4\text{-}11)$$

Where L, the Lagrangian, represents the kinetic energy minus the potential energy and q_i are the system generalized coordinates.

- In the inertial reference frame:

$$L(X,Y,Z,\dot{X},\dot{Y},\dot{Z},t) = \frac{1}{2}(\dot{X}^2 + \dot{Y}^2 + \dot{Z}^2) + U(X,Y,Z,t) \qquad (4\text{-}12)$$

- In the rotating reference frame:

$$L(x,y,z,\dot{x},\dot{y},\dot{z},t) \qquad (4\text{-}13)$$
$$= \frac{1}{2}((\dot{x} - y)^2 + (x + \dot{y})^2 + \dot{z}^2)$$
$$- U(x,y,z)$$

Then, the Lagrangian is time-independent, since distances r_1 and r_2 are invariant under rotation (4-10).

With this formulation, the Euler-Lagrange equations (4-11) can then be developed and simplified :

$$\ddot{x} - 2\dot{y} = -\bar{U}_x = -\frac{\partial \bar{U}}{\partial x}$$

$$\ddot{y} + 2\dot{x} = -\bar{U}_y = -\frac{\partial \bar{U}}{\partial y} \qquad (4\text{-}14)$$

$$\ddot{z} = -\bar{U}_z = -\frac{\partial \bar{U}}{\partial z}$$

Where, $\bar{U}$ is the effective potential:

$$\bar{U}(x,y,z) = -\frac{1}{2}(\mu_1 r_1^2 + \mu_2 r_2^2) - \frac{\mu_1}{r_1} - \frac{\mu_2}{r_2} \qquad (4\text{-}15)$$

4.2.7 Hamiltonian formulation

Equations (4-15) can be transformed into an Hamiltonian form thanks to the Legendre transformation :

$$p_i = \frac{\partial L}{\partial \dot{q}^i} \qquad H(q^i, p_i) = \sum_{i=0}^{N-1} p_i \dot{q}^i - L(q^i, p_i) \qquad (4\text{-}16)$$

$$\dot{q}^i = \frac{\partial H}{\partial p_i} \qquad \dot{p}_i = -\frac{\partial H}{\partial q^i}$$

And the Hamiltonian form of the equations of motion is, in the rotating frame:

$$\dot{x} = \frac{\partial H}{\partial p_x} = p_x + y$$

$$\dot{y} = \frac{\partial H}{\partial p_y} = p_y - x \qquad (4\text{-}17)$$

$$\dot{z} = \frac{\partial H}{\partial p_z} = p_z$$

$$\dot{p}_x = -\frac{\partial H}{\partial x} = p_y - y - \bar{U}_x$$

$$\dot{p}_y = -\frac{\partial H}{\partial y} = -p_x - y - \bar{U}_y$$

$$\dot{p} = -\frac{\partial H}{\partial z} = -\bar{U}_z$$

Since the equations of motion (4-17) are Hamiltonian, and do not depend on time, they have an energy integral of motion denoted as :

$$E(x, y, z, \dot{x}, \dot{y}, \dot{z}) = \frac{1}{2}(\dot{x}^2 + \dot{y}^2 + \dot{z}^2) \qquad (\text{4-18})$$
$$+ \overline{U}(x, y, z)$$

The **Jacobi integral** can also be used:

$$J = -2E \qquad\qquad (\text{4-19})$$

Along a trajectory solution of the system, the energy integral is constant. When the constant e is fixed, the trajectories belong to a energy surface: the **energy manifold.** It can be defined as:

$$\mathcal{M}(\mu, e) = \{(x, y, z, \dot{x}, \dot{y}, \dot{z})/E(x, y, z, \dot{x}, \dot{y}, \dot{z}) \qquad (\text{4-20})$$
$$= e\}$$

This concept is the fundamental basis of the trajectory optimization in the three-body problem. Actually, for a given initial velocity, that corresponds to a given energy, e, natural trajectories, requiring no additional energy (or velocity), are solutions of the problem.

They can be obtained by projection of the energy manifold onto the space position, in the rotating frame. The result is named the **Hill's region** and is determined by:

$$H(\mu, e) = \{(x, y, z)/\overline{U}(x, y, z) \le e\} \qquad (\text{4-21})$$

By consequence, when the initial conditions are known, the regions, reachable by the particle can be computed. When a certain region is an objective, the initial conditions have to be found so as to ensure that the particle will travel on the zero velocity curve to reach it.

The particle can, of course, only travel on trajectory where the kinetic energy is positive. When the kinetic energy is negative, the motion is not feasible.

Figure 26 presents an example of the effective potential, in the case of Earth-Moon system.
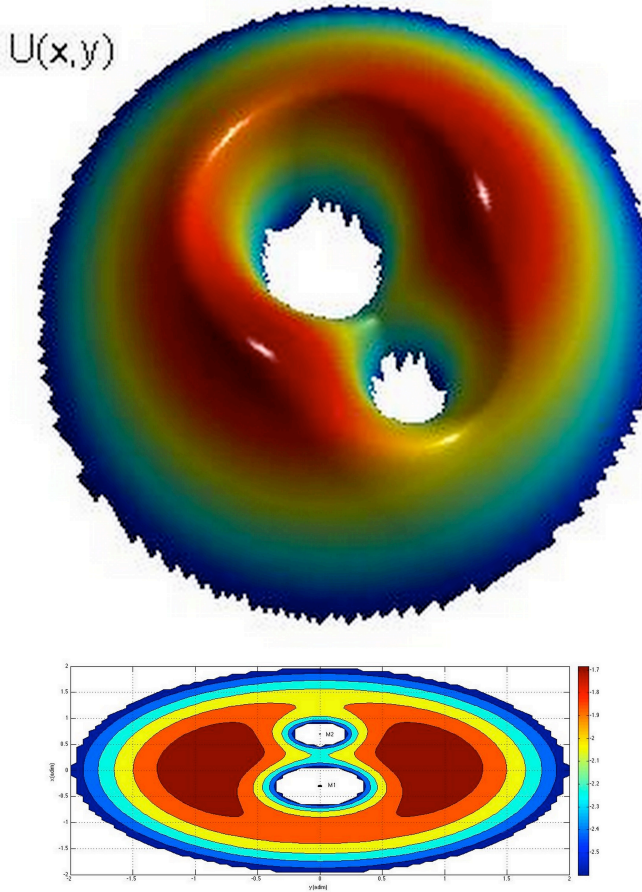
Figure 26: Effective potential for μ =0.3

This example was obtained for μ =0.3 so as to compare results with the ones presented in [27] with a planar motion (z=0). Two holes can be noticed in the vicinity of the primaries: they correspond to a potential well. Five critical points can be observed. They are denoted as the Lagrangian points (L_1… L_5). A more detailed description of their characteristics is given in paragraph 4.3.

The particle energy, E, can be compared to the energy required at the Lagrangian point ($E_1 \dots E_5$) where:

$$E_1 < E_2 < E_3 < E_4 = E_5 \quad (\text{4-22})$$

When μ is fixed, five cases can be defined, depending on the value of E, compared to $E_1 \dots E_5$.
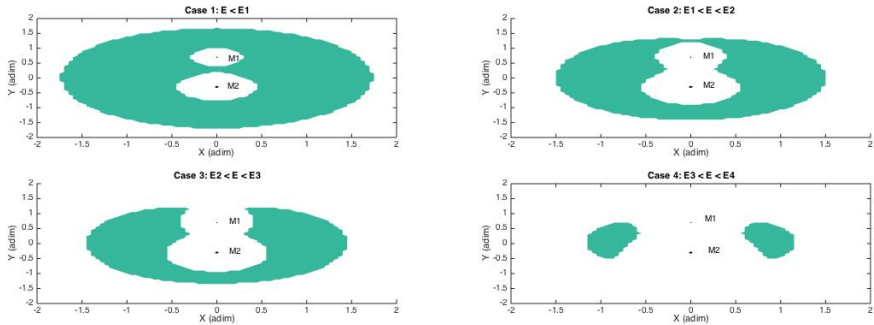
Figure 27: Realms of possible motion

Figure 27 depicts the borders between the different zones that the particle can reach or not.

- On case 1, when $E<E_1$, the particle cannot move only in the vicinity of the two primaries (the white zones).
- On case 2, when $E_1<E<E_2$, the particle can travel in the neck between the realms of the two primaries.
- On case 3, when $E_2<E<E_3$, the particle can quit the vicinity of the two primaries thanks to a narrow way after the second primary.
- On case 4, when $E_3<E<E_4$, the particle can quit the vicinity of the two primaries, from M_1 directly thanks to a way in the direction of L_3.
- On case 5 (not represented on Figure 27), there is no more forbidden realm and the particle is free to navigate in the entire space.

The curves presented on Figure 27 are the same as the ones presented in [27].

Those properties are the fundamental basis for transfer trajectories optimization. It will be detailed in chapter 5. For trajectories design, minimizing the fuel consumption (i.e. the energy), two cases are more relevant:

- Case 2 for destination in the Moon vicinity (as second primary)
- Case 3 for solar system further destinations

4.3   Lagrangian points

4.3.1   Definition

Lagrangian (or Libration) points, in a two-bodies rotating system, are locations where gravitational pulls and centripetal force are balanced. Joseph Lagrange demonstrated in 1772 (see [5]) in such context, five points can be found. For example, in the Earth-Moon system, they are called EML1 to EML5.

The three first points (L_1 to L_3) are collinear and located on the primaries axis, the last two ones, L_4 and L_5, are positioned at 60° leading and 60° trailing on the M_2 orbit (as smaller primary body). Figure 28 presents the Earth-Moon Libration points location without respect of the celestial bodies size and the distances scale.
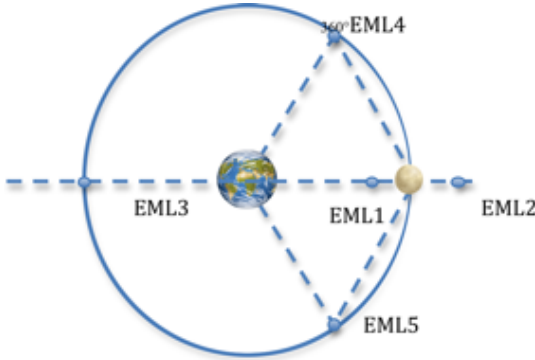
Figure 28: The Five Earth-Moon Libration points locations

Relative EML distances in the Earth-Moon reference frame are given in the Table 7:

EML	Distance in km
EML1 to the Moon	62 690
EML2 to the Moon	59 746
EML3 to the Earth	386 345
EML4 and EML5 to the Earth	384 400

Table 7: EML distance in the Earth-Moon system

By consequence, Lagrangian points, as equilibrium points of the three-body problem, are interesting destinations, as final destination or waypoint on the road to further destinations, since they required low energy to be reached and low energy to maintain the orbit in their vicinity.

4.3.2   Positions computation

The exact positions of the Libration points can be obtained by solving the Circular Restricted Three Body Problem (CR3BP), describing the motion of a particle with a

66

negligible mass in the system with the two primary bodies, evolving on circular orbits [27]. These points are not only equilibrium points for the system of equations (4-14) of the three-body problem but also extrema of the effective potential (4-15).

The state vector of one equilibrium point can be denoted as $(x_e, y_e, z_e, \dot{x}_e, \dot{y}_e, \dot{z}_e)$.

As a consequence, to compute their positions, the system (4-14) must be solved with the following conditions:

$$\dot{x}_e = 0, \dot{y}_e = 0, \dot{z}_e = 0 \qquad (4\text{-}23)$$
$$\ddot{x}_e = 0, \ddot{y}_e = 0, \ddot{z}_e = 0$$

One immediate consequence is that $z_e = 0$, equilibrium points are in the (xy) plane, containing also the primaries orbit. The system (4-14) becomes:

$$\frac{\partial \bar{U}}{\partial x} = 0, \frac{\partial \bar{U}}{\partial y} = 0 \qquad (4\text{-}24)$$

Then it has to be discussed to find the collinear equilibrium points (on the x-axis) and the equilateral equilibrium points (y≠0).

4.3.2.1 Equilateral Lagrangian points

While, when y≠0, using definition of r_1 and r_2 (4-10), the system does not depend any longer on x and y:

$$\frac{\partial \bar{U}}{\partial x} = \frac{\partial \bar{U}}{\partial r_1} \times \frac{\partial r_1}{\partial x} + \frac{\partial \bar{U}}{\partial r_2} \times \frac{\partial r_2}{\partial x} = 0 \qquad (4\text{-}25)$$
$$\frac{\partial \bar{U}}{\partial y} = \frac{\partial \bar{U}}{\partial r_1} \times \frac{\partial r_1}{\partial y} + \frac{\partial \bar{U}}{\partial r_2} \times \frac{\partial r_2}{\partial y} = 0$$

With:

$$\mu_1 = 1 - \mu \qquad (4\text{-}26)$$
$$\mu_2 = \mu$$

This leads to

$$\frac{\partial U}{\partial r_1} = \mu \left(r_2 - \frac{1}{r_2^2} \right) = 0 \qquad (4\text{-}27)$$
$$\frac{\partial U}{\partial r_2} = (1 - \mu) \times (r_1 -) = 0$$

It is equivalent to:

$$r_1 = r_2 = 1 \qquad (4\text{-}28)$$

With the coordinates of the two equilateral Lagrangian points are:

$$L_4 = \left(\frac{1}{2} - \mu, \frac{\sqrt{3}}{2}, 0\right) \qquad (4\text{-}29)$$

$$L_5 = \left(\frac{1}{2} - \mu, -\frac{\sqrt{3}}{2}, 0\right)$$

4.3.2.2   Collinear Lagrangian points

When y=0, the position x_e of the three Lagrangian points are solutions of the x-axis equation:

$$x_e - \frac{1-\mu}{(x_e+\mu)^2} - \frac{\mu}{(x_e-1+\mu)^2} = 0 \qquad (4\text{-}30)$$

This equation has no explicit solution. Several numerical methods have been suggested. Szebehely proposed in 1967 [44], the most useful one, based on series expansion.

When γ_1, respectively γ_2, is the distance from L_1, respectively L_2, to the smallest primary, M_2, positions of the collinear point, L_1 and L_2, can be defined as:

$$x_{L_1} = 1 - \mu - \gamma_1 \qquad (4\text{-}31)$$

$$x_{L_2} = 1 - \mu + \gamma_2$$

Where γ_1, respectively γ_2, is the unique solution of the equation deduced from the maximization of the effective potential at the Lagrangian point:

$$\begin{bmatrix} \gamma_1^5 - (3-\mu)\gamma_1{}^4 + (3-2\mu)\gamma_1^3 - \mu\gamma_1^2 - \mu = 0 \qquad (4\text{-}32) \\ \gamma_2^5 + (3-\mu)\gamma_2{}^4 + (3-2\mu)\gamma_2^3 + \mu\gamma_{21}^2 - \mu = 0 \end{bmatrix}$$

From Szebehely [44], distances γ_1 and γ_2, can be developed in series:

$$\gamma_1 = r_h\left(1 - \frac{1}{3}r_h - \frac{1}{9}r_h^2 + \cdots\right) \qquad (4\text{-}33)$$

$$\gamma_1 = r_h\left(1 + \frac{1}{3}r_h - \frac{1}{9}r_h^2 + \cdots\right)$$

Where r_h is the Hill radius, defined by:

$$r_h = \left(\frac{\mu}{3}\right)^{\frac{1}{3}} \qquad (\ 4\text{-}34\ )$$

The Hill radius, r_h, represents the sphere surrounding the smallest primary, M_2, on which the gravitational effects of both primaries are equivalent.

A similar methodology can be applied to find the position of L3, while considering its distance to the biggest primary, M_1.

The Figure 29 presents the evolution of the effective potential when y = 0. The three maxima can be noticed. They correspond to L1, L2 and L3. The curve was obtained for μ=0.3 and can be compared to the one presented in [27].
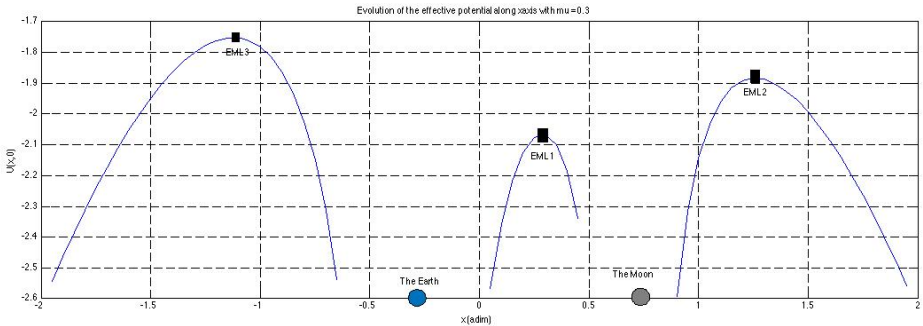
Figure 29: Evolution of the effective potential for μ = 0.3

The Figure 29 is not realistic, since μ is different from 0.3 in the Earth-Moon system. Moreover, the positions of the two celestial bodies, Earth and Moon, are not exact and their radius is wrong. They have been added to the graph so as to illustrate it.

Now that the positions of the five Lagrangian points have been computed, they can be placed on the effective potential map. In Figure 30 an example is provided for μ = 0.3, that is not realistic for the Earth-Moon system but gives a nice visualization.
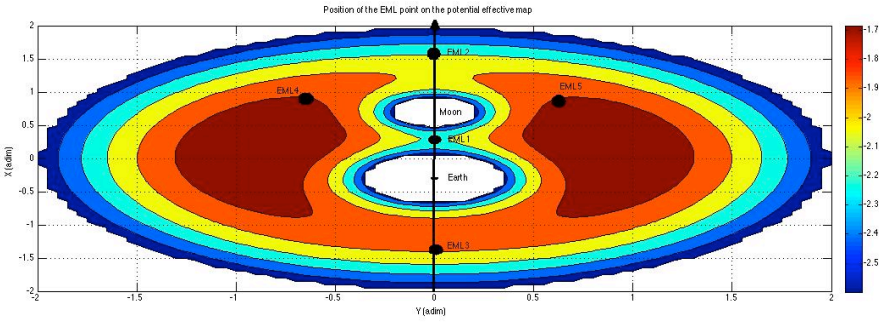
Figure 30: Position of the Lagrangian points on the effective potential map μ = 0.3

4.3.3 Stability considerations

In previous paragraphs, the interest of the Lagrangian points, their definitions and locations have been discussed. The aim of this paragraph is now to provide some stability considerations. As far as stability is concerned, the three collinear points (from EML1 to EML3, in the case of the Earth-Moon system) are considered as semi-stable. Actually, for any object orbiting in the vicinity of one of those three points, any deviation in the two transversal directions from their location will result in an acceleration back to the EML whereas any deviation in the radial directions will result in an acceleration either back to the Moon or to the Earth. Both properties are useful for space mission because it will ensure stable orbits around the Libration point (reducing fuel budget) and guarantee low cost trajectory back to the Earth (in terms of fuel).

The equations of motion of the particle have to be linearized to study the stability of the particle in the neighborhood of the collinear Lagrangian Points. Considering a small displacement $(\delta x, \delta y, \delta z)$ from the equilibrium position $X_e = (x_e, y_e, z_e)$, the linearized equations of motion can be written in the matrix form:

$$\frac{d}{dt}\begin{pmatrix} \delta x \\ \delta y \\ \delta z \\ \delta \dot{x} \\ \delta \dot{y} \\ \delta \dot{z} \end{pmatrix} = \begin{pmatrix} 0 & 0 & 0 & 1 & 0 & 0 \\ 0 & 0 & 0 & 0 & 1 & 0 \\ 0 & 0 & 0 & 0 & 0 & 1 \\ \frac{\partial^2 U}{\partial x^2}(X_e) & \frac{\partial^2 U}{\partial x^2}(X_e) & \frac{\partial^2 U}{\partial z \partial x}(X) & 0 & 2 & 0 \\ \frac{\partial^2 U}{\partial x \partial y}(X_e) & \frac{\partial^2 U}{\partial y^2}(X_e) & \frac{\partial^2 U}{\partial z \partial y}(X_e) & 0 & -2 & 0 \\ \frac{\partial^2 U}{\partial x \partial z}(X_e) & \frac{\partial^2 U}{\partial y \partial z}(X_e) & \frac{\partial^2 U}{\partial z^2}(X_e) & 0 & 0 & 0 \end{pmatrix}\begin{pmatrix} \delta x \\ \delta y \\ \delta z \\ \delta \dot{x} \\ \delta \dot{y} \\ \delta \dot{z} \end{pmatrix} \qquad (4\text{-}35)$$

By solving the characteristic equation of this dynamic system, the roots are:
- at L$_1$, L$_2$ and L$_3$: $(\pm\lambda, \pm i\omega_p, \pm i\omega_v)$ with $\lambda > 0, \omega_p > 0, \omega_v > 0$

70

- at L_4 and L_5 : $(\pm i\omega_1, \pm i\omega_2, \pm i\omega_3)$ $with$ $\omega_1 < \omega_2 < \omega_3$

In co-linear Lagrangian point, at least, one root strictly is positive, so it can be concluded that those points are unstable. The linear behavior is of the type of "saddle x center x center" with one real root (saddle point) and two complex roots (center point).

A saddle point phase portrait can be represented as shown on Figure 31:
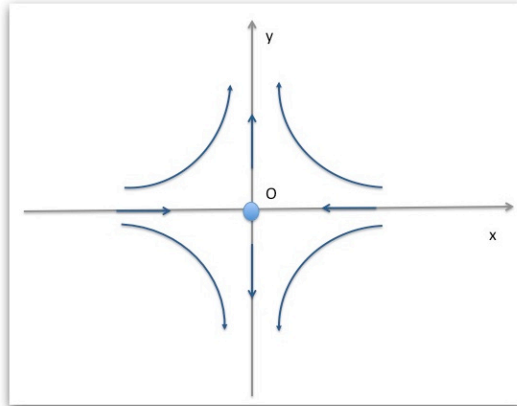
Figure 31: Saddle point phase portrait

A center point phase portrait can be represented as shown on Figure 32:
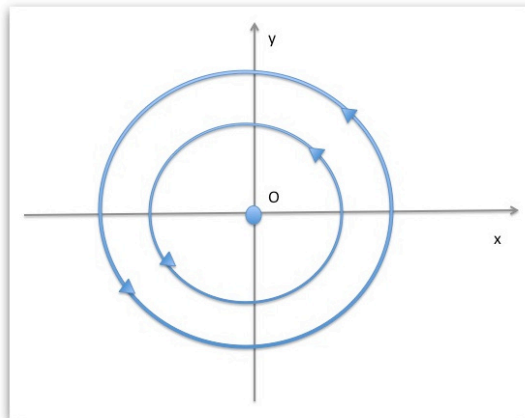
Figure 32: Center point phase portrait

For more details on phase portrait of dynamic systems, refer to [45]. The case of the equilateral points is not detailed here, since it is out of the scope of the project, but it has been often described in literature (see, for example, [46]).

Until now, the definition of Lagrangian points and the motions in their vicinity have been discussed. Now, trajectories around them, as solutions of the three-body problem at a collinear Lagrangian, are then detailed in next paragraph. At this step, the important concept to highlight is that the Lagrangian points are ideal destinations that the particle will only tend to reach.

4.4   Families of libration orbits

4.4.1   Orbits definition

According to literature four different kinds of orbits exist around libration points.
They are usually designated as:

- Lyapunov orbits are planar periodic orbits in the orbital plane of the primaries (xy-plane). Exact Lyapunov orbits only exist in the CR3BP.
- Lissajous orbits are three-dimensional quasi-periodic orbits with an in- and out-of-plane oscillation.
- Halo orbits are three-dimensional periodic orbits. R. Farquhar named them "Halo orbits" from the shape they take when seen from Earth. Exact Halo orbits can only be computed in the CR3BP.
- Quasi-Halo orbits are quasi-periodic orbits around a Halo orbit. They are intermediate between Lissajous and Halo orbits.
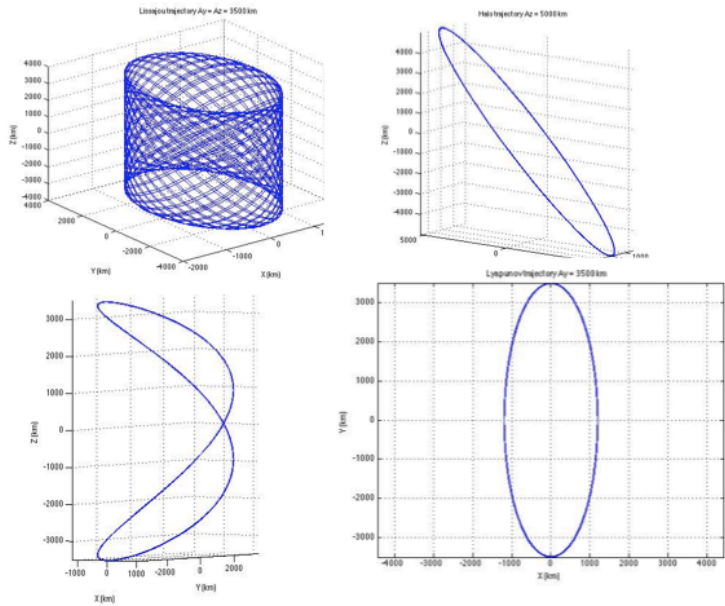
Figure 34 presents examples of orbits around EML2.

The Lyapunov orbits center of gravity is entirely in the primaries' rotation plane. Therefore there is no possibility to avoid occultation: for example, when the Moon crosses the direct line of sight from the station to the Earth. According to [8], Lyapunov orbits only exist in the CR3BP and until now, do not have any practical relevance.

To obtain a Lissajous orbit, it shall be superimposed an out-of-plane oscillation to a Lyapunov orbit. As the oscillation frequencies are not the same in the two planes (x-y plane and the out-of-plane), these orbits are not periodic and their amplitude changes. Exchange of energy between the oscillation in the in-plane (x-y plane) and the out-of-plane movement results in non-periodicity and changing amplitudes. For small amplitudes, this effect can be neglected and the trajectory can be calculated using the differential equation linearized around the Libration point.

Halo orbits only exist above certain amplitudes as they are based on the aforementioned exchange of energy. This amplitude depends on the Libration point location. The oscillations have the same frequency for in - and out-of-plane movements and resulting orbits are periodic with a never entered zone. Perfect periodic Halo orbits only exist in CR3BP. In general, the Halo orbits consist of greater amplitudes than Lissajous orbits. For example, traveling around EML2 leads to bigger orbit than around EML1.

73

4.4.2 Numerical computation of orbits around Lagrangian points

As the CR3BP cannot be solved analytically, methodologies with high order approximations have been set up and presented by K. Howell [47], G. Gòmez and J. Masdemont ([48], [49]).

The numerical methodology consists then in:
- First, to find the periodic solutions, thanks to the Lindstedt-Poincaré method (4.4.2.2)
- Then, to use a differential correction to find an accurate periodic solution (4.4.2.4)

This accurate periodic solution is then considered as an initial guess for the shooting process method (4.4.2.4) or a seed for constructing successive approximations, from the exact systems of equations. For the THOR mission project, this methodology has been developed with Matlab.

4.4.2.1 Expansion of the nonlinear equations

The equations of motion of the particle near the Lagrangian point has to be expressed in a new reference frame so as to ease the computation.

The new reference frame results from the translation of the origin from O, the center of gravity of the primaries, origin of the rotating frame to L, the Lagrangian point. Figure 33 presents an example of the new reference in the Earth-Moon system when the origin is located in EML2. On this figure, the distances are not representative.
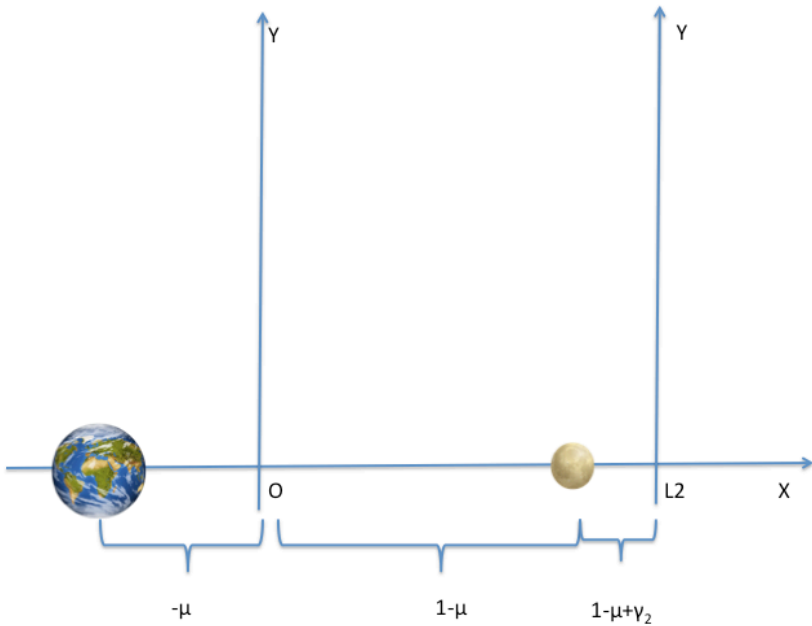
Figure 33: Reference frame in EML2

As the new coordinate system is normalized, the change of coordinates was introduced by Richardson [51] and is given by:

$$\bar{x} = \frac{x - 1 + \mu \pm \gamma}{\gamma} \qquad (4\text{-}36)$$

$$\bar{y} = \frac{y}{\gamma}$$

$$\bar{z} = \frac{z}{\gamma}$$

Where
- + is for L1 and – is for L2,
- γ is obtained thanks to (4-33)

In this coordinate system, the distance between the L_1 (respectively L_2) and the smallest primary is equal to 1.
From now on, simply the notations (x,y,z) will be used to represent the position of the particle in the rotating reference frame centered on the Lagrangian point.

75

The equations of motion in the CR3BP can be developed using a set of Legendre polynomials, P_n:

$$\ddot{x} - 2\dot{y} - (1 + 2c_2)x = \frac{\partial}{\partial x} \sum_{n \geq 3} c_n \rho^n P_n \left(\frac{x}{\rho}\right) \qquad (4\text{-}37)$$

$$\ddot{y} + 2\dot{x} + (c_2 - 1)y = \frac{\partial}{\partial y} \sum_{n \geq 3} c_n \rho^n P_n \left(\frac{x}{\rho}\right)$$

$$\ddot{z} + c_2 z = \frac{\partial}{\partial z} \sum_{n \geq 3} c_n \rho^n P_n \left(\frac{x}{\rho}\right)$$

Where:

$$\rho = x^2 + y^2 + z^2 \qquad (4\text{-}38)$$

$$c_n = \frac{1}{\gamma^3} \left((\pm 1)^n \mu + (-1)^n \frac{(1 - \mu)\gamma^{n+1}}{(1 \mp \gamma)^{n+1}} \right) \qquad (4\text{-}39)$$

With the + is for L1 and − is for L2.

Richardson [51] developed a third-order approximation, as:

$$\ddot{x} - 2\dot{y} - (1 + 2c_2)x = \frac{3}{2}c_3(2x^2 - y^2 - z^2) + 2c_4(2x^2 - 3y^2 - 3z^2) + O(4) \qquad (4\text{-}40)$$

$$\ddot{y} + 2\dot{x} + (c_2 - 1)y = -3c_3 xy - \frac{3}{2}c_4(4x^2 - y^2 - z^2) + O(4)$$

$$\ddot{z} + c_2 z = -3c_3 xz - \frac{3}{2}c_4 z(4x^2 - y^2 - z^2) + O(4)$$

Where $O(4)$ means that the terms of higher order (than 4) are neglected.

The Richardson expansion is the one that is used in this thesis.

4.4.2.2 *Periodic orbit solutions computation*

Thus, before exploring the solutions of the general non-linear systems, it is recommended to look at its periodic solutions. The numerical process relies on the **Lindstedt-Poincaré** method consisting in successive approximations. The methodology starts from a "naïve" solution of the problem, and then, introduces perturbations to the solution. In the CR3BP context, it is considered that non-linearities disturb the eigenvalues of the equations of the linearized system.

In this paragraph, the solutions of the linearized problem are presented, and then the introduction of the frequency perturbations so as to suppress secular terms.

In this case, the linearized equations of motion become:

76

$$\ddot{x} - 2\dot{y} - (1 + 2c_2)x = 0 \qquad\qquad (\text{4-41})$$
$$\ddot{y} + 2\dot{x} + (c_2 - 1)y = 0$$
$$\ddot{z} + c_2 z = 0$$

It can be noticed that the equation along the z-axis is independent from the x and y equations. The z-axis characteristic equation leads to two pure imaginary roots. The eigenvalues of the system (4-41) are:

$$\left(\pm\lambda, \pm i\omega_p, \pm i\omega_{pv}\right)$$

With:

$$\lambda^2 = \frac{c_2 + \sqrt{9c_2^2 - 8c_2}}{2} \qquad\qquad (\text{4-42})$$

$$\omega_p^2 = \frac{2 - c_2 + \sqrt{9c_2^2 - 8c_2}}{2}$$

$$\omega_v^2 = c_2$$

The solution of the linearized system is then:

$$x = A_1 e^{\lambda t} + A_2 e^{-\lambda t} - A_x \cos(\omega_p t + \phi) \qquad\qquad (\text{4-43})$$
$$y = cA_1 e^{\lambda t} - c_2 A_2 e^{-\lambda t} + \kappa A_x \sin(\omega_p t + \phi)$$
$$z = A_z \cos(\omega_v t + \psi)$$

Where A_1, A_2 and c are constants.
When the initial conditions are carefully selected (A_1 and A_2, the hyperbolic amplitudes set to zero), the periodic solutions of the system are:

$$x = -A_x \cos(\omega_p t + \phi) \qquad\qquad (\text{4-44})$$
$$y = \kappa A_x \sin(\omega_p t + \phi)$$
$$z = A_z \cos(\omega_v t + \psi)$$

Where

$$\kappa = \frac{\omega_p^2 + 1 + c_2}{2\omega_p} = \frac{2\lambda}{\lambda^2 + 1 - c_2} \qquad\qquad (\text{4-45})$$

It is then reminded that:
- c_2 is given by (4-39) with n=2
- λ is the positive real root of the characteristic equation of the system.

Remarks:
- A_x, A_z, κ, ϕ and ψ depend on the initial conditions. As a consequence, for trajectories design, those parameters have to be carefully selected to ensure the system to converge towards periodic solutions.
- $(\pm\lambda, \pm i\omega_p, \pm i\omega_{pv},)$ only depend on c_2, that only depends on γ and μ, unique parameters of the system.
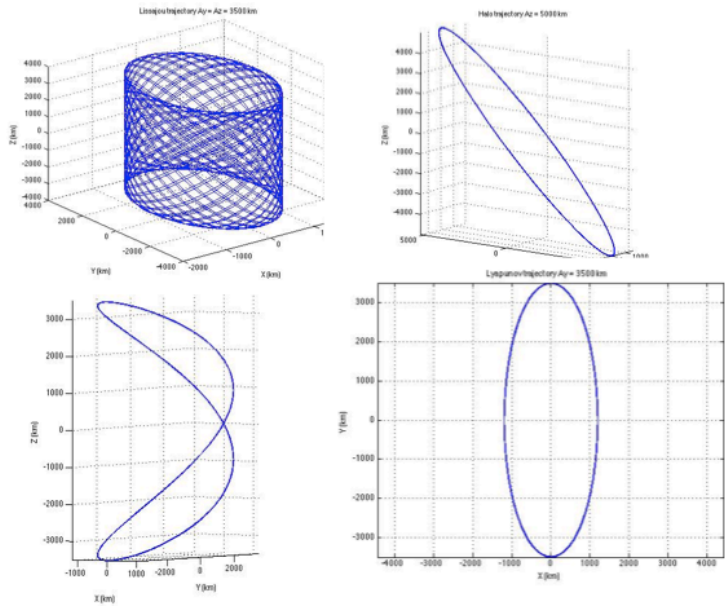
Figure 34 presents examples of periodic orbits around EML2.
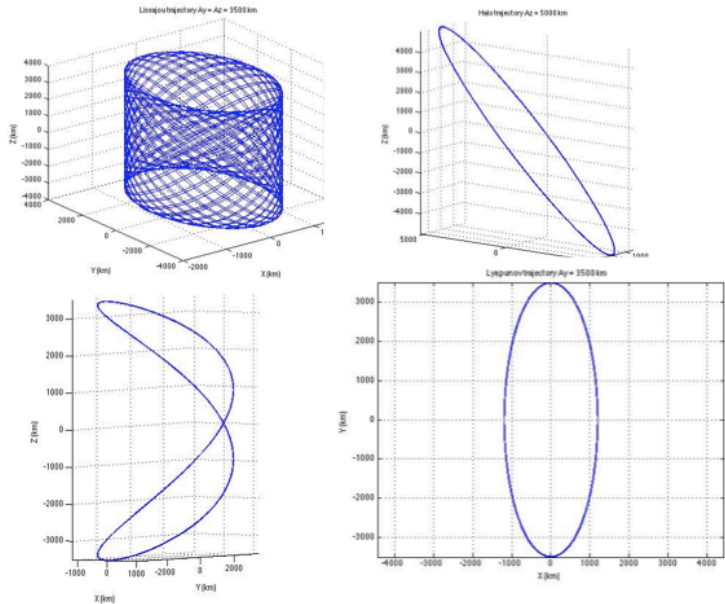
Figure 34: Examples of periodic orbits around EML2
(a) Lissajous trajectory with $A_y = A_z = 3500$ km
(b) Halo trajectory $A_z = 5000$ km
(c) Eight shape Lissajous trajectory with $A_y = A_z = 3500$ km
(d) Lyapunov trajectory with $A_y = 3500$ km

Then, the frequency of the periodic solutions (4-44) is modified, thanks to a new variable :

$$\tau = \nu t \qquad\qquad (4\text{-}46)$$

Where

$$\nu = 1 + \sum_{n \geq 1} \nu_n \; with \; \nu_n < 1 \qquad\qquad (4\text{-}47)$$

The A_x and A_z elongations are assumed to be large enough so that ν_n can be neglected according to them. The computations of the solutions in the general case are not provided in this thesis, since they were already deeply developed in many papers (see [27] and [46]). The next paragraph detailed the example of the Halo orbit.

4.4.2.3 Halo orbits computation

The results presented in the previous paragraph are now applied to the particular case of the Halo orbits, based on Richardson third-order approximation (see Appendix 3). In the particular case of the Halo orbit, the first mandatory approximation to find a solution is to assume that:

$$\omega_p = \omega_\nu \qquad\qquad (4\text{-}48)$$

A correction term must be then introduced:

$$\Delta = \omega_p^2 - c_2 = \omega_p^2 - \omega_\nu^2 \qquad\qquad (4\text{-}49)$$

This leads to the conclusion that A_x and A_z are linked by a relationship, as:

$$l_1 A_x^2 + l_2 A_z^2 + \Delta = 0 \qquad\qquad (4\text{-}50)$$

Where l_1 and l_2 are given in Appendix 3.

The minimum value for A_x elongation, for $A_z > 0$ is: $\sqrt{\dfrac{\Delta}{l_1}}$

Moreover,

$$\delta_m = \psi - \phi = m\frac{\pi}{2} \; m = 1,3 \qquad\qquad (4\text{-}51)$$

Two mirror solutions are obtained, depending on m:

- For m=1, $\delta_m > 0$, the solutions are Northern Halo orbits for EML2 (respectively, Southern orbits for EML1)
- For m=3, $\delta_m < 0$, the solutions are Southern Halo orbits for EML2 (respectively, Northern orbits for EML1)

As a synthesis a Halo obit is fully defined by two parameters: A_z and m.

The Halo orbit period can be computed as a function of its maximal elongation along z-axis, A_z, with:

$$T = \frac{2\pi}{\omega_p \upsilon} \qquad (4\text{-}52)$$

With

$$\upsilon = s_1 A_x^2 + s_2 A_z^2 \qquad (4\text{-}53)$$

Where s_1 and s_2 are given in Appendix 3.

Figure 35 presents a family of Halo orbits around EML2 for several values of A_z (from A_z = 5000 to 30000 km).
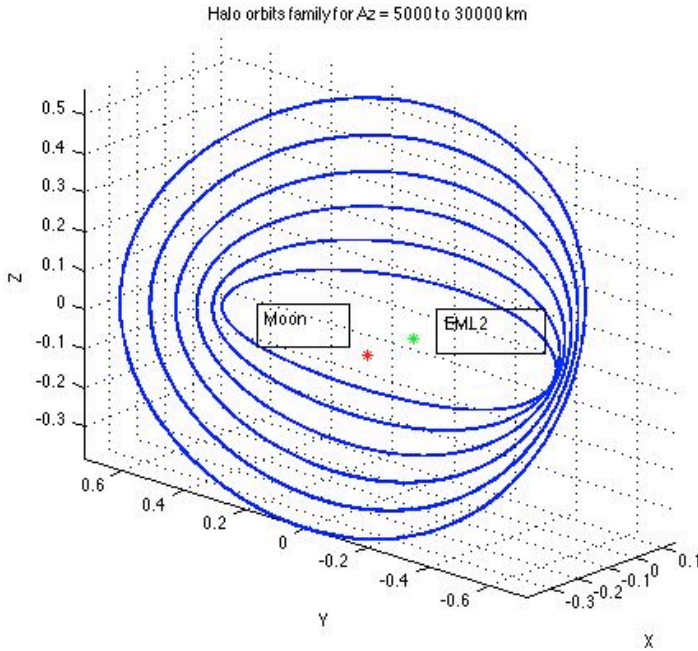
Figure 35: Halo orbits family for A_z = 5000 to 30000 km

4.4.2.4 Shooting method

The methodology applied to compute an accurate periodic orbit is denominated as a differential correction (or a shooting method). A shooting method consists in finding the zeros of an associate function to a system of differential equations. It is very sensitive to initial conditions. In the CR3BP context, this requires:

-   Initial conditions: state vector when t = t₀, $X_0 = (x_0, y_0, z_0, \dot{x}_0, \dot{y}_0, \dot{z}_0)$,
-   A first guess: an analytical approximation of the orbit as a reference trajectory.

The concept of the differential correction is to add a small change in the initial state to target the desired final point. The process will converge by iteration. But before, applying this process to the Halo orbit, flow map and state transition matrix have to be defined, as key elements of the methodology.

4.4.2.4.1 Flow map

The flow map, $\phi(t, t_0, X_0)$, of the dynamic systems (4-14) corresponds to all the trajectories that start from a state $X(t_0) = X_0$, where t₀ represents the initial time and t

the final time. The flow map describes the state of the particle from its initial location at t_0 to its final one at t. The trajectory complies with the natural dynamics, as:

$$\dot{X} = f(X) \qquad\qquad (4\text{-}54)$$

To simplify the notations, the flow map will be denoted: $\phi(t, X_0)$. Then, the flow map satisfies:

$$\frac{d\phi(t, X_0)}{dt} = f(\phi(t, X_0)), \qquad with\ \phi(t_0, X_0) = X_0 \qquad\qquad (4\text{-}55)$$

4.4.2.4.2 State transition matrix

The flow map, of course, satisfies the equations of motion. As a consequence, when a trajectory starts with a small deviation of the initial conditions $X_0 + \delta X_0$, then a displacement, at t, can be observed:

$$\delta X(t) = \phi(t, X_0 + \delta X_0) - \phi(t, X_0) \qquad\qquad (4\text{-}56)$$

Then (4-56) can be expanded in Taylor series as:

$$\delta X(t) = \frac{\partial \phi}{\partial X_0}(t, X_0)\delta X_0 + o\big(\delta X_0{}^2\big) \approx \Phi(t, t_0)\delta X_0 \qquad\qquad (4\text{-}57)$$

$\Phi(t, t_0)$ is the state transition matrix. It gives the linear relationship between the initial small displacement δX_0 and the final small displacement δX.

$\phi(t, X_0)$ is also a solution of the linearized equations (4-55). As a consequence, the state transition matrix solves the following problem:

$$\dot{\Phi}(t, t_0) = Df\big(X(t)\big)\Phi(t, t_0)\ with\ \ \Phi(t_0, t_0) = I \qquad\qquad (4\text{-}58)$$

Where $Df\big(X(t)\big)$ is the Jacobian matrix of the flow map.

4.4.2.4.3 Halo orbit application

In the Halo orbit case, the process has been clearly explained by K. Howell [47]. A synthesis is presented here after:
- Initial conditions are $X_0 = (x_0, 0, z_0, 0, \dot{y}_0, 0)$. The initial vector is then perpendicular to the x-z plane (in the rotating plane, centered on the Lagrangian point). See Figure 33.
- The initial guess is the Halo orbit, computed thanks to the Richardson third-order approximation (refer (4-44)). The orbit period is T (4-52). At T/2, the state vector of the particle is

$$X_{T/_2} = (x, 0, z, 0, \dot{y}, 0) \qquad (4\text{-}59)$$

Nevertheless, by integrating with the Runge-Kutta process the third-order approximation of the equations of motion, the state vector obtained after T/2 is not perfect, since $\dot{x}$ and $\dot{z}$ are not low enough. As a consequence, a shooting method has to be performed so as to find the total correction to be applied on the initial conditions to find the target final conditions at T/2. The orbit is symmetric about the x-z plane, and then it is not necessary to compute it on the entire T period.

The state transition matrix is given by:

$$\Phi = \begin{pmatrix} 0 & I \\ U_{xx} & -2\Omega \end{pmatrix} \qquad (4\text{-}60)$$

Where:
- 0 is a 3x3 zero matrix
- I is the 3x3 identity matrix
- $\Omega = \begin{pmatrix} 0 & 1 & 0 \\ -1 & 0 & 0 \\ 0 & 0 & 0 \end{pmatrix}$
- U_{xx} is a matrix composed of the second partial derivatives of the effective potential with respect to x, y and z.

The corrections can be applied on the initial state $(\delta x_0, 0, \delta z_0, 0, \delta \dot{y}_0, 0)$ so as to reduce $\delta \dot{x}$ and $\delta \dot{z}$. The initial state is then related to the final state thanks to the equations of motion, through a 2x3 matrix. As a consequence, it is recommended to constrain one of the initial states, so as to invert a 2x2 matrix.

For example, when z_0 is fixed to 0, changes will be performed on δx_0 and $\delta \dot{y}_0$, as:

$$\begin{pmatrix} \delta \dot{x} \\ \delta \dot{z} \end{pmatrix} = \left[\begin{pmatrix} \dfrac{\partial \phi}{\partial \dot{x} \partial x} & \dfrac{\partial \phi}{\partial \dot{x} \partial \dot{y}} \\ \dfrac{\partial \phi}{\partial \dot{x} \partial z} & \dfrac{\partial \phi}{\partial \dot{x} \partial \dot{z}} \end{pmatrix} - \dfrac{1}{\dot{y}} \begin{pmatrix} \dot{x} \\ \dot{y} \end{pmatrix} \begin{pmatrix} \dfrac{\partial \phi}{\partial y \partial x} & \dfrac{\partial \phi}{\partial y \partial \dot{y}} \end{pmatrix} \right] \begin{pmatrix} \delta x_0 \\ \delta \dot{y}_0 \end{pmatrix} \qquad (4\text{-}61)$$

This methodology will be applied as many times as required to obtain the targeted values of $\dot{x}$ and $\delta \dot{z}$. The initial and final state vectors are then known and the orbit can be computed thanks to integration with a Runge-Kutta process of the equations of motion.

4.5 End-to-end transfer trajectories
The previous paragraph 4.4 discusses the different types of orbits that exist at a Lagrangian point, their analytical formulation and their numerical computation. Designing a space mission requires not only to know the final goal with accuracy but

also to determine the path to reach this final goal. Moreover, in the Human spaceflight context, it is also mandatory to explain how to come back.

The methodology presented hereafter deals with slow transfers, when duration may be counted in weeks or months. On the contrary, "fast" transfers will take less then two weeks. This point is discussed in details in paragraph 5.2.

The concept that is there developed is to use the targeted orbits (4-20) to reach and leave the vicinity of the Lagrangian point. Actually, the stable manifold will converge to the desired orbit, while the unstable manifold will quit the region of the Lagrangian point.

The concept of unstable and stable manifolds will be first defined. Then, it will be explained how to find intersections between manifolds. Two fundamental tools are presented the Monodromy matrix and the Poincaré map.

4.5.1   Escape and no-escape directions

From (4-43), the expression of the solutions of the linearized system of equations, it can be concluded that a small variation of the trajectory can cause a small component A_1 and the trajectory becomes unstable. This concept is then used to compute trajectories that converge towards the orbit around the Lagrangian point (stable manifold) and departs from the orbit (unstable manifold).

For a given orbit, the stable (resp. unstable) invariant manifold is defined as the sub-space of the 6-dimensional phase space consisting of all vectors whose future (resp. past) positions converge to the periodic orbit. The corresponding trajectories in the vicinity of the orbit are often called asymptotic orbits since they slowly converge to or diverge from the orbit. Invariant manifolds can be seen as 4-dimensional spaces, topologically equivalent to $S^3 \times \mathbb{R}$ in the 5-dimensional energy manifold $\mathcal{M}(\mu, e)$ (4-20). These structures provide dynamical channels beneficial to the design of energy efficient trajectories (in term of fuel consumption) [14]. They are often referred to as "tubes" since they exhibit tube-like shapes when projected onto the 3-dimensional position space.

To compute the invariant manifolds, the equations of motion can be propagated. However, given the asymptotic behavior of the motion at arrival or departure, manifolds are not generated directly from a position on the orbit. Usually, a linear approximation of the manifold is calculated for any given point on the orbit using tools from the theory of the dynamical stability of systems. Then, the starting point of the trajectory is taken at a distance d_M in the initial stable or unstable direction given by the linear approximation (see Figure 37 for a visualization of d_M). For further details on the subject, see e.g. [27] and [52]. Figure 36 shows an example of the projection onto the position space of the stable (green) and unstable (red) manifolds of an EML2 southern Halo orbit (blue) with an amplitude A_z = 5000 km.
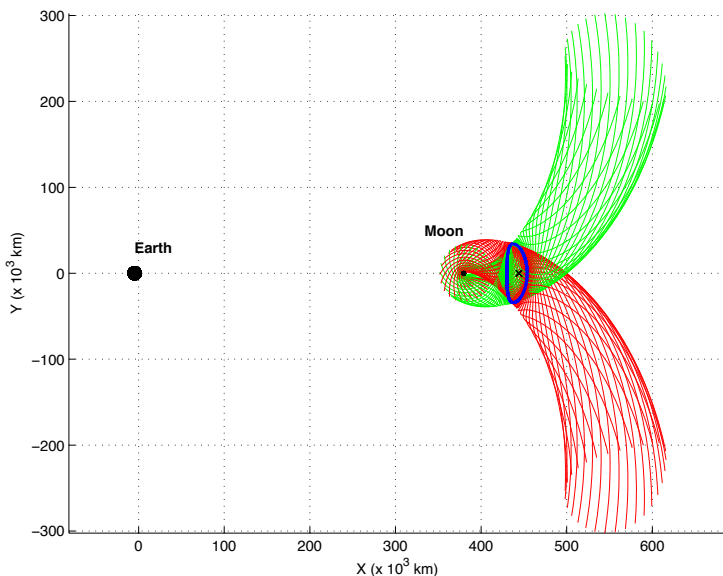
Figure 36: Stable (green) and unstable (red) manifold for an EML2 southern Halo orbit ($A_z = 5000$ km)
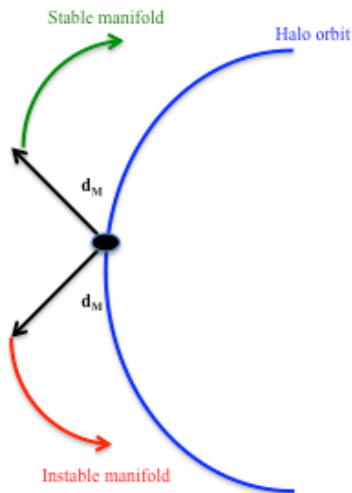
Figure 37: d_M distance definition

The manifolds are trajectories, solutions of the system of motion equations. For example, a simplified analytical expression of the manifolds can be obtained while taking into account the linearized system. The expression is identical to (4-43). The initial conditions are chosen so that this time, A_1 and A_2 are not null. The variation of the initial conditions lead to the tubes "structure".

86

The unstable manifold is obtained in the forward time (t>0, $A_1 \neq 0$, $A_2 = 0$), while the stable manifold is computed in backward time (t<0, $A_1 = 0$, $A_2 = 0$).

4.5.2 Monodromy matrix

The concept of Monodromy matrix is applied to analyze the stability of a trajectory according to the impact of the initial conditions variation on the flow. It is classically employed for the linear time periodic systems (see [45])

A particular solution X^* of the system is considered: its stability is evaluated thanks to the displacement after one period, T, when the trajectory starts from $X_0^* + \delta X_0$.

This matrix is defined by:

$$M = \Phi(T, 0) = \frac{\partial \phi(T, X_0^*)}{\partial X_0} \qquad (4\text{-}62)$$

This matrix corresponds to the state transition matrix after one period. Its properties render the system stability thanks to the growing or decreasing of the initial disturbance (δX_0).

It can be demonstrated that the Monodromy matrix admits n eigenvalues ($\lambda_1, \dots \lambda_n$) and has always one eigenvalue, λ_n, equal to 1.

Then, the stability of the periodic solution can be determined thanks to the other eigenvalues of the Monodromy matrix, ($\lambda_1, \dots \lambda_{n-1}$):

- the solution is stable when $\forall i = 1 \dots n - 1, |\lambda_i| < 1$
- the solution is unstable when $\exists i, 1 \leq i \leq n - 1, |\lambda_i| > 1$

4.5.3 Poincaré Map

The Poincaré Map or Poincaré section is a mathematical concept that is often used in System Dynamics theory, to discuss stability considerations. In this project, as it will be developed in paragraph 4.5.4, the Poincaré section will be used to connect trajectories, as solution of the system of equations.

Considering:
- $\phi(t, X_0)$, a trajectory representing one solution of the system with X_0 as initial conditions,
- Σ_p, a hypersurface.

The Poincaré map, P_{Σ_p}, is defined as the set of points of the trajectory, $\phi(t, X_0)$, when it intersects the hypersurface, Σ_p with:

$$P_{\Sigma_p} = \{X = (x, y, z, \dot{x}, \dot{y}, \dot{z})/X \in \Sigma_p \ and \ \dot{X} = f(X)\} \qquad (4\text{-}63)$$

On a Poincaré map, the flow can be observed in a lower dimensional space. Figure 38

presents an example of a Poincaré map: it is composed of the X_n, points of the flow $\phi(t, X_0)$, when it intersects the hypersurface Σ_p.
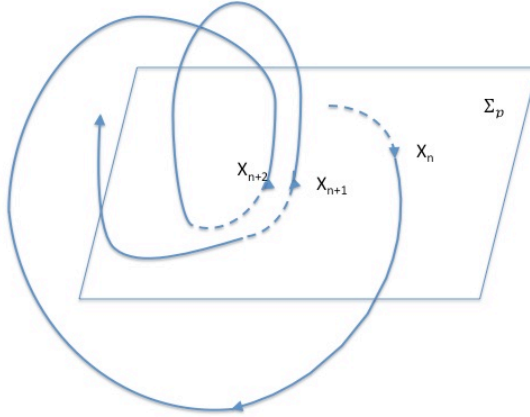
Figure 38: Example of Poincaré section

4.5.4 Connection between manifolds

As demonstrated by Koon et al [53], an intersection between two manifolds may exist. Thus, it provides an asymptotic path from one periodic solution to another one. If both manifolds are related to the same orbit, it is a homoclinic connection. On the contrary, when the manifolds are linked to different orbits, the connection is heteroclinic.

Connections between two manifolds can be obtained by using a Poincaré map (see 4.5.3). Finding the intersection between two manifolds is not a trivial question as far as the spatial problem is considered. Nevertheless, this concept is fundamental to design low cost transfer trajectories in the Earth-Moon system (see 5.2) and will be extended to rendezvous trajectories in the vicinity of the Lagrangian point (see 5.3).
The Figure 39 presents an example of heteroclinic connection from a Halo orbit (Northern type, $A_z = 15000$km) around EML1 to a Halo orbit (Northern type, $A_z = 8000$km) around EML2. The intersection is scheduled at a Poincaré map center on the Moon.
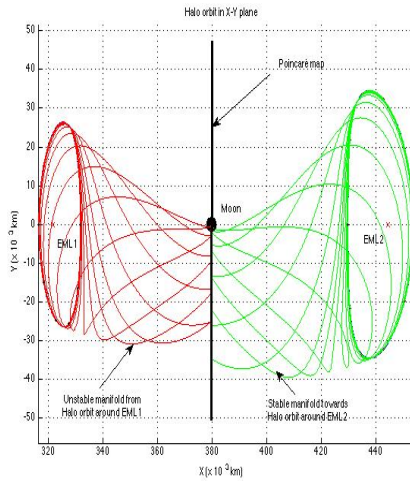
Figure 39: Example of heteroclinic connections from EML1 to EML2 (from B. Le Bihan, PhD student at ISAE-Supaero)

As a consequence, Poincaré map as a support of the manifolds intersection must be carefully defined. The Poincaré must be determined by its location in the current reference frame. The results of the mission analysis directly depend on its position. As far as the numerical computation is concerned, the concept of intersection is not as ideal as in mathematics. Actually, integration of the equations of motion to determine the evolution of the particle state in time must be performed thanks to the solver function. For example, this project relies on the Runge-Kutta process, ODE45, developed in Matlab. The solver implies that all components (time and state) have been discretized. As a consequence, the concept of intersection will then be replaced by the minimization of the distance between the positions on both manifolds at the Poincaré map location.

89
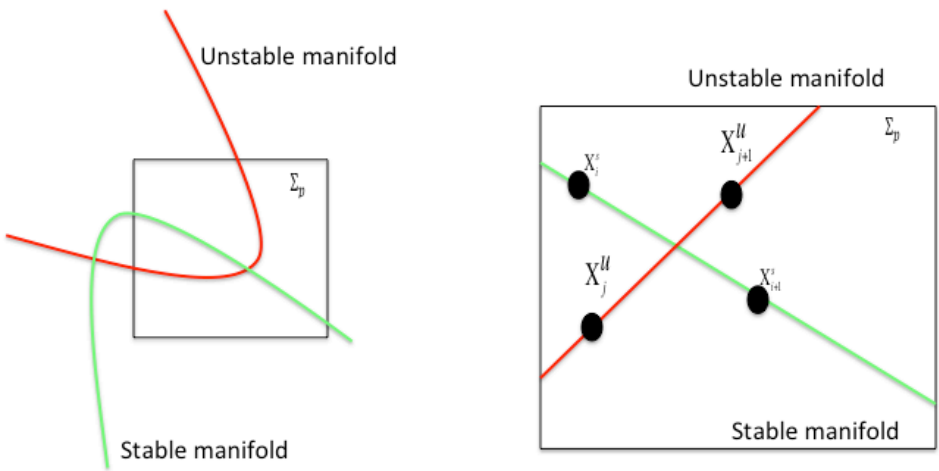
Figure 40: Schematic representation of the manifolds intersection on the
Poincaré map

Figure 40 provides a schematic representation of the manifolds intersection on the
Poincaré map. The left part presents the ideal mathematics concept, while on the right
part, the limitations due to the numerical discretization is shown.

4.6   Modeling limitations

The CR3BP is an idealization, but comparisons with existing numerical models taking
into account influence of other gravitational bodies like the Sun, more precise
trajectories, anomalies in gravitational fields, … lead to conclude that the CR3BP is
sufficient for the current study purposes.

For example, in the mission analysis paragraph (see 5), ephemerides of the position of
the Moon, the Sun and The Earth as provided in the JPL model or the IMCCE catalog
are not considered. Moreover, the slight inclination (about 5°) between the Earth-
Moon plane and the Earth-Sun plane is neglected. As a consequence, it is suggested
that further analyses shall refine the trajectories in more realistic models. But it will
add new constraints since the models based on ephemerides are time dependent.

The methodology applied for transfer and rendezvous trajectories are based on the
Three-body problem, but an extension to the Four-body problem (regarding the
influence of the Earth, the Moon and the Sun on the particle trajectory) could be
interesting.

4.7   Genetic algorithms

The first parts of this theoretical background presented the mathematical concepts
necessary to understand trajectories of the N-Body problem. Those abstract ideas are
necessary, but not sufficient to find the best trajectory for an entire round-trip from
LEO to EML2 and return. Actually, they lead to recommend a good strategy for the

90

travel, but they cannot ensure that the recommended one will minimize the fuel consumption (delta-v) and the duration.

By consequence, strategies must be then applied to optimize the trajectory according to the proposed scenario. In the project context, the solutions to be optimized are complex, non-linear, depending on heterogeneous types of initial conditions. Therefore, it has been decided to employ genetic algorithms to perform the optimization.

In [54], E. Goldberg was the first to theorize the genetic algorithms, as a methodology to generate solutions to optimization problems that can not be solved by exact methods. This process is inspired from natural evolution.

The methodology is based on five main steps :
- Initialization
- Evaluation
- Selection
- Genetic operators
- Termination

Those steps will now be detailled and are sumed up in Figure 41.
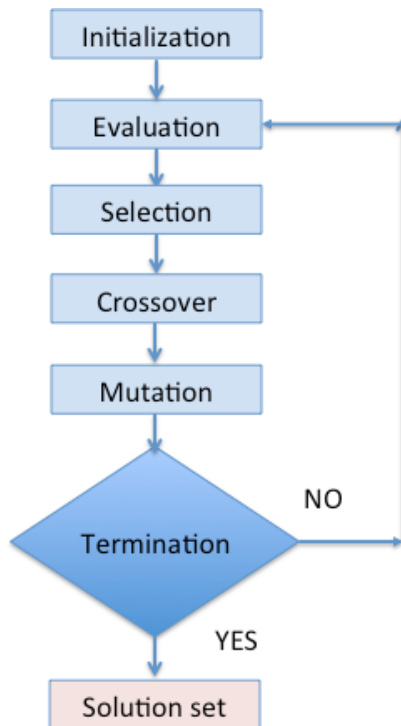
Figure 41: Genetic algorithm process

4.7.1 Initialization

The algorithm starts with the composition of the **initial population**, constituted of individuals generated at random. They are characterized by a set of properties. They are not supposed to correspond to the best solutions of the problem, but to fit with the required performances.

4.7.2 Evaluation

Once the intial population has been generated, all the individuals of the initial populsation must be evaluated so as to sort out the most promising ones.

4.7.3 Selection

Each individual of a generation is then evaluated thanks to its **fitness**. Several selection methodologies exist, and are not described here. Some methods focus the most promising individuals due to their own fitness, while other methods sort out the individual at random.

4.7.4 Genetic operators

Then, a new **generation** is produced as a combination of individuals of the initial population. Successive generations will be then created in an interative process. Since the second generation, the genetic operators is composed of two sub-stpes : the **crossover** and the **mutation**.

Crossover consists in combining individuals two-by-two to create new indiviuals.

Mutation lies in the random evolution of existing individuals. It is not certain that resulting individuals will be better or worse than the prvious ones, but they will offer new crossover possibilities.

4.7.5 Termination

The process to generate new indivitials is repeated until the termination conditions are reached: when minimal solutions are found, after a certain number of iterations, ….

4.7.6 Application to three-body problem

In this project, the genetic algorithms are employed to find best transfer trajectories to minimize the delta-v (velocity increment) and the duration, since the number of design parameters is very important and the three-body problem admits a great number of local minima.

Applied algorithms are those proposed in Matlab Global Optimization toolbox with the "gamultiobj", that finds the minima of multiple functions using genetic algorithm.

In the process applied for transfer optimization from LEO to EML2 (as described in 5) the five main steps are followed with:

- The **<u>initial population</u>** is composed at random by individuals (trajectories), characterized by three parameters: the initial angular position at LEO, the angular position of the Poincaré Map and the initial velocity increment to depart from Earth vicinity. The initial population size is then limited to 100 individuals so as to reduce the computation time.
- The individuals **<u>evaluation</u>** is performed thanks to fitness functions computing the gap distance between the two manifolds at the Poincaré section and a mixed gap combining distance and velocity.
- Selection, crossover and mutation are encapsulated in the "gamultiobj" Matlab function. Its outputs are individuals on the Pareto frontier and their objectives the other individuals of the population that fit with the fitness criteria. The Pareto frontier is the set of allocations of resources (here delta-V and duration) in which it is impossible to make any one individual better or worse off than the others (see Figure 42 for example).
- **<u>Termination:</u>** The maximal number of iterations is fixed at 30.

Figure 42 presents an example of Pareto frontier obtained to find best trajectory as far as the velocity increment (ΔV in km/s) and the time of flight (duration in days) are concerned, for the lunar flyby strategy (see 5.2.3), for several value of the Halo orbit elongation (A_z).
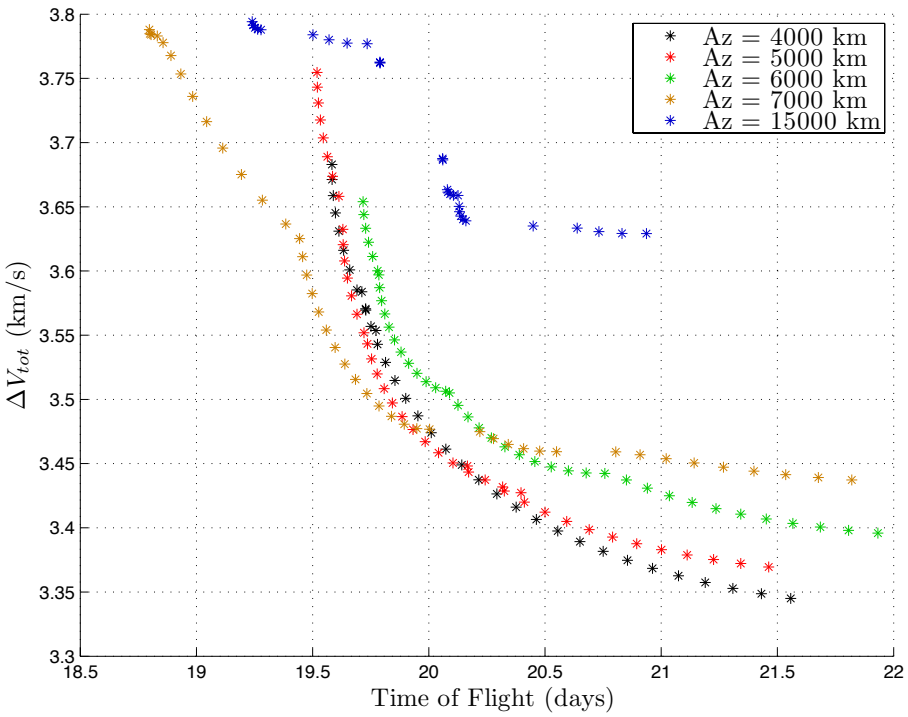
Figure 42: Pareto fronts for lunar flyby strategy

Results provided on Figure 42 are provided as an illustration. Velocity increment and time of flight performances obtained for THOR mission are commented and compared to bibliographical results in the next chapter (see particularly, 5.2).

Of course, genetic algorithms have limitations. It can be then recommended to extend the project by seeking and applying different optimization methodologies in order to compare their performances.

5   Mission analysis

Recommendations extracted from Stakeholder needs analysis (see 3.1) led to assume that the THOR space station should be rotating on a Halo orbit around EML2. The operational phase of the Space station life-profile shall be composed by at least three nominal scenarios:

- Scenario 1: the Space Station assembly
- Scenario 2: the resupply cargo delivery
- Scenario 3: the crew rotation

Station disposal scenario is not developed in this PhD, even if it would lead to a very interesting analysis. Actually, several possible sequences of events can be imagined to manage the end of life of such a station: to get it back to the Earth, to maintain it in EML2, to transfer it to another destination in the solar system so as to perform science…

The following figure presents one example of operational phase decomposition with an assembly in LEO of the Space Station, a lunar flyby transfer for the crew vehicle and a weak-stability trajectory for the cargo.
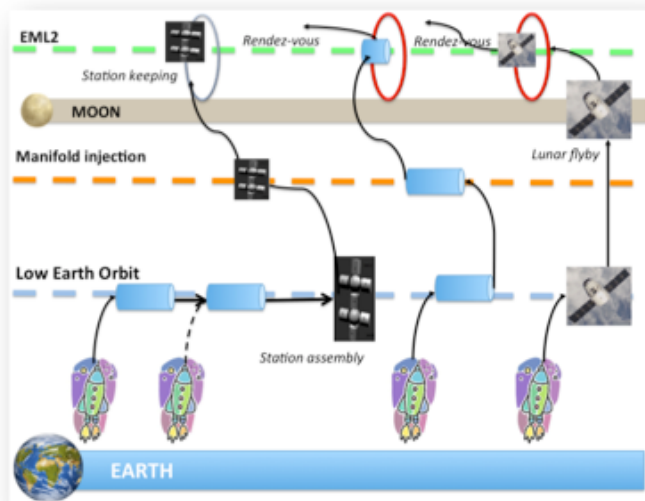
Figure 43: Example of operational phase decomposition

Common legs between all the three scenarios are: transfer from LEO to EML2 and rendezvous. Mastery of rendezvous techniques is therefore crucial to allow the space station to dock with cargo spacecraft and to exchange its crew.

The main goal of this chapter is to describe the methodology to plan a rendezvous in EML2 between the THOR space station and the delivery cargo or the crew vehicle.

This chapter is divided in four parts:
- The first one states the global optimization problem
- The second part deals with the optimization of the transfer leg
- The third part focuses on the best rendezvous strategy
- The fourth part presents results for several scenarios of the study case

5.1 Optimization problem statement

The goal of this study is to design trajectories of the Station, the cargo and the crew vehicle from a prescribed initial Low Earth Orbit to the vicinity of the Earth-Moon Lagrangian point number 2. The travel is supposed to be performed exclusively by high-thrust. All types of trajectories require powerful propulsion for impulsive increment of velocity. As the amount of fuel (mass criteria, cost criteria) is limited and the time of flight must be as short as possible so as to reduce the crew exposition to radiations. The selected strategy must minimize the duration and the cost (through delta-v).

In order to compare the possible scenarios, the cost function is computed as follows

$$\Delta v_{tot} = \Delta v_{Launch} + \Delta v_{SK\_LEO} + \Delta v_{transfer} + \Delta v_{cargo} + \Delta v_{crew} \quad (5\text{-}1)$$

Where :
- Δv_{launch} is the total delta-v for all the launches
- Δv_{SK_LEO} is the total delta-v for assembly and station-keeping in LEO before transfer
- $\Delta v_{transfer}$ is the total delta-v for all the THOR Space Station modules transfer
- Δv_{cargo} is the total delta-v for all the cargo encompassing launch, LEO station-keeping, transfer, rendezvous in EML2 and return
- Δv_{crew} is the total delta-v for all the crew trips encompassing launch, LEO station-keeping, transfer, rendezvous in EML2 and return without re-entry.

As launch cost surpasses and crushes all the other delta-v, it will not be taken into account for the scenarios comparison. Moreover, efforts must be condensed on transfer and rendezvous. As a consequence, to find the best global strategy for the entire mission of the THOR Space station corresponds to:
- Minimize Δv_{SK_LEO} (optimal solution for the Station assembly),
- Minimize $\Delta v_{transfer}$ (optimal solution for the Station modules transfer),
- Minimize Δv_{cargo}
- Minimize Δv_{crew} and crew transfer duration

The global optimization problem is split into four optimization sub-problems, of different types. Moreover, the cargo and crew sub-problems have also to be decomposed in sub-sub-problems. Once again, as the launch velocity increment would

96

eclipse all other costs, it is not taken into account. So optimization efforts will focus on transfer and rendezvous.

The main goal of the project is to find the optimal scenario, one for the assembly of the THOR space station and one for its resupply (cargo and crew). As a consequence, it is essential to compute performances (delta-v and duration) for all identified legs. However, it has been elected in this project to apply efficient modeling strategies that can lead rapidly to a good numerical estimation. The aim is to obtain accurate orders of magnitude, so as to verify the feasibility of the strategies and compare scenarios. Future additional projects can then be carried out so as to improve performances calculation accuracy.

5.2   Transfer strategies

To deploy, maintain and operate a space station located on Halo orbit around EML2, a global trajectory has to be selected. Even if launch and station keeping (in LEO or at EML) are critical legs, the focus is set in this part on the transfer and in the next one, on the rendezvous.

5.2.1   Transfer strategies comparison

As far as transfer strategy is concerned, a wide literature already exists and enlightens that four main strategies are possible: the direct transfer, the indirect transfer, the lunar flyby and the weak stability boundary transfer. The first three strategies fit into the Earth-Moon Three-Body Problem, whereas the last one patches two Three-Body problems.

In this paragraph, the four strategies are shortly described. Then a comparison is provided based on a bibliographical survey.

5.2.1.1   Direct transfer

Direct transfer consists in displacing a spacecraft between two space bodies with two direct ballistic maneuvers. It is the most fuel-consuming strategy since it does not take benefit of the manifolds.

In his last book [11], J. Parker defines a direct transfer in the Earth – Moon system as a trajectory that "*requires only the gravitational attraction of the Earth and the Moon* […] and other forces (such as the Sun or many spacecraft events) *may be considered to be perturbations*". In the direct transfer case, the required $\Delta v_{\text{transfer}}$ from the LEO to the Halo orbit is around 4000 - 4500 m/s, with transfer duration between 3 and 5 days.

5.2.1.2   Indirect transfer

The indirect transfer strategy main goal is to deposit the spacecraft at an optimized point to enter the manifold and let it glide until it reaches the selected orbit. The first step of these methods consists in generating many entrance points along the manifold in order to select the one which will lead to a minimum $\Delta v_{\text{transfer}}$ without any assumption on the position of these entrance points. In other words, the time of flight on the manifold is initially let free to vary.

For each manifold entrance point, the boosts to leave the LEO and to enter the

97

manifold will be different, the main objective being to minimize their sum. Some research teams have used this method, generating many entrance points and choosing the best trajectories among their results [55]. With this strategy, the total needed $\Delta v_{transfer}$ from the LEO to the Halo orbit is around 3200-3300 m/s, but the time of flight increases, between 50 and 150 days approximately.

Bernelli-Zazzera [26] developed an optimization process for this method with the time of flight on the manifold as a decision variable, using genetic algorithms and sequential programming. Without any additional gravitational assist from the Moon or the Sun, he computed several low-cost trajectories with $\Delta v_{transfer}$ close to 3200 m/s.

5.2.1.3 Lunar flyby

In the Lunar flyby strategy, the manifold entrance point is in the Moon vicinity in order to benefit from its slingshot effect to get into the manifold towards the Halo orbit. In this strategy, the entrance point in the manifold is chosen close to the Moon and is not a free parameter anymore. Thus, the key parameters are the altitude of the lunar flyby and the angle relative to the Moon with which the spacecraft reaches the manifold. This strategy leads to a good compromise between the $\Delta v_{transfer}$ and the time of flight. Recent publications give $\Delta v_{transfer}$ of 3300-3400 m/s approximately, for a time of flight between 10 and 25 days [25], [56] and [57].

5.2.1.4 Weak Stability Boundary transfer

Belbruno ([58] and [59]) developed the concept of Weak Stability Boundary transfer strategy. This methodology uses the gravitational influence of the Sun to lower the required fuel. For such a transfer, an extension of the C3RBP is needed: as a first approach, two patched Three-Body problems (Sun-Earth-Spacecraft and Earth-Moon-Spacecraft) are modeled to take into account the influence of the Sun, the Earth and the Moon. The Weak Stability Boundary transfer strategy utilizes a property of another manifold, the stable one from the Sun-Earth system. In this Sun-Earth 3-body problem, Earth is the smallest primary: as a consequence, this manifold comes much closer to Earth than the Earth-Moon manifolds. It is then much easier in terms of $\Delta v_{transfer}$ to reach this particular manifold and to make benefit of its rich dynamics in order to reduce the cost. The principle of this strategy is to get an advantage of the « twisting » properties of trajectories near the Sun-Earth manifold [27] so as to leave LEO with a first maneuver and then enter the Earth-Moon stable manifold with or without a new maneuver.

This fourth strategy is definitely the cheapest, with values of $\Delta v_{transfer}$ around 3100-3200 m/s. Lasting between 80 and 120 days, it is also one of the slowest possible transfers.

5.2.1.5 Return trajectories

As the project lies in the Human Spaceflight context, the way back from EML2 to Earth must be taken into account for the crew vehicle and the resupply cargo. The

return trajectories from the Halo orbit to LEO can use exactly the same trajectories as described above, provided the roles of unstable and stable manifolds are reversed. Instead of using the stable manifold to asymptotically get to the Halo orbit, the unstable manifold will be used.

When considering the Earth-Moon-spacecraft 3-body problem, the theorem of image trajectories [60] can be used. This theorem states that if a trajectory is feasible in the Earth-Moon system, its image relative to the plane containing the Earth-Moon axis and orthogonal to the plane of rotation of the Moon around Earth is also feasible if flown in the opposite direction. More recent results [61] point out that optimum Earth-Moon and Moon-Earth trajectories are mirror images of one another.

5.2.1.6 Transfer strategies selection

Bibliographical survey led to compare transfer strategies. Results are provided on Figure 44: fuel cost as a function a time of flight.
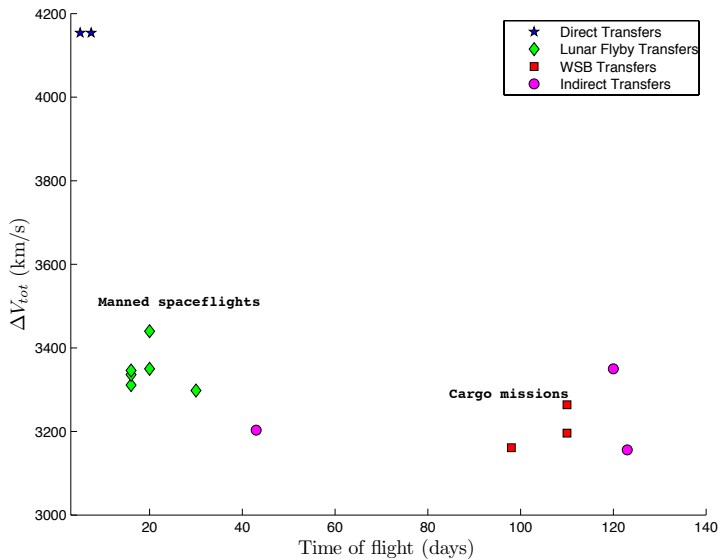
Figure 44: Comparison of transfer strategies: fuel cost as a function of the time of flight

The main recommendations from this survey are to consider a lunar flyby for human spaceflight (crew vehicle trajectories) and Weak Stability transfer for unmanned system (Station modules and cargo).

The strategies are mainly evaluated thanks to two main criteria: duration (total time of flight and delta-v). Comparison of those four strategies has been performed and the main conclusions are:

99

- As the travel is symmetric, it is enough to focus only on one way. The return will be deduced while using the same trajectory but with a travel on the unstable manifold.
- As the duration criteria is the most important in case of human spaceflight, the crew vehicle trajectory shall be sized thanks to lunar flyby strategy.
- As the consumption is the most significant criteria for cargo scenario, weak stability boundary transfer is recommended.

5.2.2   Crew vehicle transfer trajectory

As explained previously, human spaceflights between Earth and the THOR station at EML2 require both a short time of flight and low propellant consumption. Flyby strategy has thus been selected as the best compromise for this type of missions. The influence of the design parameters on the cost of the transfer in terms of time of flight and $\Delta v_{transfer}$ is analyzed. The main objective is to identify optimal trade-offs between duration and fuel consumption.
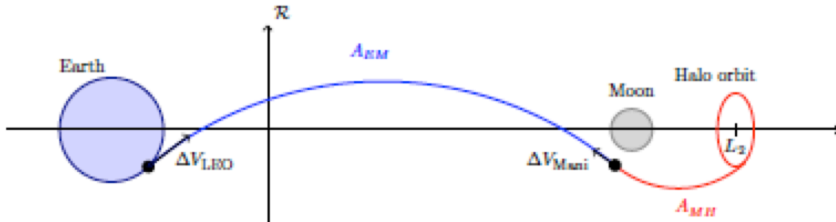
Figure 45: Crew vehicle transfer trajectory definition

Figure 45 presents the transfer trajectory from LEO to Halo orbit in EML2, in case of crew vehicle rotation. On the figure,
- Δv_{LEO} represents the initial increment velocity required to leave the LEO
- Δv_{mani} represents the increment velocity to enter the manifold
- A_{EM} is the Earth-Moon branch
- A_{MH} is the Moon-EML2 branch.

5.2.2.1   Crew vehicle transfer trajectory design parameters

Design parameters are:
- A_z: the maximal elongation (4.4.2.3) along z-axis of the Halo orbit
- m: the orbit family type (m=1 corresponds to the Northern family, m=3 to the Southern family)
- d_M: the distance (4.5.1), between the point on the Halo orbit and the actual starting point of the trajectory on the linear approximation of the stable manifold. See Figure 37 for more details. In the context of numerical simulation, d_M can be considered as a design parameter, despite its non-physical nature. It is chosen in the [1km; 100km] range for which the linear

approximation is valid. Those values have been selected thanks to literature analysis.

- Θ: the angle that gives the position of the departure point on the Halo orbit. It varies in the [0°; 360°] range. The set (A_z, θ) defines a specific unique position on a given Halo orbit. It is precisely defined hereafter.
- ϕ :   the angle providing the angular position of the injection point in the manifold, according to the Moon. This angle is defined on Figure 46. ϕ varies from 0° to 360°.
- h_{LEO} : the altitude of the initial Low Earth parking Orbit. The great influence of the LEO altitude, $h_{LEO,}$ on the overall cost is well-known and expected, see [27, 56, 62], therefore it is fixed to the common value of **200 km** to cancel its influence on the results and on the following discussion.
- φ_{LEO}: the latitude of the parking orbit.
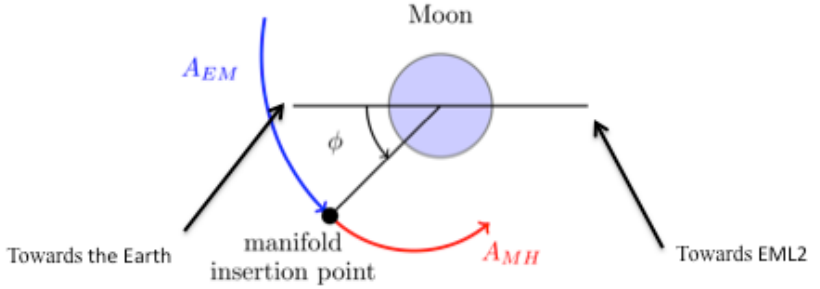
Figure 46: Definition of the angle ϕ

The θ angle is defined thanks to a continuous parameterization of the position on the Halo orbit. This parameterization will be also applied for rendezvous strategies, for departure and arrival. The concept of a pseudo-center of the Halo orbit, $\overrightarrow{X_{pc}}$, see Figure 47, is defined and computed with:

$$\overrightarrow{X_{pc}} = \frac{1}{2}(\vec{X}_0 - \vec{X}_1) \qquad (5\text{-}2)$$

Where $\overrightarrow{X_0}$ and $\overrightarrow{X_1}$ are the two points with y=0 in the Earth-Moon reference frame.

The θ angle is then defined as the angle in the x-y plane between $(\overrightarrow{X_{pc}}, \overrightarrow{X_0})$ axis and $(\overrightarrow{X_{pc}}, \vec{X})$ axis, where $\vec{X}$ denotes the position of the object (THOR station, cargo or crew vehicle) on the Halo orbit. The θ angle is counted clockwise.
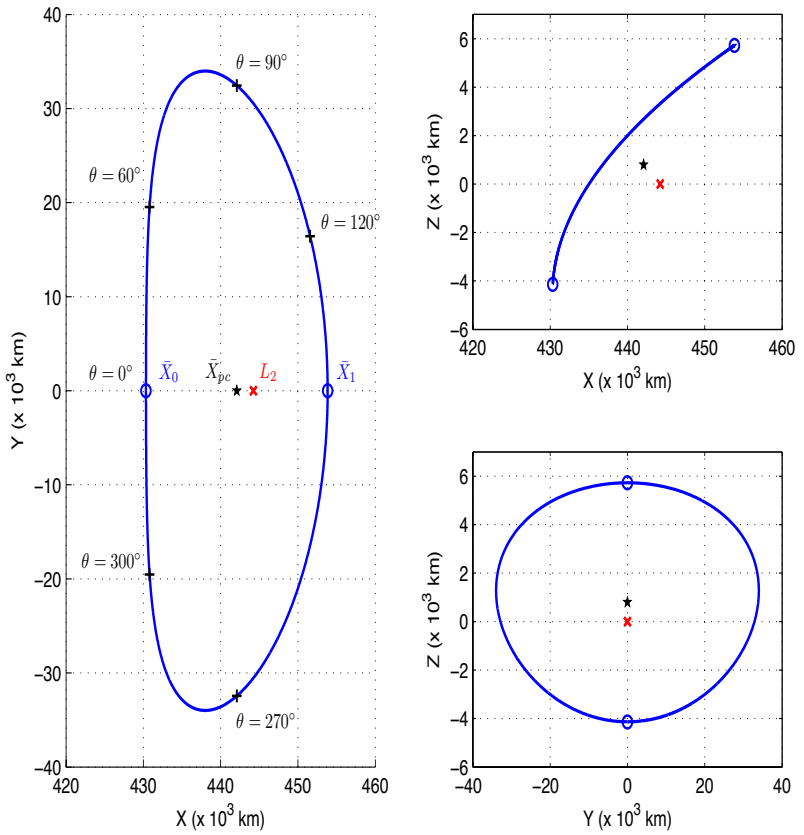
Figure 47: Halo orbit parameterization

The set (A_z, θ, d_M) gives a specific trajectory to/from the Halo orbit.

The under table sums up the assumptions:

Parameter	Value	Units
A_z	[5000; 30000]	km
m	1 or 3	
d_M	[0; 100]	km
Θ	[0; 360]	(°)
ϕ	[0; 360]	(°)
h_{LEO}	200	km
φ_{LEO}	[0; 360]	(°)

Table 8: Crew vehicle transfer design parameters assumptions

102

As consequence, A_z, m, d_M and h_{LEO} are fixed parameters, while θ, ϕ and φ are varying.

Some other parameters have to be fixed, like for example the required precisions to solve the differential equations. Those values are not design parameters but depend on the software selected for the modeling.

5.2.2.2 *Crew vehicle transfer trajectory optimization algorithm*

The main process to compute the entire transfer trajectory from a predefined LEO to a Halo orbit starts with the computation of this Halo orbit, then a backward computation of the stable manifold until a Poincaré map defined, according to the Moon position and a shooting method to obtain the optimal departure point on the LEO minimizing the total delta-v.

The sequence applied to find the best lunar flyby transfer trajectory for a fixed value of the aimed unique angular position on the Halo orbit (defined by A_z, m and θ) is:

- **The 1ˢᵗ step** consists in defining the environmental parameters to describe the selected CR3BP. This step needs as inputs the two primaries data (radius, mass, position…). Outputs are all the parameters of the CR3BP: positions of the Lagrangian points, energy and Jacobi constant of the system, …
- **The 2ⁿᵈ step** is mandatory to get the initial guess of the targeted Halo orbit around the selected Lagrangian point (here EML2). With A_z and m as inputs, outputs provide for example adimensionalized A_z, orbit family.
- **The 3ʳᵈ step** procures from a polynomial interpolation in an abacus of the initial Halo orbit, the Halo orbit and its stable and unstable manifold by differential correction (see 4.4.2). The abacus is restricted to $A_z = 76698$ km for EML2, because of the selected methodology for the initialization of the differential correction scheme. If larger A_z are required, non-classical methodology should be implemented to compute the Halo orbits and its manifolds.
- **The 4ᵗʰ step** computes the intersection of the stable Halo orbit manifold with the Poincaré section that describes the lunar flyby (fixed value of the ϕ). The outputs are the position and the velocity of the stable manifold injection point.
- **The 5ᵗʰ step** computes the Moon-Earth arc from the Poincaré section to a Low Earth orbit. Computation stops when transfer trajectory is tangent to the selected circular orbit. This means the velocity vector is perpendicular to the axis joining the Earth center to the object (h_{LEO}). The methodology drawback is that only one angular position is

selected on the LEO. This angular position ensures to reach the target position on the Halo orbit, but implies operational constraints (like launch window). In the rendezvous case, it is important not to constrain this position so as to ensure the optimal injection position on the Halo orbit. This last point will be detailed in paragraph 5.3. Outputs of this 5th step are the two necessary delta-v at LEO departure and at the flyby injection point and the total duration along the entire transfer trajectory.

Figure 48 gives a functional and temporal description of the lunar flyby transfer trajectory computation.
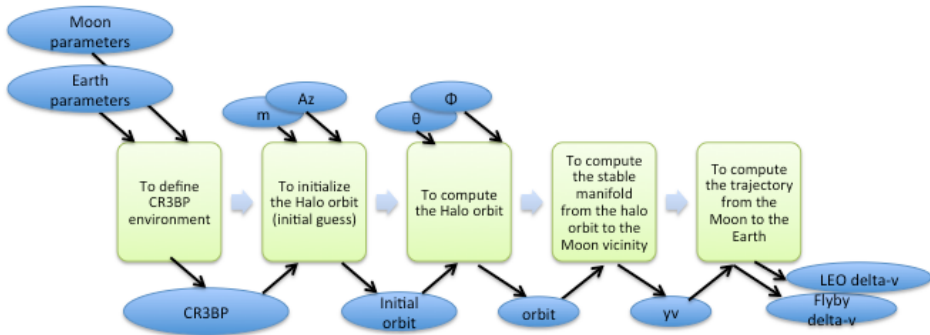
Figure 48: Lunar flyby algorithm

5.2.2.3 Crew vehicle transfer software modeling

The process described in the previous paragraph has been computed with Matlab. The solving of the differential equations (describing the dynamics of the CR3BP) has been performed with the "ode45" Matlab function, with the following precisions:

- The relative tolerance: `default.ode45.RelTol = 1e-12;`
- The absolute tolerance: `default.ode45.AbsTol = 1e-12;`

Those two thresholds define the acceptable error of the solution.

5.2.2.4 Crew vehicle transfer results

When the process is applied for a fixed set of design parameters, results, as the ones presented on   Figure 49 are obtained. In this example, the values of the designed parameters are:

Parameter	Value	Units
A_z	8000	km
m	3	
d_M	50	km
Θ	120	(°)
ϕ	120	(°)
h_{LEO}	200	km
φ_{LEO}	[0; 360]	(°)

Table 9: Example of Lunar flyby design parameters

Only φ_{LEO} is free to vary so as to find an optimal transfer trajectory.
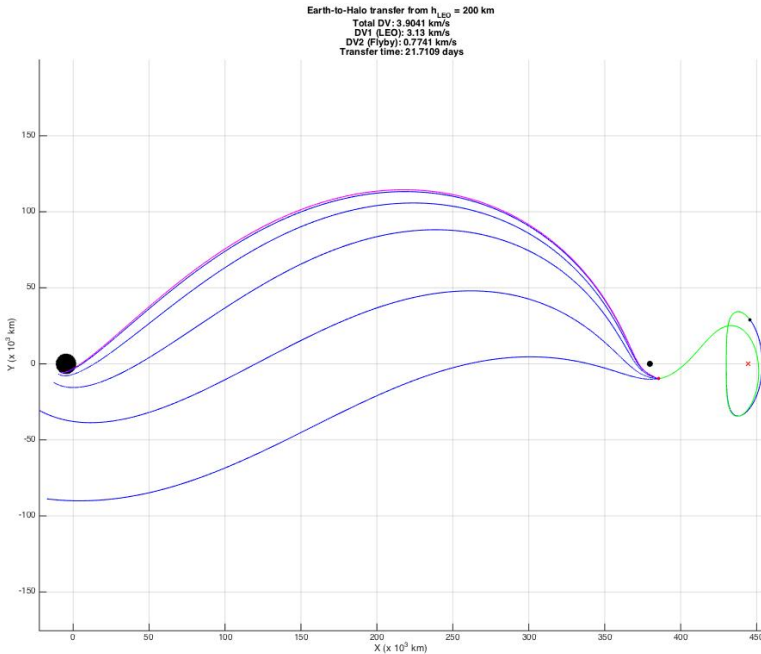
Figure 49: Example of lunar flyby

Figure 49 presents the successive steps of the process:
- the Halo orbit and its stable manifold correspond to the green plots
- the blue graphs are the succeeding shoots to obtain the Moon-Earth arc
- the magenta graph is the best trajectory.

EML2, the Moon and the Earth are also represented on the figure. It can be noticed that the succeeding transfer trajectories are getting closer and closer to the LEO.

Performances are also provided with:
- a total delta-v $\Delta v_{transfer} = 3.9041\ km/s$
- a delta-v in LEO $\Delta v_{LEO} = 3.13\ km/s$
- a delta-v at lunar flyby $\Delta v_{mani} = 0.7741\ km/s$
- a transfer total duration (TOF): 21.7109 days

These results are coherent with the biographical survey (see 5.2.1.6). The developed tools can then be verified. Compared to performances presented in other publications, those results cannot be considered as optimal as far as delta-v or duration are concerned. Local optimization of those performances is considered out of the scope of this study, since its main goal deals with scenario global optimization. Nevertheless, it appears to be interesting to evaluate the influence of all the design parameters on the results: on the one hand the total delta-v $\Delta v_{transfer}$, on the other hand the time of flight along the trajectory (TOF). All along this parametric analysis, the d_M parameter is fixed to 50 km.

5.2.2.4.1.1 Influence of the design parameters on the total delta-v

In order to understand the influence of the design parameters on $\Delta v_{transfer}$, the following set of parameters has been fixed:
- A_z varies from 5 000, 6 000… 30 000 km,
- ϕ varies from 0, 10,… 90° ,
- Θ varies from 1, 2,… 360°.

In this paragraph, the influence of the angular position, Θ, on the overall transfer cost, will be discussed first, for a fixed value of A_z, while ϕ is varying and then, for a fixed value of ϕ, while A_z is varying. That leads to the definition of a "no-go window". The impact of design parameters on this window is then presented, in the perspective of the mission analysis. At last, since this survey lies in the context of the crew vehicle transfer, the relation between the overall cost transfer and the time of flight is established.

Next figure shows the resulting costs $\Delta v_{transfer}$ (named ΔV_{tot} on the figure) as a function of Θ, for a fixed value of the out-of-plane elongation, $A_z = 5000$ km.
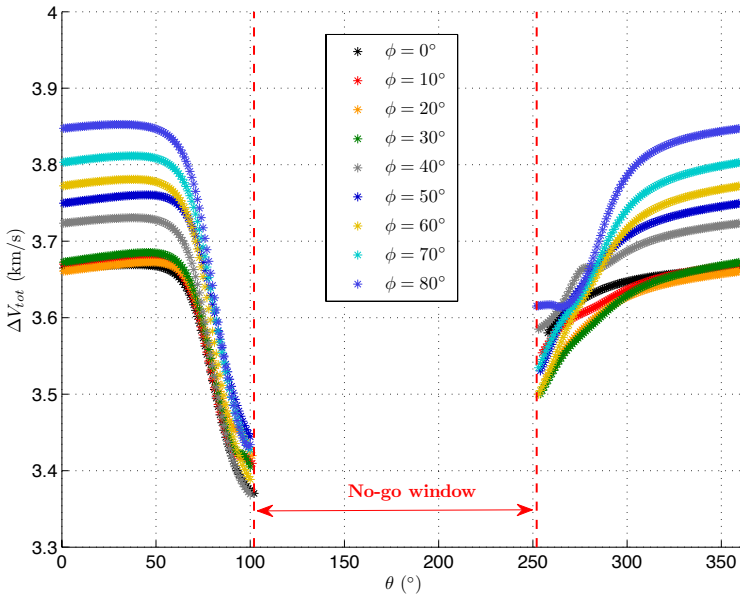
Figure 50: The overall transfer cost $\Delta v_{transfer}$ of lunar flyby trajectories as a function of the position on the orbit Θ for various values of ϕ

With this proposed methodology, some trajectories are not possible for a given departure point on the Halo orbit, comprised in a region with $\theta \in [102°, 252°]$ because of a potential collision of the corresponding manifold branch with the Moon. This region is denoted, in this study, the "**no-go window**". More definitions and analysis on the "no-go window" are provided in the paragraph 5.2.2.4.1.2.

This no-go window could be considered as contradictory to EML properties, described in Table 5. Actually, this no-go window would introduce a constraint on the launch window. Nevertheless, a small additional maneuver, while departing from the manifold, could be performed to slightly modify the trajectory and avoid the collision with the Moon. This no-go window is a direct consequence of the proposed approach, with the selected optimization parameters. The feasibility of the trajectory would be ensured by the additional maneuver that would not really degrade the performances. Computations of such an additional maneuver could extend the present analyses.

For this fixed A_z value, and for any value of the parameter ϕ, one can see a significant drop of the cost in the vicinity of the "no-go window", corresponding to the closest lunar flybys. This correlation between the overall cost and the distance to the Moon during the flyby is coherent with previous works [24, 56].

Moreover, it can be noticed that depending on the value of Θ, the minimum cost may correspond to various values of ϕ. In order to cancel the influence of ϕ, for each value of Θ, the minimum value of costs $\Delta v_{transfer}$ (i.e. ΔV_{tot}) is selected in the variation range of ϕ. The corresponding curves are plotted on Figure 51 for various values of

A_z between 4000 and 25000 km. For small A_z values, the minimum costs $\Delta v_{transfer}$ still corresponds to the closest lunar flybys, in the vicinity of the no-go window. However, it is the contrary for A_z values greater than 10 000 km.
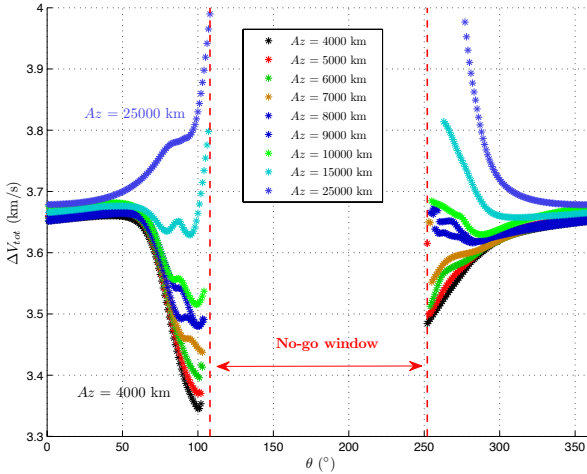
Figure 51: The minimum ϕ-independent overall cost $\Delta v_{transfer}$ of lunar flyby trajectories as a function of the position on the orbit Θ for various values of the out-of-plane amplitude A_z

The overall cost for a flyby trajectory to a Halo orbit of A_z = 25000 km is always greater than 3,6 km/s, whereas trajectories with a cost smaller than 3,35 km/s are possible if A_z = 4000 km. This result illustrates the pertinence of the flyby strategy for orbits with small out-of-plan extensions, and symmetrically shows its irrelevance for greater A_z values. In general, $\Delta v_{transfer}$ is an increasing function of A_z for almost all values of the position Θ.

As a synthesis, to minimize $\Delta v_{transfer}$, the overall cost for a flyby trajectory to a Halo orbit, it is recommended to select A_z lower than 10000 km, with the closest lunar flybys, with tangential maneuver, which correspond to positions on the Halo orbit close to the no-go window.

5.2.2.4.1.2 Influence of the design parameters on the no-go window

no-go This section aims at investigating the structure of the no-go window and introducing its influence on mission design. Given set of (A_z, m, *Θ*), the transfer on the stable manifold from Halo may collide into the Moon and leads to an unrealistic trajectory. This arc depends on (d_M, ϕ). This type of collision is usually obtained for a continuous range of positions on the orbit, both for the stable and unstable manifolds i.e. for both traveling directions. This range, noted $[\theta_1; \theta_2] \in [0; 360°]$, defines the "no-go window" for both travelling ways (from the Earth to EML2 and the way back).

This window imposes constraints on the mission design, and particularly on launch window:

- For Earth-to-Halo transfers, the set of Halo injection points at a given date may be restricted
- For Halo-to-Earth transfers, the flyby strategies may be impossible for certain positions of the THOR space station and dates

Following analysis are discussed to evaluate the impact of the window on mission design, in the very particular case of no additional maneuver is allowed (in contingency case, for example).

The temporal extent of the no-go window is denoted as T_{nogo} and is given as a fraction of the orbital period T_0 of the Halo orbit. The motion of the object (Space Station, crew vehicle or delivery cargo) on the manifold and thus the position and amplitude of the no-go window are very sensitive to the d_M value.

Figure 52 shows the spatial and temporal extent of the no-go window as a function of d_M for a fixed value of the out-of-plane elongation, $A_z = 4000$ km and for the median value $\phi = -45°$. The temporal results are given in days and in percentage of the orbital period. One can see that the duration of the window is very variable for small values of d_M, ranging between 20 and 30 % of the orbital period for this example. On Figure 52, the no-go window is also spatially variable and evolves on the orbit along with d_M. On the left, the spatial extent is represented by the values θ_1 (in red) and θ_2 (in blue) which are taken in $\mathbb{R}$ instead of $[0; 360°]$, to ensure continuity. The continuous grey range corresponds to the impossible flyby transfers.
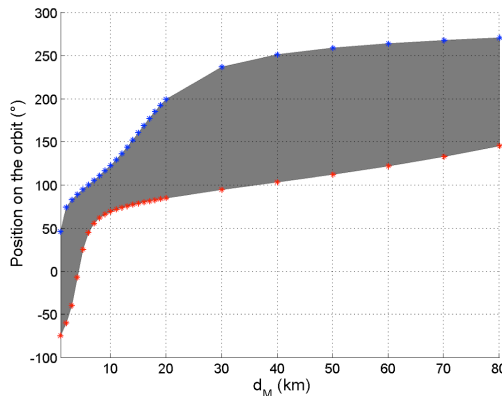
(a) The spatial extent of the no-go window as function of d_M
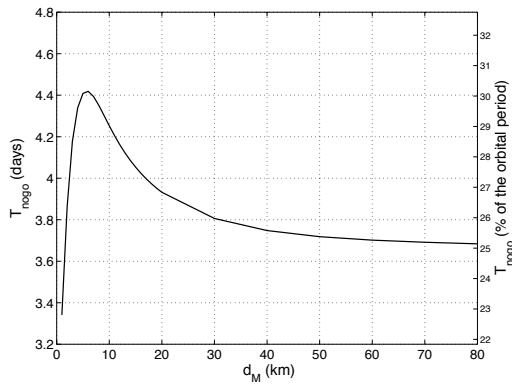
(b) The temporal extent of the no-go window as function of d_M

Figure 52: The spatial and temporal extent of the no-go window as function of d_M

Complementary studies should be carried out to characterize more precisely the influence of d_M on the no-go window and the overall mission design. In the meantime, d_M has been fixed to an arbitrary value of 50 km to cancel out its effect (according to bibliographical survey).

For a given position on the Halo orbit, a return flyby strategy from the station may be impossible to implement if it interferes with the no-go window. It is then important to quantify the delay induced by the presence of the no-go window on the return strategy. For a given set of the parameters (A_z, d_M, ϕ), the fastest Halo-to-Earth transfer has been computed for $\Theta = 1, 2, \dots 360°$ with the process described hereafter:

- For a given position θ_0, the initial transfer selected as the departure point consists in a classical flyby transfer with a time of flight $T_{transfer,0}$.
- For all the positions $\theta_i = 1, 2, \dots 360°$, the time spent on the orbital arc between θ_0 and θ_i, designated as $T_{orbit,i}$ is computed.
- The time of flight of the classical flyby transfer with θ_i taken as the departure point, is denoted $T_{transfer,i}$.
- The fastest Halo-to-Earth transfer at θ_0 is then given, with the departure point position defined by $\arg\min_{\theta_i} (T_{orbi,i} + T_{transfer;i})$ by the minimum : $\min_{\theta_i} (T_{orbit,i} + T_{transfer,i})$

Figure 53 presents the resulting return mission durations for a given set: $(A_z, d_M, \phi), = (5000\ km, 50\ km, 45°)$. As expected, the no-go window almost doubles the maximum mission duration. Quantitatively, at the beginning of the window, 44 days are needed to go back to Earth if a flyby return is decided. Thus, in the context of crew safety, other strategies than the lunar flyby transfer have to be implemented to fulfill the requirements of fast return from the station.

110
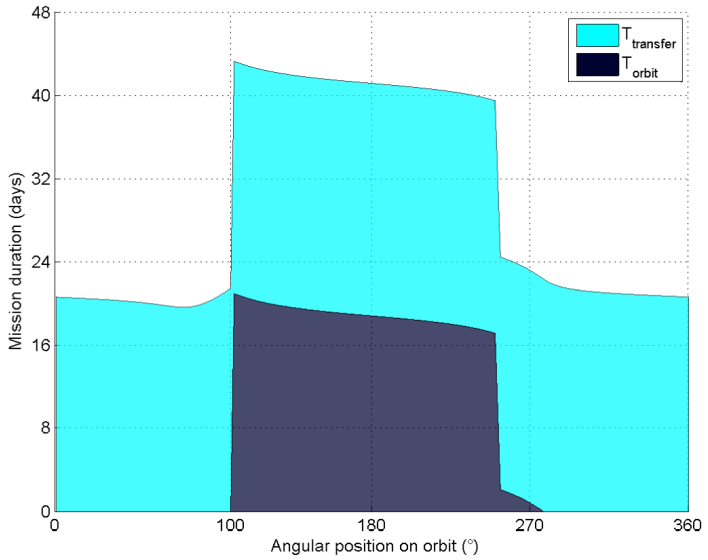
Figure 53: The fastest Halo-to-Earth flyby strategy as a function of the current angular position Θ for a fixed set of (A_z, d_M, ϕ)

5.2.2.4.1.3 Relation between the overall transfer cost and the time of flight

In this paragraph, the overall time of flight (TOF) is computed for the set of trajectories defined previously in 5.2.2.4.1.1.

For a given Halo orbit, the best solution in terms of $\Delta v_{transfer}$ has been selected in the restricted pool

ϕ = 0, 10, … 90° and Θ = 1, 2, … 360°. The overall cost $\Delta v_{transfer}$ and the time of flight (TOF) of these trajectories are presented on Table 10 for various values of the maximum out-of-plane amplitude A_z. The minimum $\Delta v_{transfer}$ is an increasing function of A_z, which is in favor of the minimization of the Halo orbit size.

(km)	$\Delta v_{transfer}$ (km/s)	TOF (days)
4 000	3,34	20,4
5 000	3,36	20,1
6 000	3,39	21,8
7 000	3,44	21,3
8 000	3,48	21,3
9 000	3,48	21,3
10 000	3,52	19,2

Table 10: The overall transfer cost and TOF for different values of A_z

111

Figure 54 shows the scatter diagram of ($\Delta v_{transfer}$, TOF) for A_z = 5000 km and for various values of ϕ. The best trajectories (cyan circles) are situated in the lower left corner of the figure, as both small $\Delta v_{transfer}$ and time of flight are sought. These trajectories create a Pareto front in the ($\Delta v_{transfer}$, TOF) space. The corresponding results are presented on Figure 42 for various values of A_z. On this figure, the trade-off between the fuel cost, $\Delta v_{transfer}$, and the time of flight clearly appears. The fastest transfers (less than 19 days of travel for A_z = 7000 km) are obtained thanks to the highest maneuvers (more than 3,7 km/s for A_z = 7000 km) and conversely, the shortest transfers are obtained for A_z = 7000 km, the most fuel efficient for A_z = 4000 km.
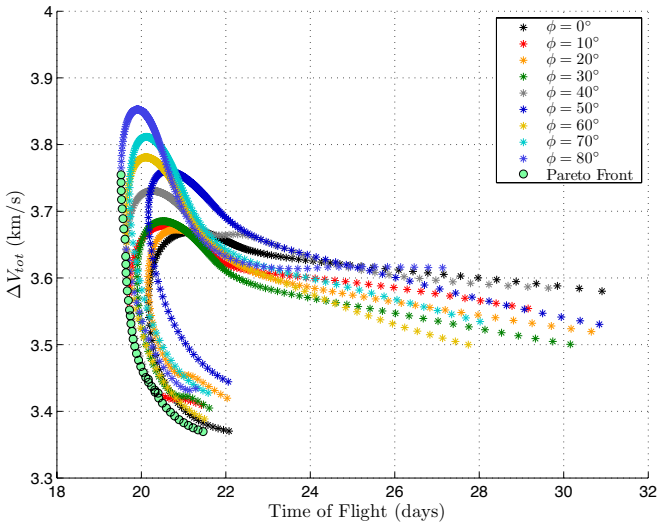
Figure 54: Scatter diagram of ($\Delta v_{transfer}$, TOF) for A_z = 5000 km and for various values of ϕ

There is a twist in the trade-off situation around the 20-days value: it is much more time consuming to reach the minimum $\Delta v_{transfer}$ in the long duration flight region than to save fuel in the short duration flight range. The best trade-offs correspond to a time of flight around 20 days and an overall fuel cost around 3.45 km/s.

5.2.2.5 Crew vehicle transfer synthesis and recommendations

As a synthesis of the analysis of the crew transfer vehicle, it can be recommended to minimize the total cost and the time of flight that:
- The A_z of the targeted Halo orbit should be lower than 10000 km,
- The introduction of an additional maneuver after departing from the manifold to avoid collision with the Moon, when the angular position, Θ, is close to the "no-go window"

The value of ϕ and d_M should be considered as design parameters and let free to vary in the optimization process when A_z and Θ have already been fixed.

Depending on the selected value of the out-of-plane elongation, A_z, the optimal transfer should be expected with a time of flight of 20 days and a total overall cost between $[3.34; 3.52] \, km/s$. Then the mission analysis should evaluate the consequences on the operational activities.

5.2.3 Station modules and cargo transfer trajectory

This paragraph focuses on another kind of transfer trajectories from LEO to EML2. The setting-up of a habitable station on a Halo orbit would imply one or several deployment missions and regular cargo flights to resupply the astronauts in food, water and other consumables. As far as the transportation of uninhabited elements (empty modules of the station or resupply cargo), main optimization criterion is the total overall cost of the transfer. The time of flight becomes a secondary figure of merit. That is the reason why, as already recommended in paragraph 5.2.1.6,, the selected strategies for this type of transfer should be the Weak Stability Boundary strategy (see 5.2.1.4). This strategy will allow taking into account the Sun influence.

5.2.3.1 Station modules and cargo transfer strategy description

In this case (WSB strategy), the considered dynamics taking into account the particle (Station, cargo or crew vehicle) travels under the influence the Earth, the Sun and the Moon, thus it is related to a four-body problem. The motions of the three massive bodies are assumed to be planar. The methodology consists in a patched three-body model with the connection of two trajectories computed in two different three-body problems.

Then, two CR3BP are employed: the Sun-Earth CR3BP and the Earth-Moon CR3BP. This strategy tries to reach a Sun-Earth low-energy trajectory with a first maneuver to quit the LEO, and then entering the Earth-Moon stable manifold with or without a second maneuver.

Figure 55 provides an example of a WSB transfer trajectory from LEO to EML2, with A_z = 8 000 km.

The transfer is divided into two steps:

- The first one leads the spacecraft from its departure LEO to the entrance point of the Earth-Moon stable manifold towards the Halo orbit. It corresponds to the blue part of the plot on Figure 55.
- The second one consists in the asymptotic drifting along the manifold to the final Halo orbit about EML2. It corresponds to the red part of the plot on Figure 55.
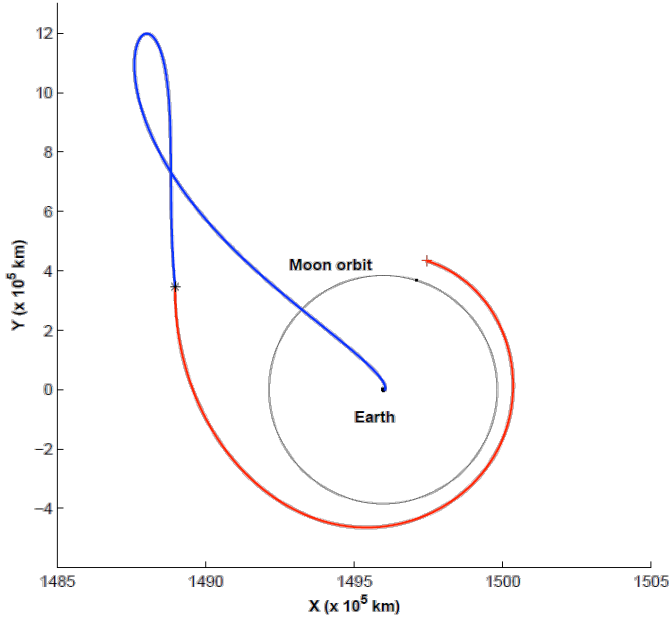
Figure 55: Example of WSB transfer trajectory (for $A_z = 8000km$)

In order to benefit from the solar dynamical assistance, the first stage is computed in the Sun-Earth CR3BP, which means the influence of the Moon is not taken into account. The initial Low Earth Orbit is chosen to lie in the ecliptic, thus the first leg of the trajectory is contained in the $z = 0$ plane. On the contrary, the second part of the trajectory is calculated in the Earth - Moon CR3BP so that the stable manifold is used to reach the Halo orbit.

Following the work of [63], two Poincaré sections, respectively named P_{SE} (for the Sun-Earth system) and P_{EM} (for the Earth-Moon system) are generated to detect connections between the two legs of the trajectory. They are defined on
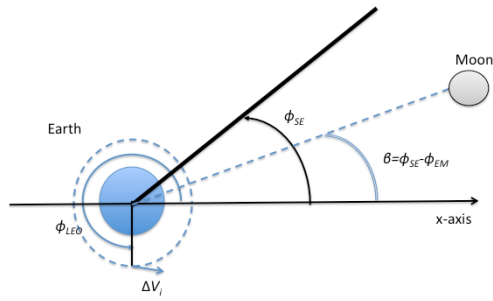
114

(a) Earth escape trajectory (Sun-Earth system)
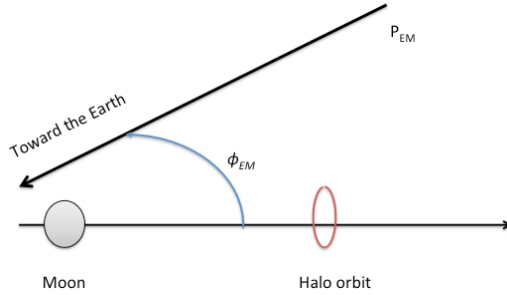
(b) Halo arrival trajectory (Earth-Moon system)

Figure 56, along with their associated angles ϕ_{SE} and ϕ_{EM}. The design of the whole Earth-to-Halo trajectory comes down to the selection of pairs of intersection points with:

$$y_{SE} \in P_{SE} \; with \; y_{SE} = \{x_{SE}, y_{SE}, z_{SE}, \dot{x}_{SE}, \dot{y}_{SE}, \dot{z}_{ES}\} \qquad (5\text{-}3)$$
$$y_{EM} \in P_{EM} with \; y_{EM} = \{x_{EM}, y_{EM}, z_{EM}, \dot{x}_{EM}, \dot{y}_{EM}, \dot{z}_{EM}\}$$

The angle between the two Poincaré sections is denoted:

$$\beta = \phi_{SE} - \phi_{EM} \qquad (5\text{-}4)$$
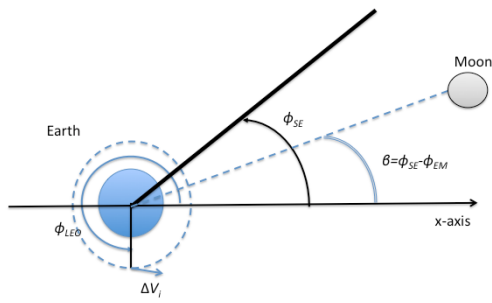
(a) Earth escape trajectory (Sun-Earth system)
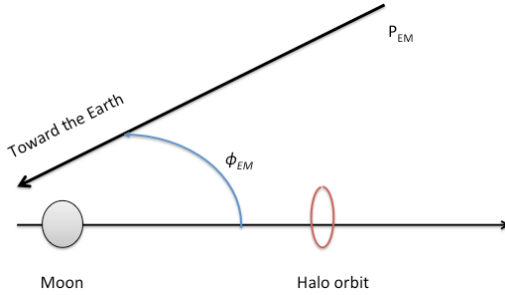
(b) Halo arrival trajectory (Earth-Moon system)

Figure 56: Definition of the design parameters for the cargo transfer optimization

The necessary condition to identify feasible trajectories is the coincidence, at least in the configuration space, of the y_{SE} and y_{EM} points. This imposes that the two Poincaré sections PSE and PEM are projected on the same line in the (xy) plane. In terms of mutual positioning of the primaries, it means that the Earth-Moon line must be tilted by the angle β (see (5-4)) with respect to the Sun-Earth line at the time the object (Station, modules or cargo) is on the Poincaré section (see
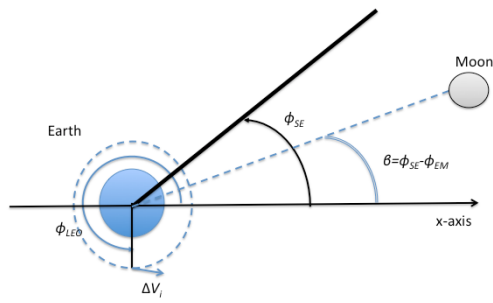
(a) Earth escape trajectory (Sun-Earth system)
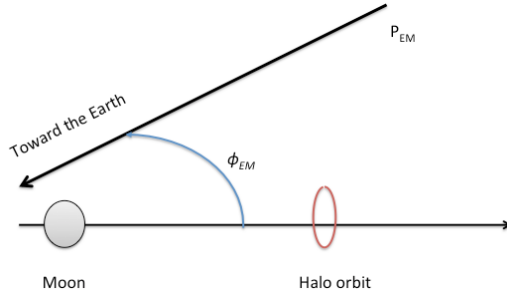
(b) Halo arrival trajectory (Earth-Moon system)

Figure 56). Moreover, since the Poincaré map PSE lies in the $z = 0$ plane, the search of possible intersections is restricted to the two points in PEM with zero z-coordinate. Since the spatial flow is never tangential to the $z = 0$ plane, and although it is possible to achieve satisfying intersections in configuration space between PSE and $P_{EM} \cap \{z = 0\}$, a small out-of-plane component of the velocity maneuver can never be avoided.

5.2.3.2 Station modules and cargo transfer design parameters

Design parameters have been selected so as to be coherent with previous analysis on the crew vehicle transfer strategy (see 5.2.2). They are:
- h_{LEO}: The cargo transfer will start from a circular LEO in the (xy) plane (no inclination). The influence of the LEO altitude (h_{LEO}) is significantly contributing to the overall cost and therefore, fixed to 200km.
- ϕ_{LEO}: The departure point angular position is not fixed but rather used as one of the optimization parameter.
- ΔV_i: The first thrust required to leave the LEO.
- ϕ_{SE}: The angle between the x-axis and the Poincaré map P_{ST} in the Sun-Earth system. It is not fixed and is let vary for optimization purpose.
- ϕ_{EM}: The angle between the x-axis and the Poincaré map P_{EM} in the Earth-Moon system. It is not fixed and is let vary for optimization purpose.

117

- A_z: It corresponds to the maximum out-of-plane amplitude in the +z direction of the considered orbit, in kilometers
- m: The Halo family. When the A_z is in the +z direction, the Halo orbit is a member of the northern family (m=1), while if A_z is in the -z direction; the Halo orbit belongs to southern family (m=3).
- d_M: The distance between the Halo orbit and the manifold

Here under table sums up the assumptions:

Parameter	Value	Units
A_z	[5000; 30000]	km
m	1 or 3	
h_{LEO}	200	km
ϕ_{LEO}	[0; 360]	(°)
ΔV_i	[3150; 3250]	m/s
d_M	[0; 100]	km
ϕ_{SE}	[0; 180]	(°)
ϕ_{EM}	[0; 180]	(°)

Table 11: Station modules and cargo transfer design parameters assumptions

Figure 57 provides a definition of the parameters $(\phi_{LEO}, \Delta V_i, \phi_{SE})$ in the Sun-Earth system.
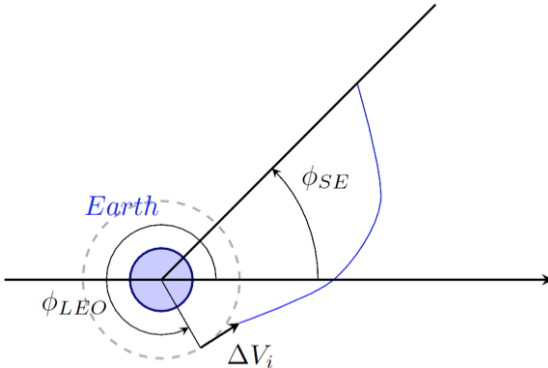
Figure 57: Parameters in the Sun-Earth system

For any pair y_{SE} and y_{EM}, the conditions for a successful connection are defined by:

$$\left\| \begin{pmatrix} x_{SE} \\ y_{SE} \end{pmatrix} - \begin{pmatrix} x_{EM} \\ y_{EM} \end{pmatrix} \right\| \leq 10 \ km$$

$$\left\| \begin{pmatrix} \dot{x}_{SE} \\ \dot{y}_{SE} \\ \dot{z}_{SE} \end{pmatrix} - \begin{pmatrix} \dot{x}_{EM} \\ \dot{y}_{EM} \\ \dot{z}_{EM} \end{pmatrix} \right\| \leq 30 \ m/s$$

5.2.3.3 *Station modules and cargo transfer optimization algorithm*
The following methodology has been developed for the application to the scenario of

118

a cargo vehicle resupplying the station. In orbit at least for six months on a Halo orbit around EML2, it could easily be adapted for the Space stations modules deployment.

The transfer optimization algorithm lies in minimizing the total transfer delta-v along the trajectory. The transfer is separated into two branches: A_{EM} (the arc in the Sun-Earth system) and A_{MH} (the arc in the Earth-Moon system). The methodology resides on two CR3BP models overlapping and aims at reducing the velocity gap to jump from first arc to the second one. It is based on backward computation that starts from the targeted Halo orbit to the LEO.

The algorithm has five main steps that will be described just after:

- **The 1st step** consists in the targeted Halo orbit computation, for the fixed values of A_z and m.
- **The 2nd step** aims at computing the transfer arc in the Earth-Moon system, from the Halo orbit to manifold entrance point. The angular position, θ, on the Halo orbit (see Figure 47 for its definition) varies between 0° and 360°. For each value of θ, the trajectory on the stable manifold is computed backward. The computation starts at a distance, d_M, from the Halo orbit and finishes at the Poincaré map, P_{EM}, at points uniquely defined by ϕ_{EM} and z=0. ϕ_{EM} varies between 0° and 180°. For each value, the velocity can be computed. The left part of Figure 58 illustrates this step.
- **The 3rd step** computes the transfer arc in the Sun-Earth system, from LEO to the entrance point. Velocity increment is determined so as to ensure a collinear velocity to the arc obtained at the previous step and a tangential arrival in LEO. The angular position of the arrival point on LEO is let free. Only the escape velocity, ΔV_i, is fixed, as (5-5) within a range +/- 10%. It is targeted using a numerical differential correction scheme such as the one developed by Gordon [56]. The right part of Figure 58 depicts this step.
- **The 4th step** optimizes the total delta-v from LEO to Halo orbit in EML2. As ΔV_i, is sorted randomly, the optimization process focuses on the intermediate delta-v (ΔV_{gap}). It is obtained by optimization, with genetic algorithms (see 4.7). It results from the velocity gap between the final point on the arc A_{MH} and the final point on the arc A_{EM} in the Earth-Sun system.
- **The 5th step** reconstructs the entire transfer trajectory based, on the selection of the best transfer trajectories issued from the 4th step.
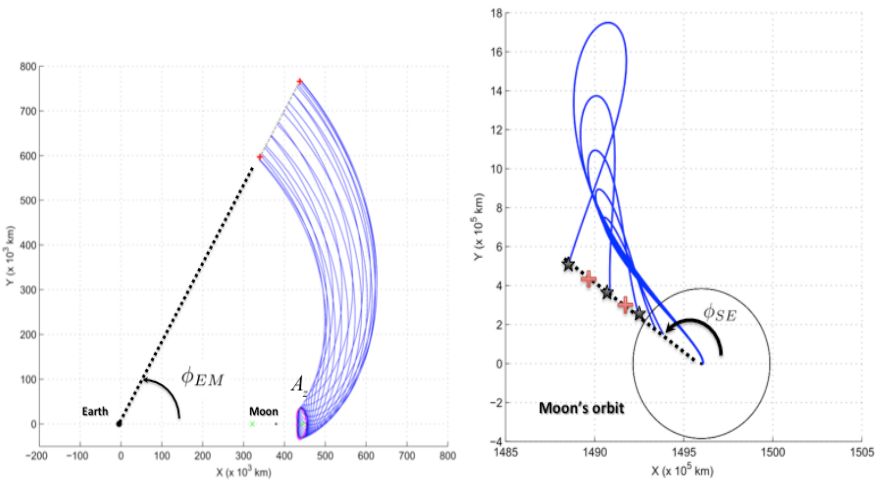
Figure 58: Parameters definition in the Earth-Moon system (left) and the Sun-Earth system (right)

Figure 59 gives a functional and temporal description of the WSB transfer trajectory computation, with eFFBD modeling. It sums up the algorithm of the four first steps of the process described previously.
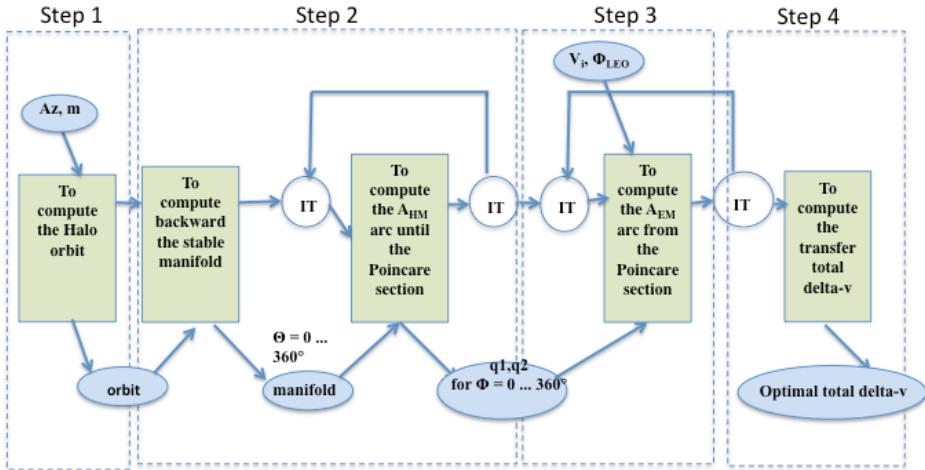
Figure 59: WSB transfer algorithm

The optimal delta-v resulting from this process is composed of two maneuvers, encompassing:

- The initial delta-v (ΔV_i) to quit the LEO and be injected on the A_{EM} arc
- The intermediate delta-v (ΔV_{gap}) to quit the A_{EM} arc and join the A_{MH}

120

An example of those maneuvers is provided on Figure 60.
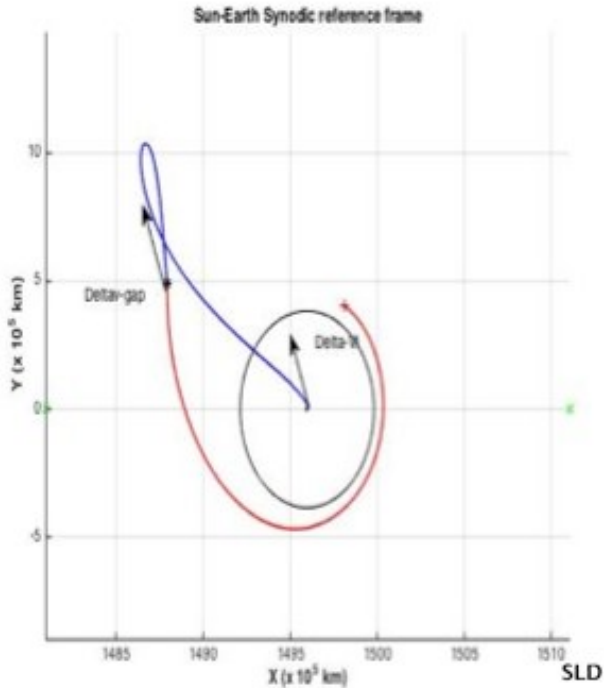
Figure 60: Example of two maneuvers for WSB strategy

Moreover, the initial delta-v (ΔV_i) to quit the LEO corresponds to a random value of the escape velocity for h_{LEO}, in a range of +/- 10%. The velocity has to be tangential to the orbit.

The initial delta-v to quit the LEO is given by the classical formula to perform a maneuver from the fixed LEO to the Moon in the two-bodies problem (when the influence of the Moon gravitation is neglected):

$$\Delta V_i = \sqrt{\frac{2\mu_E r_2}{r_1(r_1 + r_2)}} - \sqrt{\frac{2\mu_E}{r_1}} \qquad (5\text{-}5)$$

where:
- μ_E is Earth gravitational constant
- r_1 is the altitude of the LEO (see (5-6)
- r_2 is radius of the Moon orbit (see (5-7)
- R_E is the Earth radius
- $dist_{EM}$ is the Earth-Moon distance

$$r_1 = h_{LEO} + R_E \qquad (5\text{-}6)$$

$$r_2 = dist\_EM + R_E \qquad (5\text{-}7)$$

Remark: Numerical values are provided in Appendix 1.

5.2.3.4 *Station modules and cargo transfer optimization results*

Thanks to the application of the previous methodology, the cost of the transfer trajectories from LEO to EML2 has been computed for a maximal elongation A_z equal to 8000 km and 30000 km with the assumptions presented in Table 11 with $d_M = 50$ km.

A synthesis of the results (total delta-v along the transfer trajectory versus the time of flight) is presented on Figure 61 for a maximal elongation A_z equal to 8000 km (red dots) and 30000 km (blue dots).
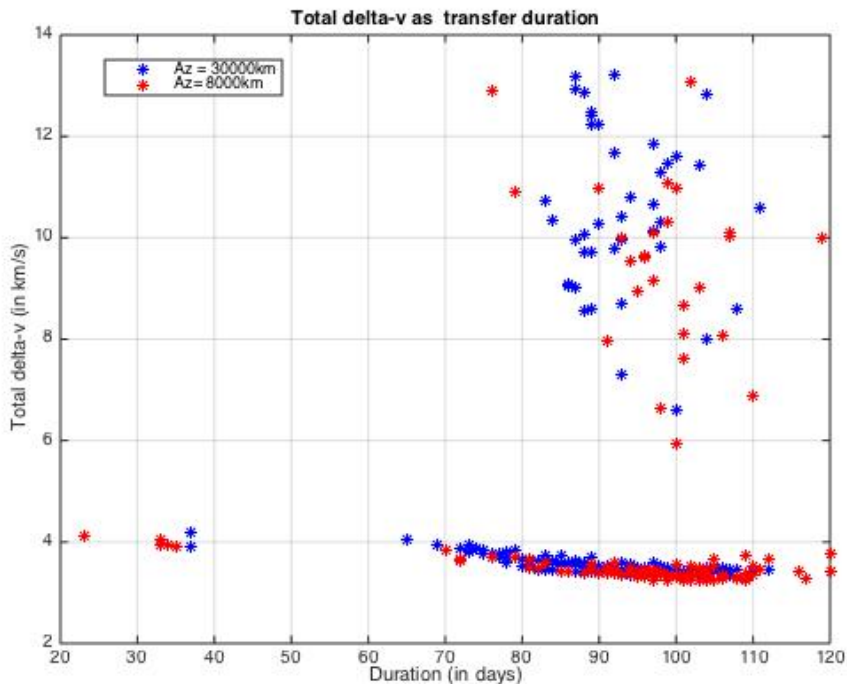
Figure 61: Total delta-v as total duration, for A_z = 8000 km and A_z = 30000 km

Results are grouped in three families:
- The " unworthy family" with a high range of total delta-v within a range of [5294; 13203] m/s and a high duration (about [70,120] days).
- The "nominal family" with a range of [3236; 4051] m/s and a time of flight of about [65,120] days. Figure 62 provides an example of a global trajectory from LEO to EML2, belonging to the nominal family.
- The "exotic family" with a time of flight lower than 37 days and a total delta-v in a range of [3898; 4179] m/s. Figure 63 provides an example of global trajectory from LEO to EML2, belonging to the exotic family.

Trajectories belonging to the "nominal family" are the most classical ones. Many comparable transfers can be found in the literature. They form a kind of Pareto front, with classical values.

The trajectories of the "exotic family" correspond, in fact, to the transfer using the exterior stable manifold to reach the Halo orbit around EML2. They are similar to the one presented by Parker [49] (with a h_{LEO} is fixed at 185 km), who did not take into account the influence of the Sun to build his Earth-to-Halo transfers. He integrated entirely his trajectory in the Earth-Moon system while using the exterior stable manifold. Even if the total delta-v is quite high, the performances obtained with this trajectories family could be interesting, as a back-up solution, for crew vehicle or for a

123

rapid cargo delivery in case of contingency, compared to direct transfer or lunar flyby. It seems to be feasible to gain some days, but while spending a lot of energy. These transfer trajectories are remarkable: the Earth leg (the AEM arc) seems to correspond to an ellipse (with a low eccentricity). Few solutions are obtained in these families, mostly due to the genetic algorithms. Nevertheless, the computation can be forced so as to obtain more results. Some attempts were performed in the BCR4BP (Bi-Circular Restricted Four-Body Problem) with the Sun, the Earth and the Moon so as to evaluate the influence of the Sun during the transfer on the AEM arc between LEO and the Halo orbit manifold entrance point. The variation on the particle energy (i.e. velocity) caused by the influence of the Sun is very low compared to the energy gap required to change from AEM arc to AMH arc. As a consequence, it has been decided that CR3BP remains the baseline for transfer.

The "unworth family" is clearly out of interest for transfer: too expensive, too slow!

Finally, it should be noticed that there is a topological gap between the three families. As "nominal family" and "exotic family" could be considered as transfer strategies, it seems worthy to go further so as to find the boundaries of both families. It could be interesting to let the design parameters evolve continuously, and fill the gap.

T_{tot} =101 jours
ΔV^{tot} =3.2358 km/s
ΔV_{gap}^{tot} =23.1511 m/s
phi LEO =163.8922 degre
DV =3.2127 km/s
phi ST =35.7996 deg
phi TL =21.7 deg
Point number1
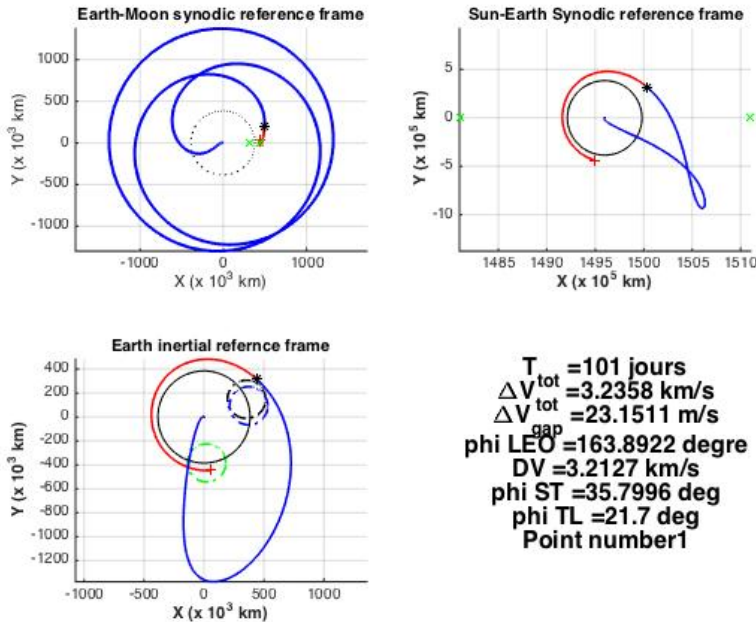
Figure 62: Example of trajectory of the « nominal family »
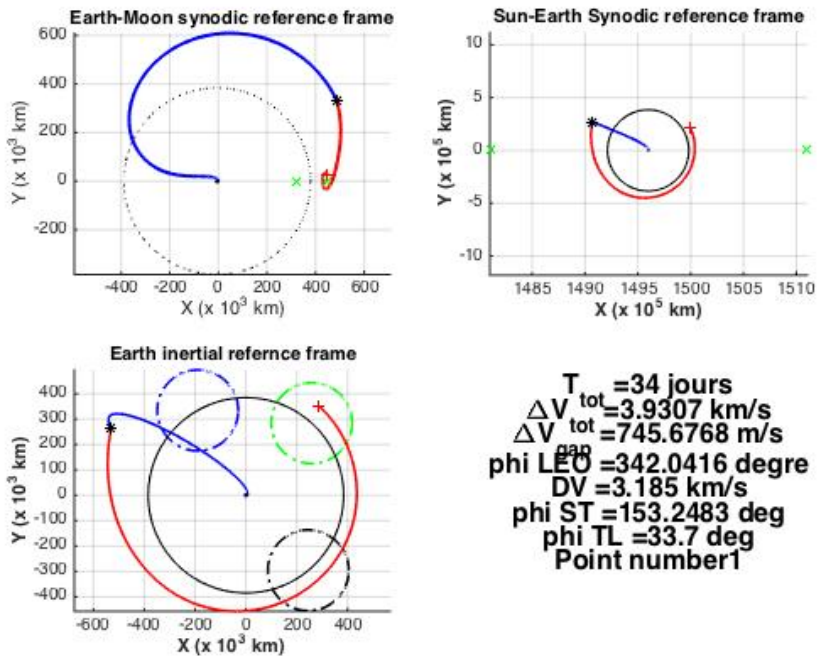
Figure 63: Example of trajectory of the « exotic family »

As a synthesis for station modules and cargo transfer: the utilization of WSB strategy could be better than lunar flyby transfer, either for duration or for total delta-v, depending on a strict selection of the design parameters. The following table provides a summary of the WSB transfer results with a comparison of direct transfer and lunar flyby, extracted from literature.

Type of transfer	Duration (days)	Delta-v (km/s)
Direct (*)	3 – 5	4.0 – 4.5
Lunar flyby (*)	10 - 25	3.3 – 3.5
Lunar flyby	≈ 20	3.3 – 3.5
WSB (exotic family)	17 - 37	3.9 – 4.2
WSB (nominal family)	65 – 120	3.2 – 4.0

(*) Data extracted from literature (see 5.2.1).

Table 12: Performances comparison of transfer strategies

There is no systematic recommendation. Actually, it has been observed on the one side there does exist transfers of the "exotic family" with lower time of flight, but higher total delta-v than lunar flyby transfer. On the other side, the nominal family of

125

the WSB strategy can have lower delta-v than lunar flyby, to the detriment of the duration.

With regard to mission analysis, a complementary figure of merit should be considered: the flexibility. Actually, the WSB performances depend on the Moon, Earth and Sun configuration (through the selection of ϕ_{EM} and ϕ_{SE}, which consequently, constraints the transfer starting time.

5.2.4 Transfer optimization limitations

This chapter deals with finding the optimal transfer trajectories between LEO and a Halo orbit around EML2, for two main scenarios: "Crew vehicle" and "Station modules and cargo delivery". It has been concluded that the best solution for Crew vehicle is a lunar flyby strategy, while for cargo delivery, it could be better to envisage a WSB strategy, taking benefit of the Sun influence.

Nevertheless, the main limitations of this study should be recalled:
- First, it is supposed that the Moon, the Sun, the Earth and the particle (modules, station, cargo, crew vehicle…) are travelling in the same plane.
- Secondly, only CR3BP are taken into account, i.e. their motion is perfectly circular. Their position is theoretical. Ephemerids should be applied to have more realistic results.
- Thirdly, the influence of each primary is taken into account two-by-two (in the Sun-Earth system or in the Earth-Moon system), which is also limited to the first order. Actually, it would be more realistic to model those trajectories in a Four-body problem.

Nowadays, additional research analyses are under going at ISAE-SUPAERO in the Bi-Circular Four Body Problem to model more precisely the transfer trajectories in the Earth-Moon system taking into account the Sun influence. Those results are out of the scope of this project, but will complement it.

5.3 Rendezvous in EML2 strategy

This paragraph studies the feasibility of rendezvous in the vicinity of EML2 by comparing several rendezvous strategies and by providing quantitative results so as to select the optimal rendezvous scenario for a cargo or a human spacecraft with the THOR station. It is assumed that the THOR space station is already rotating on a Halo orbit around EML2. Then, the cargo or the crew vehicle tries to reach it.

In THOR resupply context, the main rendezvous phases have to be modified and adapted to non-keplerian orbits around unstable Lagrangian points (here, EML2).

5.3.1 Rendezvous definitions

JC Houbolt [64] defines the rendezvous as:

"the problem of rendezvous in space, involving, for example, the ascent of a satellite or space ferry as to make a soft contact with another satellite or space station already in orbit."

The vehicle that is already in orbit is commonly called the **target**, while the one that is arriving, is named the **chaser**.

The different phases and maneuvers of a typical rendezvous mission from the launch until the docking to the target spacecraft have been extensively studied from Apollo missions to ISS resupply missions. They are mostly named: *launch, transfer, orbital injection, phasing and proximity maneuvers* (including homing, closing and final approach). Rendezvous is then followed by docking or berthing, depending on the type of the chaser.

The rendezvous operations that are considered in this study will start from the departure of the chaser from its parking orbit to the injection maneuver onto the target orbit in the vicinity of the Earth-Moon Lagrangian point EML2. Transfer trajectories have already been deeply studied in paragraph 5.2. Final maneuvers to phase the target and the chaser on the target final orbit are out of the scope of this project. Nevertheless, the main goal of the rendezvous is to conduct the chaser relatively close to the target in order to linearize the equations of motions of both vehicles until the contact.

5.3.2 Rendezvous bibliographical context

Even though rendezvous is a critical phase, it has rarely been studied in the context of the dynamics of the Lagrangian points, except by R. B. Gerding [65] in 1971 and by E. Canalias [66] in 2006. By consequence, the topic is important for the objectives of this project.

Of course, a large amount of publications from 1950s to today dealing with rendezvous can be found.
But the typical rendezvous problem considers that both vehicles are in orbit about a massive celestial body (Earth, Moon, Mars…) and lies only in the two-body problem.

Strategies for rendezvous are really important for several types of space missions like: assembly of orbital units, crew transfer, rescue, retrieval, cargo delivery, inspection, interception, formation flying or debris removal. Most of those situations are in the scope of the THOR overall mission, based on the CR3BP.

5.3.3   Rendezvous strategies

Considering the results of the bibliographical survey and lessons learned from ATV missions, it is considered that the main goal of the rendezvous between the chaser (the cargo or the crew vehicle) and the target (the THOR space station) is directed on the chaser on the orbit of the target. By assuming that the THOR space station on a Halo orbit, the delivery cargo or crew vehicle tends to join THOR. The chaser may either start the rendezvous from a manifold or from on a Halo parking orbit. According to [27], depending on the location of the chaser, two different types of rendezvous could be performed:

- The **HOI (Halo Orbit Insertion):** the chaser is parking on a particular Halo orbit (defined by A_{z_chaser}, $m_{\_chaser}$),
- The **MOI (Stable Manifold Orbit Insertion):** the chaser travels from the Earth on the stable manifold of the Halo orbit of the THOR space station.

The Figure 64 illustrates both concepts.
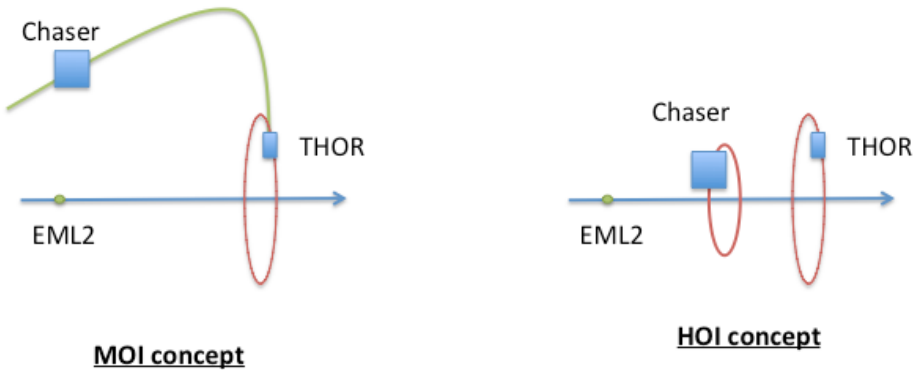
Figure 64: Rendezvous concepts

By consequence, the rendezvous operations would include the following steps:

- **Parking:**   the initial state. The THOR space station is orbiting on another Halo orbit (defined by A_{z_THOR}, $m_{\_THOR}$). The chaser is either arriving on the stable manifold, either parking on a Halo orbit.
- **Departure:**   a first maneuver (Δv_1) is applied to the chaser so that it would leave its Halo orbit and travel on the unstable manifold in the MOI case. There is no departure in HOI case.
- **Intermediate maneuver:**   In MOI case, a second maneuver (Δv_2) is applied at the intersection between the unstable manifold of the cargo Halo orbit and the stable manifold of the THOR Halo orbit, so that the chaser trajectory is reoriented. There is no final maneuver in HOI case.
- **Final maneuver:**   a last maneuver (Δv_3) is performed so that the chaser would leave the stable manifold to reach the THOR space station Halo orbit.
- **Phasing:**   As soon as the chaser and the station are rotating on the same Halo orbit, phasing operations could take place so as to ease docking

maneuvers: both vehicles must be as close as possible so as to linearize their equations of motions.

The operations are summed up on the following schema (with eFFBD modeling). Only processes are given. Data flows have not been detailed for simplification.
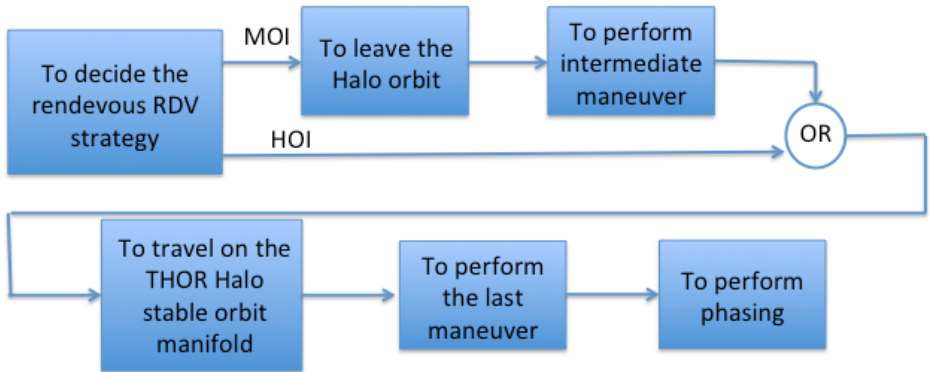
Figure 65: Rendezvous operations sequence

The most critical part of the rendezvous mission lies in the proximity operations phase (phasing) when the distance between the chaser and the target is below a small distance (some kilometers). Safety is the overriding design consideration for automated missions towards inhabited facility. To avoid collision and accident, corrections maneuvers must be performed before this final step. This is why the chaser trajectory must be computed with a very high accuracy. The phasing activities are not presented in the project, but it is an interesting extension opportunity, while referring to E. Canalias [66]. She suggested simple equations to manage the phasing on Lissajous orbits that could be adapted to Halo orbits.

As a consequence, the rendezvous design parameters are:
- HOI or MOI: initial situation of the chaser
- A_{z_THOR}:   Maximal elongation along z-axis of the Halo orbit of the THOR space station
- A_{z_chaser}:   Maximal elongation along z-axis of the initial Halo orbit of the chaser
- $m_{\_THOR}$:   Halo family of the THOR space station
- $m_{\_chaser}$:   Halo family of the chaser
- θ_{THOR}:   Initial angular position of the THOR space station on the Halo orbit when rendezvous starts
- θ_{chaser}:   Initial angular position of the chaser on the Halo orbit when rendezvous starts

Remark: the initial angular position of the THOR space station and of the chaser is computed as in Figure 47.

The Table 13 synthesizes all the possible situations. From this overview, the main conclusion is that the focus shall be set on the modeling and analysis of the **Halo-to-Halo rendezvous**. Two different Halo orbits are never coplanar; studies have been performed on optimal transfers between unstable orbits around Lagrangian points using Weak Stability Boundary and Invariant Manifolds (see part 5.2). Actually, due to unpredictable miscellaneous or discrepancies during previous steps of the trajectory (launch, LEO and transfer), it seems not realistic that the chaser will reach perfectly the Halo orbit of the THOR space station, even if the targeted Halo orbits are the same (same A_z, same m). It is then assumed that the cargo will not arrive directly on THOR orbit. This does mean that every listed situation should finally come to perform a rendezvous at least two maneuvers: a first maneuver to leave the current trajectory and a second maneuver to get on the target Halo orbit. The algorithm of this strategy is detailed in 5.3.4.

A focus is set on a Halo-to-Halo transfer, while assuming THOR already orbiting around EML2 (due to mission requirements). But every type of rendez-vous (Lissajous-to-Halo, Lyapunov-to-Halo…) should be investigated. This option will be discussed in 5.3.7.2.

Case Number	Initial maneuver type	A_z	Orbit class (m)	Initial angular position	Strategy
1	HOI	A_{z_THOR} = A_{z_chaser}	m_THOR = m_chaser	θ_{THOR} $\neq \theta_{chaser}$	THOR and the chaser are on the same Halo orbit. Only the angular position of the chaser has to be changed.
2	HOI	A_{z_THOR} $\neq$ A_{z_chaser}	m_THOR = m_chaser	θ_{THOR} and θ_{chaser} are indifferent	First, to modify A_{z_chaser} and then, θ_{chaser}. See proposed algorithm in 5.3.4.
3	HOI	A_{z_THOR} = A_{z_chaser}	m_THOR $\neq$ m_chaser	θ_{THOR} and θ_{chaser} are indifferent	No simple process to modify only the Halo orbit class. See proposed algorithm in 5.3.4
4	HOI	A_{z_THOR} $\neq$ A_{z_chaser}	m_THOR $\neq$ m_chaser	θ_{THOR} and θ_{chaser} are indifferent	See proposed algorithm in 5.3.4
5	MOI	A_{z_THOR} = A_{z_chaser}	m_THOR = m_chaser	θ_{THOR} $\neq \theta_{chaser}$	The chaser has not yet reached its final destination (the THOR Halo orbit). The final maneuver should ensure that there would be no collision.
6	MOI	A_{z_THOR} $\neq$ A_{z_chaser}	m_THOR = m_chaser	θ_{THOR} is indifferent	The chaser has not yet reached its final destination (a different orbit from the THOR Halo orbit). Two options: to modify m_chaser while the chaser is travelling on the manifold or to wait its arrival to its final destination. In case of success, the first

					option would lead to case 5. Then, the second option comes down to case 2. See proposed algorithm in 5.3.4.
7	MOI	A_{z_THOR} = A_{z_chaser}	$m_{\_THOR}$ $\neq$ $m_{\_chaser}$	θ_{THOR} is indifferent	The chaser has not yet reached its final destination (a different orbit from the THOR Halo orbit). Two options: to modify A_{z_chaser} while the chaser is travelling on the manifold or to wait its arrival to its final destination. In case of success, the first option would lead to case 5. Then, the second option comes down to case 3. See proposed algorithm in 5.3.4.
8	MOI	A_{z_THOR} $\neq$ A_{z_chaser}	$m_{\_THOR}$ $\neq$ $m_{\_chaser}$	θ_{THOR} is indifferent	The chaser has not yet reached its final destination (a different orbit from the THOR Halo orbit). Two options: to modify A_{z_chaser} and $m_{\_chaser}$ while the chaser is travelling on the manifold or to wait its arrival to its final destination. In case of success, the first option would lead to case 5. Then, the second option comes down to case 6. See proposed algorithm in 5.3.4.

Table 13: Comparison of the rendezvous situations

132

5.3.4 Rendezvous algorithm

The main goal of this part is to describe the proposed algorithm to plan and evaluate the rendezvous in EML2 between the THOR space station and its chaser (delivery cargo or crew vehicle). The rendez-vous maneuver main goal is to ensure that the chaser approaches the target within a very close distance. Rendez-vous requires a precise match of the orbital parameters (velocity, direction, …) of the two vehicles, allowing them to remain at a constant distance through station-keeping maneuvers in order to allow docking or berthing. This constant distance will be suppressed during proximity maneuvers until docking.

The previous synthesis (see Table 13 and its conclusions) shows that performing the rendezvous between a chaser and the THOR station always corresponds to a **quasi-heteroclinic** connection between two Halo orbits, by finding the intersection between their manifolds (the unstable manifold for the cargo and the stable manifold for the station), except when only the phase has to be changed. The focus is set on the HOI configuration, with different A_z.

The methodology developed describes how to model the rendezvous between two different Halo orbits, is constructed as a quasi-heteroclinic connection.

The process is consistent with previous transfer study, since the main step lies in the intersection of two manifolds thanks to a Poincaré section. It falls into five main steps:
- **Step 1:** To compute the chaser Halo orbit and unstable manifold
- **Step 2:** To compute the THOR space station Halo orbit and stable manifold
- **Step 3:** To find the optimal intersection between both manifolds thanks to a Poincaré section
- **Step 4:** To compute the chaser entire rendezvous trajectory from its Halo orbit to the Station orbit
- **Step 5:** To estimate the rendezvous performances (total delta-v, duration)

This process imposes additional design parameters, let free for the optimization:
- d_{M_THOR}:   Distance between the THOR space station Halo orbit and the manifold
- d_{M_chaser}:   Distance between the chaser Halo orbit and the manifold
- ϕ_{rdv}:   Poincaré section position

The Figure 66 provides a 3D example of a Halo-to-Halo rendez-vous strategy, with the THOR space station Halo orbit defined by (A_{z_THOR} = 30000 km, m_THOR = 1) and a chaser Halo orbit defined by (A_{z_chaser} = 8000 km, m_chaser = 3).
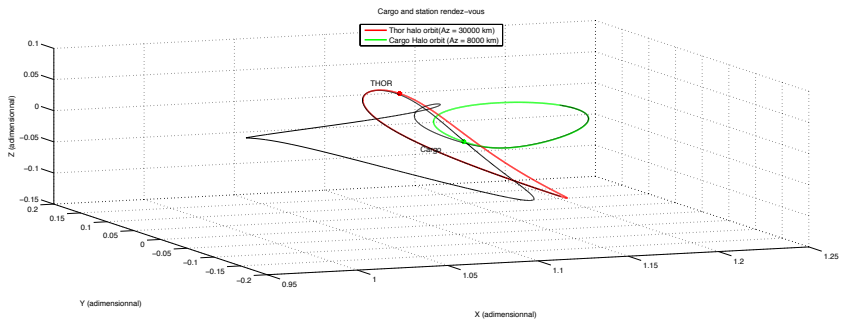
Figure 66: Example of rendezvous strategy between a chaser and the THOR space station

The chaser is first rotating on its Halo orbit (green leg), and then escapes on the unstable manifold (first black leg) to a first impulsive maneuver. At the intersection between chaser unstable manifold and station stable manifold, on the Poincaré section (see 5.3.4.2), the chaser enters the station stable manifold thanks to a second impulsive maneuver and then glides until it reaches the Station orbit. During this phase, the THOR station keeps on traveling on its Halo orbit.

5.3.4.1 Halo orbit modeling

The determination of highly accurate trajectories in the vicinity of the translunar libration point is very important. It is part of the decision criteria for mission analysis. Step 1 and 2 of the Halo-to-Halo rendezvous strategy requires precise Halo orbit models. The linearized model will not suffice. For a real mission, there should be no difference, since except in CR3BP, an exact Halo orbit does not exist. The chaser keeps on traveling on its trajectory that will converge at the infinite time to the Halo orbit. Nevertheless, numerical representations impose to consider two different models: one for the Halo orbit (as described in 4.4.2.3) and one for the manifold.

For this project, the analytical solutions for quasi-periodic orbits about EML2 that Farquhar [30] has obtained using the method of Lindstedt - Poincaré are compared to linearized model and the one of Richardson.

The next figure presents the result of the comparison of the Halo orbit obtained with Farquhar model (red plot) and Richardson model (blue plot), for $A_z = 30000$ km and m=3. The green star in the center is EML2.
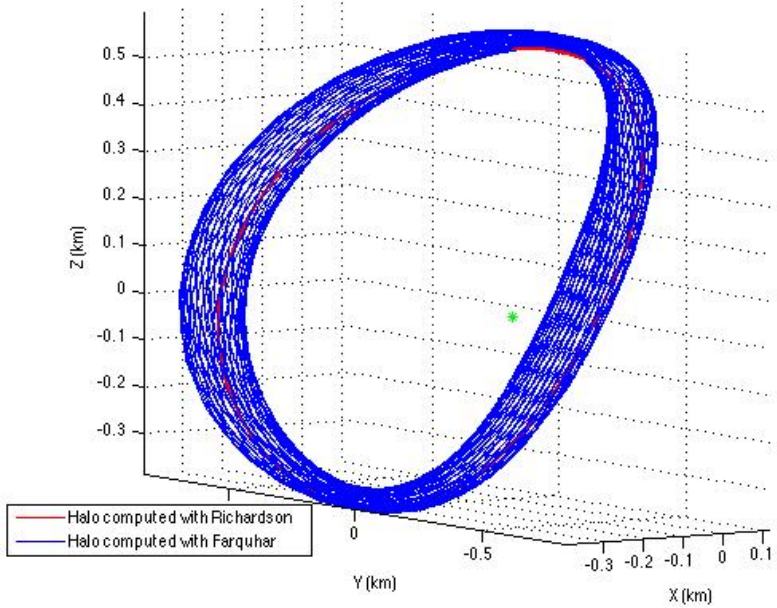
Figure 67: Comparison of Halo obtained with Farquhar model and Richardson model

It can be concluded that the Halo orbit model type has large consequences on the accuracy of the position knowledge. An imprecise model will generate degraded rendezvous performances. The Farquhar orbit model is interesting since it takes into account natural uncertainties (like for example the Sun's gravitational effect on the Earth-Moon system). The Farquhar third-order approximation is convenient for qualitative analysis, but may be insufficient for accurate performances computation. As a consequence, this orbit is then combined to a differential correction process using the Richardson model as a first guess. Moreover applying the Richardson model will reinforce constancy with the transfer trajectory algorithm.

5.3.4.2 Poincaré section definition

The Poincaré section description is consequently enhanced by a new definition, given as:

$$\{(x, y, z, \dot{x}, \dot{y}, \dot{z})/\phi = \phi_{rdv}\} \qquad (5\text{-}8)$$

With ϕ_{rdv} varying between 0° and 360°.
The origin of ϕ_{rdv} is O, the center of gravity of the Earth-Moon system (see 4.2.4).
Figure 68 presents the Poincaré section definition.
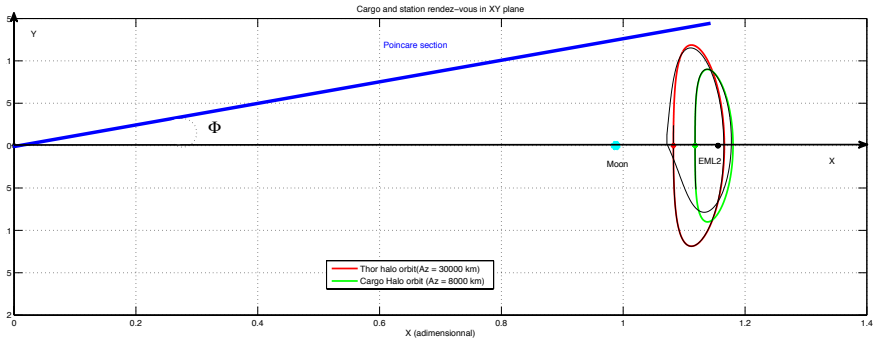
Figure 68: Poincare section definition for rendezvous optimization

ϕ_{rdv} excursion is limited to the internal realm of the Earth-Moon system [27].

Figure 69 presents an example of the effective potential, in the case of Earth-Moon system (with $\mu = 0{,}3$).
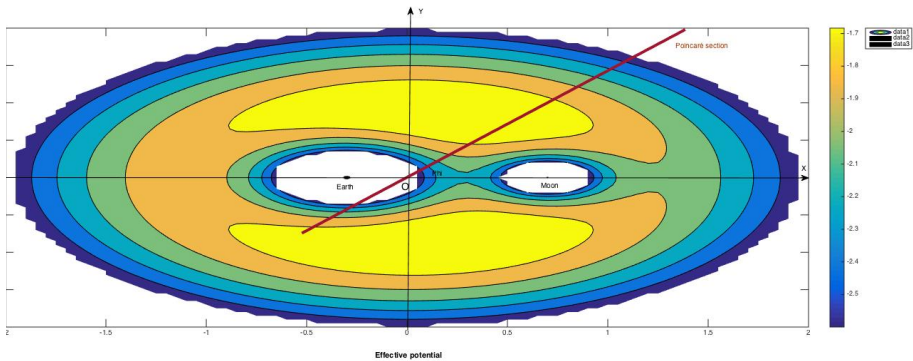
Figure 69: Poincare section and Effective potential

On this figure, it can be easily noticed that only low values of ϕ_{rdv} are expected for rendezvous.

5.3.4.3 Rendezvous total delta-v computation

The total delta-v for the rendez-vous is computed as:

$$\Delta v_{rdv} = \Delta v_1 + \Delta v_2 + \Delta v_3 \qquad (5\text{-}9)$$

Where

- Δv_1 is the necessary burst to enter the unstable manifold from the chaser initial Halo orbit
- Δv_2 is the burst to leave the unstable manifold to get on the stable manifold
- Δv_3 is the required final burst to leave the stable manifold to join the THOR Halo orbit

Figure 70 presents an example of the three rendezvous maneuvers. It was obtained for the same conditions as Figure 66. The length of the arrows representing the maneuvers is not scaled.
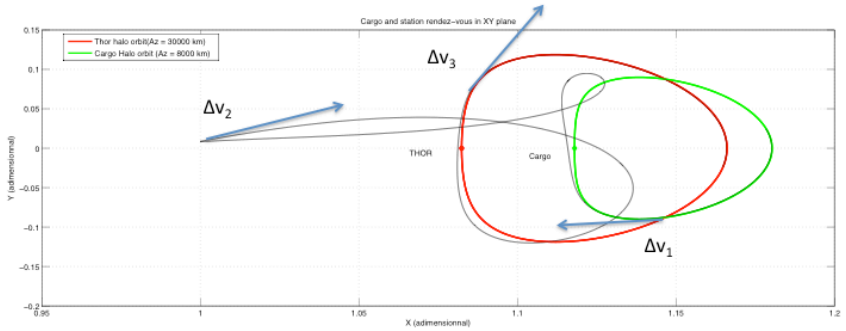
Figure 70: Example of the three rendezvous maneuvers

137

5.3.5 Assumptions for rendezvous with THOR

Here under table sums up the assumptions for the design parameters:

Parameter	Value	Units
$A_{z\ THOR}$	8000	km
m_{THOR}	3	
$d_{m\ THOR}$	50	km
θ_{THOR}	[0; 360]	(°)
$A_{z\ chaser}$	[5000; 3000]	km
m_{chaser}	1 or 3	
$d_{m\ chaser}$	50	km
θ_{chaser}	[0; 360]	(°)
ϕ_{rdv}	[0; 360]	(°)

Table 14: Rendezvous design parameters assumptions

5.3.6 Rendezvous optimization criteria

This chapter focuses on the rendezvous between a chaser (cargo or crew vehicle) and the THOR space station, but it aims at minimizing the total rendezvous delta-v (Δv_{rdv}) and the duration (see 5.3.6 for optimization description). Computation of Δv_{rdv} has been provided in 5.3.4.

The cost function for the optimization process is a combination of the distance between the two manifolds and the velocity gap at this point, since Δv_2 is the most critical maneuver. The distance has to be as low as possible:

- First to explore only physical and feasible trajectories (no teleportation is allowed)
- Then to limit the rendezvous duration, since it is a direct consequence of this distance.

Optimization process is based on two steps:

- A first **global step** aims at finding an initial guess: both Halo orbits are fixed ($A_{z\_}$ and m are constant for both orbits). Only the angular phases, θ_{THOR} and θ_{chaser} are let free to vary. Initial guess will be the trajectory will minimize the cost function (detailed in (5-10)). Results are provided 5.3.7.1
- Then, a second **local step** starts from the initial guess. Design parameters domain is then extended. Results are provided in 5.3.8.

The cost function combines the position gap and the velocity gap at manifold intersection on the Poincaré section. It can be written as the minimum of the weighted root mean square:

$$minJ = \left(\sqrt{ \alpha \left\| \begin{pmatrix} x_{chaser_{PM}} \\ y_{chaser_{PM}} \\ z_{chaser_{PM}} \end{pmatrix} - \begin{pmatrix} x_{THOR_{PM}} \\ y_{THOR_{PM}} \\ z_{THOR_{PM}} \end{pmatrix} \right\|_2^2 + \beta \left\| \begin{pmatrix} \dot{x}_{chaser_{PM}} \\ \dot{y}_{chaser_{PM}} \\ \dot{z}_{chaser_{PM}} \end{pmatrix} - \begin{pmatrix} \dot{x}_{THOR_{PM}} \\ \dot{y}_{THOR_{PM}} \\ \dot{z}_{THOR_{PM}} \end{pmatrix} \right\|_2^2 } \right) \qquad (5\text{-}10)$$

138

Where:

- $\begin{pmatrix} x_{chaser_{PM}} \\ y_{chaser_{PM}} \\ z_{chaser_{PM}} \end{pmatrix}$ is the position of the intersection of the unstable manifold (from the initial chaser Halo orbit) and the Poincaré map (PM)

- $\begin{pmatrix} x_{THOR_{PM}} \\ y_{THOR_{PM}} \\ z_{THOR_{PM}} \end{pmatrix}$ is the position of the intersection of the stable manifold (from the THOR Halo orbit) and the Poincaré map (PM)

- $\begin{pmatrix} \dot{x}_{chaser_{PM}} \\ \dot{y}_{chaser_{PM}} \\ \dot{z}_{chaser_{PM}} \end{pmatrix}$ is the velocity at the intersection of the unstable manifold (from the initial chaser Halo orbit) and the Poincaré map (PM)

- $\begin{pmatrix} \dot{x}_{THOR_{PM}} \\ \dot{y}_{THOR_{PM}} \\ \dot{z}_{THOR_{PM}} \end{pmatrix}$ is the velocity at the intersection of the stable manifold (from the THOR Halo orbit) and the Poincaré map (PM)

- $\left\lVert \begin{pmatrix} x \\ y \\ z \end{pmatrix} \right\rVert_2$ refers to the quadratic norm 2 of the vector $\begin{pmatrix} x \\ y \\ z \end{pmatrix}$

- α is the weight of the gap in position
- β is the weight of the gap in velocity

This cost function is robust, since there is no discontinuity as far as the local step of the optimization process is concerned. The cost function expression is quite simple, but the constraints are complex due to non-linear dynamics of the system. As a consequence, it is really difficult to find a simple methodology to find out optimal values for both weights (α, β). Their tuning will be detailed in 5.3.7.2.1.

5.3.7   Rendezvous results

5.3.7.1   Initial guess

A_{z_chaser} and A_{z_THOR} are assumed to be different, so as to take into account the launch and transfer maneuvers discrepancies. As already discussed in [44], Halo orbits with an A_z equal to 8000 km are less expensive than Halo orbits with an A_z equal to 30000 km.

Moreover, the simulation campaign demonstrated that the difference between both elongations has a bad impact on Δv_2. Actually, the difference, $\left| A_{z\_THOR} - A_{z-chaser} \right|$ influences Δv_2 and the total duration. Figure 71 presents the evolution of the total duration (red plot) in days and of Δv_2 the in km/s (blue plot) as a function of A_{z_chaser} (in km) when:

- A_{z_THOR} is set equal to 8000 km
- ϕ_{rdv} has a constant value of 0.5 °
- A_{z_chaser} varies from 7500 km to 8000 km/s with a step equal to 100 km
- (α, β) are set equal to 1

Graphs on Figure 71: Influence of A_{z_chaser} on the rendezvous duration and on Δv_2 Figure 71 lead to the conclusion that it would be better to select an A_{z_chaser} between 7500 km and 7900 km, or over 8400 km. As a consequence A_{z_chaser} has been set equal to 7800 km. According to the definition of the Poincaré map, ϕ_{rdv} is expected to take low values since Az_THOR is very small compared to the distance between EML2 and O (the origin of the reference frame). ϕ_{rdv} varies in the range $[-5°; +5°]$ with a step of $0.1°$.
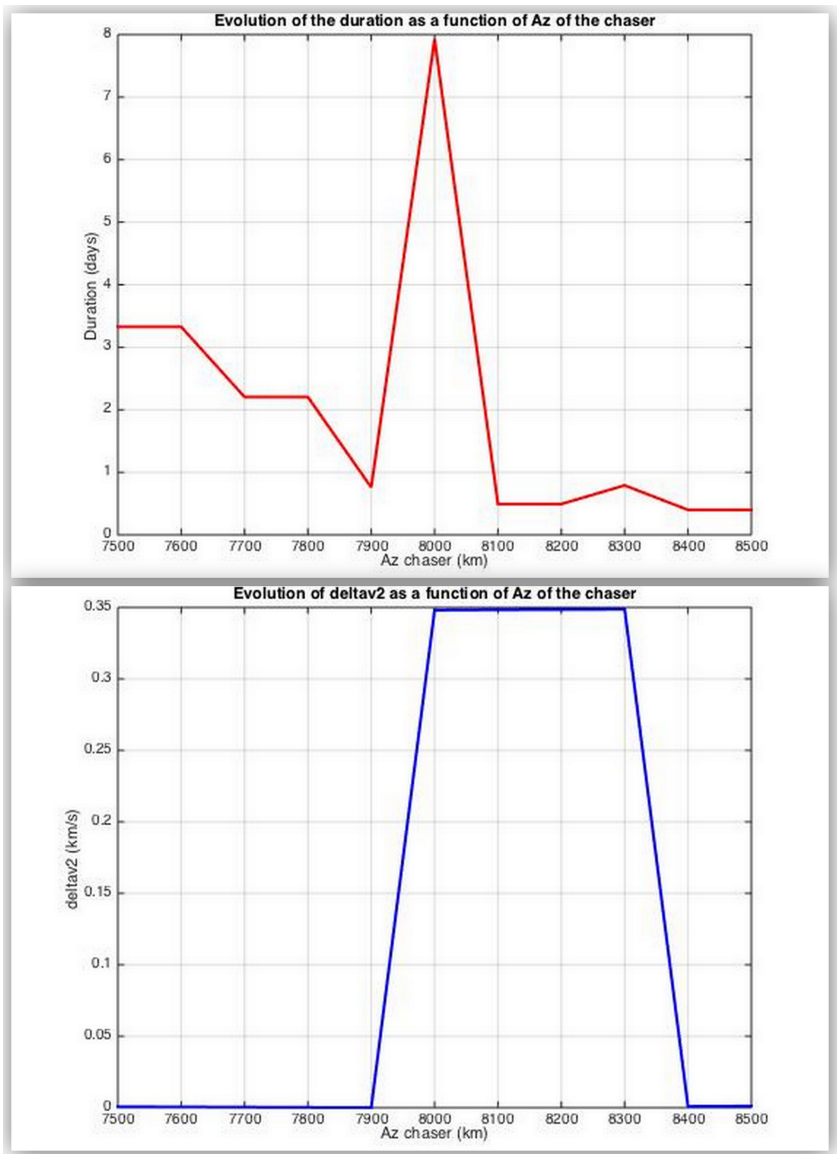
Figure 71: Influence of A_{z_chaser} on the rendezvous duration and on Δv_2

Next figure presents the evolution of the total duration (red plot) in days and of Δv_2 (blue plot) in km/s as a function of ϕ_{rdv} (in °).
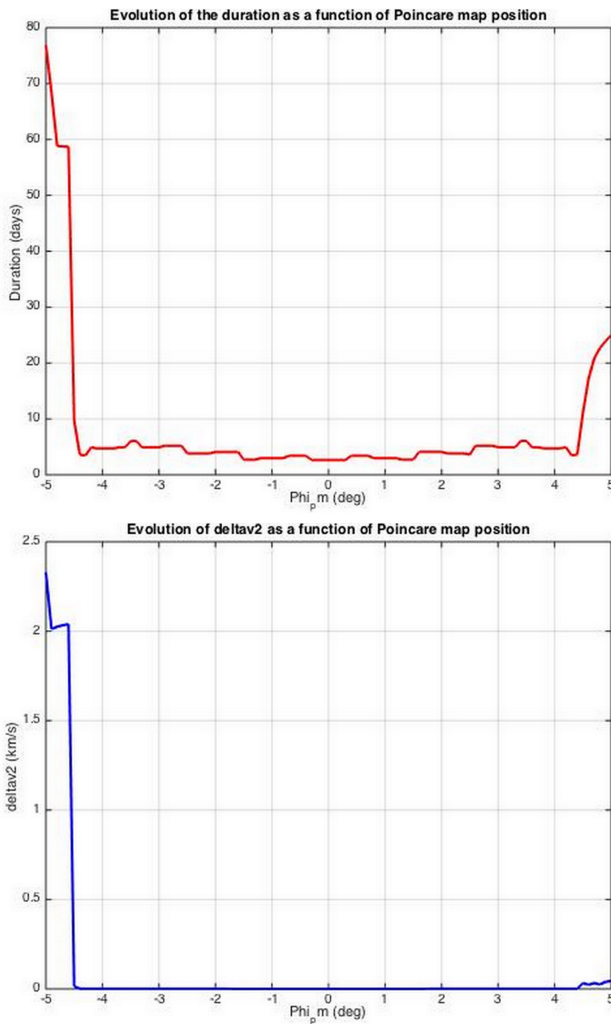
Figure 72: Influence of ϕ_{rdv} on the rendezvous duration and on Δv_2

On Figure 72, it can be observed:

- There are two areas (on the left and the right sides) where the rendezvous is not realistic (distance gap is largely greater than 50 km) and one area (in the middle) where the rendezvous is feasible. The boarder between unrealistic zone and feasible zone corresponds to the point where the Poincaré map intersection with the xy plane is tangent to the THOR Halo orbit, at its maximal elongation.
- The graph seems to be symmetrical as $\phi_{rdv} = 0°$. In that case, the Poincaré map intersection with the xy plane coincides to the x-axis, which is almost a

142

symmetric axis of the THOR Halo orbit. The Halo orbit is not really symmetric, since its maximal elongation is either on the Northern side (m=3) or the Southern side (m=1).

As a consequence, it seems to be judicious to limit the evolution of ϕ_{rdv} between 0° and 4.4°.

Figure 73 presents a focus on rendezvous distance gap with this new range for of ϕ_{rdv}.
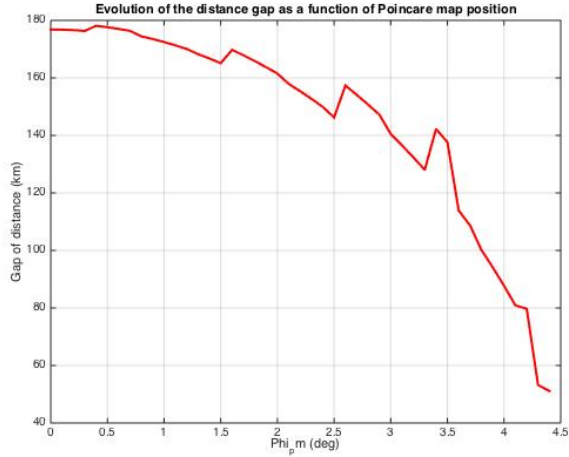
Figure 73: Rendezvous distance gap evolution when $\phi_{rdv} \in [0°; 4.4°]$

As a consequence, so as to find the initial guess it has been decided to fix:

- $A_{z\_chaser} = 7800$ km
- $A_{z\_THOR} = 8000$ km
- $\phi_{rdv} = 4.4$ °

For example, with the additional assumptions, performances obtained for the rendez-vous are:

Data	Value	Units
Δv_1	1.4296e-04	km/s
Δv_2	0.0011	km/s
Δv_3	9.0823e-05	km/s
Δv_{rdv}	0.0013	km/s
Duration	3.629	days
Distance gap	51.1163	km
θ_{THOR}	80	°
θ_{chaser}	330	°

Table 15: Initial guess performances

According to the total delta-v and duration, this initial guess is really promising. The instantaneous jump in space is about 51 km. It is reminded that the limit for linearization is considered to be equal to 50 km. Optimization process will then aim at reducing this distance without degrading the total delta-v and duration.

5.3.7.2   Rendezvous influence analyses
Results obtained at the previous step are encouraging: the methodology proposed seems to obtain good performances. Nevertheless, the results are not optimal, in particular, because the gap in distance at the intersection of both manifolds on the Poincaré Map is too high. In this paragraph, it is analyzed:
-    The influence of the weights of the cost function
-    The influence of the initial angular positions on both Halo orbit
on the rendezvous performances.

5.3.7.2.1   Influence of α and β
The main goal of the previous step was to identify an initial guess to confirm that the proposed strategy is feasible. At this step, (α, β) are set equal to 1.
While studying the evolution of the distance in position and in velocity between the two manifolds, it can be noticed that the (α, β) influences the performances. It can be then expected to find a couple of values for (α, β) that would reduce the distance gap, the total delta-v and the duration.
When $\alpha \gg \beta$, it means that the feasibility of the mission dominates.
When $\alpha \leq \beta$, it means that the cost of the mission is the most important criterion for strategy selection.

While applying the Richardson modeling for the both Halo orbits, the ratio between α and β should be chosen as follows, if one is looking for an equivalent weight between feasibility and cost:

$$\frac{\alpha}{\beta} = \frac{\left|(1+\kappa)^2\left(A_{x\_chaser} + A_{x\_THOR}\right)^2 + \left(A_{z\_chaser} + A_{z\_THOR}\right)^2\right|}{\left|\omega_p^2(1+\kappa)^2\left(A_{x\_chaser} + A_{x\_THOR}\right)^2 + \omega_v^2\left(A_{z\_chaser} + A_{z\_THOR}\right)^2\right|} \qquad (5\text{-}11)$$

Computational details are provided in Appendix 4.

Figure 74 presents the results of the analysis of the influence of (α, β) on the rendezvous performances (duration, total delta-v and teleportation gap), with the same assumptions as the proposed initial guess (see at the end of 5.3.7.1, with $\phi_{rdv} = 4.4\,°$). The first graph (upper left hand) shows the evolution of the rendezvous duration (in days) as a function of alpha: duration clearly decreases while alpha increases until it converges towards a minimal value (here 2.9 day). The second graph (upper right hand) describes the evolution of the rendezvous duration as a function of the distance gap: the duration increases with the distance gap. This means that while minimizing the distance gap, it minimizes the duration. The plot also reveals that it is possible to find a solution with a distance gap at the Poincaré lower then 50 km. The third graph (lower right hand) presents the evolution of total delta-v as a function of alpha. It can be concluded that there is no simple relationships between alpha and the delta-v. But, the minimal value of delta-v ($1.3.\ 10^{-03}$ km/s) is obtained for an alpha between to 2 and 5, which is coherent with the order of magnitude obtained with formula (5-11). Actually, in this particular case, the formula suggests that $\frac{\alpha}{\beta} = 3.48$.

Unfortunately, the minimum for delta-v does not correspond to the minimum for the duration (and the teleportation gap). That is the reason why, the last graph (lower left hand) has been plotted: it shows the rendezvous duration as a function of the total delta-v. A compromise must be found between duration and delta-v. When a crew vehicle mission is concerned, of course the strategy that would minimize the duration would be selected: the position of the Poincaré map should probably be modified. For the cargo, strategy with the lowest delta-v should be chosen. All the graphs lead us to conclude that alpha should be lower than 43.
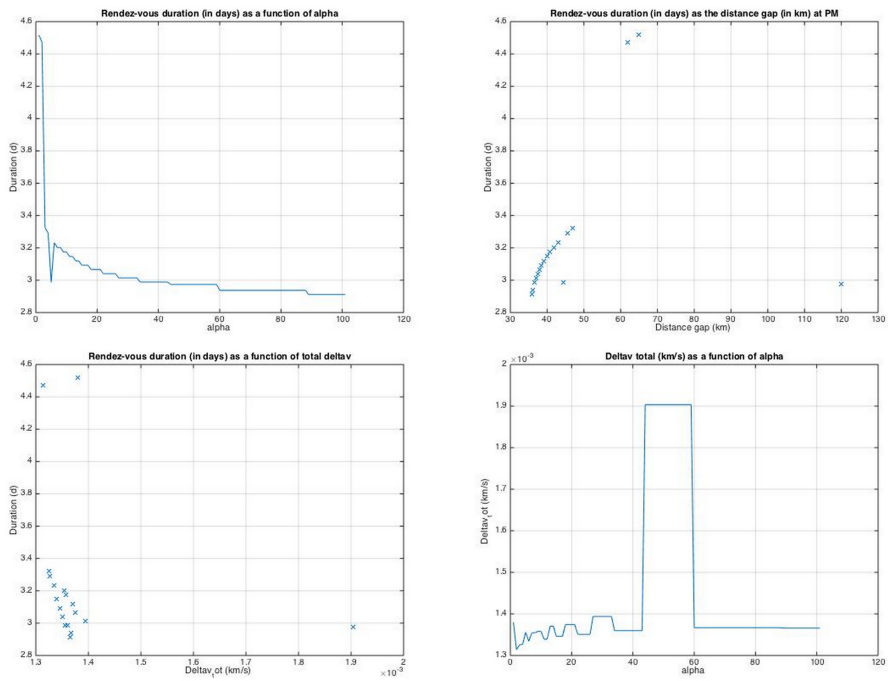
Figure 74: Influence of (α, β) on the rendezvous performances

Setting $\alpha = 4{,}35$ and $\beta = 1$ leads to the following performances, compared to the ones obtained for $\alpha = 1$ and $\beta = 1$

Data	Value ($\alpha = 4{,}35$)	Value ($\alpha = 1$)	Units
Δv_1	1.4063e-04	1.4296e-04	km/s
Δv_2	0.0011	0.0011	km/s
Δv_3	9.0823e-05	9.0823e-05	km/s
Δv_{rdv}	0.0013	0.0013	km/s
Duration	3.3299	3.629	days
Distance gap	49.008	51.1163	km
θ_{THOR}	80	80	°
θ_{chaser}	360	330	°

Table 16: Refined initial guess

The performances obtained for the new strategy are all better than the one presented in Table 15.

146

5.3.7.2.2 Influence of θ_{THOR} and θ_{chaser}

To improve the first global step of the optimization process, it has been decided to perform complementary analyses so as to determine the influence of the initial angular position (θ_{THOR} and θ_{chaser}). The graph on Figure 75 provides the evolution of total delta-v during the rendezvous as a function of the angular position on the departure Halo orbit and on the arrival Halo orbit, for two positions of the Poincaré Map $\phi_{rdv} = 4.4°$ and $\phi_{rdv} = 0.5°$. Other data are the ones selected for the initial guess trajectory.
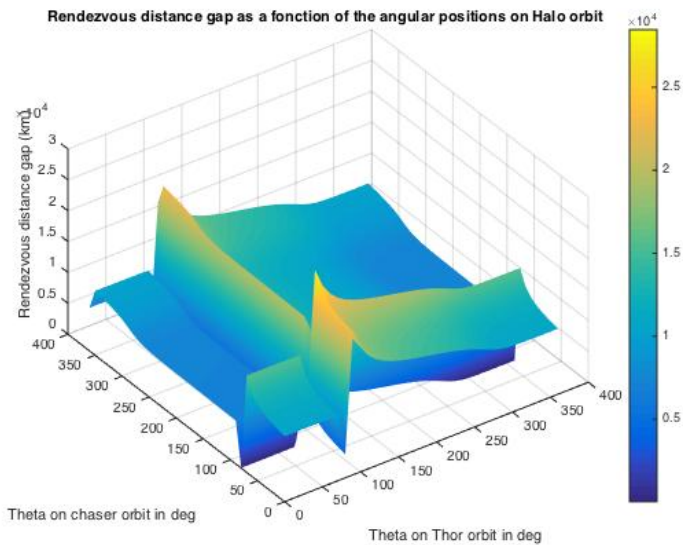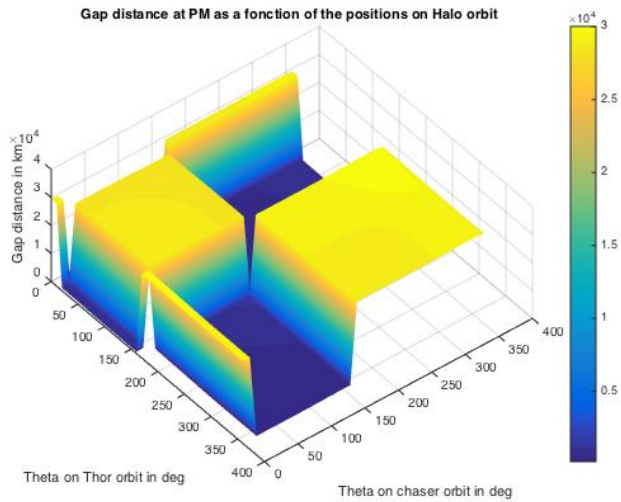
Figure 75: Distance gap as a function of the angular positions on the Halo orbit
for $\phi_{rdv} = 0.5°$ (up) and for $\phi_{rdv} = 4.4°$ (down)

On these graphs, it can be observed that there are large discontinuities on the distance gap. Similar analyses on the total duration and on the total delta-v lead to the same conclusion. Those discontinuities can be surprising, since the design parameters evolve continuously. They can be explained by the selection of the $(\theta_{THOR}, \theta_{chaser})$ pair. Two distinct areas can be observed:

- The blue ones, where the distance gap at the intersection on the Poincaré are almost feasible (less than 500 km),
- The yellow ones, where the distance gap at the intersection on the Poincaré are unrealistic (over 2.8×10^4 km)

Actually, the discontinuities correspond to the optimization process that jumps brutally from one $(\theta_{THOR}, \theta_{chaser})$ pair to another one, as the cost function takes only into account what happens at the Poincaré map. Such a behavior can have a direct impact on the mission design since the main risk of such discontinuities lies in the fact that if the mission discrepancies induce an error (of some degrees) on those initial angular positions, generating an important and sudden increase of the total delta-v.

In fact, the variation of delta-v as a function of both angular positions is continuous, only the optimization process induces the discontinuities. An error on the initial value of the departure (or arrival) position will only degrade the total duration and the total delta-v.

With further simulations, it has been observed that:

- The distance gap is satisfactory when θ_{THOR} and θ_{chaser} are on opposite sides of the Poincaré map. This situation corresponds to the blue zones.
- The distance gap is not acceptable when angular positions on both Halo orbits are on the same side of the Poincaré map. This is the case for the yellow areas.

This can be explained by the fact that the unstable manifold of the Halo orbit of the chaser is always computed clockwise (with respect to the Halo orbit pseudo-center reference frame). As a consequence, when the chaser initial position is located on the same side of the Poincaré Map as the THOR space station target angular position, the unstable manifold end-point is too far away from the stable manifold end-point to consider the rendezvous as valid (see lower part of Figure 76). Actually, it corresponds to an unrealistic jump in space. On the contrary, when the chaser initial position is located on the opposite side of the Poincaré Map as the THOR space station target angular position, both manifold end-points are close enough to perform a rendezvous (see upper part of Figure 76).

Figure 76 was obtained with the following assumptions:

Data	Value	Units
Δv_1	1.0954e-04	km/s
Δv_2	1.675e-04	km/s
Δv_3	1.0463e-04	km/s
Δv_{rdv}	3.8162-04	km/s
Duration	2.34	days
Distance gap	175,07	km
ϕ_{rdv}	0.5	°
θ_{THOR}	60	°

For realistic rendezvous

θ_{chaser}	310	°

For unrealistic rendezvous

θ_{chaser}	28	°

Table 17: Assumptions for realistic and unrealistic rendezvous
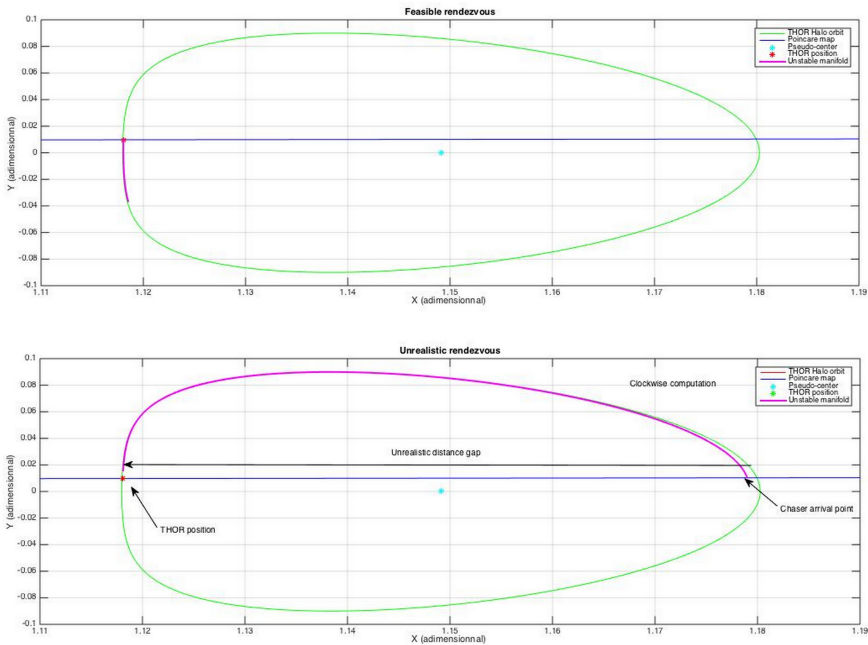
Figure 76: Influence of initial angular position on rendezvous performances

The main conclusion is that the performances of the rendezvous definitely depend on the initial angular positions on both Halo orbit, that is to say (θ_{THOR}, θ_{chaser}). Best rendezvous will be found in a scenario when θ_{THOR} and θ_{chaser} are on opposite sides of the Poincaré map.

150

Moreover, the optimal scenario corresponds to the case with the Poincare map tangent to the Halo orbit at one of its extrema along the y-axis.

5.3.8   Rendezvous optimization algorithm

The main conclusions of the previous analyses lead to propose the following process to select the optimal scenario for a rendezvous with THOR space station (when A_{z_THOR}, $m_{\_THOR}$, A_{z_chaser}, $m_{\_chaser}$) are already fixed:

-   **Step 1:** To compute the THOR and chaser Halo orbits
-   **Step 2:** To minimize the gap of distance at Poincare map when ϕ_{rdv} is varying.
-   **Step 3:** When ϕ_{rdv} is fixed, to optimize rendezvous total delta-v when $(\theta_{THOR}, \theta_{chaser})$ are let free.
-   **Step 4:** To compute the optimal rendezvous performances (duration, distance gap and total delta-v)

Figure 77 provides a synthesis of the optimization algorithm for the rendezvous between a chaser and the THOR space station.

Optimization algorithm selected to find the minimum gap of distance at Poincaré map is similar to a method of gradient descent.
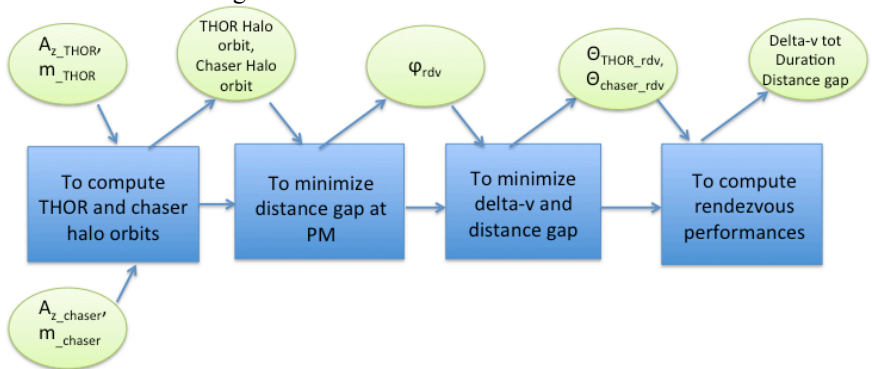
Figure 77: Rendezvous optimization algorithm

5.3.9   Rendezvous optimization synthesis and recommendations

This paragraph will first present some results of the rendezvous optimization process, then comments on analyses performed on another category of rendezvous and then recommendations.

5.3.9.1 Optimization results

Applying the optimization algorithm presented in 5.3.8, the following strategy was sorted out. Resulting performances comply with the requirement:

- Distance gap at Poincaré lower than 50 km
- Low total delta-v
- Low duration (about three days)

The strategy is then summed up in the following table:

	Parameter	Value	Units
THOR Halo orbit definition	$A_{z\ THOR}$	8000	km
	m_{THOR}	3	
	$d_{m\ THOR}$	50	km
	θ_{THOR}	**80**	(°)
Chaser Halo orbit definition	$A_{z\ chaser}$	7800	km
	m_{chaser}	3	
	$d_{m\ chaser}$	50	km
	θ_{chaser}	**330**	(°)
Rendezvous	ϕ_{rdv}	**4.48**	(°)
Performances	Δv_1	**1.4296e-04**	km/s
	Δv_2	**0.0012**	km/s
	Δv_3	**9.0823e-05**	km/s
	Δv_{rdv}	**0.0014**	km/s
	Duration	**3.6317**	days
	Distance gap	**41.6335**	km

Table 18: Example of Halo-to-halo rendezvous strategy performances

Bolded values come out the optimization process. Figure 78 presents the entire rendezvous trajectory from chaser Halo orbit ($A_{z\ chaser}$ = 7800km, m_THOR = 3) to THOR Halo orbit ($A_{z\ chaser}$ = 8000km, m_THOR = 3) with ϕ_{rdv} = 4.48°.
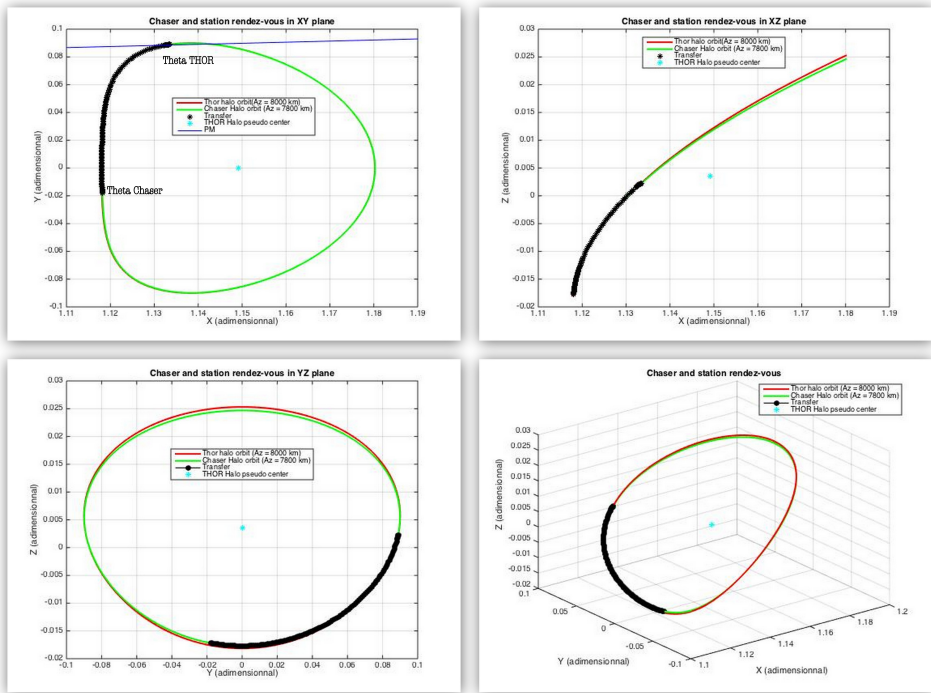
Figure 78: Halo-to-Halo rendezvous with THOR with $\phi_{rdv} = 4.48°$

On this graph, the two Halo orbits (the green for the chaser and the red for THOR) are almost mixed since both elongations are not really different. Anyway, it can be noticed that the Poincaré map is almost tangent to the THOR Halo orbit.

This strategy was selected since it minimizes the distance gap at the Poincaré map. The feasibility criterion is considered to be the most important. Actually, some other strategies could be proposed with lower duration or lower total delta-v. As a consequence, when the crew vehicle mission is concerned, different rendezvous trajectories can be selected so as to reduce the duration, even if the total delta-v would increase.

5.3.9.2 Rendezvous further analyses
Two complementary analyses have been performed to:

- Compute another type of strategy for rendezvous like for example, a Lyapunov orbit.
- Find a new criterion to decide where to apply delta-v2 (the second maneuver that leads to quit the unstable manifold of the chaser Halo orbit and reach the stable manifold of the THOR space station)

153

5.3.9.2.1 Lyapunov-to-Halo rendezvous

Previous studies have all been performed with a chaser parking on a Halo orbit so as to be nearest to the THOR Space station. From results presented in chapter 5.3.3, the chaser may be orbiting on another type of trajectory, like a Lyapunov orbit (see 4.4.1 for the definition).

Actually, it was expected the intersection between unstable manifolds of a given Lyapunov orbit and stable manifolds of a Halo orbit could provide new opportunities.

The Lyapunov orbits have no extension along the z-axis, and are entirely described, by A_x (maximal elongation along x-axis). Consequently, several important steps of the rendezvous computation process had to be adapted: particularly, the orbit generation and the differential correction.

Lyapunov-to-Halo rendezvous performances have been computed while A_{x_chaser} and the position of the Poincaré map, ϕ_{rdv}, are varying. It has been then observed that some cases correspond to shorter duration (compared to average Halo-to-Halo rendezvous), but with bigger total delta-v (total cost is almost multiplied by 100, even by 1000).

Those results can be easily explained. In fact, as the two orbits (with equivalent elongation) are almost superimposed in the xy-plane, the transfer duration is low. Nevertheless, the maneuver at the manifolds intersection requires a high level thrust along z-axis to join the THOR Halo orbit stable manifold, since until now the chaser velocity has only components along x and y axis.

Above all, the distance gap at Poincaré map is unsatisfactory. Another algorithm to find the best intersection should be suggested.

As a consequence, it has been decided not to go on with this type of rendezvous strategy, since it does not procure promising performances. Anyway, it should not be totally dismissed: first for a better understanding of the dynamics in the vicinity of EML2 and secondly, for specific scientific missions this could have any interest in Lyapunov orbits. Moreover, it could be really instructive to perform a global comparison of all types of rendezvous in the vicinity of EML2.

5.3.9.2.2 Intersection improvement

Going back to Halo-to-Halo rendezvous strategy, it has been decided to find a more generic way to find the optimal rendezvous. Main conclusion of the previous paragraphs was that the Halo-to-Halo rendezvous performances directly depend on the position of the intersection at the Poincaré map.

The idea is now to enlarge the intersection area so as to allow maneuvers at other places than at Poincaré map, but still in its vicinity. The best location to perform the second maneuver will be selected as the one that minimize the criteria given by (5-10).

The new process could be:
- **Step 1**: To fix rendezvous initial conditions (A_{z_THOR}, m_THOR, A_{z_chaser}, m_chaser, ϕ_{rdv}, θ_{THOR}, θ_{chaser})
- **Step 2**: To compute the unstable and stable manifolds until the Poincaré map
- **Step 3**: To select the n last (resp. first) positions on the unstable (resp. stable) manifold
- **Step 4**: To compute the quadratic distance criteria (see (5-10)) for each positions couple (one on the unstable manifold, one on the stable manifold)
- **Step 5**: To find the couple that minimizes the criteria.

This algorithm has been suggested so as to refine the Halo-to-Halo optimization algorithm and succeeds to it.

5.3.9.3 *Rendezvous recommendations*
The main results of the analyses performed for the rendezvous with the THOR space station on a Halo orbit around EML2 are:
- First, A_{z_chaser}, the maximal elongation of the Halo orbit of the chaser along the z-axis, should be close to A_{z_THOR}. For example, with A_{z_THOR}= 8 000km, it is recommended to select A_{z_chaser} in the range of [7 500 km; 7 900 km].
- Secondly, the position of the Poincaré map must be carefully selected. It will impose the location where the vehicle will change from the unstable stable manifold leg to the stable manifold leg. In the case where A_{z_THOR}= 8 000km, it can be suggested to fix it in the range of [-4.5°; 4.5°]. As, the problem is symmetrical; its study can be limited to the positive values of ϕ_{rdv}.
- Thirdly, the angular positions on both Halo orbit, θ_{THOR} and θ_{chaser} are decisive for the rendezvous performances. It has been concluded that θ_{THOR} and θ_{chaser} should be on both sides of the Poincaré map.
- At last, the Poincaré map should be almost tangent to the THOR Halo orbit at its maximal position along the y-axis.

Those recommendations lead to define precisely the rendezvous strategy so as to find the best compromise between the duration, the cost (in term of delta-v) and teleportation (distance gap at the Poincaré map).
Those analyses were restricted to the HOI case, with two Halo orbits belonging to the same family. Some further simulations led to the conclusions that rendezvous from a Lyapunov orbit to a Halo orbit are not worthy. Anyway, it could be really interesting to study deeply all the possible combinations of rendezvous (and more particularly the MOI strategies), to get better knowledge on heteroclinic rendezvous in the vicinity of a Earth-Moon Lagrangian points.

Until now, all the performances were computed separately (leg by leg). It is nevertheless worthy to consider the interaction between transfer and rendezvous. Two situations must be considered:

- First, the crew vehicle scenario that includes a lunar flyby transfer and a Halo-to-Halo rendezvous
- Secondly, the cargo delivery scenario with a WSB transfer and a Halo-to-Halo rendezvous

Main recommendations from the lunar flyby strategy analysis suggest that the targeted angular position for the injection of the vehicle on its Halo orbit must be close to the "no-go window". Then there are two options:

- Either to inject the chaser near the optimal angular position on the Halo orbit to prepare the rendezvous
- Or to deposit it at an angular location that optimizes the transfer from LEO and wait to reach the optimal rendezvous departure point to start the second leg of the trajectory.

On the one hand, the first option would minimize the duration and the total delta-v of the entire trajectory of the chaser from LEO to THOR Halo orbit, but it could be very risky. Actually, any discrepancy on the application of the delta-v by the propulsion sub-system might generate a modification of the trajectory. The chaser travel would by consequence be different from the theoretical one. The dynamics in the vicinity of EML2 is complex and non-linear. As a consequence, solutions are not robust to parameters modification.

On the other hand, the second option will degrade the total duration of the trajectory, since the chaser would have to wait before departing towards the Halo orbit. Moreover, additional maneuvers could be expected for station keeping during that parking phase. But, the great advantage of this option is to increase the flexibility of the rendezvous trajectory. Actually, the mission control center would be able to prepare and propose a new strategy in case of unexpected deviation to the theoretical ones.

It can be then recommended to go further in the modeling of the entire trajectory, so as to link together both legs: the transfer from LEO to chaser Halo orbit and the Halo-to-Halo rendezvous.

The cargo delivery scenario should take benefit of the WSB transfer strategy. This transfer does not impose constraint on the rendezvous. On the contrary, the global strategy must start from the criterion of the rendezvous on THOR Halo orbit so as to deduce the optimal chaser rendezvous and then find the transfer in the two patched Three-Body problems from LEO to the cargo Halo orbit. Thus, the rendezvous criterion would impose the conditions of departure from LEO with the best configuration of the position of Sun, Moon and Earth, and by consequence, the departure date, that must be compatible with operational constraints (launch window, control center availability, visibilities…).

Next paragraph will then deal with the performances computation for all the identified mission scenarios: THOR space station assembly, cargo delivery and crew rotation for the entire duration of the station life duration. This study does not only focus on trajectory cost and duration, but also on other figures of merit.

5.4 Mission evaluation

At this stage of THOR mission study, the selection of the best strategy for the entire mission needs a multi-criteria decision analysis approach. This approach mainly falls into five main steps:
1. To define potential alternatives
2. To elicit Stakeholders' needs so as to define criteria
3. To rank the criteria
4. To aggregate criteria so as to compare scenarios
5. To decide so as to select the best strategy

Remark: This process is presented here sequentially, but it can be a loop to take into account the impact of new inputs.

Stakeholder's needs analysis of the THOR (see 3.1.2.3) mission provides the following main objectives:
- **Objective n°1:** The THOR space station shall be always safe for the crewmembers. Particularly, it means that all phases of the life cycle (i.e. during assembly and operations) shall take place in a safe, adaptable and effective way.
- **Objective n°2:** Efficient and sustainable systems with commonalities to existing THOR Space Station shall be used while keeping deployment and operational cost low.

A secondary class of objectives corresponds to the success of the THOR space station exploration goals (scientific experiments, human exploration of the solar system…).

As a consequence, all efforts performed in mission analysis chapter (see 5) are necessary but are not sufficient to select the optimal strategy for the global THOR mission. Complementary criterion shall be introduced to evaluate entirely both high-level mission objectives.

This chapter will:
- First introduce the scenarios (deduced from the mission life profile, see 0),
- Secondly, give the list of figures of merit according to both previous objectives,
- Thirdly, provide processes to evaluate those figures of merit,
- Fourthly, presents the results of figures of merit evaluation,
- And last, proposes a synthesis and recommendations.

5.4.1   Scenarios description

The THOR mission life-profile has been previously decomposed (see 0, and particularly Figure 18). As a result, three main scenarios have to be considered:

- Scenario A: Space Station assembly
- Scenario B: Resupply cargo delivery
- Scenario C: Crew rotation

While combining all those potential scenarios, more than 216 cases are obtained. Only the 42 most relevant are selected and are detailed here under. The detailed decision tree for those selected scenarios is provided on

Figure 96 in Appendix 5. In those selected scenarios, none dominates the others. All of them are relevant.

Scenario A consists of several options:

- The **type of launcher:** two launch vehicles are considered. They are the SLS (Space Launch System, under development, Figure 79) or the Ariane 5 ES (Figure 80). As each THOR module maximal mass is limited to 20t, it can be launched by Ariane 5 ES as ATV. But another option could be to leave Earth on-board a heavy lift vehicle, like SLS that should be able to deliver between 70t and 130t in LEO [67]. The lowest configuration could deliver three modules and a sphere together. As consequence, three SLS launches could be enough, while in the Ariane 5 ES case at least seven launches are necessary.
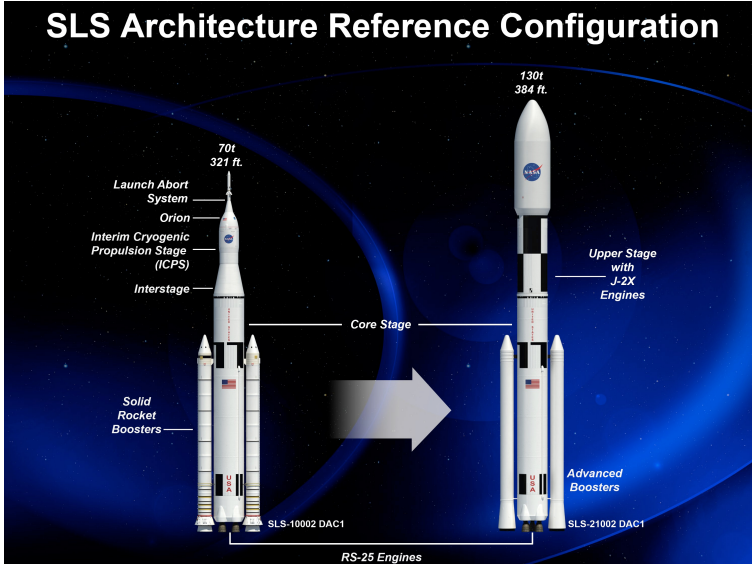
Figure 79: SLS Architecture reference configuration (copyright NASA)
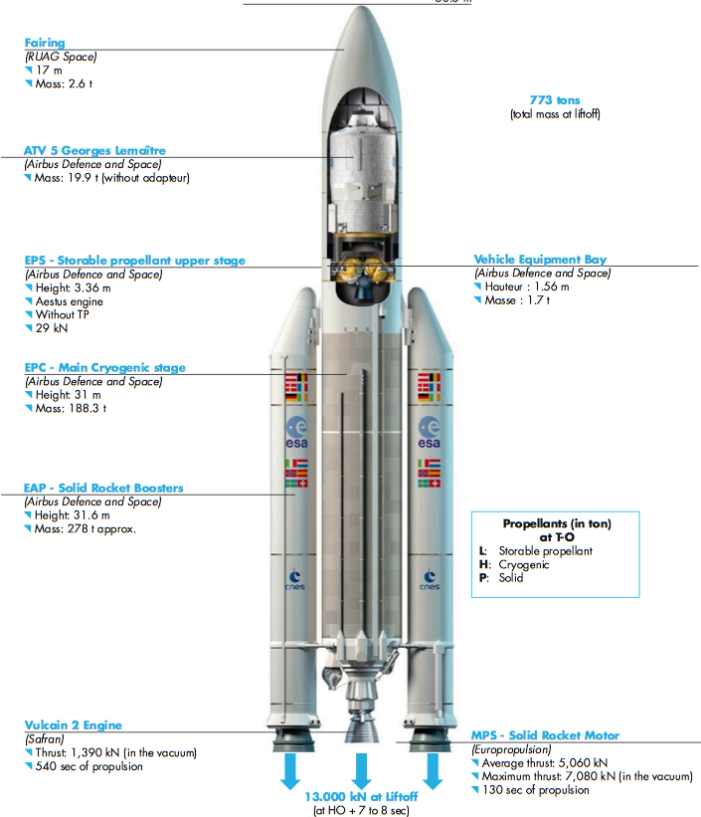
Figure 80: Ariane 5 ES architecture (Copyright ESA)

- The **assembly location**: in LEO or in EML2, and the sequence of modules integration. The modules can be assembled at different locations. The seven modules of the Space Station can be either integrated totally in LEO, then transferred to EML2 or assembled directly at EML2. The final assembly at EML2 could be a very flexible strategy, since the station would be gradually extended with the arrival of the new single modules or group of modules. It could improve the date of availability of the Space Station. The different assembly sequences of the THOR Space Station correspond to staging options. In **Ariane 5 ES case**, fifteen intermediate combinations have to be considered. In scenarios evaluation study, only four of them are presented and listed below:
    o Scenario A.1: The total assembly in LEO (noted "1x7").
    o Scenario A.2: The total assembly at EML2 (noted "7x1").
    o Scenario A.3: (noted "4 + 3x1"). Four core modules are assembled first in LEO and sent towards EML2. Then, the three remaining

159

modules are added separately, delivering three extension modules for the station capabilities.

- o Scenario A.4: (noted "3 + 2x2"). This case consists in assembling in LEO a first core of three modules and then, transferred towards EML2. Finally, the four remaining modules are grouped in LEO, two by two.

In **SLS case**, only three combinations exist, since modules have already partially assembled on Earth:

- o Scenario A.5: The total assembly in LEO (noted "1x3").
- o Scenario A.6: Two groups of modules are assembled in LEO and then, transferred together to EML2. Then, the last group of modeled is sent separately to EML2 and assembled to the station in EML2.
- o Scenario A.7: The total assembly at EML2 (noted "3x1").

Moreover, next table lists some example of qualitative pros and cons of both assembly locations. It is of course not exhaustive.

Assembly location	Pros	Cons
LEO	Known technology for assembly (ISS) Cheap and reliable delivery to LEO	Need for enhanced LEO capabilities Structure has to support the transfer Assembly services needed (LEO infrastructure)
EML2	Dedicated design for EML2 environment Initial on orbit capabilities (start with basic services, add modules for more advanced capabilities later on)	Modules need a higher degree of autonomy Only limited LEO check-out and testing

Figure 81: Disadvantages and benefits of assembly location

- The type of **propulsion**: chemical or electrical. The type of transfer (lunar flyby or WSB) can be a sub-option of chemical propulsion. Actually, electrical propulsion is not compatible with trajectories taking benefit of the Three-body problem, since delta-v generated by electrical engines cannot be considered as instantaneous. Moreover, electrical propulsion can only be envisaged when mission duration is not a constraint.

Thanks to previous analyses on the trajectories legs, the scenario B (Resupply cargo delivery) can be limited to options, linked to the type of propulsion of the cargo (electrical or chemical). The chemical cargo can use one of the three studies strategies for transfer: named here LBT (for Transfer), WSBT (for) and WSBE (for Weak Stability Boundary Exotic transfer). The scenario C (for crew rotation) is limited to only two options. Because of limitations due to transfer duration, electrical propulsion

and WSBT are not envisaged for the scenario C. Actually the lunar flyby transfer is highly recommended for crew rotation. The WSBE seems to be a good back-up option.

Finally, the selected scenarios for THOR mission evaluation are:

- o Scenario B.1: corresponds to the transfer of the cargo with a Lunar Flyby
- o Scenario B.2: is the Weak Stability Boundary Traditional transfer for the cargo
- o Scenario B.3: is the Weak Stability Boundary Exotic transfer for the cargo
- o Scenario C.1: is lunar flyby for crew vehicle
- o Scenario C.2: is the Weak Stability Boundary Exotic transfer for crew vehicle

Figure 82 depicts a hierarchical tree view summarizing all considered scenarios, while assuming no electrical propulsion. All the THOR space station modules are transferred with nominal WSB trajectory.
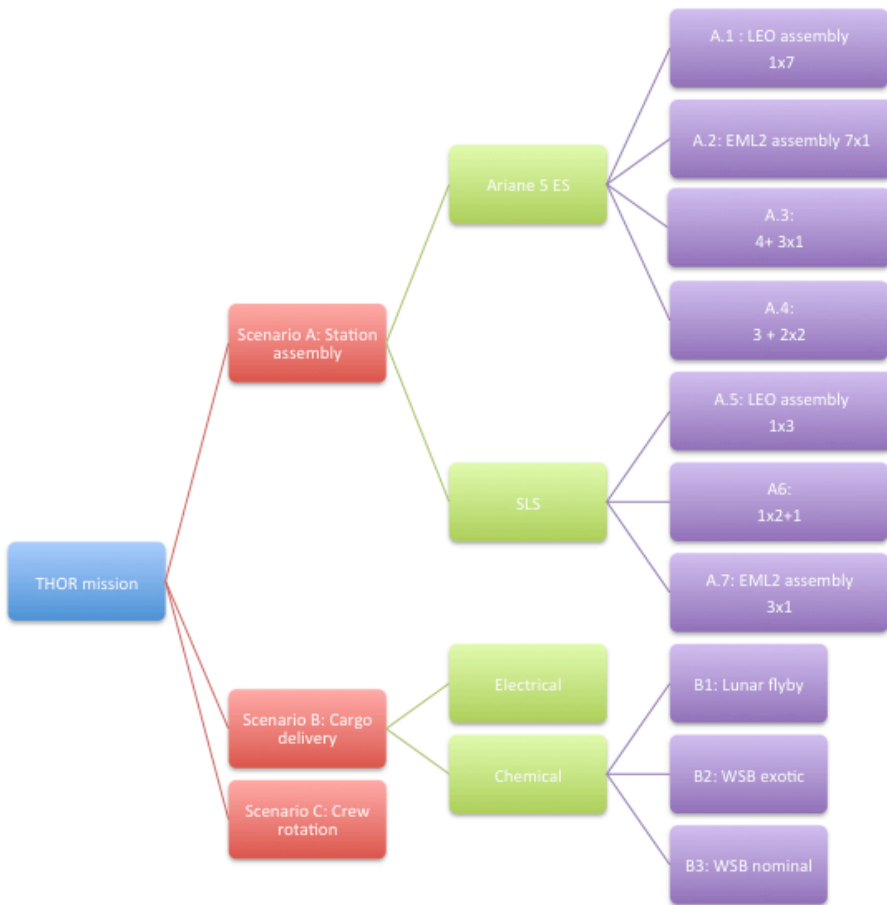
Figure 82: THOR mission scenarios overview

Having the full picture of all forty-two scenarios, they are compared by evaluating the Figures of Merit (FOM), presented in next paragraph.

5.4.2 Figures of merit

The studied scenarios are evaluated based on Figures of Merit (FOM). Those FOM are linked to system drivers, the mission objectives and must be easy to calculate or assess. On one hand, the qualitative FOM for this study are: cost, risk and operability. On the other hand, the quantitative FOM for this study are: required number of launches, the total delta-v (Δv_{tot},), IMLEO (initial mass delivered to LEO), AMEML2 (The available mass in EML2) and the time until initial operational capabilities are available (T_{init}).

Considered exhaustive, these eight FOM are not redundant. They are evaluated for each mission leg and finally the average values out of every step are multiplied for the qualitative FOM. The quantitative FOM are summed up over the entire mission.

Next table provides a synthesis of the selected figure of merit, with their class (quantitative or qualitative) and their origin (from which of both main objectives they derived).

FOM	Unit	Derived from objectives
Qualitative		
Cost	low - medium - high	Objective 2
Risk	low - medium - high	Objective 1
Operability	low - medium - high	Objective 1 and 2
Quantitative		
Number of launches	-	Objective 2
Δv_{tot}	km/s	Objective 2
IMLEO	tons	Objective 2
AMEML2	tons	Objective 2 and partially 1
T_{init}	days	Objective 1

Table 19: Qualitative and quantitative FOM

It can be noticed that most of the figures derive from Objective 2 (the cost), while lessons learned from stakeholders interview led to the conclusion that Objective 1 is the most important. This remark is particularly true for quantitative FOM. As a consequence, this aspect must be taking into account, while weighting the figure of merit in the final mark evaluation to select the best scenario (see 5.4.2.3).

5.4.2.1   Qualitative FOM
In the same time, cost, risk and operability are assessed in a qualitative way, through stakeholders' interviews and bibliographical survey. The scale ranges from one to three (low – medium – high) and is defined in the following paragraphs.

5.4.2.1.1 Cost
Estimated cost corresponds uniquely to the launch cost since other costs are taken into account in the other qualitative FOM (like operability) and the quantitative FOM (like number of launch, delta-v...). The cost is rated in comparison to the cost of existing space systems:

- **Low cost:** These options are assumed to be widely spread and very frequently used. A commercial market exists and services can be bought from a variety of service providers operating technically mature systems.
- **Medium cost:** These are either technically mature human rated systems (current example: Soyuz) or cargo systems using advanced technologies. Their common property is that there is a broad range of applications and

163

production rates for launch vehicles are more than ten units a year. The number of service providers is limited (Current example: Ariane 5 ES).
- **High cost:** These systems are using technologies and designs that are new or specific to a limited field of applications. They include new developments like heavy lift launchers, crew shuttles and crewed exploration vehicles and are usually characterized by a low production rate. Current example: SLS

5.4.2.1.2 Risk

Risk is defined as the product of probability and severity of the consequences of an event. It becomes higher for longer durations and if the consequences are more severe. Here, a qualitative measure for the risk bound to a mission leg and the entire concept is defined by:
- **Low risk:** The lowest risk in space flight results from combining proven technologies, short durations and multiple redundancies. This is mandatory for Human Spaceflight missions and incorporates conservative system design and high cost.
- **Medium risk:** This level of risk can result from longer mission durations but also from using less proven but more efficient technologies, novel combinations of hardware and reaching for new environments. This is acceptable for cargo delivery missions.
- **High risk:** Technology demonstration missions, long durations, a dependency on singular maneuvers or systems and unknown environments entail a high level of risk that should not be accepted for core components.

5.4.2.1.3 Operability

The third classical FOM is the flexibility. It contains two aspects: Flexibility of the mission, indicating if it may serve multiple purposes with minor adaptations as well as flexibility within the mission indicating for example that it can be performed using another launcher or similar technologies. But in the context of the THOR Space Station, mission scenarios evaluation, flexibility does not seem to be relevant. A. Crocker [69] defined another criterion: the operability as:

« […] the measure of a system's flight operability is the measure of the degree to which that system enables a balance of maximum mission success, minimal risk, and minimum operating cost »

It can de decomposed into six sub-criteria: simplicity, margin, robustness, flexibility, situation awareness and control.
For the THOR mission, cost and risk are already evaluated separately. Thus, it is considered that operability FOM measures complexity to support operations. Three levels are defined
- **Low operability:** Operations are feasible, with negligible challenges.

- **Medium operability:** Operations are difficult. Some operational objectives may be risky (link budget, team workload, schedule, duration, etc)
- **High operability:** Operations will reduce the mission capability. Some operational challenges may even prevent some mission objectives. It may increase risk of loss of Station modules, cargo or crew vehicle.

A fourth level can be identified, when the system is not operable. It is not applicable to THOR mission, since all legs of the trajectory are selected to ensure permanent communications with the Earth.

5.4.2.2 Quantitative FOM

5.4.2.2.1 Number of launches
The number of launches is an indicator for cost and risk. The type of a launch (Ariane 5 ES or SLS) is not considered.

5.4.2.2.2 Mission total delta-v
The total velocity increment, Δv_{tot}, for the mission is a consequence of the selected trajectories used. It is independent of the propulsion technology and the propellant type. That is taken into account in next FOM: IMLEO (see 5.4.2.2.3) and AMEML2 (see 5.4.2.2.4).
According to mission analysis, it has been decided not to take into account delta-v due to launch leg, since it surpasses all the other velocity increments. Its detailed computation process is provided in 5.4.3.2.3.3.

5.4.2.2.3 IMLEO
In the chemical propulsion case, the IMLEO is directly related to Δv_{tot}. Actually, this relationship is given by the Tsiolkovsky rocket equation [68]:

$$\Delta v = v_e ln \frac{m_i}{m_f} \qquad (5\text{-}12)$$

Where:

    m_i is the initial total mass
    m_f is the final total mass (i.e dry mass)
    v_e is the effective exhaust velocity
    Δv is delta-v
    ln is the natural logarithm function

By consequence, Δv_{tot} does not really represent totally the cost of the mission, while the IMLEO is. In fact, the highest required Δv is, the highest initial mass is. This lets only few margins for dry mass when m_i is fixed. In this study, IMLEO is obtained by addition of all the initial total mass of all the components (THOR space station

165

modules, cargo, crew vehicle). With multiple launches or multiple transfers, IMLEO would be spared. Δv_{tot} is a good criterion to compare transfer strategies. But as far as mission cost is concerned, the relevant criterion is IMLEO. Its weight must be more important than the others FOM in the scenarios evaluation.

5.4.2.2.4 AMEML2
While IMLEO is the classical FOM for space mission design, this study suggests introducing a specific one, named AMEML2 (for Available Mass in EML2), which mostly corresponds to the amount of available facilities inside the THOR modules; as soon as the transfer leg and the assembly are over. Actually, it is the remaining mass when all the ergol mass has been consumed for maneuvers. AMEML2 will size the internal layout of the Station. The higher AMEML2 is, the more confortable and the safer THOR will be for the crewmembers, but also to allow more experiments on board.

5.4.2.2.5 T_{init}
Another traditional FOM for space mission design is the mission duration. The main goal is to find the scenario that minimizes this mission duration. In the particular case of the THOR space station, the entire mission duration (T_{THOR}) is fixed to 15 years from the first modules departure towards EML2. T_{THOR} is composed of two main steps: the Space Station deployment duration (with is equivalent to T_{init}) and the operations duration (T_{ops}).
Next figure sums up the duration decomposition.
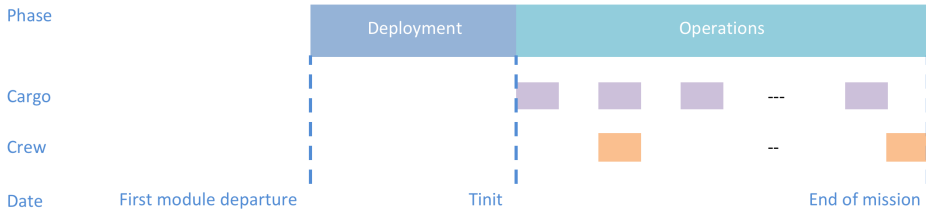
Figure 83: THOR Mission duration decomposition

Computation process of T_{init} and T_{ops} is provided in 5.4.3.2.2.1.
As T_{init} depends on the transfer strategy of the Space station modules, T_{ops} will vary from one scenario to another. Thus, it cannot be considered as a figure of merit, since it will have the same values for each selected scenario. As a consequence, T_{init} is the relevant FOM for this study, instead of the classical total duration.

5.4.2.3 *Scenario final mark*
FOM have already been now selected, the way to aggregate them in order to obtain a final mark for each scenario has to be defined. The process lies into three steps:

1. To translate quantitative FOM into a numerical mark
2. To normalize quantitative FOM
3. To compute the final mark

5.4.2.3.1 Qualitative FOM translation

The three FOM (cost, risk and operability) are evaluated based on three levels (low-medium-high). They have to be translated into a numerical scale so as to be compared and aggregated to the quantitative FOM.
The suggested correspondence is:

- LOW ⇔ 0
- MEDIUM ⇔ 1
- HIGH ⇔ 2

5.4.2.3.2 Quantitative FOM normalization

The five quantitative FOM are computed in their natural range. But, so as to be compared and aggregated in the final mark for scenario evaluation, they have to be normalized, using the maximum value of the category. Each quantitative final mark must be in [0; 2] range.

For all quantitative FOM (except AMEML2), where a higher value means less performance, this yields, for each scenario n°i, the performances of T_{init}, Δv_{tot}, IMLEO and Number of launches:

$$P_{i,j} = Int\left(2 \times \frac{C_{i,j} - C_{min,j}}{C_{max,j} - C_{min,j}}\right) \qquad (5\text{-}13)$$

Where

i is the scenario number: $i \in [1; 42]$
j belongs to $\{\Delta v_{tot}, ; \text{Number of launches; Tinit; IMLEO}\}$
Int is the floor function
$C_{i,j}$ is the value of Δv_{tot}, Number of launches, T_{init}, and IMLEO obtained for scenario n° i
$C_{max,j}$ is the maximum value of Δv_{tot}, Number of launches, T_{init}, and IMLEO
$C_{min,j}$ is the minimum value of Δv_{tot}, Number of launches, T_{init}, and IMLEO

Remark: It is assumed that $C_{i,j} \geq 0 \; \forall i, \forall j$ and $C_{max,j} > C_{min,j} \; \forall j$.

As the objective is to maximize AMEML2, its performance, for each scenario n°i, is evaluated then with:

$$P_{i,AMEML2} = Int\left(2 \times \frac{C_{max,AMEML2} - C_{i,AMEML2}}{C_{max,AMEML2} - C_{min,AMLEML2}}\right) \qquad (5\text{-}$$

Where
  i is the scenario number: $i \in [1; 42]$
  Int is the floor function
  $C_{i,AMEML2}$ is the value of AMEML2 obtained for scenario n° i
  $C_{max,AMEML2}$ is the maximum value of Δv_{tot}, Number of launches, $T_{init,}$ and IMLEO
  $C_{min,AMEML2}$ is the minimum value of Δv_{tot}, Number of launches, $T_{init,}$ and IMLEO

Remark: It is assumed that $C_{i,AMELM2} \geq 0 \; \forall i$, and $C_{max,AMEML2} > C_{min,AMEML2}$.

5.4.2.3.3 Final mark computation

This step consists in aggregating all the computed performances together. As THOR space station mission lies in the multi-criteria decision field, it has been decided to apply several types of aggregation formula so as to compare results before selecting the best scenario. They are weighted averaging, since the criteria are assumed to be independent. Final mark can be then computed with :

$$For \; i = 1 \dots 42, \qquad A_{k,j} = \sum_{j=1}^{8} w_{k,j} \times P_{i,j} \qquad (\,5\text{-}15)$$

Where
  k is the number of the method: $k \in [1; 6]$ .Actually, this study focuses on six different approaches that are detailed here after.
  i is the scenario number: $i \in [1; 42]$
  $P_{i,j}$ is the performance of the FOM n°j, computed for scenario n°i, with $j \epsilon \{cost; risk; operability; Number \; of \; launches; \Delta v_{tot}; IMLEO; AMEML2; T_{init}\}$
  $w_{k,j}$ is the weight of FOM n°j for method n°k.
  $A_{k,i}$ is the final mark of scenario n°i based on method k

Method n°1: In this method, all criteria are equivalent. As a consequence:

$$\forall j \in [1; 8], w_{1,j} = 1 \qquad (\,5\text{-}16)$$

$$For \; i = 1 \dots 42, \qquad A_{1,j} = \sum_{j=1}^{8} P_{i,j}$$

Method n°2: According to objectives' definition (see 5.4), the most important decision criterion is the risk, and then AMEML2. As operability is related to the risk, it has also the same weight. Thus, it has been decided that:

$$w_{2,risk} = 3$$
$$w_{2,operability} = 3$$
$$w_{2,AMEML2} = 2$$
$$\forall j \notin \{risk; operability; AMEML2\}, w_{2,j=1}$$

(5-

Remark: As the global evaluation tries to find the minimal final mark per method and does not compare final mark per method, weights are not normalized.

Method n°3: This method focuses first on the risk, associated to operability and twice, on the results of the mission (described by AMEML2 and T_{init}). By consequence:

$$w_{3,risk} = 3$$
$$w_{3,operability} = 3$$
$$w_{3,AMEML2} = 2$$
$$w_{3,ATinit} = 2$$
$$\forall j \notin \{risk; operability; AMEML2; T_{init}\}, w_{3,j=1}$$

(5-18)

Method n°4: This method focuses first on the risk, associated to operability and twice, on the cost. By consequence:

$$w_{4,risk} = 3$$
$$w_{4,operability} = 3$$
$$\forall j \in \{cost; Number\ of\ launches; \Delta v_{tot}; IMLEO\}\ w_{4,cost} = 2$$
$$\forall j \in \{AMEML2; T_{init}\}, w_{4,j=1}$$

(

Method n°5: This method focuses only on the cost, then:

$$\forall j \in \{cost; Number\ of\ launches; \Delta v_{tot}; IMLEO\}\ w_{5,cost} = 3$$
$$\forall j \notin \{risk; operability, AMEML2; T_{init}\}, w_{5,j=1}$$

(5-20)

Method n°6: This method focuses only on the results of the mission (described by AMEML2 and T_{init}). By consequence:

$$w_{6,operability} = 3$$
$$w_{6,AMEML2} = 3$$
$$\forall j \notin \{coperability, AMEML2\}, w_{6,j=1}$$

(5-21)

5.4.3 Scenarios evaluation

As FOM and final mark computation methods have already been presented in the previous paragraph, it can be now applied to the mission baseline scenario that has been selected for THOR.

169

5.4.3.1 Mission scenario baseline

As a consequence of previous analyses on transfer and rendezvous, the following baseline scenario has been selected:
-    Operational life-time duration, with station assembly: 15 years
-    One crew rotation every 6 months
-    One cargo delivery every 3 months
-    THOR station total mass: 150t
-    THOR Halo orbit A_z: 8000 km
-    THOR Halo orbit family, m:3
-    Cargo/ crew vehicle initial orbit A_z: 7800km
-    Cargo/ crew family, m:3
-    LEO altitude: 200km
-    Cargo or Crew: 21,25 t (based on Orion concept –see 2.3.6)
-    $I_{SP} = 435$ s (based on best chemical bi-propellant engine with LOX - LH_2)

The last design parameters to be discussed are the THOR assembly strategy and the type of transfer. Assembly of the seven cylindrical modules and two spheres can take place:
-    In LEO, before sending them all together to EML2
-    At EML2, after sending one by one to EML2
-    Partially in LEO (two by two, or by three…) before sending them by grape to EML2
-    At EML1, before sending the station in EML2

It has been decided not to considered electrical propulsion options. That implies that all modules of the Space station will be transferred according to nominal WSB trajectory. The best nominal trajectory has been selected (see Figure 62) to be the reference for THOR space station modules with:

For rendezvous in LEO: According to ATV lessons learned, it can be assumed that:
-    a total delta-v for rendezvous: 100 m/s
-    a total duration for rendezvous: 3 days

For modules rendezvous at EML2:
-    a total delta-v for rendezvous: 0.002 km/s
-    a total duration for rendezvous : 3.6 days

For transfer on WSB nominal:
-    a total duration for transfer : 101 days
-    a total delta-v for transfer : 3.2 km/s

For transfer on WSB exotic:
-    a total duration for transfer : 34 days
-    a total delta-v for transfer : 3.9 km/s

For Lunar flyby transfer:
- a total delta-v for lunar flyby transfer : 3.5 km/s
- a total duration for rendezvous : 21.3 days

To simplify the scenarios evaluation, it has been decided that the THOR modules are only transferred from LEO to EML2 thanks to nominal WSB, while cargo can travel on any kind of trajectories (LBT, WSBT or WBSE). The crew vehicle transfer legs can be LBT or WBSE.

5.4.3.2   Figures of merit computation
This paragraph presents the results of the computation of selected FOM, for the baseline mission scenario described just before.

5.4.3.2.1 Qualitative FOM
As explained previously, there are two categories of Figures of Merit for the evaluation and the comparison of the selected scenario for the entire THOR mission. The qualitative FOM cannot be computed with numerical formulas but through estimation. This paragraph presents the chosen way to assess them: cost, risk and operability.

5.4.3.2.1.1 Cost evaluation
The total cost of such a huge and complex mission as the THOR space station ones, is composed of the costs of each phase of the life-profile: for design, for integration and tests, for transportation (mostly the launch, transfer and rendezvous), for operations and for disposal. This study focuses only on the transportation costs. Moreover, only the cost of the launch is evaluated thanks to this FOM. The other ones are taken into account in Δv_{tot} (see 5.4.3.2.2.4).
According to the definition of the cost FOM (see), it can be concluded that:
- Ariane 5 ES cost is: MEDIUM
- SLS cost is: HIGH

5.4.3.2.1.2 Risk evaluation
A complete risk analysis should be performed to evaluate all the potential risks linked to the THOR mission, their occurrence probability and their impact on the mission (gravity). According to mission objective n°1 (see 5.4), efforts must mainly be concentrated on the safety of the crew and on the success of the mission.

Main risks are identified hereafter:
- Launch failure
- Assembly failure
- Cargo mission failure
- Crew mission failure

Risk can computed as follows:

$$Risk = Gravity \times Probability \quad (5\text{-}22)$$

Where:

Probability is the probability of occurrence of the risk. It has three levels: LOW – MEDIUM – HIGH.

Gravity is the impact of the risk on the crewmember and on the mission. It has also three levels: LOW – MEDIUM – HIGH.

Gravity levels can be defined as:
- LOW means that the leg has to be executed once gain.
- MEDIUM corresponds to a situation when the mission is partially lost.
- HIGH is when the crew is in danger or the mission cannot go on.

Formula (5-22) can be applied for each individual risk. The total scenario risk is obtained with:

$$Risk_{tot} = Risk_{Launch} \times Risk_{Assembly} \times Risk_{cargo} \times Risk_{crew} \quad (5\text{-}23)$$

Risk can be represented on a matrix like the following one:
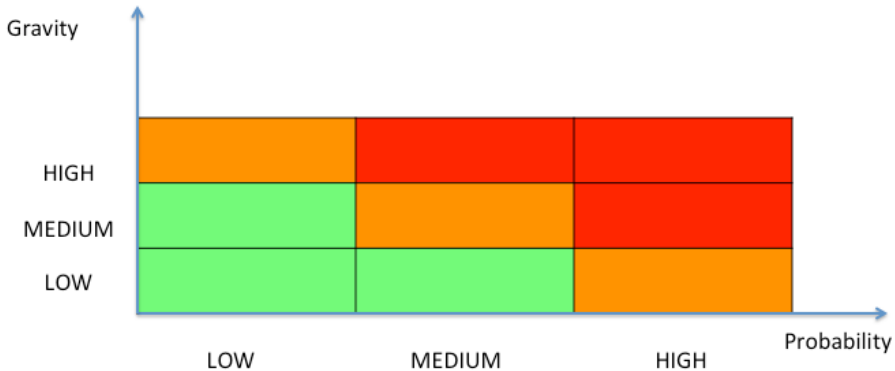
Figure 84: Risk matrix example

5.4.3.2.1.3 Operability evaluation

In this study, operability FOM is defined as the product of the duration and the cost of the operations required ensuring a dedicated scenario. A unitary operability FOM is then calculated as following:

$$Ops = Duration \times Complexity \quad (5\text{-}24)$$

Where:

> *Ops* stands for Operability
> *Duration* is the time length of the operational activities. It has three levels:
> LOW – MEDIUM – HIGH.
> *Complexity* is the level of difficulty of those operations (innovation, dangerous maneuvers, specific activities, controllers stress…). It has also three levels: LOW – MEDIUM – HIGH.

Then the operability level for the entire THOR mission takes into account the ones of each step (Launch, Assembly, Cargo transfer, Crew rotation), and can be computed as:

$$Ops_{tot} = Ops_{Launch} \times Ops_{Assembly} \times Ops_{cargo} \times Ops_{crew} \qquad (5\text{-}25)$$

5.4.3.2.2 Quantitative FOM

The quantitative FOM belong to the second category: they can be computed with numerical formulas. This paragraph presents the formulas selected to calculate them.

5.4.3.2.2.1 T_{init} computation

T_{init} is used to estimate the mission duration. Assuming that modules transfer occurs one after each another, T_{init} is obtained with:

$$T_{init} = N_{mod\_transfer} \times Duration_{mod\_transfer} + N_{mod\_rdv} \times Duration_{mod\_rdv} \qquad (5\text{-}26)$$

Where

> $N_{mod\_transfer}$ is the number of modules transfer
> N_{mod_rdv} is the number of modules rendezvous in EML2
> $Duration_{mod\_transfer}$ is the total duration of one transfer
> $Duration_{mod\_rdv}$ is the total duration of the rendezvous at EML2

Then T_{ops} can be deduced as:

$$T_{ops} = T_{THOR} - T_{init}. \qquad (5\text{-}27)$$

5.4.3.2.2.2 Number of cargo transfers

The number of cargo deliveries, N_{cargo}, depends directly on T_{ops}. In a full year, 4 cargos deliveries can be planned, so about one cargo every 90 days.

Thus,

$$N_{cargo} = Int\left(\frac{T_{ops}}{90}\right) \qquad (5\text{-}28)$$

Where
Int is the floor function
T_{ops} is given in days

5.4.3.2.2.3 Number of crew rotations

The number of crew rotations, N_{crew}, also depends directly on T_{ops}. In a full year, it is assumed that 2 crew rotations are scheduled, so about one every 180 days. Thus,

$$N_{crew} = Int\left(\frac{T_{ops}}{180}\right) \qquad (5\text{-}29)$$

5.4.3.2.2.4 Total delta-v

Total delta-v corresponds to the sum of all the velocity increment required for one strategy. Cargo and crew vehicle have to perform to transfer: one to go from LEO to EML2 and return. According to the optimization statement set in 0, the formula that takes into account the three scenarios, is given by (5-1) and reminded here below:

$$\Delta v_{tot} = \Delta v_{Launch} + \Delta v_{SK\_LEO} + \Delta v_{transfer} + \Delta v_{cargo} + \Delta v_{crew} \qquad (5\text{-}1)$$

As Δv_{Launch} surpasses all the others delta-v, it is not taken into account so as to compare the influence of the others legs cost on the scenario. For example, in Ariane 5 ES, Δv_{Launch} is about 65 km/s. It is then certain that the selection of the launch vehicle has a great influence on the total delta-v of the mission. Moreover, as it discussed in 5.4.3.5, the location of the spaceport must be carefully chosen since it has a direct impact on the LEO initial conditions.

The time spent in LEO by the THOR modules should be as low as possible so as to avoid unnecessary maneuvers. As a consequence, the estimated delta-v for station keeping and one rendezvous in LEO is assumed to be equal to ATV rendezvous order of magnitude, i.e. $\Delta v_{rdv\_LEO} = 0.1\ km/s$. By consequence, Δv_{SK_LEO} depends directly on the number of rendezvous in LEO, with:

$$\Delta v_{SK\_LEO} = N_{rdv\_LEO} \times \Delta v_{rdv\_LEO} \qquad (5\text{-}30)$$

Where N_{rdv_LEO} is the number of rendezvous performed in LEO.

Thanks to results of the previous analyses, it has been decided to transfer all THOR Space station modules thanks to a nominal trajectory of WSB strategy. By

consequence, the delta-v required for THOR modules transfer is composed of total velocity increment for maneuvers on the LEO to EML2 leg and for maneuvers to perform rendezvous At EML2

$$\Delta v_{transfer} = N_{mod\_transfer} \times \Delta v_{mod\_transfer} + N_{rdv\_EML2} \times \Delta v_{rdv\_EML2} \quad (5\text{-}31)$$

Where

$N_{mod\_transfer}$ is the number of modules transfer

$\Delta v_{mod\_transfer}$ is the total delta-v of one transfer of nominal WSB

N_{rdv_EML2} is the number of rendezvous performed at EML2 for modules integration

Δv_{rdv_EML2} is the total delta-v of one rendezvous at EML2

The computation of the entire cargo mission delta-v has to take into account the total number of cargo deliveries, but also the fact that each cargo will perform a round-trip. That means two transfers per cargo.

$$\Delta v_{cargo} = 2 \times N_{cargo} \times \Delta v_{cargo\_transfer} + N_{cargo} \times \Delta v_{rdv\_EML2} \quad (5\text{-}32)$$

Where

N_{cargo} is the number of cargo delivery

$\Delta v_{cargo\_transfer}$ is the total delta-v of one transfer for one cargo delivery. It depends on the strategy: exotic WSB, nominal WSB or Lunar flyby.

Δv_{rdv_EML2} is the total delta-v of one rendezvous at EML2

The computation of the entire crew rotation mission delta-v has also to take into account the total number of rotation, but also the fact that each rotation will perform a round-trip. That means two transfers per crew rotation.

$$\Delta v_{crew} = 2 \times N_{crew} \times \Delta v_{crew\_transfer} + N_{crew} \times \Delta v_{rdv\_EML2}$$

Where

N_{crew} is the number of crew rotation

$\Delta v_{crew\_transfer}$ is the total delta-v of one transfer for one crew rotation. It depends on the strategy: exotic WSB or Lunar flyby.

Δv_{rdv_EML2} is the total delta-v of one rendezvous at EML2

5.4.3.2.2.5 THOR available payload mass

Computing the THOR available mass for payload falls into two steps:
- Step 1: Rendezvous in LEO consumption
- Step 2: Transfer consumption

Remark: This mass budget does not take into account the consumed fuel mass during rendez-vous in EML2, since Δv_{rdv_EML2} is really low compared to the other delta-v and can be then neglected.

Step 1: Remaining mass after rendezvous in LEO, m_{rdv_LEO} can be computed as:

$$m_{rdv\_LEO} = m_0 \times \left(N_{mod\_transfer} + N_{rdv\_LEO} \times e^{-\frac{\Delta v_{rdv\_LEO}}{v_e}} \right) \qquad (5\text{-}34)$$

Where

      m_0 is the initial total mass of the THOR Space Station
      $N_{mod\_transfer}$ is the number of modules transfer
      N_{rdv_LEO} is the number of rendezvous performed in LEO
      Δv_{rdv_LEO} is the delta-v for one rendezvous in LEO
      v_e is the average exhausted velocity along the engine axis. It can be computed with:

$$v_e = Isp \times g_0 \qquad (5\text{-}35)$$

Where

      Isp is the Specific impulse of the engine
      g_0 is the Earth acceleration

Step 2: Remaining mass after transfer, $AMEML2$ can be computed as:

$$AMEML2 = m_{rdv\_LEO} \times e^{-\frac{\Delta v_{mod\_transfer}}{v_e}} \qquad (5\text{-}36)$$

Where

      m_{rdv_LEO} is the remaining mass after rendezvous in LEO
      $\Delta v_{mod\_transfer}$ is the total delta-v of one transfer of nominal WSB
      v_e is the average exhausted velocity along the engine axis.

5.4.3.2.3 Results
This paragraph provides numerical results for the following figures of merit:
- Risk
- Operability
- Delta-v
- IMLEO
- Available mass, AMEML2
- T_{init}

Scenarios are numbered from 1 to 42. An equivalence matrix is provided in Appendix 5.

5.4.3.2.3.1 Risk

Four main contingencies have been identified and presented in 5.4.3.2.1.2. They correspond to nine contingency situations to be studied:

- C1: Ariane 5 ES failure
- C2: SLS failure
- C3: THOR assembly in LEO failure
- C4: THOR assembly in EML2 failure
- C5: Cargo transfer through LBT failure
- C6: Cargo transfer through WBST failure
- C7: Cargo transfer through WBSE failure
- C8: Crew transfer through LBT failure
- C9: Crew transfer through WBSE failure

Then, risk is assessed for each contingency. All detailed results are provided in Appendix 6.

Launch failure:
In the case of Ariane 5 ES, THOR modules are launched one by one. As a consequence, one failure would imply a new launch that means additional cost and delay, but no critical impact on the mission. Gravity's level is then set equal to LOW. Moreover, as Ariane 5 is one of the most reliable launch vehicle, the probability is then LOW.

As SLS would carry THOR modules three by three, the consequence of a launch failure is more serious than in the case of Ariane 5 ES: more extra cost and perhaps, more delay. So, the gravity's level is set this time equal to MEDIUM. As SLS is a new launcher, still under development, the probability of failure is then HIGH.

Assembly failure:
Techniques to assemble in LEO huge system like THOR modules are today well-known thanks to ISS lessons learned. As a consequence, the failure probability is LOW. Moreover, in case of rendezvous failure between two parts of the station, a new attempt can be scheduled. Thanks to rendezvous lessons learned (like ATV…), the risk of collisions between the two elements is quasi null. The only consequences are on the mission cost and the delay. Thus, gravity can be considered as LOW.
Until now, no rendezvous has ever taken place in EML2. Consequently, probability of failure is HIGH. Nevertheless, the gravity is assessed to MEDIUM, since assembly would be performed without crew. So crewmembers won't be in danger. In case of failure, despite the increase of cost and delay, the mission could not be aborted, just postponed.

Cargo transfer failure:
Transfers of vehicle thanks to WBS or Lunar flyby are very seldom. Some missions have already been performed (see 2.3.5). In THOR mission, WSB transfer should have already been tested on THOR modules transfer before. Nevertheless, the three types of transfer are assessed at the same levels. As the consequence, probability may be estimated at a MEDIUM level. Furthermore, the consequence of the transfer of a cargo is not critical on the mission but would generate delay and additional cost. So the gravity is set equal to MEDIUM.

Crew rotation failure:
In case of crew transfer, the probability to failure can be set equal to MEDIUM. Actually, it can be imagined that this mission would inherit from Orion design. Besides, the gravity has the highest possible level, i.e. HIGH since the crew could be in danger.

Next figure presents a synthesis of risk evaluation.
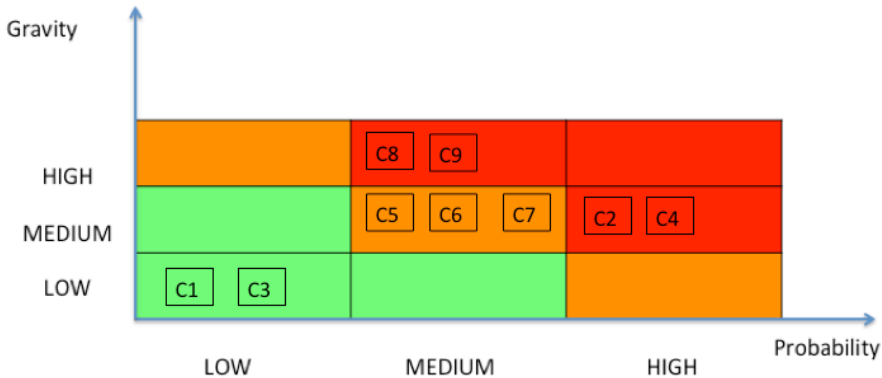
Figure 85: THOR mission risk evaluation

At one glance, it can be seen that the THOR mission is a risky project.
Figure 86 depicts the total risk evaluation for the 42 selected scenarios per scenario. It can be easily noticed that risk fluctuates widely from one scenario to another. As THOR mission lies in the human spaceflight context, risk is one of the most important FOM. It may denote that scenario from n°31 to 42 can be discarded. This is logical since they involve a new launch vehicle (SLS) and new operational activities (assembly in EML2).
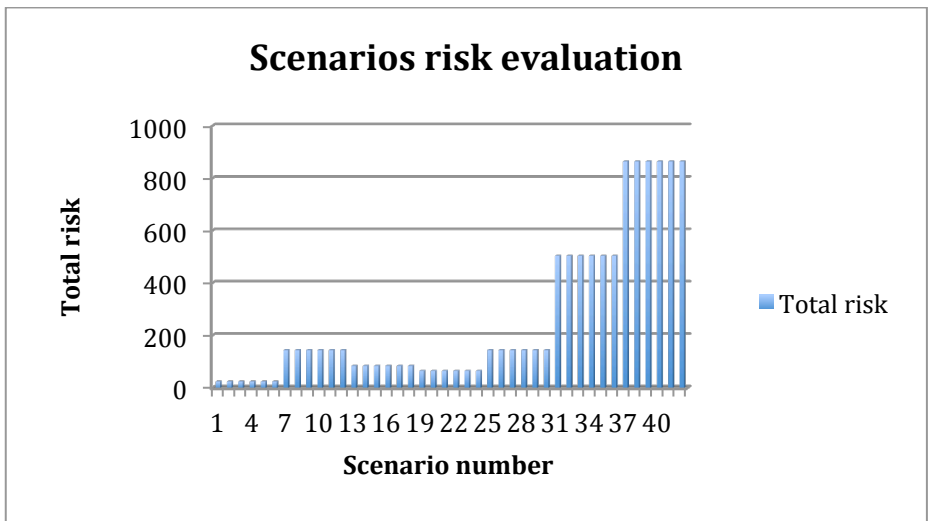
Figure 86: Scenario risk evaluation

5.4.3.2.3.2 Operability

Results obtained while applying formula (5-25) to evaluate the global operability level of the THOR space station are presented on next figure.
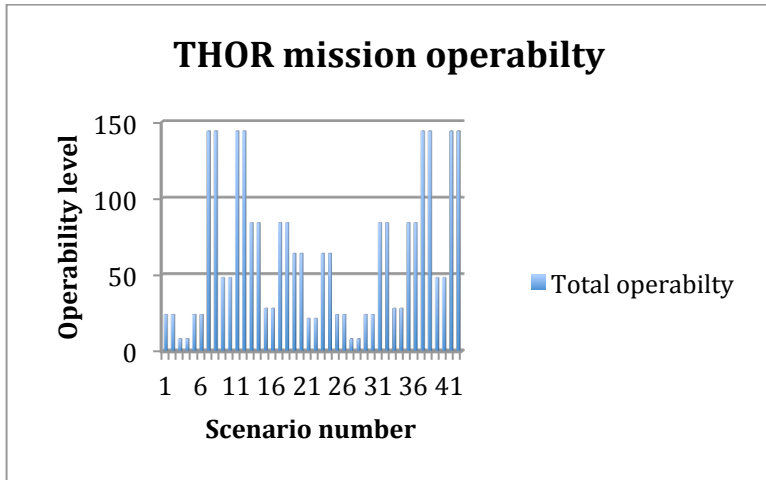
Figure 87: THOR mission operability level per scenario

Duration of operations is not exactly equal to the duration of the entire mission. Operations depend on the criticality of each step. For example, it may be considered that:

- Assembly in LEO can be performed in a semi-autonomous way. Then, complexity level is MEDIUM

179

- Assembly in EML2 is obviously not automatic and must be monitored permanently. As a consequence, in this case, complexity is HIGH.
- Complexity level of crew transfer operations is HIGH, whatever the transfer strategy is.
- On the contrary, cargo transfer requires less monitoring since there is no human being on-board. As the transfer duration is quite long, the cargo travel may not be monitored permanently between LEO and EML2. Only maneuvers require operational team in the control center.

Figure 87 shows that there is a great gap between scenarios. When only the operability criterion is concerned, it can be recommended to focus on scenarios n°1 to n°6 (Ariane 5 ES launcher and assembly in LEO) and scenarios n°25 to 30 (SLS launcher and assembly in LEO).

5.4.3.2.3.3 Delta-v

According to formulae provided in 5.4.3.2.2.4, total delta-v for the global THOR mission are computed and presented on next figure.
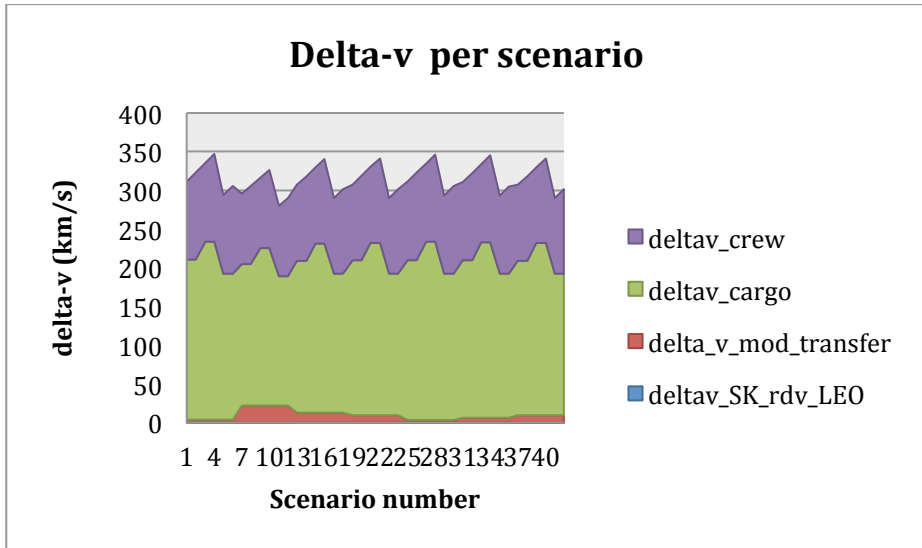
Figure 88: Total delta-v per scenario

Best scenario is n°11, with Ariane 5 ES launch, then assembly in EML2, WBST for cargo transfer and for LBT crew transfer. For each, group of scenario, a combination with WBST for cargo transfer and LBT for crew rotation leads to the best results. It is coherent with mission analysis results. This is normal because this WBST strategy is the longest lasting one; it reduces N_{cargo} and N_{crew}. Therefore, using delta-v as the only criterion proves not to be the optimal strategy, relative to all the mission objectives.

Furthermore, this proves that when delta-v is the only considered criterion, the scenario that optimizes the entire set of mission objectives may be missed.

Next figure presents an example of the distribution of the leg delta-v in the computation of the total delta-v, for scenario n°11 (THOR space station launched by Ariane 5 ES, assembled in LEO, cargo transferred with WBST and crew with LBT).
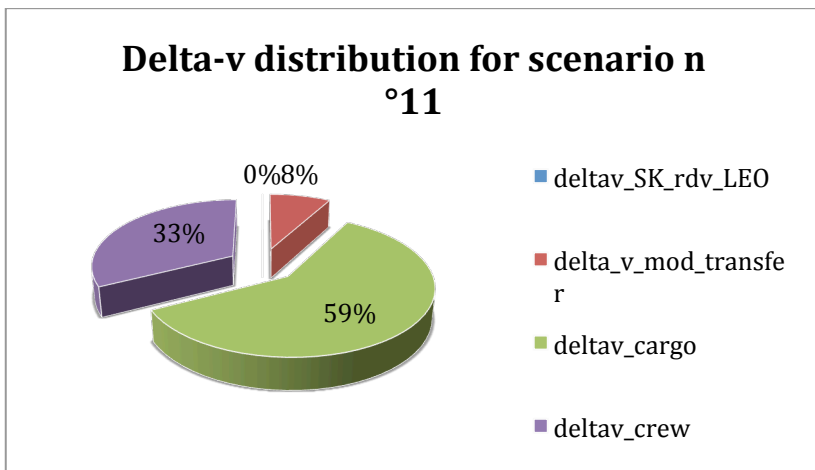
Figure 89: Delta-v distribution for scenario n°11

5.4.3.2.3.4 IMLEO

Next figure presents the evolution of the initial mass in LEO per scenario (in tons).
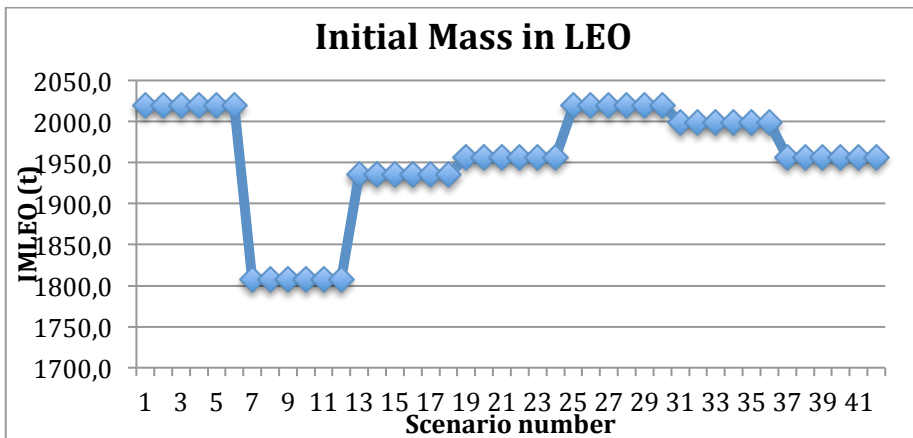
Figure 90: Evolution of IMLEO per scenario

This figure shows that there is one group of scenarios (scenario n° 7 to 12) that minimizes the IMLEO FOM. It corresponds to scenarios with an Ariane 5 ES launch and an assembly in EML2.

5.4.3.2.3.5 AMEML2

It has already been discussed that IMLEO is not really accurate in the THOR mission scenario comparison. That is the reason why the AMEML2 FOM has been suggested and computed for all the selected scenarios. The results of the computations are presented on next figure.
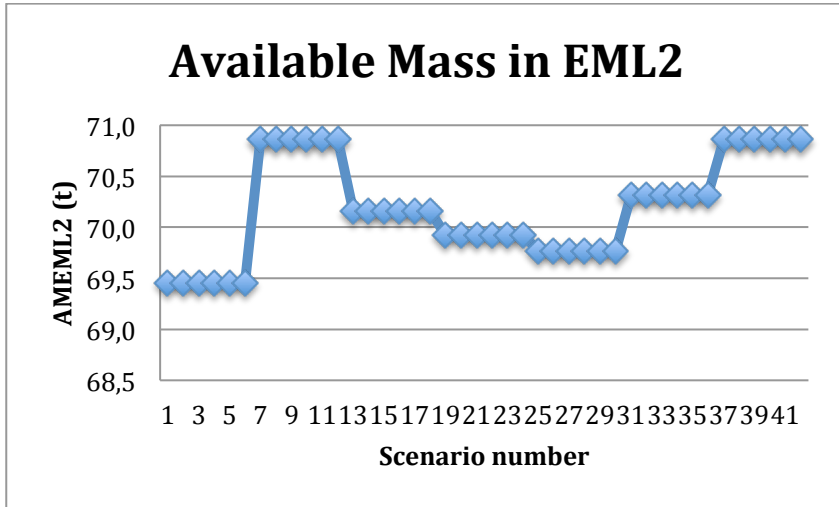
Figure 91: Evolution of AMEML2 per scenario

This figure enlightens that the group of scenarios minimizing the AMEML2 FOM is constituted by scenario n° 1 to 6. It corresponds to scenarios with an Ariane 5 ES launch and an assembly in LEO. The available mass corresponds to only 47% of the mass that has to be launched.

5.4.3.2.3.6 T_{init}

Another relevant FOM for THOR mission performances is the availability of the Station facilities in EML2, that is to say the first time the station will be available for operations (first crew ingress, experiments...).
The evolution of the T_{init} FOM is provided on Figure 92.
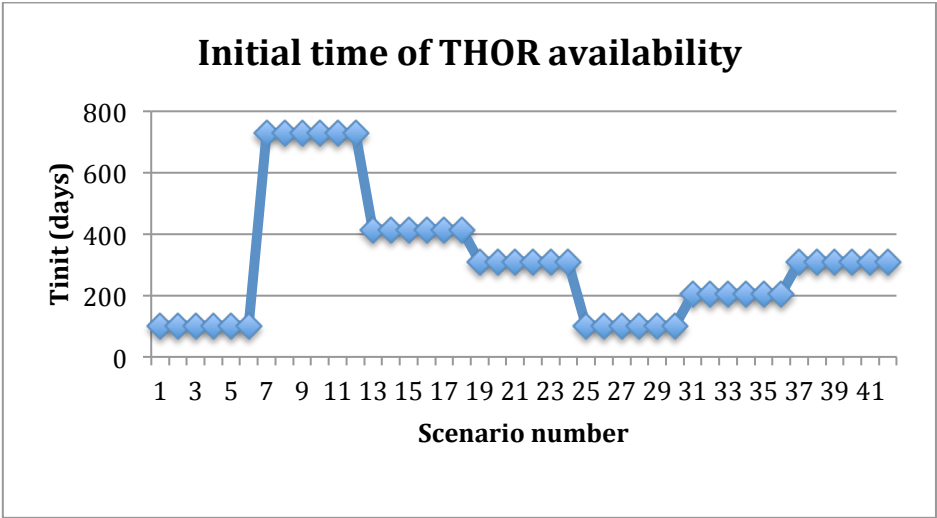
Figure 92: Evolution of T_{init} per scenario

This figure demonstrates that two groups of scenarios can be interesting as far as initial date of availability is concerned: group 1 composed of scenarios 1 to 6 and group 2 with scenarios 25 to 30. Group 1 corresponds to Ariane 5 ES launch and assembly in LEO, while group 2 to SLS launch and assembly in LEO. It shows clearly the influence of the assembly location on this criterion.

5.4.3.3 Scenarios comparison

The previous chapter did not present exhaustively all FOM computations. Detailed calculations of THOR mission criteria are provided in 5.4.3.2. Nevertheless, Table 20 compiles the final FOM for the forty-two selected scenarios.

Scenario Nbr		Qualitative FOM			Quantitative FOM			
	Cost	Flexibility	Risk	Deltav (km/s)	Launch Nbr	Tinit (days)	IMLEO (t)	AMEML 2 (t)
1	Medium	Low	Low	311,8	7,0	101,0	2020,0	69,5
2	Medium	Low	Low	323,4	7,0	101,0	2020,0	69,5
3	Medium	Low	Low	335,4	7,0	101,0	2020,0	69,5
4	Medium	Low	Low	347,0	7,0	101,0	2020,0	69,5
5	Medium	Low	Low	294,1	7,0	101,0	2020,0	69,5
6	Medium	Low	Low	305,7	7,0	101,0	2020,0	69,5
7	Medium	High	Medium	295,4	7,0	728,6	1807,5	70,9
8	Medium	High	Medium	305,8	7,0	728,6	1807,5	70,9
9	Medium	Medium	Medium	316,2	7,0	728,6	1807,5	70,9
10	Medium	Medium	Medium	326,6	7,0	728,6	1807,5	70,9
11	Medium	High	Medium	279,8	7,0	728,6	1807,5	70,9
12	Medium	High	Medium	290,2	7,0	728,6	1807,5	70,9
13	Medium	Medium	Medium	307,1	7,0	414,8	1935,0	70,2
14	Medium	Medium	Medium	318,3	7,0	414,8	1935,0	70,2
15	Medium	Low	Medium	329,5	7,0	414,8	1935,0	70,2
16	Medium	Low	Medium	340,7	7,0	414,8	1935,0	70,2
17	Medium	Medium	Medium	290,3	7,0	414,8	1935,0	70,2
18	Medium	Medium	Medium	301,5	7,0	414,8	1935,0	70,2
19	Medium	Medium	Low	307,5	7,0	310,2	1956,3	69,9
20	Medium	Medium	Low	318,7	7,0	310,2	1956,3	69,9
21	Medium	Low	Low	330,3	7,0	310,2	1956,3	69,9
22	Medium	Low	Low	341,5	7,0	310,2	1956,3	69,9
23	Medium	Medium	Low	290,4	7,0	310,2	1956,3	69,9
24	Medium	Medium	Low	301,6	7,0	310,2	1956,3	69,9

Scenario Nbr	Qualitative FOM			Quantitative FOM				
	Cost	Flexibility	Risk	Deltav (km/s)	Launch Nbr	Tinit (days)	IMLEO (t)	AMEML 2 (t)
25	High	Low	Medium	311,4	7,0	101,0	2020,0	69,8
26	High	Low	Medium	323,0	7,0	101,0	2020,0	69,8
27	High	Low	Medium	335,0	7,0	101,0	2020,0	69,8
28	High	Low	Medium	346,6	7,0	101,0	2020,0	69,8
29	High	Low	Medium	293,7	7,0	101,0	2020,0	69,8
30	High	Low	Medium	305,3	7,0	101,0	2020,0	69,8
31	High	Medium	High	311,0	3,0	205,6	1998,8	70,3
32	High	Medium	High	322,6	3,0	205,6	1998,8	70,3
33	High	Low	High	334,2	3,0	205,6	1998,8	70,3
34	High	Low	High	345,8	3,0	205,6	1998,8	70,3
35	High	Medium	High	293,6	3,0	205,6	1998,8	70,3
36	High	Medium	High	305,2	3,0	205,6	1998,8	70,3
37	High	High	High	307,1	3,0	310,2	1956,3	70,9
38	High	High	High	318,3	3,0	310,2	1956,3	70,9
39	High	Medium	High	329,9	3,0	310,2	1956,3	70,9
40	High	Medium	High	341,1	3,0	310,2	1956,3	70,9
41	High	High	High	290,0	3,0	310,2	1956,3	70,9
42	High	High	High	301,2	3,0	310,2	1956,3	70,9

Table 20: Overview of the FOM for all 42 scenarios

The highlighted boxes of the Table 20 contain the best value of each criterion. In this table, values are provided with their real value (a level for the quantitative FOM and numerical results for the quantitative FOM). This shows that no scenario is optimal for all criteria together. Moreover, no scenario can be discarded, since none of them appears to be clearly worse than the other ones.

According to process described in 5.4.2.3.1, qualitative FOM are then translated into quantitative FOM and normalized (see 5.4.2.3.2) in the [0; 2] range. Afterwards, all FOM can be aggregated.

The results of the first method (same weight for all the FOM) are provided in the Figure 93. Best scenarios are the ones that minimize the final mark.
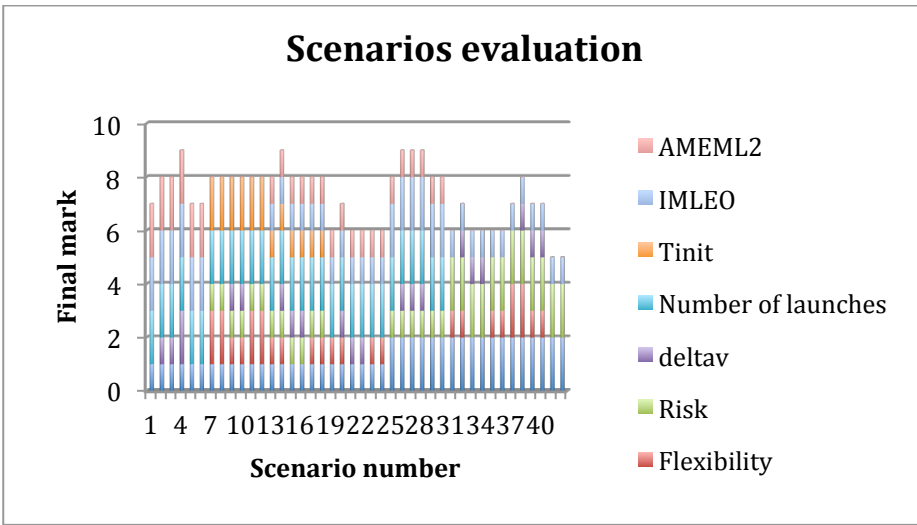
Figure 93: Scenarios comparison with an equivalent weight for all the FOM

This synthesis helps to rank the scenarios and sort out the three best ones. On Figure 93, these values are all piled up for each scenario leading to a maximum value of eight index points indicating the worst case. The colors give the decomposition of the rating and the purpose of the comparison is to show, what factors are dominant in the specific scenarios. Thus, the best scenario, with the same final mark, are: scenario n°41 (launch with SLS – assembly in EML2 – cargo transfer with WSBT – crew rotation with LBT) or scenario n°42 (SLS – assembly in EML2 - cargo transfer with WSBT- crew rotation with WSBE). These results seem to contradict that the safest scenario has to be selected.

Scenarios with a higher final mark, but especially good ratings in one category, may be still be favorable for special purposes like minimum total delta-v. Actually, according to stakeholders' needs analysis, crewmember safety must be the priority objective of the THOR mission. All the other aggregations must be applied so as to check those preliminary results.

Figure 94 compares the final mark obtained for all of the 42 scenarios, computed with the six selected aggregation method (see 5.4.2.3.3). Marks must be compared with relative values, and not the absolute ones since the FOM weights have not been normalized.
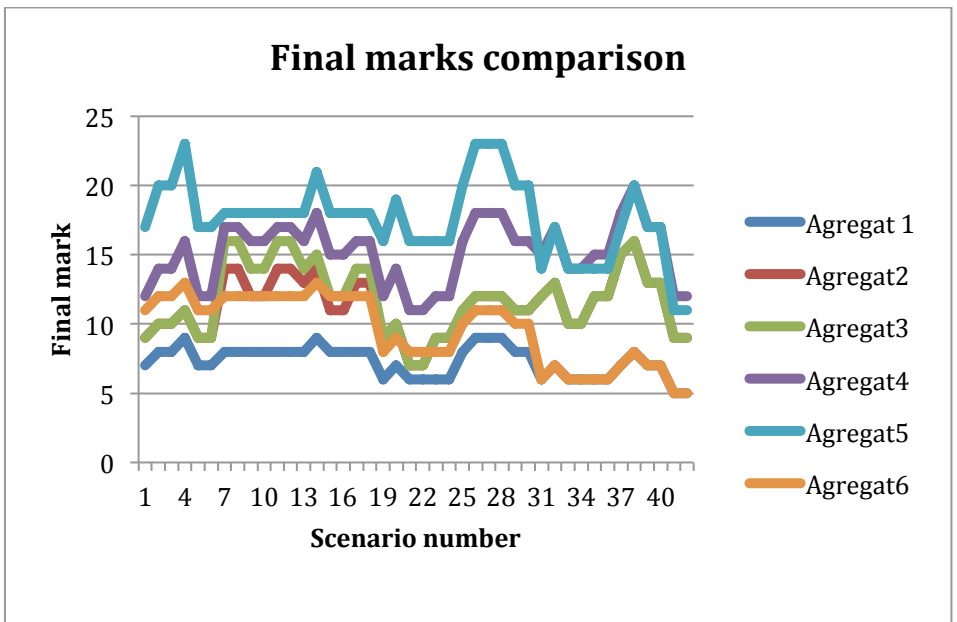
Figure 94: Final marks comparison depending on aggregation method

From the results exposed in Figure 94, it can be deduced that there is two trends of optimal scenarios:
- The ones that mostly minimize the cost: scenarios n°41 and n°42
- The ones that mostly minimize the risk and ensures mission performances: scenarios n°21 and 22.

This is not surprising since cost and safety are often opposite, but this analysis confirms this point. Considering that safety objectives are given preference over cost, they have also preference over mission performances. Thus, the scenarios can be ranked and the worst eliminated.

5.4.3.4 Synthesis and recommendations

With the results presented in Table 20, it can be obtained that according to risk criterion, only the scenarios n°1 to n°6 and scenarios n°19 to n° 24 have to be preserved.
Then, according to cost criterion, no scenario can be eliminated. But considering the delta-v FOM, only scenario n°5 and n°23 are relevant. Finally, as scenario n°5 has the best T_{init}, the best scenario n°5 can be declared as the optimal one.

The optimal scenario is summed up on Figure 43.

The main recommendations for a THOR project manager is to launch the THOR modules with Ariane 5 ES, to assemble the station in LEO, then transfer it to EML2, to resupply it frequently with cargo travelling on WBST trajectory and to transfer crewmember with a lunar flyby.

It might be considered disappointing that the SLS scenario is not the optimal one. Looking at the FOM evaluation, scenario A2 suffers from the risk due its high level of innovation. In the THOR mission time frame, SLS may probably be tested and validated. Moreover, in this analysis, qualitative assessment of the FOM is obviously limited. In order to further compare the Ariane 5 ES and SLS scenarios, quantitative numbers for cost, flexibility and risk are necessary. A next iteration has to be scheduled, that may most probably change the ranking.

This final optimization study entails that the information when and where to perform maneuvers during the mission is lost. When closely comparing two scenarios, the underlying data should be used the overview that was presented here aims at characterizing the scenarios and finding trends that are worth pursuing.

This analysis does also not take into account the potential for further use of the electrical propulsion infrastructure for modules deployment and operational phase (cargo transfer for example). However, this should be considered for a new loop of the global optimization of the THOR Space Station life-profile. Of course, using electrical propulsion will introduce additional risk, but will considerably lower IMLEO or increase AMEML2. Thus it may open new potentials for operational cost savings.

5.4.3.5 *Influence of the launch vehicle spaceport*

In all previous WSB transfer strategies analyzed, the initial angular position on the parking orbit was let free to vary, as an optimization criterion for the differential correction process used to compute the trajectories. However, the spacecraft is initially injected into near-Earth space at latitudes limited by the performances of the launch vehicle and the location of the spaceport. Thus, an additional maneuver may be required to reach the parking orbit from the original orbit of insertion. To reduce the cost of this maneuver, the initial angular position constrains the latitude of the spaceport. This additional analysis presented in this section aims to quantify the range of variation of the latitude of the parking orbit to have an estimation of the most suitable spaceport. The position of the LEO boost is computed, while taking into account the obliquity of the Earth and the inclination of the Earth-Moon plane with respect to the ecliptic.

For each value of Θ, the departure angular position on LEO (see 5.2.2.1), the minimum value of Δv_{tot} and the corresponding Earth latitude are selected in the field of variation of ϕ, the angular position of the injection point in the manifold, according to the Moon (see 5.2.2.1). The results are presented on Figure 95 for various values of the out-of-plane amplitude Az. The average latitude is 28° for every A_z, which roughly corresponds to a low-Earth orbit into the Earth-Moon plane. The deviation range around this value is about [- 2°; +4°]. As a consequence, it is recommended to

select the latitude of the low-Earth orbit plane close to 28° for the flyby trajectories (crew rotation transfer). This latitude has to be reached by the spacecraft from the insertion orbit of its launch vehicle trajectory. The latitude of the Kennedy Space Center is equal to 28°31'. Then, it would allow the insertion orbit to be very close to the parking orbit, and thus can be considered as the most suitable spaceport for this type of mission. This may orient the final decision to select the SLS strategy, at least for crew transfer.
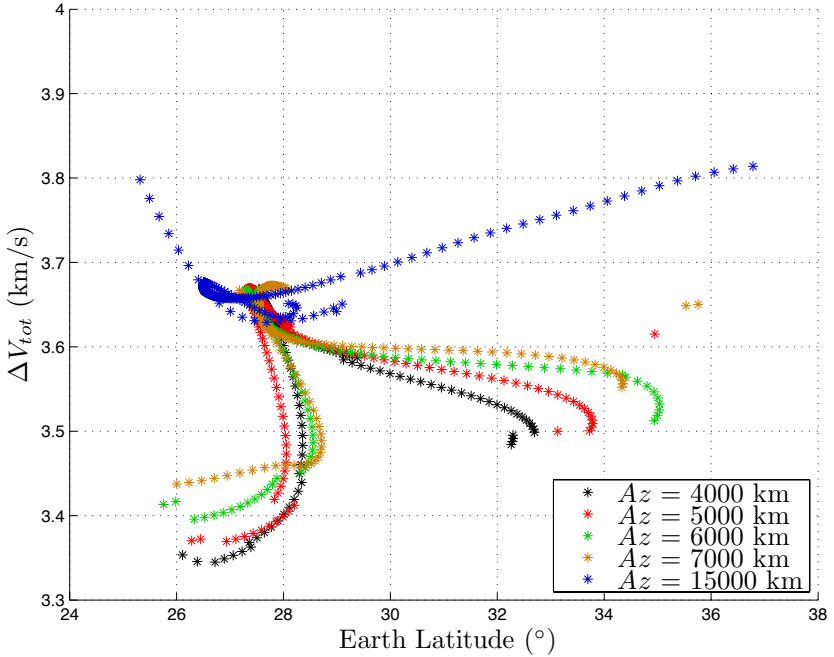
Figure 95: Minimum overall cost as a function of the latitude of the Low-Earth parking Orbit for various values of the out-of-plane amplitude A_z

6   Perspectives and conclusion

The next steps for future human space exploration of the solar system could be to operate a space station in the vicinity of the Earth-Moon Lagrangian points. This outpost would not only facilitate connections with further destinations like Mars or NEOs, but also support missions on the Moon surface. It would also procure facilities to test innovative technologies and activities and to ensure crew well being.

In this context, the present PhD project aimed at identifying solutions to manage the space station servitude, during its integration and during operational activities. After a first Systems Engineering step dedicated to set up the fundamental basis of the space station architecture, the project focused on the optimization of the operational scenarios and, particularly, on trajectories selection (for transfer and rendezvous). The main challenge was to minimize velocity increments (directly related to energy consumption) and transportation duration (crew safety).

It was first decided to locate the THOR space station on a Halo orbit around EML2, since that would permit to test safely crew resistant to visual occultation of the Earth, while preserving communications with ground stations and allow fast return in case of extreme contingency. From systems engineering outputs, the Station architecture is composed of seven cylindrical modules (based on the ATV concept) and two spherical hubs, that would ease displacement inside the station, but also docking of the visiting vehicles.

Mission analysis was performed while considering the CR3BP to model the dynamics in the vicinity of EML2, but also to compute trajectories from a Low Earth Orbit to the final destination. A great amount of scenarios have been sorted out mostly depending on the station assembly location and the types of transfer strategies for the station modules, the cargo and crew vehicle. As classical Hohmann transfer has been estimated as to expensive (according to time of flight and energy criteria), efforts were concentrated on lunar flyby trajectories or Weak Stability Boundaries transfer. Results for time of flight and velocity increment obtained for transfer trajectories are comparable to performances presented in classical papers. Nevertheless, a group of exotic solutions in the family of WSB arcs seems to be promising for crew rotation as a back-up option to lunar flyby. Moreover, modules or cargo transfers can be performed either taking advantage of the Weak Stability Boundaries trajectories or to lunar flyby.

The next task was then to determine how to perform the rendezvous at EML2. Actually, whatever the transfer strategy is, rendezvous is mandatory for THOR mission to manage safe human activities during at least fifteen years. In the past five decades, only very few research teams took an interest in rendezvous in the neighborhood of the Lagrangian points. The strategy proposed for the THOR project is an extrapolation of heteroclinic connections usually set up to transfer a particle from one Lagrangian point to another one. Assuming that the chaser (station module, cargo

or crew vehicle) is waiting on a Halo parking orbit different from the space station ones, rendezvous composed of three maneuvers would deposit the chaser on the station Halo orbit. The final maneuvers to perform the docking are not taken into account. Optimization processes applied to the proposed methodology led to affordable trajectories as far as duration and energy consumption are concerned. Moreover, those solutions are compliant with human spaceflight safety constraints, ensuring permanent communications with the crew during those critical operations and offering station keeping points for go/no go before next step.

The last part of the project consisted in selecting the optimal scenario for the entire THOR mission, while gathering performances from mission analysis and qualitative figures of merit (cost, risk, operability). Main recommendations are then to launch the THOR modules with Ariane 5 ES (because of its reliability), to assemble the station modules in LEO, then transfer entirely it to EML2, to resupply it frequently with cargo travelling on Weak Stability Boundaries transfer trajectories and to transfer crewmember with a lunar flyby arc. Nevertheless, the usage of a new heavy launcher, as SLS, must be considered as a serious back-up solution, when its availability and reliability would be confirmed, in particularly, because of the advantageous location of its spaceport.

However the THOR project tried to be as complete as possible, it cannot pretend to be exhaustive. It was the intention to open the path for extended research studies. First, the design of the THOR space station is very preliminary. It shall be worthy to go deeper into its conception, in particular, to evaluate the impact of the assembly sequence on the internal layout. Then, efforts can be supported on sub-systems design: propulsion improvement, universal docking definition, etc. Secondly, the selection of crew transfer trajectories shall be correlated to operational constraints (permanent communications, safety, launch window, rendezvous opportunity, contingencies…). The analysis performed on Weak Stability Boundaries arouses the curiosity on the exotic family and invite to go through the existence of a continuum between the two groups of trajectories. Above all, as this project was limited to the CR3BP model, it seems to be obvious to try to transpose it to a more accurate model (like the Four-body problem or the application of ephemeris). Third, the rendezvous methodology proposed in this project is a first step in the understanding of rendezvous dynamics in the vicinity of Lagrangian points. Further analyses should be undertaken to complete those preliminary results, while considering combination of orbits or with a departure point in the stable manifold of the station orbit. It could also offer an extension to look at connections from Earth-Moon Lagrangian point to Mars system, in the context of future human spaceflight.

Finally, the THOR project finds fresh hope to invite the international human spaceflight community to support the next steps for exploration mission towards the Earth-Moon Lagrangian points, as a safe oasis on the road to far destinations.

Appendix 1   Numerical values

Symbol	Description	Value	Units
μ_{EM}	Earth-Moon mass ratio	0.0121506037932213	-
L_{EM}	Earth-Moon distance	384748.91	km
T_{EM}	Orbital period of Earth-Moon system	$2.361.10^6$	s
R_E	Earth radius	6378.14	km
R_M	Moon radius	1738.2	km
μ_E	Earth gravitational constant	398600.4418	USI
γ_{EM}	Distance ratio for EML2 point	0.1678331476	-
μ_{ST}	Sun-Earth mass ratio	$3.04040.10^{-6}$	-
L_{ST}	Sun-Earth distance	$1.49597870.10^8$	km
T_{ST}	Orbital period of Sun-Earth system	$3.147.10^7$	s
R_S	Sun radius	695508	km

Appendix 2 Historical overview of Human spaceflight and missions

Period	Year	Milestones	Theoretical concepts	Space stations Russia	Space stations US	Space stations Europe	Space stations Others	Launch Vehicles Russia	Launch Vehicles US	Launch Vehicles Europe	Launch Vehicles Others	Crew/ Resupply vehicle Russia	Crew/ Resupply vehicle US	Crew/ Resupply vehicle Europe	Crew/ Resupply vehicle Others	Lagrangian points missions
Concepts	1911		Tsiolkovsky (Ru)													
	1928		Noordung (Austria)													
	1949		Ross/Smith (GB)													
	1952		Von Braun													
National programs	1957	Spoutnik (Ru)						R-7 Semiorka								
	1958	Nasa Foundation (Us)							Mercury - RedSTone							
	1961	Gagarine (Ru)										Vostok	Mercury			
	1962	Kennedy's speech							Atlas							
	1963															
	1964											Voskhod	Gemini			
	1966				MOL											
	1969	Lunar landing (Us)							Titan-III							
	1971			Saluyt-1				Proton-K				Soyuz				
	1973			Saluyt-2	Skylab				Saturn V							
	1974			Saluyt-3			Long March 2A (China)					Progress				
				Saluyt-4												
	1975	ESA foundation (Eu)														
	1976			Saluyt-5												
	1977			Saluyt-6										Hermès		
	1978															ISEE-3
	1979									Ariane-1						
	1981								STS							
	1982			Saluyt-7			Long March 2C									
	1983					Spacelab										
	1984									Ariane-3						
	1986			MIR						Ariane-2						
	1988									Ariane-4		Buran				
	1990						Long March 2E									HITEN (MUSES-A)
	1992						Long March 2D									
	1993					Spacehab										
	1994															Wind
	1995															SOHO
	1996									Ariane-5						ACE
International Cooperation	1998					ISS										
	1999						Long March 2F								Shenzhou-1 5 (China)	
	2001														Shenzhou-1	WMAP - GENESIS
	2002														Shenzhou-3 & 4	
	2003														Shenzhou-5	SMART-1
	2005														Shenzhou-6	
	2007															THEMIS
	2008					Columbus								ATV	Shenzhou-7	
	2009														HTV (Japan)	Herschel - Planck
	2010												Dragon			
	2011														Shenzhou-8	GRAIL
	2012														Shenzhou-9	
	2013												Cygnus		Shenzhou-10	GAIA
	2014							GSLV (India)							CARE (India)	

193

Appendix 3   Richardson Halo orbits third order approximation

This appendix presents the Halo orbits modeling with the third order approximation proposed by Richardson [51]. The third-order solution is given by:

$$x = a_{21}A_x^2 + a_{22}A_z^2 - A_x \cos(\tau_1) + (a_{23}A_x^2 - a_{24}A_z^2)\cos(2\tau_1) + (a_{31}A_x^3 - a_{32}A_xA_z^2)\cos(3\tau_1)$$
$$y = \kappa A_x \sin(\tau_1) + (b_{21}A_x^2 - ab_{22}A_z^2)\sin(2\tau_1) + (b_{31}A_x^3 - b_{32}A_xA_z^2)\sin(3\tau_1)$$
$$z = \delta_m A_x \cos(\tau_1) + \delta_m d_{21}A_xA_z (\cos(2\tau_1) - 3) + \delta_m(d_{32}A_xA_z^2 - d_{32}A_z^3)\cos(3\tau_1)$$

where :

- $\tau_1 = \omega_p\tau + \phi$
- $\delta_m = 2 - m \text{ and } m = 1,3$
- $a_{21} = \frac{3c_3(\kappa^2-2)}{4(1+2c_2)}$
- $a_{22} = \frac{3c_3}{4(1+2c_2)}$
- $a_{23} = -\frac{3c_3\lambda}{4\kappa d_1}(3\kappa^3\lambda - 6\kappa(\kappa-\lambda) + 4)$
- $a_{24} = -\frac{3c_3\lambda}{4\kappa d_1}(2 + 3\kappa\lambda)$
- $b_{21} = -\frac{3c_3\lambda}{2d_1}(3\kappa\lambda - 4)$
- $b_{22} = -\frac{3c_3\lambda}{d_1}$
- $d_{21} = -\frac{c_3}{2\lambda^2}$
- $a_{31} = -\frac{9\lambda}{4d_2}\left(4c_3(\kappa a_{23} - b_{21}) + \kappa c_4(4 + \kappa^2)\right) + \frac{9\lambda^2+1-c_2}{2d_2}\left(3c_3(2a_{23} - \kappa b_{21}) + c_4(2 + 3\kappa^2)\right)$
- $a_{32} = -\frac{9\lambda}{4d_2}(4c_3(3\kappa a_{24} - b_{22}) + \kappa c_4) - \frac{3}{2d_2}(9\lambda^2 + 1 - c_2)(c_3(\kappa b_{22} + d_{21} - 2a_{24}) - c_4)$
- $b_{31} = \frac{3}{8d_2}8\lambda\left(3c_3(\kappa b_{21} - a_{23}) - c_4(2 + 3\kappa^2)\right) + \frac{3}{8d_2}(9\lambda^2 + 1 + c_2)\left(4c_3(\kappa a_{23} - b_{21}) + \kappa c_4(4 + \kappa^2)\right)$
- $b_{32} = \frac{9\lambda}{d_2}(3c_3(\kappa b_{22} + d_{21} - 2a_{24}) - c_4) + \frac{3(9\lambda^2+1+c_2)}{8d_2}(4c_3(\kappa a_{24} - b_{22}) + \kappa c_4)$
- $d_{31} = \frac{3}{64\lambda^2}(4c_3a_{24} + c_4)$
- $d_{32} = \frac{3}{64\lambda^2}(4c_3(a_{23} - d_{21}) + c_4(4 + \kappa^2))$
- $l_1 = \frac{3}{2}c_3(2a_{21} + a_{23} + 5d_{21}) - \frac{3}{8}c_4(12 - \kappa^2) + 2\lambda^2 s_1$
- $d_1 = \frac{3\lambda^2}{\kappa}(\kappa(6\lambda^2 - 1) - 2\lambda)$
- $d_2 = \frac{8\lambda^2}{\kappa}(\kappa(11\lambda^2 - 1) - 2\lambda)$

Appendix 4   Weight estimation for the cost function

It is reminded that:
- The THOR space station is assumed to be rotating on a Halo orbit (defined by A_{z_THOR}, m_{THOR})
- The chaser is on its Halo parking orbit (defined by A_{z_chaser}, m_{cargo})

By applying Richardson modeling, assuming that $m\_{chaser} = m\_{THOR}$, the motion of on both orbits can be described as follows:

$$\begin{cases} x_{chaser} = A_{x\_chaser}cos(\omega_p t + \phi_{chaser}) \\ y_{chaser} = \kappa A_{x\_chaser}sin(\omega_p t + \phi_{chaser}) \\ z_{chaser} = A_{z\_chaser}cos(\omega_v t + \psi_{chaser}) \end{cases} \begin{cases} x_{THOR} = A_{x\_THOR}cos(\omega_p t + \phi_{THOR}) \\ y_{THOR} = \kappa A_{x\_THOR}sin(\omega_p t + \phi_{THOR}) \\ z_{THOR} = A_{z\_THOR}cos(\omega_v t + \psi_{THOR}) \end{cases} \quad \text{(App 1)}$$

Where:
- t is the time

   $\kappa, \omega_p, \omega_v$ are the same for both Halo orbits since they around the same Lagrangian point (EML2) and belong to the same family
- $(\phi_{chaser}, \psi_{chaser})$ and $(\phi_{THOR}, \psi_{THOR})$ dependson initial conditions

While deriving (App 1) according to time, the velocity can be obtained:

$$\begin{cases} \dot{x}_{chaser} = -\omega_p A_{x\_chaser}sin(\omega_p t + \phi_{chaser}) \\ \dot{y}_{chaser} = \omega_p \kappa A_{x\_chaser}cos(\omega_p t + \phi_{chaser}) \\ \dot{z}_{chaser} = -\omega_v A_{z\_chaser}sin(\omega_v t + \psi_{chaser}) \end{cases} \begin{cases} \dot{x}_{THOR} = -\omega_p A_{x\_THOR}sin(\omega_p t + \phi_{THOR}) \\ \dot{y}_{THOR} = \omega_p \kappa A_{x\_THOR}cos(\omega_p t + \phi_{THOR}) \\ \dot{z}_{THOR} = -\omega_v A_{z\_THOR}sin(\omega_v t + \psi_{THOR}) \end{cases} \quad \text{(App 2)}$$

The cost function that was selected for rendezvous optimization (see 5.3.65.3.6) is:

$$J = \left(\sqrt{ \alpha \left\| \begin{pmatrix} x_{chaser} \\ y_{chaser} \\ z_{chaser} \end{pmatrix} - \begin{pmatrix} x_{THOR} \\ y_{THOR} \\ z_{THOR} \end{pmatrix} \right\|_2^2 + \beta \left\| \begin{pmatrix} \dot{x}_{chaser} \\ \dot{y}_{chaser} \\ \dot{z}_{chaser} \end{pmatrix} - \begin{pmatrix} \dot{x}_{THOR} \\ \dot{y}_{THOR} \\ \dot{z}_{THOR} \end{pmatrix} \right\|_2^2 } \right)$$

While applying (App 1) and (App 2), the quadratic norms of position and velocity gap can be computed and maximized as follows:

$$\left\| \begin{pmatrix} x_{chaser} \\ y_{chaser} \\ z_{chaser} \end{pmatrix} - \begin{pmatrix} x_{THOR} \\ y_{THOR} \\ z_{THOR} \end{pmatrix} \right\|_2 \leq \sqrt{ (1+\kappa)^2 \left(A_{x\_chaser} + A_{x\_THOR} \right)^2 + \left(A_{z\_chaser} + A_{z\_THOR} \right)^2 } \quad \text{(App 3)}$$

$$\left\| \begin{pmatrix} \dot{x}_{chaser} \\ \dot{y}_{chaser} \\ \dot{z}_{chaser} \end{pmatrix} - \begin{pmatrix} \dot{x}_{THOR} \\ \dot{y}_{THOR} \\ \dot{z}_{THOR} \end{pmatrix} \right\|_2 \quad \text{(App 4)}$$

$$\leq \sqrt{ \omega_p^2 (1+\kappa)^2 \left(A_{x\_chaser} + A_{x\_THOR} \right)^2 + \omega_v^2 \left(A_{z\_chaser} + A_{z\_THOR} \right)^2 }$$

As a consequence, the order of magnitude for $\frac{\alpha}{\beta}$, when the same weight is expected for both components, could be:

$$\frac{\alpha}{\beta} = \frac{\left|(1+\kappa)^2\left(A_{x\_chaser} + A_{x\_THOR}\right)^2 + \left(A_{z\_chaser} + A_{z\_THOR}\right)^2\right|}{\left|\omega_p^2(1+\kappa)^2\left(A_{x\_chaser} + A_{x\_THOR}\right)^2 + \omega_v^2\left(A_{z\_chaser} + A_{z\_THOR}\right)^2\right|} \qquad \text{(App 5)}$$

Appendix 5   Scenarios description
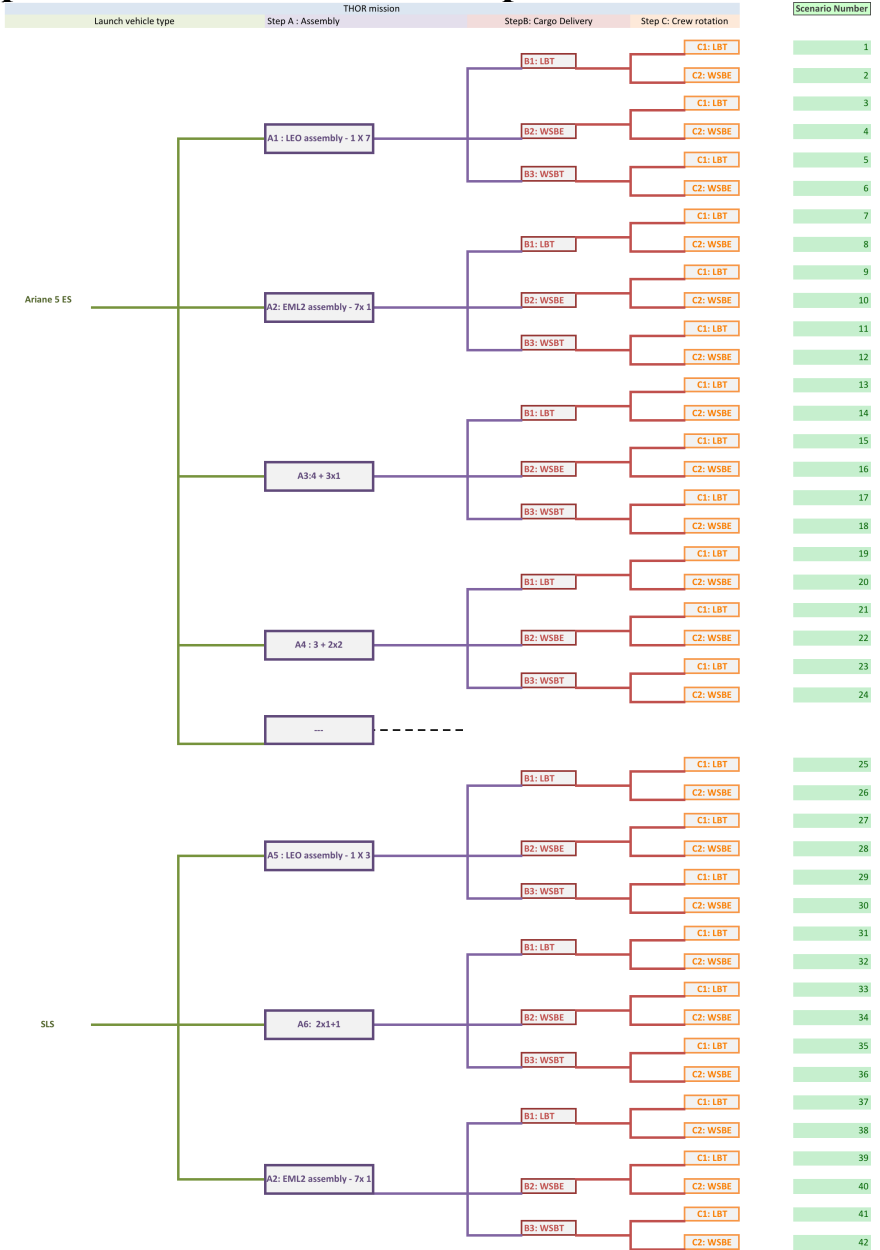
Figure 96: Scenarios decision tree

Appendix 6   THOR mission figures of merit computation

1   Delta-v

	Scenarios			Delta-v computation (km/s)				Results
Launch vehicle	THOR Assembly	Cargo delivery	Crew rotation	deltav_SK rdv LEO	delta v mod_transfer	delta v cargo	deltav crew	deltav (km/s)
Ariane 5 ES	A1		C1	0,6	3,2	206,5	101,5	311,8
		B1	C2	0,6	3,2	206,5	113,1	323,4
			C1	0,6	3,2	230,1	101,5	335,4
		B2	C2	0,6	3,2	230,1	113,1	347
			C1	0,6	3,2	188,8	101,5	294,1
		B3	C2	0,6	3,2	188,8	113,1	305,7
	A2		C1	0	22,4	182	91	295,4
		B1	C2	0	22,4	182	101,4	305,8
			C1	0	22,4	202,8	91	316,2
		B2	C2	0	22,4	202,8	101,4	326,6
			C1	0	22,4	166,4	91	279,8
		B3	C2	0	22,4	166,4	101,4	290,2
	A3		C1	0,3	12,8	196	98	307,1
		B1	C2	0,3	12,8	196	109,2	318,3
			C1	0,3	12,8	218,4	98	329,5
		B2	C2	0,3	12,8	218,4	109,2	340,7
			C1	0,3	12,8	179,2	98	290,3
		B3	C2	0,3	12,8	179,2	109,2	301,5
	A4		C1	0,4	9,6	199,5	98	307,5
		B1	C2	0,4	9,6	199,5	109,2	318,7
			C1	0,4	9,6	222,3	98	330,3
		B2	C2	0,4	9,6	222,3	109,2	341,5
			C1	0,4	9,6	182,4	98	290,4
		B3	C2	0,4	9,6	182,4	109,2	301,6

Scenarios				Delta-v computation (km/s)				Results
Launch vehicle	THOR Assembly	Cargo delivery	Crew rotation	deltav_SK_rdv_LEO	delta_v_mod_transfer	deltav_cargo	deltav_crew	deltav (km/s)
SLS	A5	B1	C1	0,2	3,2	206,5	101,5	311,4
		B1	C2	0,2	3,2	206,5	113,1	323
		B2	C1	0,2	3,2	230,1	101,5	335
		B2	C2	0,2	3,2	230,1	113,1	346,6
		B3	C1	0,2	3,2	188,8	101,5	293,7
		B3	C2	0,2	3,2	188,8	113,1	305,3
	A6	B1	C1	0,1	6,4	203	101,5	311
		B1	C2	0,1	6,4	203	113,1	322,6
		B2	C1	0,1	6,4	226,2	101,5	334,2
		B2	C2	0,1	6,4	226,2	113,1	345,8
		B3	C1	0,1	6,4	185,6	101,5	293,6
		B3	C2	0,1	6,4	185,6	113,1	305,2
	A7	B1	C1	0	9,6	199,5	98	307,1
		B1	C2	0	9,6	199,5	109,2	318,3
		B2	C1	0	9,6	222,3	98	329,9
		B2	C2	0	9,6	222,3	109,2	341,1
		B3	C1	0	9,6	182,4	98	290
		B3	C2	0	9,6	182,4	109,2	301,2

2 AMEML2

Scenario Number	Launch vehicle	THOR Assembly	Cargo delivery	Crew rotation	Mass after rdv LEO (t)	IMLEO (t)	AMEML2 (t)
1				C1	147,0	2020,0	69,5
2			B1	C2	147,0	2020,0	69,5
3		A1		C1	147,0	2020,0	69,5
4			B2	C2	147,0	2020,0	69,5
5				C1	147,0	2020,0	69,5
6			B3	C2	147,0	2020,0	69,5
7				C1	150,0	1807,5	70,9
8			B1	C2	150,0	1807,5	70,9
9		A2		C1	150,0	1807,5	70,9
10			B2	C2	150,0	1807,5	70,9
11				C1	150,0	1807,5	70,9
12	Ariane 5 ES		B3	C2	150,0	1807,5	70,9
13				C1	148,5	1935,0	70,2
14			B1	C2	148,5	1935,0	70,2
15		A3		C1	148,5	1935,0	70,2
16			B2	C2	148,5	1935,0	70,2
17				C1	148,5	1935,0	70,2
18			B3	C2	148,5	1935,0	70,2
19				C1	148,0	1956,3	69,9
20			B1	C2	148,0	1956,3	69,9
21		A4		C1	148,0	1956,3	69,9
22			B2	C2	148,0	1956,3	69,9
23				C1	148,0	1956,3	69,9
24			B3	C2	148,0	1956,3	69,9

Scenario Number	Launch vehicle	THOR Assembly	Cargo delivery	Crew rotation	Mass after rdv LEO (t)	IMLEO (t)	AMEML2 (t)
25				C1	147,7	2020,0	69,8
26			B1	C2	147,7	2020,0	69,8
27		A5		C1	147,7	2020,0	69,8
28			B2	C2	147,7	2020,0	69,8
29				C1	147,7	2020,0	69,8
30			B3	C2	147,7	2020,0	69,8
31				C1	148,8	1998,8	70,3
32			B1	C2	148,8	1998,8	70,3
33	SLS	A6		C1	148,8	1998,8	70,3
34			B2	C2	148,8	1998,8	70,3
35				C1	148,8	1998,8	70,3
36			B3	C2	148,8	1998,8	70,3
37				C1	150,0	1956,3	70,9
38			B1	C2	150,0	1956,3	70,9
39		A7		C1	150,0	1956,3	70,9
40			B2	C2	150,0	1956,3	70,9
41				C1	150,0	1956,3	70,9
42			B3	C2	150,0	1956,3	70,9

3 Tinit

Scenarios				Tinit (days)
Launch vehicle	THOR Assembly	Cargo delivery	Crew rotation	
Ariane 5 ES	A1	B1	C1	101
			C2	101
		B2	C1	101
			C2	101
		B3	C1	101
			C2	101
	A2	B1	C1	728,6
			C2	728,6
		B2	C1	728,6
			C2	728,6
		B3	C1	728,6
			C2	728,6
	A3	B1	C1	414,8
			C2	414,8
		B2	C1	414,8
			C2	414,8
		B3	C1	414,8
			C2	414,8
	A4	B1	C1	310,2
			C2	310,2
		B2	C1	310,2
			C2	310,2
		B3	C1	310,2
			C2	310,2

Scenarios				
Launch vehicle	THOR Assembly	Cargo delivery	Crew rotation	Tinit (days)
SLS	A5	B1	C1	101
			C2	101
		B2	C1	101
			C2	101
		B3	C1	101
			C2	101
	A6	B1	C1	205,6
			C2	205,6
		B2	C1	205,6
			C2	205,6
		B3	C1	205,6
			C2	205,6
	A7	B1	C1	310,2
			C2	310,2
		B2	C1	310,2
			C2	310,2
		B3	C1	310,2
			C2	310,2

4 Risk

Scenario Number	Launch vehicle	THOR Assembly	Cargo delivery	Crew rotation	Scenario description	Launch			Assembly			Cargo transfer			Crew transfer			Risk evaluation	
						Gravity	Probabilty	Risk	Gravity	Probabilty	Risk	Gravity	Probabilty	Risk	Gravity	Probabilty	Risk	Total risk	Risk level
1	Ariane 5 ES	A1		C1	A5 - RdV LEO - LBT - LBT	1	1	1	1	1	1	2	2	4	3	2	6	24	Low
2			B1	C2	A5 - RdV LEO - LBT - WSBE	1	1	1	1	1	1	2	2	4	3	2	6	24	Low
3				C1	A5 - RdV LEO - WSBE - LBT	1	1	1	1	1	1	2	2	4	3	2	6	24	Low
4			B2	C2	A5 - RdV LEO - WSBE - WSBE	1	1	1	1	1	1	2	2	4	3	2	6	24	Low
5				C1	A5 - RdV LEO - WSBT - LBT	1	1	1	1	1	1	2	2	4	3	2	6	24	Low
6			B3	C2	A5 - RdV LEO - WSBT- WSBE	1	1	1	1	1	1	2	2	4	3	2	6	24	Low
7		A2		C1	A5 - RdV EML2 - LBT - LBT	1	1	1	2	3	6	2	2	4	3	2	6	144	Medium
8			B1	C2	A5 - RdV EML2 - LBT - WSBE	1	1	1	2	3	6	2	2	4	3	2	6	144	Medium
9				C1	A5 - RdV EML2 - WSBE - LBT	1	1	1	2	3	6	2	2	4	3	2	6	144	Medium
10			B2	C2	A5 - RdV EML2 - WSBE - WSBE	1	1	1	2	3	6	2	2	4	3	2	6	144	Medium
11				C1	A5 - RdV EML2 - WSBT - LBT	1	1	1	2	3	6	2	2	4	3	2	6	144	Medium
12			B3	C2	A5 - RdV EML2 - WSBT- WSBE	1	1	1	2	3	6	2	2	4	3	2	6	144	Medium
13		A3		C1	A5 - 4 + 3x1 - LBT - LBT	1	1	1			3,5	2	2	4	3	2	6	84	Medium
14			B1	C2	A5 - 4 + 3x1 - LBT - WSBE	1	1	1			3,5	2	2	4	3	2	6	84	Medium
15				C1	A5 - 4 + 3x1 - WSBE - LBT	1	1	1			3,5	2	2	4	3	2	6	84	Medium
16			B2	C2	A5 - 4 + 3x1 - WSBE - WSBE	1	1	1			3,5	2	2	4	3	2	6	84	Medium
17				C1	A5 - 4 + 3x1 - WSBT - LBT	1	1	1			3,5	2	2	4	3	2	6	84	Medium
18			B3	C2	A5 - 4 + 3x1 - WSBT- WSBE	1	1	1			3,5	2	2	4	3	2	6	84	Medium
19		A4		C1	A5 - 3 + 2x2 - LBT - LBT	1	1	1			2,7	2	2	4	3	2	6	64,8	Low
20			B1	C2	A5 - 3 + 2x2 - LBT - WSBE	1	1	1			2,7	2	2	4	3	2	6	64,8	Low
21				C1	A5 - 3 + 2x2 - WSBE - LBT	1	1	1			2,7	2	2	4	3	2	6	64,8	Low
22			B2	C2	A5 - 3 + 2x2 - WSBE - WSBE	1	1	1			2,7	2	2	4	3	2	6	64,8	Low
23				C1	A5 - 3 + 2x2 - WSBT - LBT	1	1	1			2,7	2	2	4	3	2	6	64,8	Low
24			B3	C2	A5 - 3 + 2x2 - WSBT- WSBE	1	1	1			2,7	2	2	4	3	2	6	64,8	Low
25	SLS	A5		C1	SLS - RdV LEO - LBT - LBT	2	3	6	1	1	1	2	2	4	3	2	6	144	Medium
26			B1	C2	SLS - RdV LEO - LBT - WSBE	2	3	6	1	1	1	2	2	4	3	2	6	144	Medium
27				C1	SLS - RdV LEO - WSBE - LBT	2	3	6	1	1	1	2	2	4	3	2	6	144	Medium
28			B2	C2	SLS - RdV LEO - WSBE - WSBE	2	3	6	1	1	1	2	2	4	3	2	6	144	Medium
29				C1	SLS - RdV LEO - WSBT - LBT	2	3	6	1	1	1	2	2	4	3	2	6	144	Medium
30			B3	C2	SLS - RdV LEO - WSBT- WSBE	2	3	6	1	1	1	2	2	4	3	2	6	144	Medium
31		A6		C1	SLS - 1x2 + 1 - LBT - LBT	2	3	6			3,5	2	2	4	3	2	6	504	High
32			B1	C2	SLS - 1x2 + 1 - LBT - WSBE	2	3	6			3,5	2	2	4	3	2	6	504	High
33				C1	SLS - 1x2 + 1 - WSBE - LBT	2	3	6			3,5	2	2	4	3	2	6	504	High
34			B2	C2	SLS - 1x2 + 1 - WSBE - WSBE	2	3	6			3,5	2	2	4	3	2	6	504	High
35				C1	SLS - 1x2 + 1 - WSBT - LBT	2	3	6			3,5	2	2	4	3	2	6	504	High
36			B3	C2	SLS - 1x2 + 1 - WSBT- WSBE	2	3	6			3,5	2	2	4	3	2	6	504	High
37		A7		C1	SLS - RdV EML2 - LBT - LBT	2	3	6	2	3	6	2	2	4	3	2	6	864	High
38			B1	C2	SLS - RdV EML2 - LBT - WSBE	2	3	6	2	3	6	2	2	4	3	2	6	864	High
39				C1	SLS - RdV EML2 - WSBE - LBT	2	3	6	2	3	6	2	2	4	3	2	6	864	High
40			B2	C2	SLS - RdV EML2 - WSBE - WSBE	2	3	6	2	3	6	2	2	4	3	2	6	864	High
41				C1	SLS - RdV EML2 - WSBT - LBT	2	3	6	2	3	6	2	2	4	3	2	6	864	High
42			B3	C2	SLS - RdV EML2 - WSBT- WSBE	2	3	6	2	3	6	2	2	4	3	2	6	864	High

5   Operability

Scenario Number	Launch vehicle	THOR Assembly	Cargo delivery	Crew rotation	Scenario description	Launch Duration	Launch Complexity	Launch Ops	Assembly Duration	Assembly Complexity	Assembly Ops	Cargo transfer Duration	Cargo transfer Complexity	Cargo transfer Ops	Crew transfer Duration	Crew transfer Complexity	Crew transfer Ops	Total operability	Level operabilty
1	Ariane 5 ES	A1		C1	A5 - RdV LEO - LBT - LBT	2	1	2	1	1	1,0	3	2	6	1	2	2	24	Low
2			B1	C2	A5 - RdV LEO - LBT - WSBE	2	1	2	1	1	1,0	3	2	6	1	2	2	24	Low
3				C1	A5 - RdV LEO - WSBE - LBT	2	1	2	1	1	1,0	1	2	2	1	2	2	8	Low
4			B2	C2	A5 - RdV LEO - WSBE - WSBE	2	1	2	1	1	1,0	1	2	2	1	2	2	8	Low
5				C1	A5 - RdV LEO - WSBT - LBT	2	1	2	1	1	1,0	3	2	6	1	2	2	24	Low
6			B3	C2	A5 - RdV LEO - WSBT- WSBE	2	1	2	1	1	1,0	3	2	6	1	2	2	24	Low
7		A2		C1	A5 - RdV EML2 - LBT - LBT	2	1	2	2	3	6,0	3	2	6	1	2	2	144	High
8			B1	C2	A5 - RdV EML2 - LBT - WSBE	2	1	2	2	3	6,0	3	2	6	1	2	2	144	High
9				C1	A5 - RdV EML2 - WSBE - LBT	2	1	2	2	3	6,0	1	2	2	1	2	2	48	Medium
10			B2	C2	A5 - RdV EML2 - WSBE - WSBE	2	1	2	2	3	6,0	1	2	2	1	2	2	48	Medium
11				C1	A5 - RdV EML2 - WSBT - LBT	2	1	2	2	3	6,0	3	2	6	1	2	2	144	High
12			B3	C2	A5 - RdV EML2 - WSBT- WSBE	2	1	2	2	3	6,0	3	2	6	1	2	2	144	High
13		A3		C1	A5 - 4 + 3x1 - LBT - LBT	2	1	2			3,5	3	2	6	1	2	2	84	Medium
14			B1	C2	A5 - 4 + 3x1 - LBT - WSBE	2	1	2			3,5	3	2	6	1	2	2	84	Medium
15				C1	A5 - 4 + 3x1 - WSBE - LBT	2	1	2			3,5	1	2	2	1	2	2	28	Low
16			B2	C2	A5 - 4 + 3x1 - WSBE - WSBE	2	1	2			3,5	1	2	2	1	2	2	28	Low
17				C1	A5 - 4 + 3x1 - WSBT - LBT	2	1	2			3,5	3	2	6	1	2	2	84	Medium
18			B3	C2	A5 - 4 + 3x1 - WSBT- WSBE	2	1	2			3,5	3	2	6	1	2	2	84	Medium
19		A4		C1	A5 - 3 + 2x2 - LBT - LBT	2	1	2			2,7	3	2	6	1	2	2	64	Medium
20			B1	C2	A5 - 3 + 2x2 - LBT - WSBE	2	1	2			2,7	3	2	6	1	2	2	64	Medium
21				C1	A5 - 3 + 2x2 - WSBE - LBT	2	1	2			2,7	1	2	2	1	2	2	21	Low
22			B2	C2	A5 - 3 + 2x2 - WSBE - WSBE	2	1	2			2,7	1	2	2	1	2	2	21	Low
23				C1	A5 - 3 + 2x2 - WSBT - LBT	2	1	2			2,7	3	2	6	1	2	2	64	Medium
24			B3	C2	A5 - 3 + 2x2 - WSBT- WSBE	2	1	2			2,7	3	2	6	1	2	2	64	Medium
25	SLS	A5		C1	SLS - RdV LEO - LBT - LBT	1	2	2	1	1	1,0	3	2	6	1	2	2	24	Low
26			B1	C2	SLS - RdV LEO - LBT - WSBE	1	2	2	1	1	1,0	3	2	6	1	2	2	24	Low
27				C1	SLS - RdV LEO - WSBE - LBT	1	2	2	1	1	1,0	1	2	2	1	2	2	8	Low
28			B2	C2	SLS - RdV LEO - WSBE - WSBE	1	2	2	1	1	1,0	1	2	2	1	2	2	8	Low
29				C1	SLS - RdV LEO - WSBT - LBT	1	2	2	1	1	1,0	3	2	6	1	2	2	24	Low
30			B3	C2	SLS - RdV LEO - WSBT- WSBE	1	2	2	1	1	1,0	3	2	6	1	2	2	24	Low
31		A6		C1	SLS - 1x2 + 1 - LBT - LBT	1	2	2			3,5	3	2	6	1	2	2	84	Medium
32			B1	C2	SLS - 1x2 + 1 - LBT - WSBE	1	2	2			3,5	3	2	6	1	2	2	84	Medium
33				C1	SLS - 1x2 + 1 - WSBE - LBT	1	2	2			3,5	1	2	2	1	2	2	28	Low
34			B2	C2	SLS - 1x2 + 1 - WSBE - WSBE	1	2	2			3,5	1	2	2	1	2	2	28	Low
35				C1	SLS - 1x2 + 1 - WSBT - LBT	1	2	2			3,5	3	2	6	1	2	2	84	Medium
36			B3	C2	SLS - 1x2 + 1 - WSBT- WSBE	1	2	2			3,5	3	2	6	1	2	2	84	Medium
37		A7		C1	SLS - RdV EML2 - LBT - LBT	1	2	2	2	3	6,0	3	2	6	1	2	2	144	High
38			B1	C2	SLS - RdV EML2 - LBT - WSBE	1	2	2	2	3	6,0	3	2	6	1	2	2	144	High
39				C1	SLS - RdV EML2 - WSBE - LBT	1	2	2	2	3	6,0	1	2	2	1	2	2	48	Medium
40			B2	C2	SLS - RdV EML2 - WSBE - WSBE	1	2	2	2	3	6,0	1	2	2	1	2	2	48	Medium
41				C1	SLS - RdV EML2 - WSBT - LBT	1	2	2	2	3	6,0	3	2	6	1	2	2	144	High
42			B3	C2	SLS - RdV EML2 - WSBT- WSBE	1	2	2	2	3	6,0	3	2	6	1	2	2	144	High

6   Final evaluation

Scenario Number	Launch vehicle	THOR Assembly	Cargo delivery	Crew rotation	Scenario description	Cost	Flexibility	Risk	deltav	Number of launches	Tinit (days)	IMLEO (t)	AMEML2
						Qualitative FOM			Quantitative FOM				
1	Ariane 5 ES	A1	B1	C1	A5 - RdV LEO - LBT - LBT	Medium	Low	Low	311,8	7,0	101,0	2020,0	69,5
2				C2	A5 - RdV LEO - LBT - WSBE	Medium	Low	Low	323,4	7,0	101,0	2020,0	69,5
3			B2	C1	A5 - RdV LEO - WSBE - LBT	Medium	Low	Low	335,4	7,0	101,0	2020,0	69,5
4				C2	A5 - RdV LEO - WSBE - WSBE	Medium	Low	Low	347,0	7,0	101,0	2020,0	69,5
5			B3	C1	A5 - RdV LEO - WSBT - LBT	Medium	Low	Low	294,1	7,0	101,0	2020,0	69,5
6				C2	A5 - RdV LEO - WSBT- WSBE	Medium	Low	Low	305,7	7,0	101,0	2020,0	69,5
7		A2	B1	C1	A5 - RdV EML2 - LBT - LBT	Medium	High	Medium	295,4	7,0	728,6	1807,5	70,9
8				C2	A5 - RdV EML2 - LBT - WSBE	Medium	High	Medium	305,8	7,0	728,6	1807,5	70,9
9			B2	C1	A5 - RdV EML2 - WSBE - LBT	Medium	Medium	Medium	316,2	7,0	728,6	1807,5	70,9
10				C2	A5 - RdV EML2 - WSBE - WSBE	Medium	Medium	Medium	326,6	7,0	728,6	1807,5	70,9
11			B3	C1	A5 - RdV EML2 - WSBT - LBT	Medium	High	Medium	279,8	7,0	728,6	1807,5	70,9
12				C2	A5 - RdV EML2 - WSBT- WSBE	Medium	High	Medium	290,2	7,0	728,6	1807,5	70,9
13		A3	B1	C1	A5 - 4 + 3x1 - LBT - LBT	Medium	Medium	Medium	307,1	7,0	414,8	1935,0	70,2
14				C2	A5 - 4 + 3x1 - LBT - WSBE	Medium	Medium	Medium	318,3	7,0	414,8	1935,0	70,2
15			B2	C1	A5 - 4 + 3x1 - WSBE - LBT	Medium	Low	Medium	329,5	7,0	414,8	1935,0	70,2
16				C2	A5 - 4 + 3x1 - WSBE - WSBE	Medium	Low	Medium	340,7	7,0	414,8	1935,0	70,2
17			B3	C1	A5 - 4 + 3x1 - WSBT - LBT	Medium	Medium	Medium	290,3	7,0	414,8	1935,0	70,2
18				C2	A5 - 4 + 3x1 - WSBT- WSBE	Medium	Medium	Medium	301,5	7,0	414,8	1935,0	70,2
19		A4	B1	C1	A5 - 3 + 2x2 - LBT - LBT	Medium	Medium	Low	307,5	7,0	310,2	1956,3	69,9
20				C2	A5 - 3 + 2x2 - LBT - WSBE	Medium	Medium	Low	318,7	7,0	310,2	1956,3	69,9
21			B2	C1	A5 - 3 + 2x2 - WSBE - LBT	Medium	Low	Low	330,3	7,0	310,2	1956,3	69,9
22				C2	A5 - 3 + 2x2 - WSBE - WSBE	Medium	Low	Low	341,5	7,0	310,2	1956,3	69,9
23			B3	C1	A5 - 3 + 2x2 - WSBT - LBT	Medium	Medium	Low	290,4	7,0	310,2	1956,3	69,9
24				C2	A5 - 3 + 2x2 - WSBT- WSBE	Medium	Medium	Low	301,6	7,0	310,2	1956,3	69,9
25	SLS	A5	B1	C1	SLS - RdV LEO - LBT - LBT	High	Low	Medium	311,4	7,0	101,0	2020,0	69,8
26				C2	SLS - RdV LEO - LBT - WSBE	High	Low	Medium	323,0	7,0	101,0	2020,0	69,8
27			B2	C1	SLS - RdV LEO - WSBE - LBT	High	Low	Medium	335,0	7,0	101,0	2020,0	69,8
28				C2	SLS - RdV LEO - WSBE - WSBE	High	Low	Medium	346,6	7,0	101,0	2020,0	69,8
29			B3	C1	SLS - RdV LEO - WSBT - LBT	High	Low	Medium	293,7	7,0	101,0	2020,0	69,8
30				C2	SLS - RdV LEO - WSBT- WSBE	High	Low	Medium	305,3	7,0	101,0	2020,0	69,8
31		A6	B1	C1	SLS - 1x2 + 1 - LBT - LBT	High	Medium	High	311,0	3,0	205,6	1998,8	70,3
32				C2	SLS - 1x2 + 1 - LBT - WSBE	High	Medium	High	322,6	3,0	205,6	1998,8	70,3
33			B2	C1	SLS - 1x2 + 1 - WSBE - LBT	High	Low	High	334,2	3,0	205,6	1998,8	70,3
34				C2	SLS - 1x2 + 1 - WSBE - WSBE	High	Low	High	345,8	3,0	205,6	1998,8	70,3
35			B3	C1	SLS - 1x2 + 1 - WSBT - LBT	High	Medium	High	293,6	3,0	205,6	1998,8	70,3
36				C2	SLS - 1x2 + 1 - WSBT- WSBE	High	Medium	High	305,2	3,0	205,6	1998,8	70,3
37		A7	B1	C1	SLS - RdV EML2 - LBT - LBT	High	High	High	307,1	3,0	310,2	1956,3	70,9
38				C2	SLS - RdV EML2 - LBT - WSBE	High	High	High	318,3	3,0	310,2	1956,3	70,9
39			B2	C1	SLS - RdV EML2 - WSBE - LBT	High	Medium	High	329,9	3,0	310,2	1956,3	70,9
40				C2	SLS - RdV EML2 - WSBE - WSBE	High	Medium	High	341,1	3,0	310,2	1956,3	70,9
41			B3	C1	SLS - RdV EML2 - WSBT - LBT	High	High	High	290,0	3,0	310,2	1956,3	70,9
42				C2	SLS - RdV EML2 - WSBT- WSBE	High	High	High	301,2	3,0	310,2	1956,3	70,9

7   Final mark

Scenario Number	Launch vehicle	THOR Assembly	Cargo delivery	Crew rotation	Scenario description	Cost	Flexibility	Risk	deltav	Number of launches	Tinit (days)	IMLEO (t)	AMEML2	Agregat 1	Agregat2	Agregat3	Agregat4	Agregat5	Agregat6
					Scenarios		Qualitative FOM			Quantitative FOM				3 R + 2 AMEML2	3R+2(Mission)		3R+ 2 COST	3 COST	3 Mission
1	Ariane 5 ES	A1	B1	C1	A5 - RdV LEO - LBT - LBT	1	0	0	0	2	0	2	2	7	9	9	12	17	11
2				C2	A5 - RdV LEO - LBT - WSBE	1	0	0	1	2	0	2	2	8	10	10	14	20	12
3			B2	C1	A5 - RdV LEO - WSBE - LBT	1	0	0	1	2	0	2	2	8	10	10	14	20	12
4				C2	A5 - RdV LEO - WSBE - WSBE	1	0	0	2	2	0	2	2	9	11	11	16	23	13
5			B3	C1	A5 - RdV LEO - WSBT - LBT	1	0	0	0	2	0	2	2	7	9	9	12	17	11
6				C2	A5 - RdV LEO - WSBT- WSBE	1	0	0	0	2	0	2	2	7	9	9	12	17	11
7		A2	B1	C1	A5 - RdV EML2 - LBT - LBT	1	2	1	0	2	2	0	0	8	14	16	17	18	12
8				C2	A5 - RdV EML2 - LBT - WSBE	1	2	1	0	2	2	0	0	8	14	16	17	18	12
9			B2	C1	A5 - RdV EML2 - WSBE - LBT	1	1	1	1	2	2	0	0	8	12	14	16	18	12
10				C2	A5 - RdV EML2 - WSBE - WSBE	1	1	1	1	2	2	0	0	8	12	14	16	18	12
11			B3	C1	A5 - RdV EML2 - WSBT - LBT	1	2	1	0	2	2	0	0	8	14	16	17	18	12
12	Ariane 5 ES			C2	A5 - RdV EML2 - WSBT- WSBE	1	2	1	0	2	2	0	0	8	14	16	17	18	12
13		A3	B1	C1	A5 - 4 + 3x1 - LBT - LBT	1	1	1	0	2	1	1	1	8	13	14	16	18	12
14				C2	A5 - 4 + 3x1 - LBT - WSBE	1	1	1	1	2	1	1	1	9	14	15	18	21	13
15			B2	C1	A5 - 4 + 3x1 - WSBE - LBT	1	0	1	1	2	1	1	1	8	11	12	15	18	12
16				C2	A5 - 4 + 3x1 - WSBE - WSBE	1	0	1	1	2	1	1	1	8	11	12	15	18	12
17			B3	C1	A5 - 4 + 3x1 - WSBT - LBT	1	1	1	0	2	1	1	1	8	13	14	16	18	12
18				C2	A5 - 4 + 3x1 - WSBT- WSBE	1	1	1	0	2	1	1	1	8	13	14	16	18	12
19		A4	B1	C1	A5 - 3 + 2x2 - LBT - LBT	1	1	0	0	2	0	1	1	6	9	9	12	16	8
20				C2	A5 - 3 + 2x2 - LBT - WSBE	1	1	0	1	2	0	1	1	7	10	10	14	19	9
21			B2	C1	A5 - 3 + 2x2 - WSBE - LBT	1	0	0	1	2	0	1	1	6	7	7	11	16	8
22				C2	A5 - 3 + 2x2 - WSBE - WSBE	1	0	0	1	2	0	1	1	6	7	7	11	16	8
23			B3	C1	A5 - 3 + 2x2 - WSBT - LBT	1	1	0	0	2	0	1	1	6	9	9	12	16	8
24				C2	A5 - 3 + 2x2 - WSBT- WSBE	1	1	0	0	2	0	1	1	6	9	9	12	16	8
25	SLS	A5	B1	C1	SLS - RdV LEO - LBT - LBT	2	0	1	0	2	0	2	1	8	11	11	16	20	10
26				C2	SLS - RdV LEO - LBT - WSBE	2	0	1	1	2	0	2	1	9	12	12	18	23	11
27			B2	C1	SLS - RdV LEO - WSBE - LBT	2	0	1	1	2	0	2	1	9	12	12	18	23	11
28				C2	SLS - RdV LEO - WSBE - WSBE	2	0	1	1	2	0	2	1	9	12	12	18	23	11
29			B3	C1	SLS - RdV LEO - WSBT - LBT	2	0	1	0	2	0	2	1	8	11	11	16	20	10
30				C2	SLS - RdV LEO - WSBT- WSBE	2	0	1	0	2	0	2	1	8	11	11	16	20	10
31		A6	B1	C1	SLS - 1x2 + 1 - LBT - LBT	2	1	2	0	0	0	1	0	6	12	12	15	14	6
32				C2	SLS - 1x2 + 1 - LBT - WSBE	2	1	2	1	0	0	1	0	7	13	13	17	17	7
33	SLS		B2	C1	SLS - 1x2 + 1 - WSBE - LBT	2	0	2	1	0	0	1	0	6	10	10	14	14	6
34				C2	SLS - 1x2 + 1 - WSBE - WSBE	2	0	2	1	0	0	1	0	6	10	10	14	14	6
35			B3	C1	SLS - 1x2 + 1 - WSBT - LBT	2	1	2	0	0	0	1	0	6	12	12	15	14	6
36				C2	SLS - 1x2 + 1 - WSBT- WSBE	2	1	2	0	0	0	1	0	6	12	12	15	14	6
37		A7	B1	C1	SLS - RdV EML2 - LBT - LBT	2	2	2	0	0	0	1	0	7	15	15	18	17	7
38				C2	SLS - RdV EML2 - LBT - WSBE	2	2	2	1	0	0	1	0	8	16	16	20	20	8
39			B2	C1	SLS - RdV EML2 - WSBE - LBT	2	1	2	1	0	0	1	0	7	13	13	17	17	7
40				C2	SLS - RdV EML2 - WSBE - WSBE	2	1	2	1	0	0	1	0	7	13	13	17	17	7
41			B3	C1	SLS - RdV EML2 - WSBT - LBT	2	0	2	0	0	0	1	0	5	9	9	12	11	5
42				C2	SLS - RdV EML2 - WSBT- WSBE	2	0	2	0	0	0	1	0	5	9	9	12	11	5

Appendix 7   Bibliography

References are organized according to the document outline.

8   Abstract
[1]   ISECG, *Global Exploration Roadmap*, August 2013

9   Space exploration context
[2]   Kepler, J., *Astronomia Nova*, Heidelberg, 1609
[3]   Galileo Galilei, *Discorsi e Dimostrazioni Matematiche Intorno a Due Nuove Scienze*, 1638
[4]   Newton, I., *Philosophiae naturalis principia mathematica*, London, 1687
[5]   Lagrange J-L, 1772, *Essai sur le problème des trois corp*s, Prix de l'Académie Royale des Sciences de Paris, tome IX, in vol. 6 of Oeuvres de Lagrange , Gauthier – Villars, Paris 1873, 272-282
[6]   Poincaré, H., 1890, *Sur le problème des trois corps et les équations de la dynamique*, Acta Math, 13, 1 – 271
[7]   Poincaré, H.*,* Les méthodes nouvelles de mécanique céleste, Gauthier-Villars, Paris – 1893
[8]   Farquhar, R. *Lunar Communications with Libration-Point Satellites*. Journal of Spacecraft and Rockets. 1967, Vol. 4, 10
[9]   Farquhar, Robert W. *A Halo-Orbit Lunar Station*. Astronautics and Aeronautics. 1972, pp. 59 - 63.
[10]   Farquhar, R., and al. *Utilization of libration points for human exploration in the Sun–Earth–Moon system and beyond*. Acta Astronautica. 2004, 55, pp. 687 – 700.
[11]   J. S. Parker, R.L. Anderson*, Low energy lunar trajectory design*, Jet Propulsion Laboratory July 2013
[12]   Messerscmid, E. and Bertrand R., *Space Stations Systems and Utilization* – Springer -1999
[13]   Verne J., *De la Terre à la Lune,* Paris,1865
[14]   Verne J., *Autour de la Lune*, Paris, 1870
[15]   Tsiolkovsky K., *The Rocket into Cosmic Space* - Moscow, 1903
[16]   Oberth H., *The Rocket into Interplenatary Space* - R. Oldenbourg, Munich, 1923
[17]   Noordung (Potocnik), H., *Das Problem der Befahrung des Weltraums (the problem of space travel)*, Schmidt and Co., 1928
[18]   Ross, H. L., *Orbital Bases*, J. British Interplanetary Soc., vol. 8, no.1, 1949, pp. 1-19.
[19]   Von Braun, W. and al – *Across the space frontier* - Viking Press, New York Munich, 1952
[20]   Howell, K.C. *Families of Orbits in the Vicinity of the Collinear Libration Points*. The Journal of the Astronautical Sciences. 2001, Vol. 49, 1, pp. 107 – 125
[21]   Howell, K.C, and al. *Representations of Invariant Manifolds for Applications in Three-Body Systems.* The Journal of the Astronautical Sciences. 2006, Vol. 54, 1.

[22]   Renk, Florian. *Mission Analysis for Exploration Missions utilizing Near-Earth Libration Points.* Dissertation, Munich : Dr. Hut, 2009.

[23]   Renk, F., Hechler, M. and Messerschmid, E. *Exploration missions in the Sun-Earth-Moon system: A detailed view on selected transfer problems*. Acta Astronautica. 2010, Vol. 67, pp. 82 - 96.

[24]   Mingtao, Li and Jianhua, Zheng. *Impulsive lunar Halo transfers using the stable manifolds and lunar flybys.* Acta Astronautica. 2010, Vol. 66, pp. 1481 - 1492

[25]   Canalias, E, Gomez, G. and Marcote, M., Masdemont, J.J. *Assessment of Mission Design Including Utilization of Libration Points and Weak Stability Boundaries*. ESA Advanced Concepts Team, Ariadna Final Report (03-4103a). 2004.

[26]   Zazzera, F.B., Topputo, F. and Massari, M. *Assessment of Mission Design Including Utilization of Libration Points and Weak Stability Boundaries.* ESA Advanced Concepts Team, Ariadna Final Report (03-4103b). 2004..

[27]   Koon, W. S., et al. *Dynamical Systems, the Three-Body Problem and Space Mission Design.* Free online Copy : Marsden Books, 2008.

[28]   Mendell, Wendell W. *A gateway for human exploration of space? The weak stability boundary. Space Policy.* 2001, Vol. 17, pp. 13 - 17.

[29]   Mendell, Wendell W. and S., Hoffman. *Considerations for Cislunar Space Infrastructure*. 44th IAF Congress Graz, Austria. 1993, Paper: IAF-93-Q.5.416.

[30]   Lo, Martin. *The Interplanetary Superhighway and the Origins Program*. IEEE Space 2002 Conference. 2002.

[31]   Lo, Martin and Ross, Shane. *The Lunar L1 Gateway: Portal to the Stars and Beyond*. AIAA Space 2001 Conference. 2001.

[32]   JSC. *Lunar L1 Gateway Conceptual Design Report.* Technical Report : NASA, 2001. EX 15-01-001.

[33]   Thronson, Harley and Talay, Ted. *"Gateway" Architectures: A Major "Flexible Path" Step to the Moon and Mars after the International Space Station*? The Future in Space Operations (FISO) working group.

[34]   Thronson, Harley, Lester, Dan and Talay, *Ted. Human operations beyond LEO by the end of the decade: An affordable near-term stepping stone.* The Space Review.

[35]   Nasaspaceflight.com. *An Alternative Lunar Architecture*.
http://forum.nasaspaceflight.com/index.php?topic=1337.0.

[36]   Lockheed Martin. *Early Human L2 Farside Missions*.
http://www.lockheedmartin.com/data/assets/ssc/Orion/Toolkit/LMFarsideWhitepaper Final.pdf.

10   Space station design

[37]   INCOSE, *Systems Engineering Handbook*, INCOSE-TP-2003-002-03.2.1, San Diego, 2011

[38]   NASA, *Systems Engineering Handbook*, NASA/SP-2007-6105 rev 1, Washington, D.C, 2007

[39]   Kanas N., Manzey. D, *Space psychology and psychiatry*. 2nd edition, Microcosm Press, El Segundo, California, and Springer, Dordrecht, The Nederlands, 2008

209

[40]   Morphew, M.E, *Psychological and human factors in long duration spaceflight*. MJM 2001 6:74-80

[41]   Martin, Gary L., *NASA's Strategy for Human and Robotic Exploration,* slide 11, Space Architect, June 10, 2003

[42]   L.M. Jagger, *Spacecraft Architectural Design with Minimal Artificial Weightness Concept*, Cranfield University College of Aeronautics, ENSICA, 1998

[42b]   Wiley J. Larson et al, *Human Spaceflight Mission Analysis and Design,*., Chapet 11: Designing and Sizing Space Elements. Space Technology Series, Mc Graw-Hill, 1999, ISBN-0-07-236811-X

11   Theoretical background

[43]   Marsden, J.E and Ratiu, *Introduction to Mechanics and Symmetry*, volume 17 of text in Applied Mathematics, Springer-Verlag, 1999

[44]   Szebehely, V, *Theory of orbits: The Restricted Problem of Three Bodies*, Academic, New-York, 1967

[45]   Pac, J-L, *Systèmes dynamiques*, Dunod, 2012

[46]   Archambeau, G, *Etude de la dynamique autour des points de Lagrange*, Université Paris-Sud XI, 2008

[47]   Howell, K., *Three-dimensionnal, periodic, 'Halo' orbits,* Celestial mechanics, 1984

[48]   Gómez, G., W. S. Koon, M. Lo, J. E. Marsden, J. Masdemont, and S. D. Ross, *Invariant manifolds, the spatial three-body problem and space mission design,* Adv. Astronaut. Sci. 109, 3–22, 2001

[49]   Gómez, G., W. S. Koon, M. Lo, J. E. Marsden, J. Masdemont, and S. D. Ross, *Connecting orbits and invariant manifolds in the spatial three-body problem*, Nonlinearity, 17, pp. 1571-1606, 2004

[50]   Farquhar R. W., Kamel, A. A., Quasi-periodic orbits about the translunar libration point, Celestial Mechanics 7, 1973

[51]   Richardson, D. L, *Analytical construction of periodic orbits about the collinear points*, Celestial Mechanics, 1980

[52]   Patterson C. E., *Representations of invariant manifolds for applications in system-to-system transfer design*, Master's thesis, School of Aeronautics and Astronautics, Purdue University, West Lafayette, Indiana, 2004.

[53]   Koon, W. S., Lo, M. W. Marsden, J. E. and Ross, S. D., *Low energy transfer to the Moon*, Celestial Mechanics and and Dynamical Astronomy, 2001

[54]   Goldberg, D.E., *Genetics algorithms in search, optimization and machine learning*, Addison-Wesley 1989

12   Mission analysis

[55]   Alessi, E. M., Gomez, G., Masdemont, J, *Two-manoeuvres transfers between LEOs and Lissajous orbits in the Earth-Moon system*, Advances in Space Research, vol. 45, pp. 1276 - 1291, 2010

[56]   Gordon, D.P., *Transfers to Earth-Moon L2 Halo orbits using lunar proximity and invariant manifolds*, Master's thesis, School of Aeronautics and Astronautics, Purdue University, West Lafayette, Indiana, 2008

[57]   Rausch, R. R., *Earth to Halo Orbit transfer trajectories*, Master's thesis,

School of Aeronautics and Astronautics, Purdue University, West Lafayette, Indiana, 2005.

[58] Belbruno, E.A., Carrico, J.P. *Calculation of weak stability boundary ballistic lunar transfer trajectories*. AIAA/AAS Astrodynamics Specialist Conference, Paper No. AIAA 2000–4142, 2000

[59] Belbruno, E.A., *Analytic estimation of weak stability boundaries and low energy transfers*. Contemp Math 292, 17–45, 2002

[60] Miele, A., *Theorem of image trajectories in the Earth-Moon space*, Boeing Scientific Research Laboratories, 1960

[61] Miele, A., Mancuso, S., *Optimal trajectories for Earth-Moon-Earth flight,* Acta Astronautica, vol. 49, no. 2, pp. 59-71, 2001

[62] Topputo F., Vasile M., and Bernelli-Zazzera F., *Earth-to-Moon Low Energy Transfers Targeting L1 Hyperbolic Transit Orbits*, Annals of the New York Academy of Sciences, vol. 1065, no. 1, pp. 55-76, 2005

[63] Zanzottera A., Migotti G., Castelli R., and Dellnitz M., *Intersecting invariant manifolds in spatial restricted three-body problems: Design and optimization of Earth-to-halo transfers in the Sun-Earth-Moon scenario*, Commun Nonlinear Sci Numer Simulat, vol. 17, pp. 832-843, 2012

[64] Houbolt, J. C., *Considerations of the Rendezvous Problems for Space Vehicles,* April 1960

[65] Gerding, R. B., *Rendezvous equations in the vicinity of the second libration point*, Journal of Spacecraft and Rockets, Vol. 8, No. 3 (1971), pp. 292-294. doi: 10.2514/3.30263

[66] Canalias, E., Masdemont J. J., *Rendezvous in Lissajous Orbits using the Effective Phases Plane*, 2006 - arc.aiaa.org

[67] Gebhardt, C., *SLS: NASA identifies DAC-1configuration candidates for wind tunnel tests*

[68] Tsiolkovsky, K., *The Investigation of Space by Means of Reactive Devices*, 1903

[69] Crocker, A., *A Technique for the assessment of flight operability characteristics of human rated spacecraft*, American Institute of Aeronautics and Astronautics, 2010

Appendix 8   Author's Curriculum Vitae

ISAE-SUPAERO Space Systems Engineering and Operations Associate Professor

TEACHINGS AND RESEARCH EXPERIENCE

Since 1st July 2009:
- Space Systems Engineering and Operations Associate Professor at ISAE-SUPAERO(Institut Supérieur de l'Aéronautique et de l'Espace) in the Aeronautics and Space Center
- Head of the third year of the ISAE-SUPAERO Graduate Program
- Head of program of « Space Systems Engineering » Advanced Master of ISAE
- Head of « Space Systems » main stream of the ISAE-SUPAERO Master of Science
- Responsible for the INCOSE Certification training

Main teachings:
- Space Mechanics (undergraduate students, 10h)
- Introduction to Space Systems (post-graduate students, 10h)
- Space Systems Design (undergraduate and postgraduate students, 20h)
- Introduction to Systems Engineering (undergraduate and postgraduate students, 20h)
- Inter-disciplinary applications (undergraduate students, 20h)
- Functional design: eFFBD modeling Systems (post-graduate students, 4h)
- Stakeholders needs engineering (post-graduate students, 20h)
- Requirement engineering (post-graduate students, 20h)

Research field of interest:
- Deployment and operational scenarios optimization for a human space station located in EML2
- AOCS for scientific cubesat

Publications :

Lizy-Destrez S., Le Buan C., Francillout L, *Analyse of the resilience of the ATV Operations* – AIAA 2010 – 2278 - SpaceOps 2010 – Huntsville Alabama

Deconink F., Souchard B., Dumas P-A., Lizy-Destrez S., Mimoun D., Barata A., Burr S., Durantin G., Goulamhoussen J., Koanda M., Rocheron C., *STR: a student developed star tracker for the ESA-LED ESMO moon mission* - GLUC-10-3.2.7- GLUC 2010 – 31 May 3 - June 2010 - Beijing – CHINA

Bouchired S., Lizy-Destrez S., *System engineering approach applied to Galileo system*, Complex Systems Design & Management 2010 - CSDM 2010, 27-29 October 2010 - Paris – France

Lizy-Destrez S., Causse M., Kamali S., *Application de la démarche d'ingénierie de système pour la conception d'une plate-forme d'ingénierie simultanée pour les avant projets spatiaux*, Génie Logiciel n° 96 (mars 2011), ISSN 1265-1397

Jalabert E., Fabacher E., Guy N., Lizy-Destrez S., Rappin W, Rivier. G, *Optimization of Star research algorithm for ESMO star tracker* – GNC 2011 – 5-10

June 2011 – Karlovy Vary - Czech Republic

6. **Lizy-Destrez S., Blank C.,** *Mission analysis for a space medical center of an exploration gateway at lunar libration point*, IAC-11.A5.4.8 - IAC 2011 - 3- 7 October 2011 Cape Town - South Africa

7. **Rivier G., Lizy-Destrez S., Hugues J.**, *Enseignement de l'Ingénierie Système : retour sur la conception d'un senseur stellaire pour ESEO et ESMO* - Génie Logiciel n° 100 (mars2012), ISSN 1265-1397

8. **Christoph Pierl, Jean-Charles Chaudemar, Stéphanie Lizy-Destrez** *Application of the Systems Engineering methodology to the design of the AOCS of an Earth Observation satellite* - Complex Systems Design & Management 2012 - CSDM 2012, December 12-14 - Paris – France

9. **Bruno Aizier, Vincent Chapurlat, Stéphanie Lizy-Destrez, Daniel Prun, Charlotte Sneider, Jean-Luc Wippler,** *xFFBD: Towards a formal, but simple and complete functional modeling technique for system designers* – INCOSE 2012 , July 2012 – Roma - Italy

10. **Stéphanie Lizy-Destrez, Giuseppe Ferraioli, Chloé Audas, Jason Piat**, How to save delta-V and time for a round trip to EML2 Lagrangian point? IAC-12.A5.4.12,x13323- IAC 2012 - 1-5 October 2012 Naples - Italy

11. **Stéphanie Lizy-Destrez** *Mission analysis for a Space Medical Center of an exploration gateway at a lunar libration point* - Space Exploration Conference – 17-19 December 2012 – Paris, France

12. **J. Grave, W. Lucas, P. Peille, A. Rouanet-Labe, S. Lizy-Destrez,** *JUMPSAT: Qualifying three equipments in one Cubesat mission,* IAA-CU-12-0S-0P, 2nd IAA Conference, February 3rd – 9th, Roma – Italy

13. **Crescenzio Amendola, Stéphanie Lizy-Destrez**, *Panorama of ideas on structure and materials for the design of a multi-modular Space Station at EML2*, IAC-2013, D3.1, 6x17742 – 23-27 Septembre 2013 Beijing - China

14. **Giuseppe Ferraioli, Dr. Mickael Causse, Mrs. Stéphanie Lizy-Destrez, Prof. Yves Gourinat,** *Habitability of manned vehicles : the impact of human factors on future long duration human space exploration missions en route to Mars*, IAC-13, A1.1.1, 23-27 Septembre 2013 Beijing - China

15. **Roser Farre-Ponsa, Joachim H. Strenge, Andrea Gutierrez, Julien Grave, Anne Rouanne-Labe, William Lucas, Mr. Philippe Peille, Christoph Pierl, Stéphanie Lizy-Destrez, Jean Mignot,** *JUMPSAT: Qualifying three equipments in one Cubesat mission*, IAC-13,E2.4,4x1732923-27 Septembre 2013 Beijing - China

16. **Pierre Kokou, Bastien Le Bihan, Jean-Baptiste Receveur, Stéphanie Lizy-Destrez,** *Computing an optimized trajectory between Earth and an EML2 halo orbit*, SciTech 2014, 13-17 National Harbor, Maryland, USA

17. **Frank, Christopher and Durand, Jean-Guillaume and Evain, Hélène and Tyl, Clémence and Mechentel, Flora and Brunel, Antoine and Lizy-Destrez, Stéphanie Preliminary** *Design of a New Hybrid and Technology Innovative Suborbital Vehicle for Space Tourism,* 19th AIAA International Space Planes and Hypersonic Systems and Technologies Conference, 16 June 2014 - 20 June 2014 (Atlanta, United States)

18. **Stéphanie Lizy-Destrez, Bastien Le Bihan, Mohammad Iranmanesh,** *Transfer and rendez-vous strategies for the deployment and the servicing of an inhabited space station at Earth-Moon L2*, IAC-14, C1.8.10, 29 September – 03 October 2014,

213

Toronto, Canada

Stéphanie Lizy-Destrez, Chloé Audas, *Scenarios optimization for a servicing inhabited space station at Eath-Moon Lagrangian point (EML2)*, IAC-14, C1.8.10, 29 September – 03 October 2014, Toronto, Canada

Crescenzio Amendola, Stéphanie Lizy-Destrez, Regine Leconte, *The Thor space station at EML2 : Analysis and preliminary design of an innovative adaptable docking system,* IAC-14, C2.1.21593, 29 September – 03 October 2014, Toronto, Canada

Emilien Fabacher, Stéphanie Lizy-Destrez, Daniel Alazard, Finn Ankersen, Jean-François Jourdas, *Guidance and Navigation for Electromagnetic Formation Flight Orbit Modification,* EuroGNC, 13 - 15 April 2015, Toulouse, France

Francesco Sanfedino, Marco Scardino, Jérémie Chaix, Stéphanie Lizy-Destrez, *CubeSat Attitude Estimation via AUKF using Magnetometer measurements and MRPs,* EuroGNC, 13 - 15 April 2015, Toulouse, France

Stéphanie Lizy-Destrez., *Rendezvous optimization with an inhabited space station at EML2*, 25th International Symposium on Space Flight Dynamics ISSFD - October 19 – 23, 2015, Munich, Germany

From 1996 to 2009: Trainer in occupational environment (Altran Sud-Ouest):
Author and trainer for « Introduction to space systems » lectures
Author and trainer for « Introduction to Matlab » lectures
Young professionals coaching (integration and training)

From September 2003 to July 2009:
Member of the board of « La Fondation ALTRAN pour l'Innovation», then of the Scientific Council
Participation to main important steps of the annual competition (theme selection, jury selection, short-listing, work group animation)
Trainer for « Savoir parler de la Fondation » lectures
Member of NextSAT Steering Group (international conference for space technologies utilization in Air Traffic Service in 2015-2020)

From December 1996 to July 2009: Consultant for ALTRAN
2007 - 2009: Member of the Vehicle Engineer Team of the first ATV mission, Jules Verne, in charge of monitoring and control operations (from launch to re-entry), at ATVCC in CNES Toulouse
2006: Technical manager of the Altran SO team (6 consultants) for AOCS studies at Airbus DS Toulouse
2005: Consultant for bid to tender writing for « Frégates de type FLF » maintenance at DCN Toulon
2004-2005: Costs estimation for phase 0 studies at PASO (Advanced Studies department), at CNES Toulouse
2002-2004: Expertise and organization of functional validation tests for DEMETER micro-satellite at CNES Toulouse
2002: Consultant for systems activities for Myriade project for CNES Toulouse
2001-2002: Procurement for Solar Array drive mechanism (Septa 41 de Snecma) for micro-satellites of the Myriade project at CNES Toulouse
2001: Interfaces management for equipment's of the platform and the payload of the DEMETER satellite at CNES Toulouse
1999-2000: AOCS analyses for FBM and Picard micro - satellites, for CNES Toulouse
1997-1999: AOCS analyses for SPOT – Hélios satellites line, for CELESTRI constellation and STENTOR satellite telecommunications at Airbus DS Toulouse
1997: Consultant for OMNIS mechanism design at Airbus DS Toulouse
1996-1997: Mechanical Study Engineer for space composite structures for SESSAT RDMA equipment at Airbus DS - Les Mureaux

November 1995 – November 1996: **Engineer at EADS Space Transportation**
Mechanical Study Engineer for space composite structures at Airbus DS – Les Mureaux

FOREIGN LANGUAGES
French: Mother tongue
English: Fluent
German: Good skills, both written and oral
Russian: Beginner level

EDUCATION
1995:   Final Internship at Airbus DS at Munich, Germany
          Sensors calibration for geostationary satellites

1995:   Engineering Degree at Ecole Nationale Supérieure de l'Aéronautique et de l'Espace (ISAE-SUPAERO), Space Systems specialisation
          DESIA - Diplôme d'Etudes Supérieures en Ingénierie d'Affaire delivered by ISAE- SUPAERO
1992   Preparatory class for entrance to Grandes Ecoles Maths Sup. and Maths Spé.M' (at Lycée Thiers Marseille)